MECHANISMS OF ISCHAEMIC STROKE DAMAGE

Vanessa Helena Brait

B. Biomed Sci (Hons)

Submitted in total fulfilment of the requirements of
the degree of Doctor of Philosophy

October 2010

Department of Pharmacology
Monash University

TABLE OF CONTENTS

SUMMARY

Brain inflammation contributes to ischaemic and reperfusion injury, and thus worsens outcome after stroke. This thesis aimed to identify and investigate some of the inflammatory mechanisms that occur after cerebral ischaemia-reperfusion, to further enhance our understanding of them, and to potentially target them for future ischaemic stroke therapies.

This study primarily used C57Bl6/J mice, as well as genetically modified mice. The model of focal cerebral ischaemia utilised was the intraluminal filament-induced middle cerebral artery occlusion. Real-time PCR and Western blotting were used to examine mRNA and protein expression levels, respectively, in the brain, and immunofluorescence and immunohistochemistry were used to localise proteins and cells in the brain. T lymphocytes were isolated from the blood and spleen using Dynal negative isolation kits, and T lymphocyte-generated superoxide was measured using L-012-enhanced chemiluminescence.

Chapters 3 and 4 provided the first evidence that the larger infarct volume in males versus females following cerebral ischaemia is reperfusion-dependent and may be due to greater neuro-inflammation and brain infiltration of Nox2-expressing $CD3^+$ T lymphocytes in male mice. Moreover, this gender* difference was found to be dependent on Nox2 expression. The study also demonstrated for the first time that Nox2-expressing circulating $CD3^+$ T lymphocytes produce ~15-fold more superoxide after stroke, compared to $CD3^+$ T lymphocytes from control mice. These findings raise the possibility that therapies to reduce $CD3^+$ T lymphocyte infiltration and/or the production of superoxide from these cells in ischaemic stroke patients who receive recombinant t-PA, might be useful for reducing reperfusion injury.

*Nb. Although the term "sex" rather than "gender" may perhaps be more appropriate when referring to the biological and physiological characteristics that define males and females, "gender" is commonly used in publications. Therefore, I have chosen to use the term "gender" throughout the thesis.

Chapter 5 confirmed and extended the above findings and demonstrated for the first time that circulating Nox2-containing $CD4^+$ and $CD8^+$ T lymphocytes generate substantially higher levels of superoxide after cerebral ischaemia-reperfusion compared with similar T lymphocyte subsets from control mice.

Chapter 6 demonstrated that the mRNA expression of various chemokines and chemokine receptors, including the potent neutrophil chemoattractants, CXCR2, CXCL1 and CXCL2, are increased in the brain after ischaemia-reperfusion. Administration of the CXCR2 antagonist, SB 225002, reduced the expression of these chemokines in the brain, as well as the infiltration of neutrophils, but did not improve outcome at 72 h after ischaemia-reperfusion. These findings suggest that the infiltration of neutrophils do not contribute to ischaemia-reperfusion injury.

Chapter 7 examined for the first time the role of the endogenous calcineurin inhibitor, Down syndrome candidate region 1 (*DSCR1*), on outcome following cerebral ischaemia-reperfusion. We found that the over-expression of *DSCR1* improves neurological outcome, and reduces infarct and oedema volume. This protection was most likely through the inhibition of calcineurin in neurons and also potentially in T lymphocytes, and the subsequent reduction in pro-inflammatory mediators. Interestingly, we also found preliminary evidence that the deficiency of *DSCR1* improves neurological outcome and reduces infarct and oedema volume. *DSCR1*-deficiency thus may also reduce calcineurin activity, however the precise mechanisms underlying this are still unclear.

Overall, this thesis presents important findings on the role of inflammation in ischaemic injury following cerebral ischaemia-reperfusion, and supports the concept that strategies targeting inflammation in combination with recombinant t-PA may be a successful stroke therapy.

DECLARATION

In accordance with Monash University Doctorate Regulation 17/Doctor of Philosophy and Master of Philosophy (MPhil) regulations the following declarations are made:

I hereby declare that this thesis contains no material which has been accepted for the award of any other degree or diploma in any university or other institution and I affirm that to the best of my knowledge this thesis contains no material previously published or written by another person, except where due reference is made in the text of the thesis.

All of the results chapters are based on collaborations between researchers within our laboratory or in external laboratories, and recognises a team-based research approach to the studies in my PhD. Their contributions are acknowledged in the following section.

The ideas, development and writing up of all of the chapters in this thesis were the principal responsibility of myself, the candidate, working under the supervision of A/Prof Christopher G. Sobey.

Signed:..... Date:.....

Vanessa Helena Brait

Notice 1:

Under the Copyright Act 1968, this thesis must be used only under the normal conditions of scholarly fair dealing. In particular no results or conclusions should be extracted from it, nor should it be copied or closely paraphrased in whole or in part without the written consent of the author. Proper written acknowledgement should be made for any assistance obtained from this thesis.

Notice 2:

I certify that I have made all reasonable efforts to secure copyright permissions for third-party content included in this thesis and have not knowingly added copyright content to my work without the owner's permission.

PREFACE

The following work was carried out in collaboration with others:

Chapter 4:

- Dr Anna Walduck (Department of Microbiology and Immunology, University of Melbourne) helped with the running of the FACS, and performed the analysis
- Mr. Henry Diep and Ms. Anja Mast performed the Western blotting experiments
- Dr Stavros Selemidis performed the isolation of the T lymphocytes and the superoxide measurements
- Dr Brad Broughton and Ms. Elizabeth Guida performed the immunofluorescence and the immunohistochemistry experiments

Chapter 5:

- Mr. Henry Diep performed the majority of the T lymphocyte isolations and the superoxide measurements
- Dr Samy Sakkal (Monash Immunology and Stem Cell Laboratories, Monash University) performed the purity analyses of T lymphocyte subpopulations using flow cytometry

Chapter 6:

- Ms Jennifer Rivera performed the PCR experiments
- Dr Brad Broughton and Ms. Sandy Lee performed the immunofluorescence experiments

Chapter 7:

- Dr Melanie Pritchard (Department of Biochemistry and Molecular Biology, Monash University) generated the *DSCR1* Tg and KO mice

- Ms Katherine Martin (PhD student; Department of Biochemistry and Molecular Biology, Monash University) performed the PCR experiments, and part of the Western blotting experiments

- Dr Mariona Arbones and Dr Maria Jose Barallobre (Centre de Regulació Genòmica, Barcelona, Spain) performed part of the Western blotting experiments

I personally performed all of the surgeries, took care of all the animals post-operatively, removed, weighed, froze and sectioned all of the brains, performed all of the infarct and oedema volume analysis, performed the tail cuffing experiments, performed the T lymphocyte proliferation studies, performed a number of the leukocyte isolations, performed the FACS experiments under the supervision of Dr. Anna Walduck, performed a number of the T lymphocyte isolations and superoxide measurements, performed the von Willebrand factor immunofluorescence, and all other data analysis.

ACKNOWLEDGEMENTS

First and foremost I would like to thank my supervisor and mentor Associate Professor Chris Sobey. Chris, your endless enthusiasm in my project has kept me motivated throughout my PhD. I hope to one day be as proficient a scientist, and as wonderful and supportive a supervisor as you.

I'd also like to thank Dr Alyson Miller for having complete faith in my scientific ability during my honours year, and for taking me under her wing. Al, you have always supported me and believed in my future success. I will be forever grateful for that.

To Dr Kath Jackman for teaching me the stroke model, and for her support whenever I was questioning my ability. Her friendship in the lab was invaluable, and I will always have very fond memories of good times spent in the stroke lab. Can't wait until we're working together again.

Another special thank you goes to Michael De Silva. I felt that we really shared an enthusiasm for each other's successes during our PhDs, and it was really lovely being able to share my achievements with someone who genuinely cared.

To all the past and present members of the VBIG lab (in no particular order) – Brad, Grant, Stav, Barb, Jen, Janahan, Craig, Anja, Henry, Courtney, Elizabeth H, Klaudia, Soph, Michelle, Ravina, Steph, Elizabeth G, Sandy, Jeff, Kate and Jacqui. Thanks for all the help, advice, laughs and fun times we had together. I feel very lucky to have been a part of a lab with such vibrant, intelligent and lovely people. Also thanks to everyone in the Pharmacology department at Monash University. This department was a very special place to complete my honours and PhD, for the general laid back approach, and the welcoming environment. Coming to work each day was always a pleasure.

To all my friends, I will now have entire days, nights and weekends to spend with you. In particular, to my current house-mate and beautiful friend Danya; her advice and counselling were essential to me getting through the thesis writing process with my sanity intact. I'd also like to make special mention of Christina and Julia, for their genuine interest and excitement in my progress. Our weekly get togethers were really important to me throughout the writing process.

Lastly, I'd like to thank my family; my parents for their infinite pride in my achievements, their endless support, and for coming to uni to help with the printing debacle, and Pabs and Taegen for simply being a fantastic brother and sister-in-law that I always look forward to seeing.

Finally, I'd also like to acknowledge the people who helped with some of the experiments I am presenting in this thesis. Dr Anna Walduck from the Department of Microbiology and Immunology at the University of Melbourne, Dr Melanie Pritchard and Katherine Martin from the Department of Biochemistry and Molecular Biology at Monash University, Dr Mariona Arbones and Dr Maria Jose Barallobre from the Centre de Regulació Genòmica in Barcelona, Spain, Dr Samy Sakkal from the Monash Immunology and Stem Cell Laboratories at Monash University, Dr Brad Broughton, Jennifer Rivera, Henry Diep, Dr Stavros Selemidis, Elizabeth Guida, Sandy Lee and Anja Mast from our lab at Monash University.

I could never have completed my PhD without all of your support. THANK YOU.

ABBREVIATIONS

Aβ	amyloid beta
ANOVA	analysis of variance
APC	allophycocyanin
BA	basilar artery
BBB	blood brain barrier
BP	blood pressure
BSA	bovine serum albumin
° C	degrees celcius
Ca^{2+}	calcium ion
CCA	common carotid artery
CCIV	corrected cortical infarct volume
CIV	corrected infarct volume
cDNA	complementary DNA
CNS	central nervous system
Cox-2	cyclo-oxygenase-2
CSF	cerebrospinal fluid
CSIV	corrected subcortical infarct volume
CSP1	calcipressin 1
CXCL1	chemokine (C-X-C motif) ligand 1
CXCL2	chemokine (C-X-C motif) ligand 2
CXCR2	chemokine (C-X-C motif) receptor 2
dH_2O	distilled water
DMSO	dimethyl sulfoxide
DSCR1	down syndrome candidate region 1
DSCR1.1	down syndrome candidate region 1 isoform 1
DSCR1.4	down syndrome candidate region 1 isoform 4

ECA	external carotid artery
EDTA	ethylenediaminetetraacetic acid
EtOH	ethanol
FACS	fluorescent activated cell sorting
FCS	foetal calf serum
FITC	fluorescein isothiocyanate
g	grams or g-force
GABA	gamma-aminobutyric acid
Gdf5	growth differentiation factor 5
gDNA	genomic DNA
HMOX1	heme-oxygenase-1
HPA	hypothalamic-pituitary axis
HRP	horseradish peroxidase
IκBα	inhibitory kappa B alpha
ICA	internal carotid artery
ICAM-1	intercellular cell adhesion molecule-1
IFN-γ	interferon gamma
IL-1α	interleukin-1 alpha
IL-1β	interleukin-1 beta
IL-2	interleukin-2
IL-4	interleukin-4
IL-6	interleukin-6
IL-16	interleukin-16
IL8Ra	interleukin receptor 8 type a
IL8Rb	interleukin receptor 8 type b
iNOS	inducible nitric oxide synthase
I-NR	ischaemia with no reperfusion

i.p.	intraperitoneally
I-R	ischaemia with reperfusion
i.v.	intravenously
K^+	potassium ion
KC	keratinocyte-derived chemokine
KO	knock-out
LCA	left cortical area
LCV	left cortical volume
LHA	left hemisphere area
LHV	left hemisphere volume
Lif	leukaemia inhibitory factor
mAb	monoclonal antibody
MCA	middle cerebral artery
MCAO	middle cerebral artery occlusion
MCIP1	modulatory calcineurin-interacting protein 1
MCP-1	monocyte chemotactic protein-1
MeOH	methanol
MHC	major histocompatability complex
min	minutes
MIP-1α	macrophage inflammatory protein-1alpha
MIP-2	macrophage inflammatory protein-2
MMP-9	matrix metalloproteinase-9
MMPs	matrix metalloproteinases
MPO	myeloperoxidase
mRNA	messenger RNA
NADPH	nicotinamide adenine dinucleotide phosphate
NFAT	nuclear factor of activated T cells

NF-κB	nuclear factor-kappa B
NK cell	natural killer cell
NKT cell	natural killer T cell
nNOS	neuronal nitric oxide synthase
NO	nitric oxide
$ONOO^-$	peroxynitrite
PBMC	peripheral blood mononuclear cell
PBS	phosphate buffered saline
PCA	posterior communicating artery
PCR	polymerase chain reaction
PDB	phorbol 12,13-dibutyrate
PE	phycoerythrine
PFA	paraformaldehyde
pH	potential of Hydrogen
PVDF	polyvinylidene fluoride
Rag	recombination-activating gene
RCA	right cortical area
rCBF	regional cerebral blood flow
RCAN1	regulator of calcineurin 1
RCIA	right cortical infarct area
RIA	right infarct area
RLU	relative light units
RNS	reactive nitrogen species
ROS	reactive oxygen species
rt-PA	recombinant tissue plasminogen activator
s	seconds
SB 225002	CXCR2 antagonist

s.c.	subcutaneously
SNS	sympathetic nervous system
SOD1	superoxide dismutase 1
TBS	tris buffered saline
TBX21	T box transcription factor 21
TCR	T cell receptor
Tg	transgenic
TGF-β1	transforming growth factor beta 1
T_H1	T helper 1
T_H2	T helper 2
TNF-α	tumour necrosis factor alpha
T_{reg} cell	regulatory T cell
Trem1	triggering receptor expressed on myeloid cells 1
U	units
V	volts
VCAM-1	vascular cell adhesion molecule-1
Wt	wild-type
Wt_{KO}	wild-type littermates for the *DSCR1* KO mice
Wt_{Tg}	wild-type littermates for the *DSCR1* Tg mice

PUBLICATIONS ARRISING FROM THIS THESIS

Original research articles:

1. **V.H. BRAIT,** K.A. JACKMAN, A.K. WALDUCK, S. SELEMIDIS, H. DIEP, A.E. MAST, E. GUIDA, B.R.S. BROUGHTON, G.R. DRUMMOND AND C.G. SOBEY (2010). Mechanisms Contributing To Cerebral Infarct Size after Stroke – Gender, Reperfusion, T Lymphocytes and Nox2-Derived Superoxide. *Journal of Cerebral Blood Flow and Metabolism*, 30: 1306-1317.

2. **V.H. BRAIT*,** J. RIVERA*, S. LEE, B.R.S. BROUGHTON, G.R. DRUMMOND AND C.G. SOBEY. Effect of a CXCR2 antagonist on CXCL1, CXCL2 and CXCR2 brain expression and infarct volume after stroke in C57Bl6 mice (in preparation). *Equal contributions.

3. **V.H. BRAIT,** K.R. MARTIN, T.V. ARUMUGAM, M.A. PRITCHARD AND C.G. SOBEY. Overexpression of human Down syndrome candidate region 1 (*DSCR1*) gene improves outcome following cerebral ischemia-reperfusion in mice (in preparation).

Abstracts from work presented by the candidate at scientific meetings:

1. **V.H. BRAIT,** K.A. JACKMAN, A.K. WALDUCK, S. SELEMIDIS; H. DIEP, A.E. MAST, E. GUIDA, B.R.S. BROUGHTON, G.R. DRUMMOND & C.G. SOBEY (2010). "Mechanisms Contributing To Cerebral Infarct Size After Stroke – Gender, Reperfusion, T Lymphocytes and Nox2-Derived Superoxide". *XIX. European Stroke Conference, Barcelona, Spain.* Abstract 903.

2. **V.H. BRAIT**, K.R. MARTIN, M.A. PRITCHARD & C.G. SOBEY (2009). "Improved outcome following cerebral ischaemia-reperfusion in mice when the human down syndrome candidate region 1 (DSCR1) gene is overexpressed". *Australasian Society of Clinical and Experimental Pharmacologists and Toxicologists (ASCEPT), Sydney, Australia.* Abstract 2–5.

3. **V.H. BRAIT**, K.A. JACKMAN, A.K. WALDUCK, S. SELEMIDIS, H. DIEP, B.R.S. BROUGHTON, G.R. DRUMMOND & CG SOBEY (2009). "Mechanisms contributing to infarct size after stroke – gender, reperfusion, T lymphocytes and Nox2". *Australasian Society of Clinical and Experimental Pharmacologists and Toxicologists (ASCEPT), Sydney, Australia.* Abstract 1–42 & 102.

4. **V.H. BRAIT,** K.A. JACKMAN, H. DIEP, B.R.S. BROUGHTON, A.K. WALDUCK, G.R. DRUMMOND & C.G. SOBEY (2009). "Smaller cerebral infarct size in females versus males is reperfusion-dependent and associated with less inflammation and nox2-containing infiltrating T lymphocytes". *XXIVth International Symposium on Cerebral Blood Flow, Metabolism and Function ("Brain09"), Chicago, USA.* Abstract 0165.

5. C.G. SOBEY, K.R. MARTIN, M.A. PRITCHARD & **V.H. BRAIT** (2009). "Overexpression of human down syndrome candidate region 1 (DSCR1) gene improves outcome following cerebral ischemia-reperfusion in mice". *XXIVth International Symposium on Cerebral Blood Flow, Metabolism and Function ("Brain09"), Chicago, USA.* Abstract 0232.

6. **V.H. BRAIT**, K.A. JACKMAN, A.E. MAST, H. DIEP, A.K. WALDUCK, G.R. DRUMMOND & C.G. SOBEY (2008). "Cerebral infarct size is gender-dependent following transient but not permanent middle cerebral artery occlusion in mice". *Australian Health and Medical Research Congress (AHMRC), Brisbane, Australia.* Abstract 114.

7. **V.H. BRAIT**, K.A. JACKMAN, A.E. MAST, G.R. DRUMMOND & C.G. SOBEY (2007). "Cerebral infarct size is gender-dependent following transient but not permanent middle cerebral artery occlusion in mice". *Experimental Biology, San Diego, USA.* Abstract 719.7

8. **V.H. BRAIT**, K.A. JACKMAN, G.R. DRUMMOND & C.G. SOBEY (2007). "Cerebral infarct size is gender-dependent following transient but not permanent middle cerebral artery occlusion in mice". *Australasian Society of Clinical and Experimental Pharmacologists and Toxicologists (ASCEPT), Adelaide, Australia.* Abstract 24.

Chapter 1:

General Introduction

1.1 Ischaemic stroke

Ischaemic stroke is characterised by a transient or permanent reduction in blood supply to a part of the brain due to the blockage of a major cerebral artery. It can be caused either by an embolus or a thrombus (Dirnagl *et al.*, 1999), and accounts for approximately 80 % of all strokes (Eaker *et al.*, 1993; Manolio *et al.*, 1996). 60,000 strokes will occur in Australia in 2010 with a stroke occurring every 10 minutes (NSF, 2010). Furthermore, the incidence of strokes will increase annually due to the ageing population, as the vast majority of stroke sufferers are aged over 65 (NHLBI, 2006; Senes, 2006). In Australia, stroke is the 2nd leading cause of death after ischaemic heart disease, and the most common cause of permanent disability (AIHW, 2006). In the USA, despite a large reduction in stroke-related death, stroke remains the 5th and 2nd leading cause of death in males and females, respectively (Towfighi *et al.*, 2010), and approximately 14 % and 18 % of all 65 year old males and females, respectively, will suffer at least one stroke in their lives (Seshadri *et al.*, 2006). Currently the only available therapy for acute ischaemic stroke - approved in 1996 for use within 3 hours after stroke onset - is the thrombolytic recombinant tissue plasminogen activator (rt-PA). The use of rt-PA attempts to dissolve the clot, thus inducing recanalisation and reperfusion, and limiting the damaging effects of stroke injury (Hacke *et al.*, 1999; QSSAAN, 1996). The proportion of stroke patients that actually receive rt-PA is ≤15 % (Barber *et al.*, 2001; Johnston *et al.*, 2001; Katzan *et al.*, 2004; Koennecke *et al.*, 2001; van Wijngaarden *et al.*, 2009). In addition, the efficacy is modest and variable with 6-78 % of cases having partial or complete recanalisation within 2 hours of i.v. rt-PA infusion (78 %: Alexandrov and Grotta, 2002; 46 %: Alexandrov *et al.*, 2004; 6-44 %: Saqqur *et al.*, 2007; 17 %: Tsivgoulis *et al.*, 2010; 6-22 %: van Wijngaarden *et al.*, 2009), with re-occlusion reported to occur in 42 % of patients that experienced partial recanalisation and 22 % of patients that experienced complete recanalisation (Alexandrov and Grotta, 2002). Furthermore, tissue reperfusion is the ultimate aim of arterial recanalisation, and a study reported that only 19 % of patients that had complete recanalisation, achieved complete reperfusion (Khatri *et al.*, 2005). Since 1996, apart

from the recent approval of rt-PA use for up to 4.5 hours after stroke onset (del Zoppo *et al.,* 2009), there have been no new therapies approved. Hence, there remains a great need for therapies that can prevent or reduce brain damage during and after stroke.

1.2 Influence of gender

The incidence of stroke is lower in pre-menopausal females than age-matched males. Stroke incidence increases in females after menopause (average age of onset is 51), due to the loss of circulating oestrogen, at a much greater rate than in males at the corresponding age. By the age of approximately 75 to 84, the incidence of stroke in females catches up to males, and then in those ≥85 years of age, stroke incidence in females surpasses that of males (NHLBI, 2006). In addition to incidence, gender may influence stroke severity and outcome. Although, gender-based recovery from stroke has not been heavily studied, the few clinical studies that have examined this found that more females die from stroke then males (AIHW, 2006; NHLBI, 2006), and that females have increased functional impairment in areas of motor and cognitive function in the first 2 weeks after stroke and up to 1 year after (Gargano and Reeves, 2007; Wyller *et al.*, 1997). However, due to many confounding factors, such as the fact that female stroke patients are older, have a greater life expectancy, and are more likely to be permanently institutionalised when they experience a stroke, the findings are difficult to interpret. In any case, they do suggest that not only does the loss of oestrogen at menopause increase the incidence of stroke, but it may also result in increased neurobehavioural dysfunction after stroke. This is perhaps not surprising, as oestrogen is a complex, multi-faceted hormone with many actions, including the ability to reduce oxidative stress and free radical activity (Behl *et al.*, 1997), and various inflammatory mechanisms, such as iNOS (inducible nitric oxide synthase) expression, NF-κB (nuclear factor-kappa B) activation and leukocyte adhesion (Park *et al.*, 2006; Santizo *et al.*, 2000; Wen *et al.*, 2004), all of which are important events in the pathogenesis of stroke (see section 1.4 below).

Processes that oestrogen can inhibit occur during ischaemia, but also during reperfusion (see section 1.4.5 below), and it is possible that the anti-inflammatory and anti-oxidative effects of oestrogen may be more relevant for protection when reperfusion does occur. In addition, the vast majority of stroke studies have been performed in male rodents, using the transient ischaemia protocol (ischaemia with reperfusion; I-R), and only 3 studies (with conflicting findings) have been reported comparing genders following the permanent ischaemia protocol (ischaemia with no reperfusion; I-NR) (Cai *et al.*, 1998; Carswell *et al.*, 1999; Loihl *et al.*, 1999). Therefore, some of the goals of this thesis were to test whether there is a gender difference in outcome following I-NR, to clarify the nature of mechanisms of reperfusion injury, and to investigate whether these occur to a similar extent in males and females (Chapters 3 and 4).

1.3 Experimental models of ischaemic stroke in mice

There are numerous models of focal cerebral ischaemia that can be employed in rodents. The middle cerebral artery (MCA) or one of its branches, are the vessels most commonly affected in clinical ischaemic stroke (Bogousslavsky *et al.*, 1988). In accordance with this, the vast majority of experimental ischaemic stroke studies utilise a model in which a segment of the MCA is occluded. The induction of an MCA occlusion can be achieved either by surgical models (direct ligation or cauterisation of the MCA via the eye or cranium), a thrombo-embolic model (injection of a fibrin-rich or artificial thrombus), chemical models (direct application of the vasoconstrictor endothelin-1 or a photochemical reaction between a photoactive dye and a light beam), or the intraluminal filament model (introduction of a filament via the internal carotid artery which blocks the MCA at its origin with the circle of Willis) (For reviews see Durukan *et al.*, 2008; Durukan and Tatlisumak, 2007; Hossmann, 2008). No one model is an exact replication of human ischaemic stroke, and they each have their respective pros and cons. The thrombo-embolic model is arguably the most relevant to human stroke, but as it has a high degree of variability, and spontaneous reperfusion often occurs, it is quite inconsistent. The studies in this

thesis utilise the intraluminal filament model of ischaemic stroke, which was first described by Koizumi in 1986 (Koizumi *et al.*, 1986). Since then it has been modified numerous times, and is now the most commonly used model of ischaemic stroke. One advantage of this model is that it can be used to mimic I-NR by keeping the filament in place; or simply by retracting the filament, it can become a model of I-R. For the studies completed in Chapters 3 and 4, this was an important consideration, as the outcomes in male and female mice following the two protocols are compared. The intraluminal filament model produces reproducible infarcts and is a relatively simple, minimally invasive procedure. Some limitations to this model include occasional subarachnoid haemorrhage and incomplete occlusion, although, with the combined use of a silicone-coated filament and transcranial laser Doppler flowmetry, the incidence of subarachnoid haemorrhage can be markedly reduced. Furthermore, use of the correct sized filament with laser Doppler flowmetry will reduce the incidence of incomplete occlusion (Schmid-Elsaesser *et al.*, 1998).

1.4 Pathogenesis of cerebral ischaemia

Ischaemic brain injury following stroke results from a complex sequence of mechanisms that evolve in a spatial and temporal pattern. Within minutes, in the ischaemic core - the region most severely affected by the reduction in blood flow - energy failure and excitotoxicity lead to necrotic cell death. Adjacent to the core region, is the zone termed the penumbra (Markus *et al.*, 2003; Quast *et al.*, 1993; Touzani *et al.*, 1995). The penumbra retains structural integrity and metabolic activity due to residual circulation provided by collateral blood vessels, but it is functionally inactive (Ginsberg, 1997). The penumbra is potentially salvageable; however, if blood supply is not rapidly restored (i.e. reperfusion, either if the patient is successfully treated with rt-PA, or if the vessel spontaneously reperfuses), the disruption of cellular homeostasis in the penumbra leads to slow apoptotic cell death, resulting in a step-by-step growth of the lesion (see Figure 1.1).

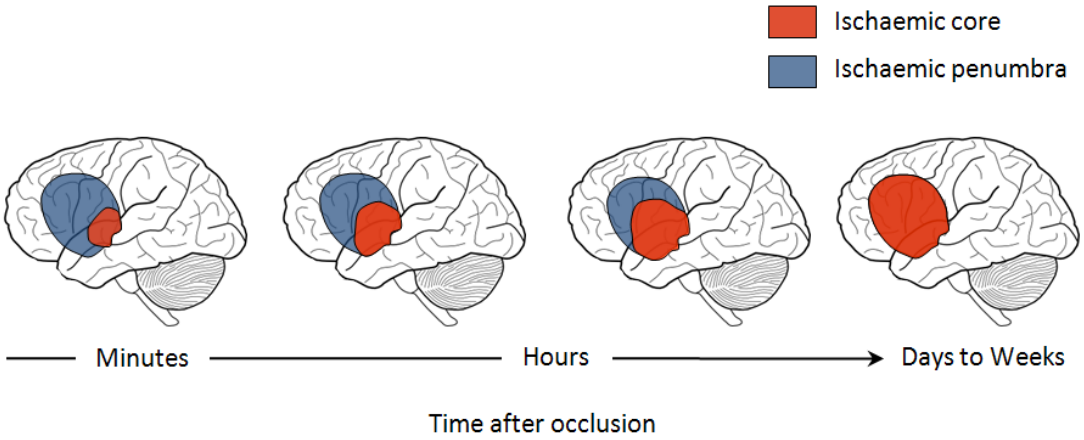

Figure 1.1. Step-by-step growth of the lesion and reduction of the penumbra over time.
Diagram depicting the putative time course and spatial pattern of the step-by-step growth of the lesion and the resultant reduction in the penumbra (Adapted from Dirnagl *et al*, 1999).

Reperfusion may be regarded as a double-edged sword because it can also cause additional brain injury through the excessive production of reactive oxygen species (ROS) and inflammatory products (For review see Schaller and Graf, 2004). The major pathogenic mechanisms of this cascade will be reviewed below, and although one event triggers the following one, it is important to note that they are inextricably linked and often occur over the same time frame (see Figure 1.2).

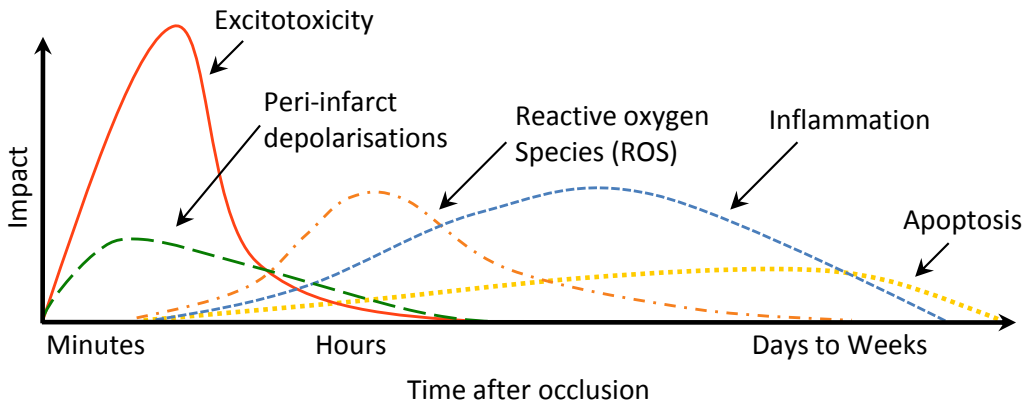

Figure 1.2. Putative cascade of the pathogenesis of cerebral ischaemia.
Diagram depicting the putative time-course and impact of the different events in the pathogenic cascade after ischaemic stroke (Adapted from Dirnagl *et al*, 1999).

1.4.1 Energy failure and ionic imbalance

As the brain cannot store energy, it is almost exclusively dependent on the continuous steady flow of glucose and oxygen from the blood for energy production. During ischaemic stroke, the reduction in cerebral blood flow causes oxygen and glucose deprivation within minutes. Initially, this loss of energy disrupts ionic gradients, with large increases in extracellular potassium (K^+) and small changes in other ion concentrations (Hansen and Zeuthen, 1981; Martin *et al.*, 1994; Nedergaard and Hansen, 1993). This triggers membrane depolarisation in neurons and glia, and further increases in intracellular sodium and chloride, and especially large increases in intracellular calcium (Ca^{2+}) (Hansen and Zeuthen, 1981; Martin *et al.*, 1994), through the activation of voltage gated Ca^{2+} channels (Goldin *et al.*, 1995).

1.4.2 Excitotoxicity

Cellular depolarisation and an increased concentration of intracellular Ca^{2+} triggers a large and prolonged release of excitotoxic neurotransmitters, especially glutamate, into the extracellular compartment (Castillo *et al.*, 1997; Davalos *et al.*, 1997). There is also a loss of excitatory amino acid transporter expression and function, impairing excitatory amino acid re-uptake, resulting in an accumulation of these amino acids in the synapse (Huang *et al.*, 1993; Rao *et al.*, 2001; Yeh *et al.*, 2005). These then activate the ionotropic NMDA (N-methyl-D-aspartate) and AMPA (α-amino-3-hydroxy-5-methyl-4-isoxazolepropionic acid) receptors, as well as metabotropic glutamate receptors. The prolonged activation of these glutamate receptors causes further increases in intracellular Ca^{2+} concentrations that are sufficient to trigger excitotoxic processes (Furukawa *et al.*, 1997), such as the degradation of cytoskeletal and extracellular matrix proteins, via lipases, proteases and nucleases (Chen and Strickland, 1997; Furukawa *et al.*, 1997), resulting in cell death. During and immediately after glutamate release, in the regions with the greatest concentration of glutamate (the ischaemic core), neurons die via necrosis - the increased intracellular Na^+ concentration causes a passive influx of H_2O, leading to cell oedema and

ultimately, osmotic lysis. However, neuronal cells in the penumbra survive the initial insult, as they still receive a sufficient supply of energy. Excitotoxicity in these cells initiate molecular events that lead to the production of ROS (see section 1.4.4 below) (Girouard *et al.*, 2009) and inflammation (see section 1.4.5 below) (Dirnagl *et al.*, 1999), that eventually undergo apoptosis (see section 1.4.6 below) (Ankarcrona *et al.*, 1995; Bonfoco *et al.*, 1995).

1.4.3 Peri-infarct depolarisations

Spreading depolarisation and repolarisation occurs in the healthy brain under control conditions. However, repolarisation is an energy-dependent event. After depolarisation following cerebral ischaemia, cells in the core region can no longer repolarise, due to a lack of these substrates, and they become necrotic (Back *et al.*, 1994). In contrast, in the penumbra, cells undergo spontaneous repetitive waves of depolarisations, due to the high levels of extracellular K^+ and glutamate (Back *et al.*, 1996; Dohmen *et al.*, 2008; Iijima *et al.*, 1992; Mies *et al.*, 1993; Nedergaard and Hansen, 1993; Strong *et al.*, 2000). These peri-infarct depolarisations slowly consume the remaining oxygen and glucose, until they too can no longer repolarise (Els *et al.*, 1997; Graf *et al.*, 1995). The frequency and duration of these peri-infarct depolarisations correspond to accelerated infarct growth (Back *et al.*, 1996; Busch *et al.*, 1996; Mies *et al.*, 1993).

1.4.4 Reactive oxygen and nitrogen species production

The brain is especially vulnerable to oxidative stress, due to its high consumption of oxygen, high concentration of easily oxidised lipids, and relatively low level of endogenous antioxidants (the brain has almost no catalase and low levels of glutathione peroxidase and vitamin E) (For review see Cui *et al.*, 2004). During ischaemia and after reperfusion, higher levels of ROS, such as superoxide, hydrogen peroxide and hydroxyl radicals, and reactive nitrogen species (RNS), such as nitric oxide (NO), are generated. NO can react with superoxide to produce the highly reactive radical, peroxynitrite ($ONOO^-$) (Blough and Zafiriou, 1985). These species are generated by a

variety of mechanisms, including excitotoxicity, intracellular Ca^{2+} overload, up-regulation of cytosolic pro-oxidant enzymes such as neuronal nitric oxide synthase (nNOS) and iNOS, cyclo-oxygenase 1 and 2 (Cox-1 and Cox-2, respectively), xanthine oxidase and NADPH oxidase, as well as the mitochondrial respiratory chain. Bone-marrow derived immune cells, such as neutrophils and monocytes, as well as the major resident brain immune cell, activated microglia, also contribute to the generation of ROS, and their involvement in I-R injury will be discussed further in the following section. Additionally, due to the energy required for the activation of endogenous antioxidant systems, these safety mechanisms, including a number of enzymes (superoxide dismutase, catalase, glutathione peroxidise) and chelators such as vitamin E, become compromised. The excess ROS can directly damage lipids, protein and DNA, as well as causing mitochondrial dysfunction, leading to apoptosis (see section 1.4.6 below) (For reviews see Chan, 2001; Schaller and Graf, 2004). Furthermore, studies in mice over-expressing antioxidants or with a deficiency in pro-oxidant enzymes have reported smaller infarct volumes (Iadecola *et al.*, 2001b; Iadecola *et al.*, 1997; Kinouchi *et al.*, 1991; Sampei *et al.*, 2000; Weisbrot-Lefkowitz *et al.*, 1998; Yang *et al.*, 1994), and studies with antioxidant-deficient mice have reported larger infarcts (Crack *et al.*, 2001; Kondo *et al.*, 1997; Murakami *et al.*, 1998), confirming the contribution of ROS to ischaemic damage.

NADPH oxidase is the major source of ROS in the vasculature (Griendling *et al.*, 1994a; Miller *et al.*, 2009; Miller *et al.*, 2005), and all cells in the vascular wall - endothelial cells, smooth muscle cells and fibroblasts - contain at least one of the isoforms of NADPH oxidase (Griendling *et al.*, 2000). Under normal conditions, the Nox2 isoform (previously named gp91*phox*), is expressed throughout many regions of the brain including the hippocampus, cortex, striatum, thalamus and amygdala (Kim *et al.*, 2005; Serrano *et al.*, 2003), in neurons (Dai *et al.*, 2006; Hilburger *et al.*, 2005; Noh and Koh, 2000; Serrano *et al.*, 2003), microglia (Li *et al.*, 2005) and astrocytes (Abramov *et al.*, 2005; Noh and Koh, 2000). Following cerebral I-R, there is an increase in brain Nox2 expression

(Kusaka *et al.*, 2004; McCann *et al.*, 2008), and mice with a dysfunctional Nox2 subunit, or completely lacking Nox2, attained a smaller infarct and oedema volume, less ROS production and less blood brain barrier (BBB) disruption than their wild-type littermates, suggesting that Nox2 is detrimental in ischaemic injury (Chen *et al.*, 2009; Jackman *et al.*, 2009a; Kahles *et al.*, 2007; Kunz *et al.*, 2007; Walder *et al.*, 1997). In contrast however, one study found no change in infarct volume when utilising Nox2-deficient mice (Kleinschnitz *et al.*, 2010a). Nox2 is also expressed in monocytes, neutrophils and T lymphocytes (Jackson *et al.*, 2004; Selemidis *et al.*, 2008), and can also potentially contribute to stroke damage via these immune cells (Walder *et al.*, 1997). Nox1 mRNA has been detected in cerebellar granule neurons (Coyoy *et al.*, 2008) and microglia (Cheret *et al.*, 2008), but its expression after stroke has not been previously studied. Only three studies have investigated the involvement of the Nox1 isoform of NADPH oxidase in cerebral I-R; two reported no effect on total infarct volume in mice deficient in Nox1 (Jackman *et al.*, 2009b; Kleinschnitz *et al.*, 2010a), whereas the other reported a smaller infarct volume and improved outcome (Kahles *et al.*, 2010), suggesting that it may play a role.

1.4.5 Inflammation

This thesis focuses on the complex inflammatory response that occurs from a few hours up to 3 days following occlusion and subsequent reperfusion of a major cerebral artery (see Figure 1.4). However, the inflammatory response is thought to still continue for up to a few weeks after occlusion (see Figure 1.2).

A few hours after the ischaemic insult, resident brain cells such as neurons, astrocytes, microglia and endothelial cells, as well as circulating immune cells, become activated, and produce pro-inflammatory genes, such as TNF-α (tumour necrosis factor-alpha), IL-1β (interleukin-1beta), IL-6 (interleukin-6) and IFN-γ (interferon-gamma) (Buttini *et al.*, 1994; Gong *et al.*, 1998; Hurn *et al.*, 2007; Kostulas *et al.*, 1999; Liu *et al.*, 1993; Offner *et al.*, 2006a; Tarkowski *et al.*, 1995; Uno *et*

al., 1997; Wang *et al.*, 1994; Zhang *et al.*, 1998c). This triggers an increased expression of adhesion molecules (eg. ICAM-1, VCAM-1, selectins) at the cerebral vascular endothelium (Connolly *et al.*, 1996; Haas *et al.*, 2007; Haring *et al.*, 1996; Justicia *et al.*, 2006; Lindsberg *et al.*, 1996; Zhang *et al.*, 1998a). These adhesion molecules bind to complementary cell surface receptors (eg. α- and β-integrins, selectin ligands) on circulating immune cells, allowing for their tethering and rolling (mediated by selectins), adhesion to the endothelium (mediated by integrins and adhesion molecules) and transmigration into the perivascular space, and ultimately into the parenchyma (For review see Engelhardt and Ransohoff, 2005). This transmigration is facilitated by the disruption of the BBB that occurs after stroke (see below). Chemokines also contribute to the infiltration of immune cells. They are produced by injured brain cells and immune cells and guide circulating immune cells into the brain. Some of the most important pro-inflammatory chemokines are CXCL8 (also named interleukin-8; IL-8), CCL2 (also named monocyte chemotactic protein-1; MCP-1) and CCL3 (also named monocyte inflammatory protein-1alpha; MIP-1α). Increases in these and other chemokines have been reported in the brain and blood after stroke (Chapman *et al.*, 2009; Ivacko *et al.*, 1997; McColl *et al.*, 2007; Minami and Satoh, 2003; Schmerbach *et al.*, 2008; Wang *et al.*, 1998; Wang *et al.*, 1999). The role of chemokines in cerebral I-R will be investigated in Chapter 6.

Leukocytes from the innate immune system (neutrophils, monocytes, NK cells), and the adaptive immune system (T and B lymphocytes), as well as leukocytes that do not fall into either category, but act to link the two (dendritic cells, natural killer T cells; NKT cells), infiltrate into the brain parenchyma and can cause ischaemic injury through the production of pro-inflammatory cytokines and chemokines, ROS and proteolytic enzymes. This can produce direct neurotoxicity, but can also increase the expression of adhesion molecules, and increase the infiltration of more leukocytes to continue the damaging cycle (For review see Huang *et al.*, 2006). In addition to leukocyte brain infiltration, there is also activation of glia. Microglia, the resident brain immune

cells, as well as astrocytes, are especially activated in the penumbra. These cells can also produce pro-inflammatory cytokines and ROS. The levels of microglial activation are higher than neutrophil or macrophage infiltration for up to 28 days after stroke (Schilling *et al.*, 2003). Gelderblom and colleagues recently completed a study investigating the time-course of resident cell activation and immune cell infiltration after cerebral I-R (see Figure 1.3). Activated microglia and macrophages were the first cells to increase in number in the ischaemic hemisphere and this was found to occur 24 h after I-R. A large infiltration of neutrophils and dendritic cells, and a smaller scale but still significant infiltration of T lymphocytes and NKT cells was observed 72 h after I-R (Gelderblom *et al.*, 2009).

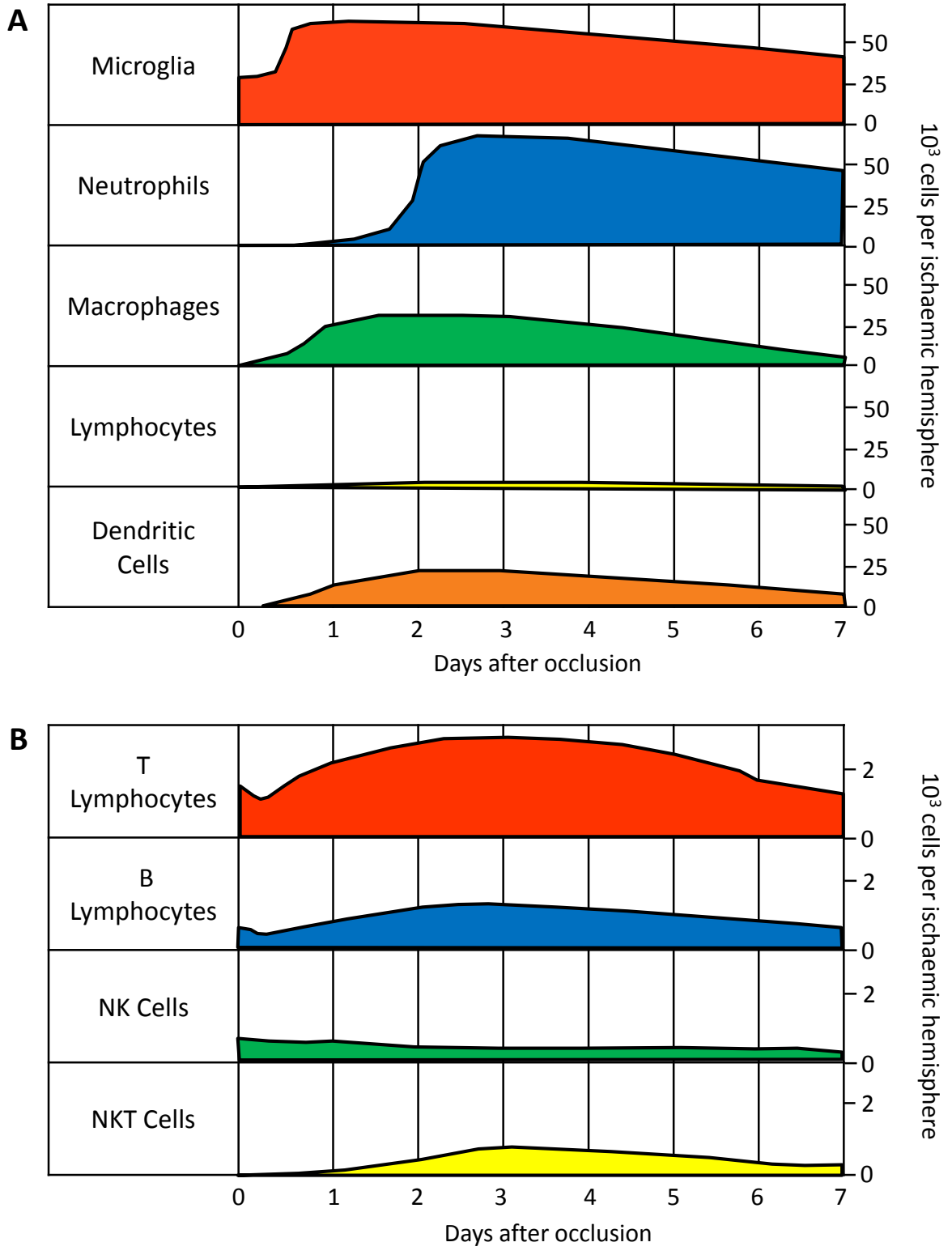

Figure 1.3. Putative immune cell infiltration after cerebral ischaemia.

A: Diagram depicting the putative time-course of immune cell brain infiltration after ischaemic stroke. **B:** Diagram depicting the putative time-course of lymphocyte subset infiltration after ischaemic stroke (Adapted from Gelderblom *et al*, 2009).

Of particular interest for this thesis, is the contribution of T lymphocytes, which are well established to be integral cells of the adaptive immune system. $CD3^+$ T lymphocytes account for 95 % of all mature T lymphocytes and these can be divided into two main subsets – the $CD4^+$ T lymphocytes (the T helper lymphocytes; T_H lymphocytes) that do not kill cells directly, but boost the capabilities of the immune system by activating and directing other cells of the immune system (Korn *et al.*, 2009; Santana and Rosenstein, 2003) and the $CD8^+$ T lymphocytes (the cytotoxic T lymphocytes) that directly kill pathogen-infected cells (Barry and Bleackley, 2002; Russell and Ley, 2002). T_H lymphocytes can be further divided into two main subsets – the T_H1 lymphocytes, which produce pro-inflammatory cytokines, such as IL-2, IFN-γ and TNF-α, and the T_H2 lymphocytes, which produce anti-inflammatory cytokines, such as IL-4 and IL-10 (Arumugam *et al.*, 2005). Another very important T_H lymphocyte subset, which accounts for ~10 % of all T_H lymphocytes, is the regulatory T cell (T_{reg}; $CD4^+CD25^+Foxp3^+$) (Zouggari *et al.*, 2009), which like T_H2 lymphocytes, reduce the pro-inflammatory response (Sakaguchi *et al.*, 2006). Stroke research with respect to immune cells has mainly focussed on neutrophils and monocytes; however, recently, a few studies have reported smaller infarct volumes in mice deficient in T lymphocytes (Hurn *et al.*, 2007; Kleinschnitz *et al.*, 2010b; Shichita *et al.*, 2009; Yilmaz *et al.*, 2006). T lymphocytes appear in the ischaemic hemisphere within 24 h after ischaemia (Jander *et al.*, 1995), and this infiltration has been reported to peak at ~72 h after I-R (Gelderblom *et al.*, 2009; Shichita *et al.*, 2009; Stevens *et al.*, 2002) (see Figure 1.3), although it is unclear which subsets are predominant. The exact mechanism(s) of T lymphocyte-mediated injury is currently unclear, however, T lymphocytes may exacerbate the inflammation occurring in the brain following stroke by releasing cytokines and chemokines that increase the expression of adhesion molecules and activate other immune cells to enter the brain, which may eventually lead to apoptosis (i.e. T_H lymphocytes) (Arumugam *et al.*, 2005). Alternatively, the action of T lymphocytes may directly cause cell necrosis as well as apoptosis via the release of cytotoxins or the activation of the Fas receptor (i.e. cytotoxic T lymphocytes) (For review see Barry and

Bleackley, 2002). Moreover, T lymphocytes were also recently reported to contain a functional Nox2-containing NADPH oxidase (Jackson *et al.*, 2004; Purushothaman and Sarin, 2009), and therefore may produce superoxide. T lymphocyte infiltration, localisation and superoxide production is investigated in male and female mice following stroke in Chapter 4, and superoxide production by the $CD3^+$, $CD4^+$ and $CD8^+$ T lymphocyte subsets after I-R will be investigated in Chapter 5.

The transcription factor NFAT (nuclear factor of activated T cells) transcribes many pro-inflammatory and pro-apoptotic genes (For reviews see Crabtree, 1999; Hogan *et al.*, 2003; Rao *et al.*, 1997). In line with the contribution of T lymphocytes to ischaemic injury, one of its major target genes is interleukin-2 (IL-2), a cytokine that helps to drive T lymphocyte proliferation (Murphy *et al.*, 2008). NF-κB is another transcription factor that transcribes a large number of cytokines, chemokines and immune-related genes (For reviews see Lee and Burckart, 1998; Pahl, 1999), and is thought to be very important in inflammation following stroke. Its activity is up-regulated after cerebral I-R (Gabriel *et al.*, 1999; Schneider *et al.*, 1999) and it contributes to cell death in stroke (Schneider *et al.*, 1999; Zhang *et al.*, 2005). An important activator of NFAT is calcineurin, which dephosphorylates and activates NFAT, and consequently activates the transcription of its target genes (Crabtree, 1999; Hogan *et al.*, 2003; Santana *et al.*, 2000). Calcineurin is also thought to activate NF-κB, through the dephosphorylation of IκB (Frantz *et al.*, 1994; Steffan *et al.*, 1995). The Down syndrome candidate region 1 (*DSCR1*) gene is an interesting endogenous calcineurin inhibitor (Rothermel *et al.*, 2000), and the role of its expression and activity in cerebral I-R will be investigated in Chapter 7.

The inflammatory cascade promotes the expression of the pro-oxidant enzymes iNOS and Cox-2. Thus, iNOS (Iadecola *et al.*, 1996; Iadecola *et al.*, 1995) and Cox-2 (Iadecola *et al.*, 1999; Miettinen *et al.*, 1997; Nogawa *et al.*, 1997; Planas *et al.*, 1995; Sairanen *et al.*, 1998) protein

expression and activity are both increased in the brain after stroke. Inflammatory cytokines can also increase NADPH-oxidase activity (Cheranov and Jaggar, 2006; De Keulenaer *et al.*, 1998; Griendling *et al.*, 1994b; Miller *et al.*, 2005), and Nox2-deficient mice were reported to have less ICAM-1 expression and less neutrophil infiltration after cerebral I-R, compared to wild-type littermates (Chen *et al.*, 2009), consistent with the established close link between Nox2 and inflammation. As mentioned in section 1.4.4 (above), these enzymes produce large amounts of NO and ROS, respectively, (as well as prostanoids), which can contribute to the continuation of the pathogenic cascade.

It was recently established that immunodepression occurs following ischaemic stroke. This is defined as the suppression of the activation or efficacy of the body's normal immune response. Although ischaemia and reperfusion initially induce a large pro-inflammatory response, these pro-inflammatory mediators in systemic and local CNS inflammation, are thought to trigger the activation of the sympathetic nervous system (SNS) and the hypothalamic-pituitary axis (HPA) producing a release of glucocorticoids and catecholamines. This produces monocyte de-activation, inhibits the production of additional pro-inflammatory mediators and causes a shift from T_H1 cell cytokine production (pro-inflammatory) to T_H2 cytokine production (anti-inflammatory (Prass *et al.*, 2003). Offner and colleagues found this shift from pro-inflammatory to anti-inflammatory cytokine release (including IL-10 and TGF-β; transforming growth factor-beta) to occur by 96 h after I-R (Offner *et al.*, 2006a; Offner *et al.*, 2006b). The release of glucocorticoids and catecholamines also cause increased apoptosis of immune cells in the spleen, thymus and lymph nodes, and as a result, these secondary lymphatic organs atrophy, and the number of circulating immune cells decrease (Haeusler *et al.*, 2008; Liesz *et al.*, 2009a; Offner *et al.*, 2006b; Prass *et al.*, 2003). T_{reg} cell levels were also increased by 96 h after I-R (Offner *et al.*, 2006b), and these cells have been reported to be neuroprotective in experimental stroke through the release of the anti-inflammatory cytokine, IL-10 (Liesz *et al.*, 2009b). As the infiltration of

immune cells contributes to ischaemic injury, the immunosuppression that occurs is believed to act as the body's protective mechanism. However, this effect substantially weakens the immune system, especially the adaptive immune system, and therefore increases the chance of infection (Prass *et al.*, 2003; Urra *et al.*, 2009). It should be noted that infection is currently the most common cause of death in the post-acute phases of stroke (Heuschmann *et al.*, 2004; Vernino *et al.*, 2003). Therefore when attempting to manipulate the immune response after stroke for therapeutic reasons, a fine balance between the inhibition of the damaging immune system with the maintenance of the infection-fighting immune system must be met.

Reperfusion produces a large influx of leukocytes that can exacerbate the inflammatory response. The leukocytes adhere to the endothelium, and either infiltrate into the brain parenchyma, or accumulate in the microvessels, leading to what is known as the "no-reflow" phenomenon, which prevents the complete restoration of cerebral blood flow (del Zoppo *et al.*, 1991). Furthermore, inflammation and oxidative and nitrosative stress, which are greater after reperfusion, activate matrix metalloproteinases (MMPs), such as MMP-9, which degrade extracellular matrix proteins, disrupting the integrity of the vascular wall, and increasing BBB permeability (Asahi *et al.*, 2000; Romanic *et al.*, 1998). This, in addition to the movement of water from the intravascular to the extravascular compartments, causes vasogenic cerebral oedema, which increases intracranial pressure (For review see Ayata and Ropper, 2002), and is a major contributor to clinical deterioration and mortality (Hacke *et al.*, 1996).

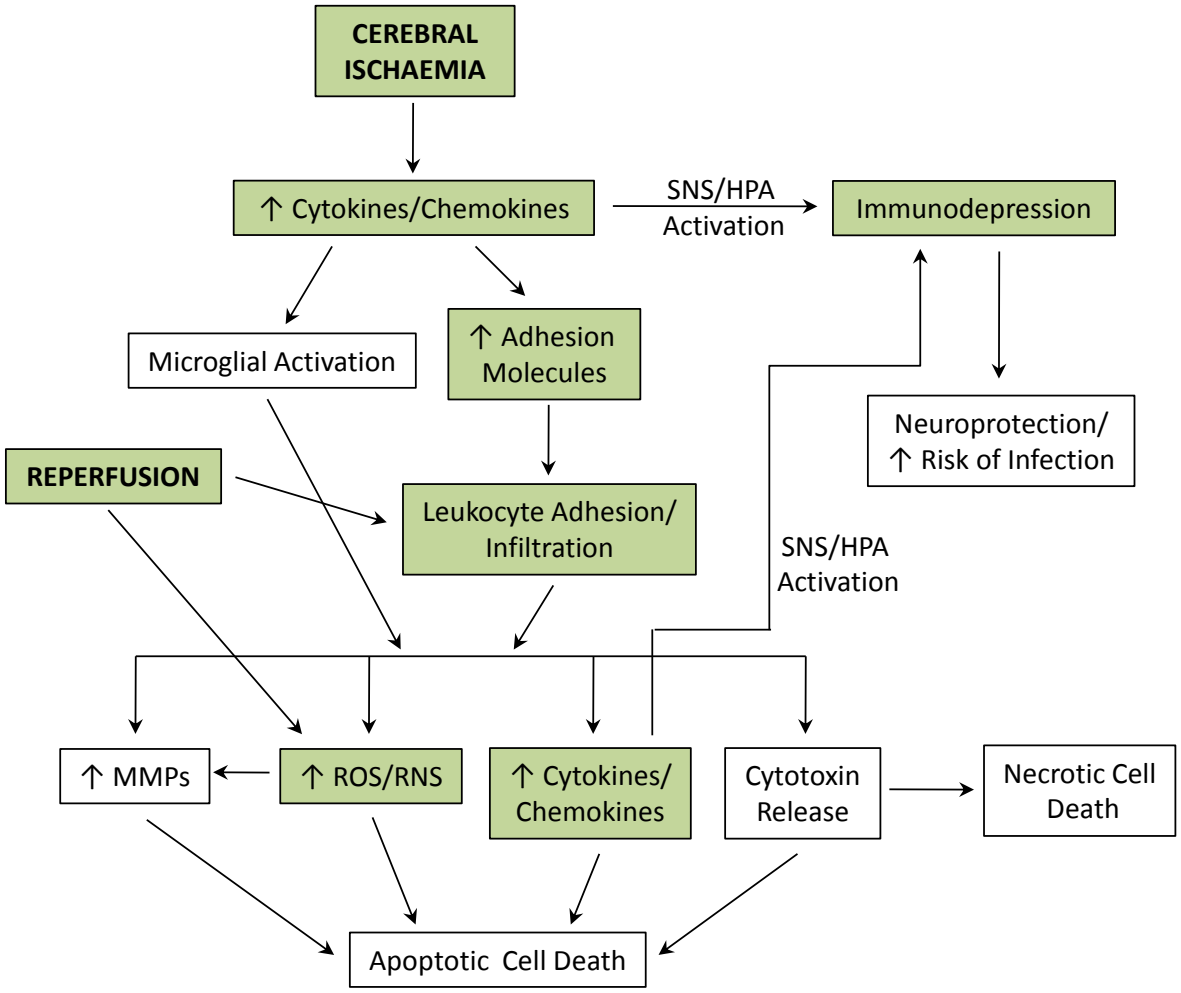

Figure 1.4. Flow chart of the inflammatory response after stroke.

The coloured boxes represent events and mechanisms that are addressed in this thesis. SNS, sympathetic nervous system; HPA, hypothalamic-pituitary axis; MMPs, matrix metalloproteinases; ROS, reactive oxygen species; RNS, reactive nitrogen species (Adapted from Wang *et al.*, 2007).

1.4.6 Apoptosis

Unlike necrotic cell death, which occurs due to irreversible cellular damage after a severe ischaemic insult, apoptosis - or programmed cell death - is a controlled physiological sequence of events that cells undergo as a type of cell suicide. Neurons undergoing apoptosis characteristically exhibit blebbing, cell body shrinkage, chromatin condensation and DNA fragmentation, and in contrast to necrosis, present no danger to their neighbouring cells as macrophages and microglia recognise and phagocytose apoptotic neurons (For reviews see

Lipton, 1999; Mattson *et al.*, 2000). Cell death via apoptosis is induced preferentially to necrosis, when ischaemic injury is mild. Due to the collateral blood flow in the penumbra, this region sustains a milder injury than the core, and consequently, if the cells ultimately die, it is apoptotic cell death that predominates. Apoptosis begins hours after ischaemia (see Figure 1.2), and Li and colleagues previously reported that signs of apoptosis persisted for at least 4 weeks after cerebral I-R (Li *et al.*, 1995). Both the intrinsic (mitochondria-dependent pathway induced by high levels of glutamate, intracellular Ca^{2+}, ROS and DNA damage) and the extrinsic ("death receptor pathway" via the activation of the FAS and TNF receptors, induced by inflammation) apoptotic pathways operate after ischaemia in neurons (For review see Broughton *et al.*, 2009).

1.5 Lack of success for clinical neuroprotective drugs

In the late 1980's, the first experimental studies to test neuroprotective drugs aimed at rescuing ischaemic tissue were published. Since then, there have been more than 1800 experimental studies and 600 clinical trials published (PubMed, 2010). However, although these clinical trials originated from experimental studies that reported protection in models of ischaemic stroke, all except the thrombolytic, rt-PA, have failed. This can be attributed to a number of reasons. The first of these is the design and quality of the experimental studies the clinical trials were based on - there is a considerable lack of randomisation, blinding and clear exclusion criteria in experimental stroke studies (van der Worp *et al.*, 2005). Secondly, the experimental studies that some of the clinical trials were based on only showed weak evidence overall that the drug in question was actually neuroprotective, and thus were probably not well justified without more compelling rationale. Thirdly, there are large discrepancies between the general protocols of experimental studies and clinical trials. These include the timing of drug administration (administration is usually before or just after ischaemia in animal trials, but many hours after the onset of ischaemia in clinical trials), the greater reliance on the reduction of infarct volume in the animal studies versus improvement in functional tests in the clinic, and the greater reliance on

early outcomes in experimental studies versus late assessments in clinical trials (For reviews see Cheng *et al.*, 2004; Ginsberg, 2009; Gladstone *et al.*, 2002). Lastly, the majority of drugs tested in clinical trials to date have targeted early metabolic events in cerebral ischaemia, especially excitotoxic mechanisms, such as the use of glutamate receptor (NMDA or AMPA) antagonists or GABA (gamma-aminobutyric acid) agonists (For reviews see Ginsberg, 2008; Gladstone *et al.*, 2002; Jain, 2000). It makes sense to inhibit one of the earliest steps in the cascade, as it triggers the other pathogenic events, however, because excitotoxicity occurs immediately after stroke, attempted inhibition of these mechanisms a few hours after clinical stroke onset (when the majority of patients get to the hospital) may not be able to realistically rescue any brain tissue as the excitotoxic processes will have already peaked, and the pathogenic cascade already progressed too far for the inhibition to have a protective effect. Inflammation occurs at a later time-point in the pathogenic cascade, and lasts for up to a few weeks (see Figure 1.2), mainly inducing apoptotic cell death. Furthermore, the expression of many cytokines, chemokines and adhesion molecules, as well as the infiltration of immune cells, reach peak levels in the brain between 6 and 72 h after the ischaemic insult (For review see Nilupul Perera *et al.*, 2006). Therefore, inflammatory processes occur at a more reasonable time-frame for therapeutic intervention.

At present, combination therapies are believed to be the best way forward for successful neuroprotection after ischaemic stroke. There is a special interest in therapies that use neuroprotectants in combination with rt-PA (For reviews see Gladstone *et al.*, 2002; Rogalewski *et al.*, 2006), and although rt-PA is not able to be used in the majority of patients due to time limitations and the large number of exclusion criteria, it is the best (and only) current treatment for ischaemic stroke. Furthermore, with new technologies (Alexandrov *et al.*, 2004; Smith *et al.*, 2008; Tsivgoulis *et al.*, 2010) and media campaigns to educate people of the signs of stroke so that they can get to hospital earlier (Davis *et al.*, 2007), the number of patients administered rt-PA, and the number of successful recanalisations and reperfusions are slowly increasing. It also seems

sensible to first restore cerebral blood flow and then try to protect remaining vulnerable tissue. After recanalisation by rt-PA, reperfusion injury, which is mainly caused by inflammatory and oxidative mechanisms, causes a large amount of tissue damage, resulting in cell death. Therefore, the co-administration of anti-inflammatory treatments alongside rt-PA may potentially salvage at risk brain tissue (the penumbra), as well as perhaps increasing the time-window for safe rt-PA administration. There have been several studies in which experimental animals were co-administered rt-PA and anti-inflammatory drugs, specifically anti-leukocytic adhesion molecules, that demonstrated an increased therapeutic efficacy, as well as an increase in the time window of its administration (Bowes *et al.*, 1995; Zhang *et al.*, 2003; Zhang *et al.*, 1999). Furthermore, although not designed to test the effect of UK-279,276, a CD11b/CD18 inhibitor, as an adjuvant with rt-PA, a clinical trial reported neurological improvements in the small powered subgroup where both drugs were administered together (Sughrue *et al.*, 2004). These studies show potential for this type of synergistic therapy, and thus, in Chapter 6 we investigate chemokine-related targets in the brain after stroke and examine the efficacy of administering a CXCR2 antagonist at the time of reperfusion.

1.6 Thesis aims

The aims of this thesis focus on the contribution of the inflammatory response to ischaemic injury following cerebral I-R. Specifically, the aims of this thesis were:

1. a) To examine the effects of gender and reperfusion on outcome following ischaemic stroke (Chapter 3).

   b) To examine the effect of Nox2-deficiency on outcome following cerebral I-R in male and female mice (Chapter 3).

2. a) To investigate whether gender has an effect on the expression of key pro-inflammatory proteins, and the infiltration and localisation of T lymphocytes and Nox2 protein in brain (Chapter 4).

   b) To test the effect of gender, ischaemia and reperfusion on the levels of various immune cells in the spleen and the blood (Chapter 4).

   c) To assess the effect of gender and I-R on proliferation of T lymphocytes (Chapter 4).

   d) To test whether T lymphocytes generate Nox2-derived superoxide, and if so, to test whether this is altered after I-R in males and/or females (Chapter 4).

3. To investigate which subset(s) of $CD3^+$ T lymphocytes might be involved in the increased superoxide production 24 h after I-R (Chapter 5).

4. a) To examine the brain mRNA expression profiles of a large number of chemokines, chemokine receptors and immune-related genes 4, 24 and 72 h after cerebral I-R (Chapter 6).

   b) To identify a family of chemokines that are increased following cerebral I-R, and to examine the effect of pharmacologically targeting them on outcome following cerebral I-R (Chapter 6).

5. a) To examine the effect and the possible underlying mechanisms of *DSCR1* over-expression on outcome following cerebral I-R (Chapter 7).

   b) To examine the effect of *DSCR1*-deficiency on outcome following cerebral I-R (Chapter 7).

Chapter 2:

General Methods

2.1 Ethics Approval

All experimental procedures were approved by the Monash University School of Biological Sciences B Animals Ethics Committee.

2.2 Total Animals Studied

In total, 511 mice were used. These comprised 391 C57Bl6/J mice (280 male and 111 female), 26 Nox2-deficient mice ($Nox2^{-/-}$; 15 male and 11 female); 39 male *DSCR1* transgenic mice and 39 *DSCR1* wild-type littermate (Wt_{Tg}) mice; and 11 male *DSCR1* knock-out (KO) mice and 5 *DSCR1* wild-type littermate (Wt_{KO}) mice.

2.3 Focal Cerebral Ischaemia in Mice

Focal cerebral ischaemia was induced by either transient (30 min) or permanent intraluminal filament occlusion of the right middle cerebral artery (MCA). Mice were anaesthetised with a mixture of ketamine (80 mg/kg, i.p.) and xylazine (10 mg/kg, i.p.). Rectal temperature was monitored throughout the procedure and until animals regained consciousness. Temperature was maintained at 37.5 ± 0.5 °C via an electronic temperature controller (Digitemp EX1310TC, Extech Equipment Pty. Ltd.; Boronia, VIC, Australia) linked to a ceramic heat lamp (100W PT-2046, Exo Terra, Australian Reptiles Pty. Ltd.; Hoppers Crossing, VIC, Australia). Regional cerebral blood flow (rCBF) in the area of cerebral cortex supplied by the MCA (~2 mm posterior and ~5 mm lateral to bregma) was monitored and recorded, beginning at the start of surgery, which typically lasted 15-20 min and continued for 1 h after the induction of ischaemia, using trans-cranial laser-Doppler flowmetry (PF5010 LDPM Unit, Perimed; Järfälla, Sweden). Under a dissecting microscope (MZ6, Leica Microsystems; Wetzlar, Germany), the right carotid bifurcation was exposed through a ventral midline neck incision and was carefully dissected free from surrounding connective tissue. A branch of the external carotid artery (ECA) was cauterised with an Aaron low temperature fine tipped hot wire cautery (Bovie Medical

Corporation; Clearwater, FL, USA), and the ECA was ligated with 6-0 silk suture (Dynek Pty Ltd; Hendon, SA, Australia) distal to the bifurcation of the common carotid artery (CCA) and cut, forming an ECA stump. The CCA and internal carotid artery (ICA) were carefully separated from the adjacent vagus nerve, and a suture bridge was placed underneath the ICA. The CCA was then clamped and tension was applied to the ICA via the suture bridge, to prevent bleeding. A small nick was made in the ECA stump, and a 6-0 nylon monofilament with silicone-coated tip (Doccol Co., Redlands, CA, USA) was inserted and advanced distally along the ICA (11-12 mm distal to the carotid bifurcation), causing occlusion of the MCA at its junction with the circle of Willis. Severe (~80 %) reduction in rCBF in the MCA territory, measured by a real time trans-cranial laser-Doppler, confirmed accurate placement of the filament. This filament was then tied in place, the CCA clamp removed and the suture bridge released.

In the protocol for transient ischaemia (ie. ischaemia-reperfusion; I-R), occlusion was maintained for 30 min, and the monofilament was then retracted to allow reperfusion for 3.5, 5.5, 23.5 or 71.5 h. Reperfusion was confirmed by an immediate increase in rCBF, which reached the pre-ischaemic level within 5 min. In the protocol for permanent ischaemia (i.e. ischaemia with no reperfusion; I-NR), the monofilament was kept in place and the occlusion maintained for 24 h. Sham-operated mice were anaesthetised and the right carotid bifurcation was exposed and dissected free from surrounding connective tissue, but no arterial ligation was made or filament was inserted. The neck and head wounds were then closed using 5-0 nylon suture (Dynek Pty Ltd), covered with betadine and OpSite spray dressing (Smith & Nephew; Mount Waverley, VIC, Australia), and when the mice regained consciousness they were returned to their cages.

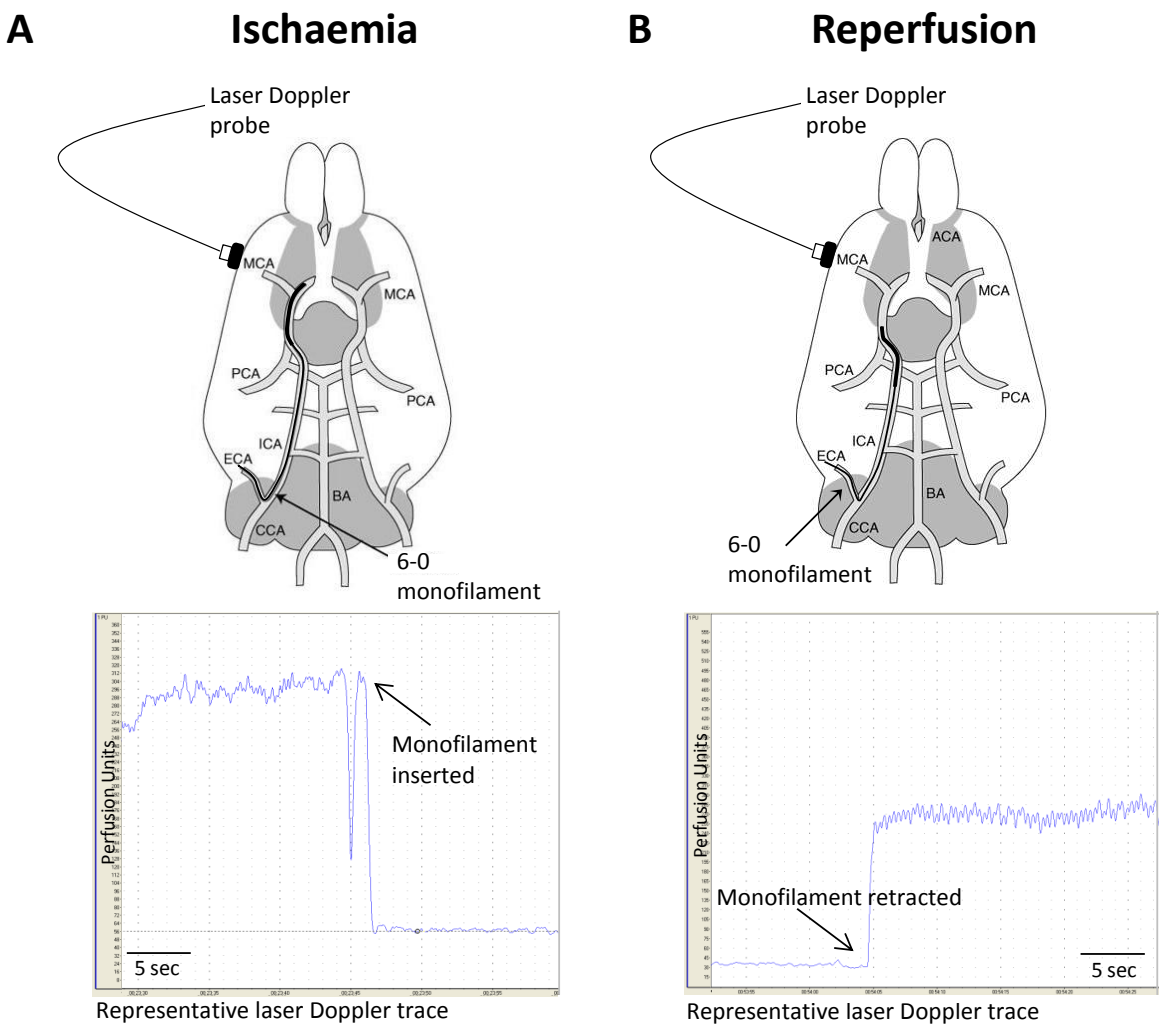

Figure 2.1. Occlusion of the MCA.

A. Upon insertion of the silicone-coated monofilament, the MCA is occluded, causing a sudden drop in cerebral blood flow measured using trans-cranial laser Doppler flowmetry in the territory of the MCA, as depicted in the representative laser Doppler trace. **B.** Following the ischaemic period (0.5 h) in the protocol for transient cerebral ischaemia (I-R), the filament is retracted, inducing reperfusion, as illustrated by the representative laser Doppler flow trace. In the case of permanent cerebral ischaemia (I-NR), 'A' is maintained for the entire 24 h, and 'B' does not occur (Adapted from O'Neill and Clemens, 2000). MCA, middle cerebral artery; CCA, common carotid artery; ECA, external carotid artery; ICA, internal carotid artery; PCA, posterior communicating artery; BA, basilar artery.

2.4 Evaluation of Neurological Function

At the end of the experiment (either 24 or 72 h), neurological assessment was performed using a five-point scoring system commonly used in mice to test neurological impairment after cerebral ischaemia (Iadecola *et al.*, 1997). The specific scoring system we used (0 to 4), was originally based on Bederson and colleagues, and Yang and colleagues (Bederson *et al.*, 1986; Yang *et al.*, 1994), and was modified by Iadecola and colleagues (Iadecola *et al.*, 1997). For studies conducted in chapters 3 and 7, mice were assigned a score from 0 to 4 according to the following criteria: 0, normal motor function; 1, flexion of torso and contralateral forelimb exclusively to the contralateral side when mouse is lifted by the tail; 2, circling to contralateral side when mouse is held by the tail on a flat surface, but normal posture at rest; 3, leaning to contralateral side at rest; 4, no spontaneous motor activity. Mice that were rolling uncontrollably in their cages were also assigned a score of 4. Neurological assessment was performed by an investigator blinded to the experimental treatment. For chapter 6 (the final study of my PhD, chronologically speaking), we amended the five-point scoring system, due to the fact that >90 % of all the mice following stroke – whether male or female, and whether or not reperfusion was instituted - were assigned a score of either 3 or 4, which did not correlate with the differences found in their infarct volumes. After personal communication with a colleague from Dr. Iadecola's laboratory in New York, we modified the criteria to: 0, normal motor function; 1, flexion of torso and forelimb to either side when mouse is lifted by the tail; 2, circling to either side when mouse is held by the tail on a flat surface, but normal posture at rest; 3, leaning to either side at rest; 4, no spontaneous motor activity. The most important amendment was that the tests were carried out sequentially; and if a mouse exhibited the appropriate behaviour at one step but not at the following step, it was assigned the score of the former step. However, this was not the case when assigning a score of 4, as a score of 4 indicates that the mice were unable to move, and therefore were unable to exhibit the appropriate behaviour for scores 1 or 2.

At the end of the experiment (either 24 or 72 h), the hanging wire test was also performed to test their motor function, gripping ability and forelimb strength (Hattori *et al.*, 2000). Mice were placed so that their front paws were gripping onto a wire (~1 mm diameter, tied horizontally between two poles 60 cm apart, elevated 30 cm above a padded surface). The length of time suspended from the wire, up to a maximum of 60 seconds was noted, and the average time of 3 trials with 5-min rests in between, was recorded.

2.5 Evaluation of Cerebral Infarct and Oedema Volume

Mice were killed at 24 or 72 h by inhalation of CO_2 and O_2 (80:20), followed by decapitation. The brains were immediately removed, snap frozen with liquid nitrogen and stored at -80 °C. Using a cryostat (-21 °C, CM1850, Leica Microsystems; Wetzlar, Germany), evenly spread (separated by ~420 μm) coronal sections (30 μm thick) were obtained spanning the infarct, (which equated to ~15 sections/brain following I-R, and ~20 sections/brain following I-NR). These sections were then thaw-mounted onto poly-L-lysine coated glass slides (0.1 % poly-L-lysine in distilled water; dH_2O). To delineate the infarct, sections were immersed in thionin (0.1 %; 2 min), dipped a few times into two separate containers of dH_2O to rinse off the excess thionin, then immersed in 70 % ethanol (EtOH; 2 min), followed by 100 % EtOH (2 min). Slides were then dried, dipped in xylene and cover-slipped with DPX mounting media. Images of the sections were captured with a CCD camera (Cohu Inc., San Diego, CA, USA) mounted above a light box (Biotec-Fischer Colour Control 5000, Reiskirchin, Germany). Total infarct volume was quantified using image analysis software (ImageJ, NIH; Bethesda, MD, USA), correcting for brain oedema, according to the following formula: CIV = [LHA – (RHA – RIA)] X (thickness of section + distance between sections); in which CIV is corrected infarct volume, LHA is left hemisphere area, RHA is right hemisphere area and RIA is right hemisphere infarct area (Tsuchiya *et al.*, 2003; Xia *et al.*, 2006). Oedema volume was calculated using the following formula: [RHA – LHA] X (thickness of section + distance between sections). Similarly, cortical

infarct volume was quantified, correcting for brain oedema, according to the following formula: CCIV = [LCA – (RCA – RCIA)] X (thickness of section + distance between sections); in which CCIV is corrected cortical infarct volume, LCA is left cortical area, RCA is right cortical area and RCIA is right cortical infarct area. Subcortical infarct volume (CSIV) was calculated by subtracting oedema-corrected cortical infarct volume (CCIV) from oedema-corrected total infarct volume (CIV). Oedema-corrected infarct volumes of individual brain sections were then added giving a three-dimensional approximation of the total (ΣCIV), cortical (ΣCCIV) or subcortical infarct volume (ΣCSIV).

In order to be sure to correct for variations in apparent brain size (eg. due to strain or gender differences, or the fixing and processing of the sections), we also estimated infarct volume as a percentage of the hemisphere using the non-ischaemic hemisphere as a reference volume. This was calculated according to the following formulas: (ΣCIV/Σ[LHA X (thickness of section + distance between sections)]) X 100, for total infarct volume, and (ΣCCIV/Σ[LCA X (thickness of section + distance between sections)]) X 100, for cortical infarct volume; in which Σ[LHA X (thickness of section + distance between sections)] is the sum of [LHA X (thickness of section + distance between sections)] of all the individual sections, to get an approximation of the left hemisphere volume (ΣLHV), and Σ[LCA X (thickness of section + distance between sections)] is the sum of [LCA X (thickness of section + distance between sections)] of all the individual sections, to get an approximation of the left cortical volume (ΣLCV). Subcortical infarct volume was calculated according to the following formula: [ΣCSIV/(ΣLHV – ΣLCV)] X 100.

Longitudinal distribution of the infarct area was also calculated. Using the same coronal sections taken for infarct evaluation, with a mouse brain atlas (Paxinos and Franklin, 2001) as a guide to the brain structures at certain stereotaxic coordinates, a coronal section was assigned the position of bregma +1.6 mm. The CIA (oedema-corrected infarct area; LHA – [RHA – RIA]) previously

calculated was noted down for this coordinate, as were the CIAs for every section ~840 μm from that point, spanning the entire infarct. If the infarct began at a more rostral point to bregma +1.6 mm, the CIA of brain sections ~840 μm earlier were also recorded. The same process was also performed for cortical infarct distribution, using CCIA (oedema-corrected cortical infarct area; LCA – [RCA – RCIA]) instead of CIA, and subcortical infarct distribution was calculated by subtracting the CCIA at each coordinate from the CIA.

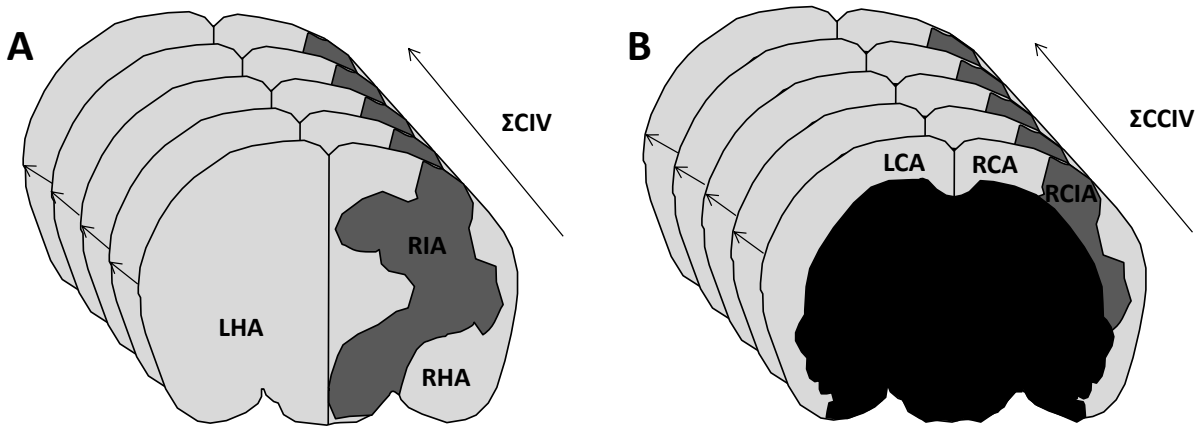

Figure 2.2. Quantification of infarct volume.
Cartoon depicting areas measured for quantification of oedema-corrected (**A**) total and (**B**) cortical infarct volume. LHA, left hemisphere area; RHA, right hemisphere area; RIA, right infarct area; LCA, left cortical area; RCA, right cortical area; RCIA, right cortical infarct area. Each small arrow represents the 'thickness of section + distance between sections'.

2.6 Tail cuffing

Systolic blood pressure (BP) was measured in some mice prior to MCAO via tail cuffing, using a MC4000 Blood Pressure Analysis System (Hatteras Instruments; Cary, NC, USA). The mice were placed into the individual dark chambers on the preheated platform. The tail of each mouse was inserted into a tail cuff, placed into a tail slot in the device and secured with a piece of masking tape. The tail cuff was then positioned so that it was directly touching the rump of the mouse. The mouse tail cover was then placed over the tail slot. The day before the actual

experimental measurements were taken, each mouse was placed into the MC4000 Blood Pressure Analysis System to undergo 15 preliminary cycles, for the mouse to become accustomed to the process, to reduce their anxiety levels the following day. On the experimental day, the mice firstly underwent 5 preliminary cycles, for which data was not recorded. This allowed the mouse time to become accustomed to the chamber and to having the tail cuff inflate and deflate around its tail, and also time to warm up which improves blood flow to the tail. Following the preliminary cycles, 30 measurement cycles were completed. Measurements taken from cycles lacking the ideal profile were rejected (eg. if the mouse was moving and the pulse wasn't consistent or if no pulse could be detected), and the average of the systolic BP measurements of the remaining successful cycles was used. For each individual mouse we collected a minimum of 15 successful measurement cycles. If this could not be achieved, the mouse was re-positioned, and the above procedure was repeated. In order to enhance the reliability and reproducibility of the BP measurements, the room in which the measurements were performed was kept quiet with no loud talking or noise.

2.7 Western Blotting

In separate mice, the expressions of various proteins were measured in homogenates of the ischaemic (right) or non-ischaemic (left) brain hemisphere using Western blotting. Mice were killed and brains removed and frozen as for 'Evaluation of Cerebral Infarct and Oedema Volume' (see section 2.5 above). Brains were cut into hemispheres, and the ischaemic and non-ischaemic hemispheres were homogenised over liquid nitrogen and prepared in 4 ml Laemmli buffer (25 % Glycerin, 12.5 % β-mercaptoethanol, 7.5 % sodium docedyl sulfate, 25 % 1 M TrisHCl pH 8.0, 0.25 mg/ml bromophenol blue). Homogenates were sonicated on ice, heated (37 °C; 10 min) and then centrifuged (15,700 g; 10 min at 4 °C). 5 µl of the sample was taken to determine the protein concentration, and the remainder was stored at -80 °C. Protein concentration was determined using the RCDC protein assay (Bio-Rad; Hercules, CA, USA), as

per the manufacturer's instructions. Absorbance of each well was then read using a Spectra Max 340 spectrophotometer (Molecular Devices; Sunnyvale, CA, USA) set at 720 nm and analysed with SOFTmax PRO software (Version 1.2.0, Molecular Devices).

Equal quantities of protein, along with a dual colour molecular weight marker (Bio-Rad) were loaded onto 1 mm thick polyacrylamide gels and mounted in a mini PROTEAN® 3 cells (Bio-Rad). Voltage was set at 60 V for migration of protein through the upper gel and raised to 100 V for migration through the lower gel.

Once the proteins had migrated the desired distance according to the molecular weight marker, gel tanks were disassembled and gels were carefully removed from glass plates and placed in buffer 2 (25 mM Tris, 20 % MeOH, 80 % dH_2O; pH 7.4) on a shaker for 10 min. Polyvinylidene Fluoride (PVDF) membranes were then placed in methanol (MeOH) for 10 sec, rinsed with dH_2O for 5 min followed by a further rinse with buffer 2 for 10 min. Two pieces of Whatmans blotting paper (GE Healthcare; Waukesha, WI, USA) were soaked in buffer 1 (300 mM Tris, 20 % MeOH, 80 % dH_2O; pH 10.4), one piece in buffer 2 and two pieces in buffer 3 (38 mM Tris, 20 % MeOH, 80 % dH_2O; pH 10.4). Blotting paper, PVDF membrane and gel were arranged in a TE 77 Semi Dry Transfer Unit (Amersham Biosciences; Waukesha, WI, USA) as shown in Figure 2.3. The proteins were then transferred by the semi dry transfer method (0.4 mA per cm^2 of gel for 70 min at room temperature). Successful protein transfer was confirmed by Ponceau S staining before washing a few times with tris-buffered saline containing 0.1 % Tween 20 (TBS-T; 20 mM Tris, 15 mM NaCl, 0.1 % Tween 20; pH 7.5).

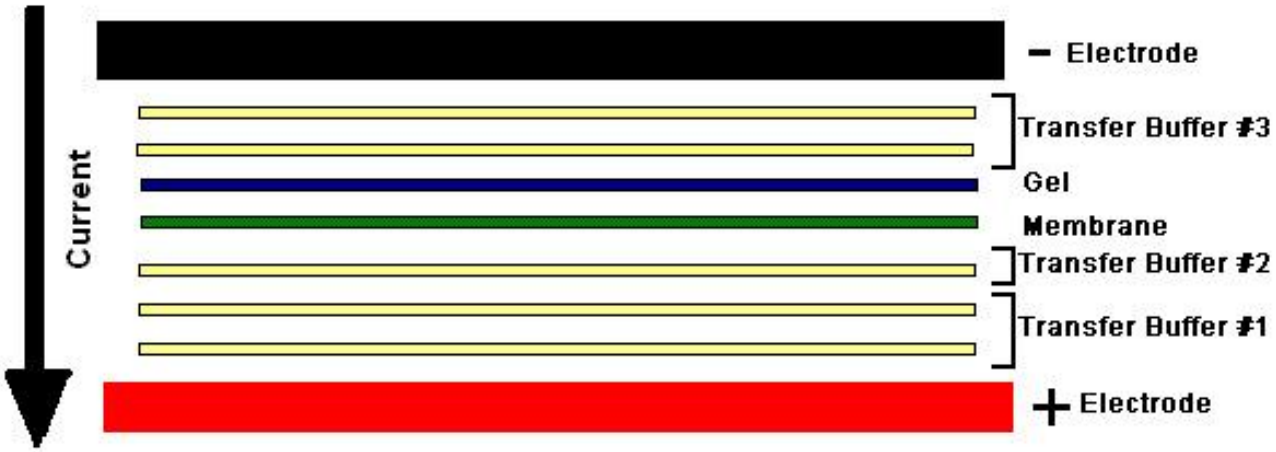

Figure 2.3. Arrangement of blotting paper, PVDF membrane and gel in the TE 77 Semi Dry Transfer Unit.

Membranes were blocked in 5 % skim milk dissolved in TBS-T for 1 h (room temperature) to reduce non-specific binding of antibodies, and were then incubated overnight (4 °C) with the appropriate primary antibody in 5 % skim milk in TBS-T with constant gentle agitation, followed by three 15 min washes with TBS-T. Following washes, membranes were incubated with a horseradish peroxidase (HRP)–conjugated secondary antibody made up in 5 % skim milk with TBS-T for 1 h (room temperature) with constant gentle agitation followed by three 15 min washes with TBS-T.

Immunoreactive bands were detected by enhanced chemiluminescence. The membrane was saturated in Immobilon Western Chemiluminescence HRP substrate ECL reagent (Millipore; Billerica, MA, USA). The membrane was wrapped in a plastic pocket and placed into a hyper-cassette. In a dark room, photographic paper (Fujifilm SuperRx, Fujifilm; Tokyo, Japan) was placed over the membrane and exposed for 1-30 min depending on the antibody used. The film was then developed with an AGFA CP1000 processor (AGFA; Mortsel, Belgium) and quantified using a ChemiDoc XRS molecular imager (Bio-Rad). Relative intensities were normalised to the intensity of corresponding bands for β-actin.

2.8 Real-time PCR

In separate mice, the mRNA expression of various genes was measured in homogenates of the ischaemic (right) or non-ischaemic (left) brain hemisphere using quantitative PCR. Mice were killed and brains removed and frozen as for 'Evaluation of Cerebral Infarct and Oedema Volume' (see section 2.5 above). RNA was extracted from each brain hemisphere using the Qiagen RNeasy Mini Kit and the Qiagen RNase-free DNase Kit (Qiagen; Hilden, Germany). Briefly, brains were cut into hemispheres, and the ischaemic and non-ischaemic hemispheres were homogenised over liquid nitrogen until ground into a fine powder. The RLT buffer from the kit was then added to the samples (2.5 ml RLT buffer with 0.01 % β-mercaptoethanol per sample). Homogenates were sonicated and then centrifuged (18,400 g; 3 min at room temperature). The pellet was discarded, and 700 µl of the supernatant (lysate) was transferred to a 1.5 ml eppendorf tube. The remainder of the lysate was kept in the -80 °C freezer to make up more RNA if needed. 700 µl of 70 % EtOH was added to the eppendorf tube and mixed. 700 µl of the sample was then transferred to an RNeasy spin column and centrifuged (9,400 g; 15 s at room temperature). The flow-through from the collection tube was then discarded. 350 µl of Buffer RW1 (wash buffer) was added to the RNeasy spin column and centrifuged (9,400 g; 15 s at room temperature), and then the flow-through was discarded. Next, 10 µl of DNase stock solution was mixed with 70 µl of Buffer RDD (DNase digestion buffer) per sample, and added directly to the RNeasy spin column membrane and incubated (15 min at room temperature). 350 µl of Buffer RW1 was then added to the RNeasy spin column. It was centrifuged (9,400 g; 15 s at room temperature) and the flow-through was discarded. Next, 500 µl of Buffer RPE (concentrated wash buffer) was added to the RNeasy spin column and centrifuged (9,400 g; 15 s at room temperature) and the flow-through was discarded. Another 500 µl of Buffer RPE was then added to the RNeasy spin column and centrifuged (9,400 g; 2 min at room temperature) and the flow-through was discarded. The RNeasy spin column was then placed into a new 2 ml collection tube and centrifuged (18,400 g; 1 min at room temperature) to eliminate possible

carryover of Buffer RPE or any remaining residual flow-through on the outside of the spin column. The collection tube and the flow-through were then discarded. Next, the RNeasy spin column was placed into an Eppendorf tube and 30 µl of RNase free water was added directly onto the spin column membrane. It was then centrifuged (9,400 g; 1 min at room temperature) to elute the RNA, and the spin column was discarded. RNA was measured at 260 nm using the NanoDrop™ 1000 spectrophotometer (Thermo Scientific; Wilmington, DE, USA) and was then stored at -80 °C until ready for use.

RNA was converted into cDNA using various kits. The mRNA expression of a range of mouse immune genes, including cytokines and chemokines, were measured using either a PCR array from SABiosciences (Frederick, MD, USA) or Applied Biosystems (Carlsbad, CA, USA), or specific gene expression assays (Applied Biosystems).

To carry out the real-time PCR, the PCR mixture was prepared, added to the 96-well plate and then placed into a real-time PCR system. The real-time PCR was then run for 40 cycles, using the appropriate thermal-cycling parameters.

To analyse the real-time PCR data for both the PCR array and the gene expression assays, the relative expressions of each target gene were normalised to the house-keeping gene, and then further normalised to a control sample. This was calculated according to the following formula: $2^{-\Delta\Delta CT}$; in which CT is the cycle threshold, ΔCT is CT (target gene) – CT (house-keeping gene), and ΔΔCT = ΔCT (treatment sample) – ΔCT (average of control sample).

2.9 Immunohistochemistry and Immunofluorescence

The cellular localisation of various proteins in brain sections was performed by immunohistochemistry or immunofluorescence. Separate mice were killed and brains removed

and frozen as for 'Evaluation of Cerebral Infarct and Oedema Volume' (see section 2.5 above). Multiple serial coronal sections of 30 μm were taken throughout the forebrain, and thaw-mounted onto poly-L-lysine coated glass slides (0.1 % poly-L-lysine in dH_2O). Tissue sections were fixed in acetone (immunohistochemistry) or 4 % paraformaldehyde (PFA; immunofluorescence), washed in tris-buffered saline (TBS; 50 mM Tris base, 154 mM NaCl; pH 8.4; for immunohistochemistry) or 10 mM phosphate buffered saline (PBS; 5 mM Na_2HPO_4, 154 mM NaCl, 5 mM $NaH_2PO_4.2H_2O$; pH 7.4; for immunofluorescence) and then incubated in a mixture of primary antibodies overnight in a humid chamber. The following day, tissues were washed in TBS or PBS (for immunohistochemistry and immunofluorescence, respectively) and incubated with the appropriate secondary antibodies in a humid chamber. Slides were washed in TBS or PBS (for immunohistochemistry and immunofluorescence, respectively), mounted in mounting medium and cover-slipped. Staining was then viewed and photographed on an Olympus light microscope (Olympus; Hamburg, Germany; for immunohistochemistry) or a fluorescent microscope (Olympus; for immunofluorescence), and analysed. All appropriate control experiments were performed.

2.10 Isolation of Leukocytes from Blood and Spleen

Mice were killed at 24 h following sham or stroke surgery by isoflurane inhalation and exsanguination. A midline abdominal incision (from the base of the ribs to the bladder) was made, the organs were retracted, and blood was withdrawn from the inferior vena cava into a 1 ml syringe containing 0.1 ml Clexane (400 U/ml), and transferred to an eppendorf tube. The spleen was then removed, and placed in media (RPMI 1640 + 5 % foetal calf serum; FCS) if the leukocytes were being used in 'Fluorescence Activated Cell Sorting (FACS) Analysis' (see section 2.11 below) or PBS + 4 % FCS if they were being used for the 'Measurement of Superoxide Production by T Lymphocytes' (see section 2.13 below). Single cell suspensions of the spleen cells were prepared either by passing the tissue through a 75 μm nylon cell strainer or by gently

rubbing the spleen between two rough slides in a circular motion. The cells from both blood and spleen were washed in media by centrifugation (1000 g for 5 min, 4 °C), and red cells were lysed with red cell lysis buffer (155.17 mM NH_4Cl, 9.99 mM $KHCO_3$, 0.24 mM EDTA, filter sterilised in distilled H_2O; 2 x 5 min, 37 °C) with a wash in media in between and afterwards (1000 g for 5 min, 4 °C) to stop the lysis reaction and rid the sample of lysed red cells. The cells were then resuspended in FACS wash buffer (PBS + 2 % FCS) for the 'Fluorescence Activated Cell Sorting (FACS) Analysis' or PBS + 4 % FCS if they were being used for the 'Measurement of Superoxide Production by T Lymphocytes', and counted using a haemocytometer, with trypan blue dye, whereby lymphocytes appeared small and round with a white halo, and dead cells, which were excluded from the count, appeared dark blue.

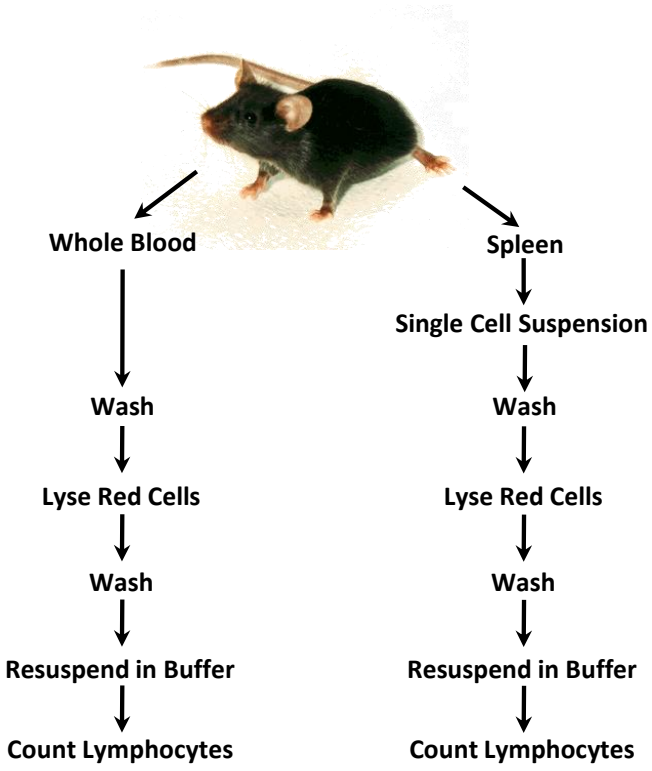

Figure 2.4. Isolation of leukocytes from blood and spleen.

Flow diagram showing the steps involved in the isolation of leukocytes from the blood and spleen.

2.11 Fluorescence Activated Cell Sorting (FACS) Analysis

Fluorescence flow cytometric analyses were performed to determine the numbers of various immune cells in the blood and/or spleen. Cells (~$1x10^6$) were first incubated on ice for 10 min in 100 µl of staining buffer (PBS containing 1 % normal mouse serum, 5 % FCS and 0.001 % rat anti-mouse CD16/CD32, FC receptor block; BD Biosciences; North Ryde, NSW, Australia). This was to allow the antibody time to bind, and reduce FC receptor-mediated non-specific binding. The cells were then centrifuged (1000 g for 5 min, 4 °C) and the supernatant discarded. Next, the cells were labelled for cytofluorimetry by resuspending in 100 µl of staining buffer containing optimal dilutions of the appropriate primary antibodies conjugated with varying fluorophores. The samples were vortexed and then left at room temperature for at least 30 min. Cells were washed, by the addition of ~1 ml FACS wash buffer, vortexed, and centrifuged (1000 g for 5 min, 4 °C), and the supernatant discarded. This was repeated three times, and after the final wash, the cells were resuspended in 300 µl of PBS. Flow cytometry was performed using a BD FACS Canto II flow cytometer and CELLQuest 8.0 software (BD Biosciences). Forward height and forward area parameters were used to identify and separate single-cells from duplicates. Forward and side scatter parameters were chosen to identify lymphocytes and granulocytes. For each experiment, cells were stained with appropriate isotype control antibodies to establish background staining and to set quadrants before calculating the percentage of positive cells. In addition, there were single stained controls and an unstained control to use for compensation. Data were analysed using FlowJo (V8.8.2, Tree Star, Inc.; Ashland, OR, USA).

2.12 Isolation of T Lymphocytes (Dynal negative isolation kits)

After the 'Isolation of Leukocytes from Blood and Spleen' (see section 2.10 above), a purified suspension of $CD3^+$, $CD4^+$ or $CD8^+$ T lymphocytes was obtained using either the Dynal® Mouse T Cell Negative Isolation Kit, the Dynabeads® FlowComp™ Mouse $CD4^+CD25^+$ T_{reg} Cells Kit, or the Dynal® Mouse CD8 Negative Isolation Kit (Invitrogen; Carlsbad, CA, USA), respectively.

Briefly, a mixture of monoclonal rat anti-mouse antibodies to all immune cells (B lymphocytes, T lymphocytes, monocytes, NK cells, dendritic cells, erythrocytes and granulocytes), except for the T lymphocyte subset of interest, was mixed with the leukocyte suspension and then incubated for 20 min on ice. The cells were then washed by centrifugation (300 g for 8 min, 4 °C) to remove any excess antibody. The magnetic beads, coated with a polyclonal sheep anti-rat antibody were then added, and incubated for 15 min at room temperature with a gentle tilting and rotating motion, to allow for binding of the cells to the antibodies. Every few minutes during the incubation period, the cells were gently resuspended using a 1 ml pipette. Next, the 15 ml Falcon tubes containing the samples were each placed into the DynaMag™-15 magnet (Invitrogen). After approximately 2 min, the beads had adhered to the side of the tubes facing the magnet, and the remaining suspension contained the purified T lymphocytes.

2.13 Superoxide Measurements (L-012-enhanced chemiluminescence)

Basal and phorbol 12,13-dibutyrate (PDB; 1 μM)-stimulated superoxide production by T lymphocytes from blood and spleen of mice following I-R was measured by 100 μmol/L L-012-enhanced chemiluminescence (Daiber *et al.*, 2004). In triplicates, 50 μl of the T lymphocyte suspension (see section 2.12 'Isolation of T Lymphocytes (Dynal negative isolation kits)' above) was added into separate wells of a white 96-well plate containing 150 μl L-012 in Krebs-HEPES assay solution (99.01 mM NaCl, 4.69 mM KCl, 1.87 mM $CaCl_2$, 1.20 mM $MgSO_4$, 1.03 mM K_2HPO_4, 25.0 mM $NaHCO_3$, 20.0 mM Na-HEPES, 11.1 mM glucose; pH 7.4). 20 μl of PDB in Krebs-HEPES assay solution was then added to the appropriate wells. The white plate was then carefully covered with a clear topseal. L-012-enhanced chemiluminescence in each well was then measured for 2 s and repeated for 30 cycles by a Plate Chameleon Luminescence Reader (Hidex Ltd.; Turku, Finland). L-012-enhanced chemiluminescence was also measured in adjacent wells with L-012 in Krebs-HEPES assay solution devoid of cells (blank). In all experiments, the triplicates were averaged, and the results were expressed as an average of the 30

cycles. The chemiluminescence signal (relative light units per s) obtained in the blank wells were then subtracted. Superoxide production per cell (for blood samples) and per 10^3 cells (for spleen samples) was calculated by normalising the average chemiluminescence signal to T lymphocyte number. FACS analysis was used to confirm purity of $CD3^+$, $CD4^+$ and $CD8^+$ T lymphocytes in some samples.

2.14 Drugs and Chemicals

Ketamine (Parnell Laboratories; Alexandria, NSW, Australia), xylazine (Troy Laboratories; Smithfield, NSW, Australia), poly-L-Lysine (Sigma Aldrich; St. Louis, MO, USA), thionin (Sigma Aldrich), xylene (Scharlau Chemie; Barcelona, Spain), DPX mounting media (BDH Chemicals Ltd.; Poole, UK), paraformaldehyde (PFA; Merck; Darmstadt, Germany), isoflurane (Baxter Healthcare; Old Toongabbie, NSW, Australia), clexane (Sanofi-Aventis Australia Pty Ltd.; Macquarie Park, NSW, Australia), RPMI 1640 (Sigma Aldrich), trypan blue (Fluka; Buchs, Switzerland), foetal calf serum (FCS; Multiser; Noble Park, VIC, Australia), phorbol 12,13-dibutyrate (PDB; Calbiochem; Gibbstown, NJ, USA), L-012 (Wako Pure Chemical Industries; Osaka, Japan). All other chemicals were purchased from Sigma Aldrich or Merck.

2.15 Statistical Analyses

Data are typically presented as mean ± standard error. Statistical analyses were performed using GraphPad Prism version 5 (GraphPad Software Inc., San Diego, CA, USA). Between-group comparisons of rCBF during the 30 min ischaemic period and rCBF during the first 30 min of reperfusion in the I-R protocol, or rCBF during the first 60 min of ischaemia in the I-NR protocol, were compared using a two-way analysis of variance (ANOVA). Between-group comparisons of infarct volume, oedema volume, hanging wire, protein expression, FACS and T lymphocyte-generated superoxide were compared using an ANOVA or a Student's unpaired *t* test with Bonferroni *post-hoc* test, as appropriate. Between-group comparisons of distribution of

infarct area at each 'distance relative to bregma' point were compared using a Student's unpaired *t* test. Neurological score was compared using a Mann-Whitney test or a Kruskal-Wallis test followed by Dunn's *post-hoc* test, as appropriate. Mortality data were analysed using a log-rank test. Group numbers are shown in parentheses. Statistical significance was accepted when $P < 0.05$.

Chapter 3:

The Effects of Gender and Reperfusion on Cerebral Infarct Size after Stroke

3.1 INTRODUCTION

Studies of experimental stroke commonly employ models of cerebral ischaemia-reperfusion (I-R; i.e. transient ischaemia), and report that stroke severity is lower in females than males due to the greater level of circulating oestrogen in females (Alkayed *et al.*, 1998; Park *et al.*, 2006; Zhang *et al.*, 1998b). These experimental findings are supported by epidemiological studies indicating that females are more resistant to cerebral ischaemia (Prencipe *et al.*, 1997; Sudlow and Warlow, 1997). Studies assessing the effect of gender on outcome after cerebral ischaemia with no reperfusion (I-NR; i.e. permanent ischaemia) are surprisingly very few, and they report conflicting findings as to whether or not females undergo less ischaemic damage (Cai *et al.*, 1998; Carswell *et al.*, 1999; Loihl *et al.*, 1999).

Reperfusion is well established to cause a large inflammatory response (For review see Schaller & Graf, 2004). Oestrogen is a multi-faceted hormone which has powerful anti-inflammatory properties, and thus may mediate most of its benefit when reperfusion occurs (Schaller and Graf, 2004). However, reperfusion often may not occur in clinical stroke. Spontaneous reperfusion is common (≤70 % within one week after ischaemia) (Bowler *et al.*, 1998; Fieschi *et al.*, 1989; Jorgensen *et al.*, 1994), although it is usually incomplete (Barber *et al.*, 1998), and re-occlusion often occurs (Alexandrov and Grotta, 2002; Alexandrov *et al.*, 2004). Currently, recombinant tissue plasminogen activator (rt-PA) is the only available clinical treatment for acute stroke, and it has its effect by causing thrombolysis, thus allowing reperfusion to occur. rt-PA has a very limited time window for effective therapeutic use - initially treatment was approved for within 3 h of stroke onset, but it has recently been increased to 4.5 h (del Zoppo *et al.,* 2009), as it was still found to have significant benefit when administered between 3 and 4.5 h of stroke onset (Hacke *et al.,* 2008). Due to this relatively small therapeutic time window, in addition to the large number of exclusion criteria, which include any signs of bleeding in the brain (QSSAAN, 1996), only ~7-16 % of all stroke patients are eligible (Batmanian *et al.*, 2007; Johnston *et al.*, 2001; Katzan *et al.*,

2004), and even less receive it (Barber *et al.*, 2001; Batmanian *et al.*, 2007; Johnston *et al.*, 2001; Katzan *et al.*, 2004; Koennecke *et al.*, 2001; van Wijngaarden *et al.*, 2009). In addition, rt-PA does not achieve reperfusion in all patients, and it has been reported that complete reperfusion within 2 hours of i.v. infusion occurs in ~6-34 % of cases, and partial reperfusion in ~25-48 % of cases (Alexandrov and Grotta, 2002; Alexandrov *et al.*, 2004; Molina *et al.*, 2009; Saqqur *et al.*, 2007; Tsivgoulis *et al.*, 2010; van Wijngaarden *et al.*, 2009). Therefore, although I-NR is certainly a clinically relevant protocol for experimental stroke, no previous study has assessed the effect of gender on outcome after both I-R and I-NR.

Given that oestrogen is also known to be a cerebral vasodilator (Duckles and Krause, 2007), it is conceivable that the brain is better perfused in females during ischaemia and/or reperfusion. Because the salvage of brain tissue following post-ischaemic reperfusion may, on the one hand, be limited by pro-inflammatory mechanisms occurring during reperfusion, but on the other hand improved by restoration of blood flow to the ischaemic tissue, it is important to better identify the mechanisms involved in reperfusion, which will be further elucidated in Chapter 4, and to clarify whether females and males are equally vulnerable to reperfusion-induced damage.

NADPH oxidase is the major source of reactive oxygen species (ROS) in both systemic and cerebral vasculatures (Griendling *et al.*, 1994a; Miller *et al.*, 2005; Miller *et al.*, 2009), as well as in circulating leukocytes (eg. monocytes, neutrophils, T lymphocytes) (Jackson *et al.*, 2004; Selemidis *et al.*, 2008), and NADPH oxidase-derived ROS have been implicated in brain damage following ischaemic stroke (Kahles *et al.*, 2007; Kunz *et al.*, 2007). Specifically, the Nox2 (previously named gp91*phox*) isoform of NADPH oxidase was found to contribute to damage following stroke. After cerebral I-R, male mice either deficient in the Nox2 subunit, or with a dysfunctional Nox2 subunit, were reported to attain a 46-61 % smaller infarct than their wild-type littermates (Chen *et al.*, 2009; Kahles *et al.*, 2007; Kunz *et al.*, 2007; Walder *et al.*, 1997). Furthermore, apocynin

(4-hydroxy-3-methoxy-acetophenone), a relatively selective inhibitor of Nox1- and Nox2-containing NADPH oxidase, has also been shown to reduce infarct volume (Chen *et al.*, 2009; Jackman *et al.*, 2009a; Tang *et al.*, 2007; Tang *et al.*, 2008), and our lab has previously reported that apocynin reduces cerebral infarct volume via the inhibition of Nox2 (Jackman *et al.*, 2009a). These results suggest that Nox2 activity is detrimental in ischaemic injury following reperfusion in male mice. To our knowledge, no one has yet investigated whether Nox2 also contributes to stroke damage in females.

In this study, we performed either 30 min middle cerebral artery (MCA) occlusion with 23.5 or 71.5 h reperfusion (I-R), or 24 h MCA occlusion with no reperfusion (I-NR). Following I-NR, full development of infarct volume is believed to be reached by 24 h (Aronowski *et al.*, 1997; Iadecola *et al.*, 2001b), however, after a 30 min MCA occlusion, infarcts may not reach their maximum until ~48 h after reperfusion (Kunz *et al.*, 2007; Li *et al.*, 2000). For this reason, it is important to confirm what is observed at 24 h with a later time-point after the end of infarct progression (eg. at 72 h).

The aims of this study were firstly, to test the effects of gender and reperfusion on outcome following ischaemic stroke, and secondly, to assess the role of Nox2 expression in cerebral infarct volume in male and female mice after cerebral I-R. We evaluated neurological impairment, as well as infarct and oedema volume, at 24 h after I-R and I-NR in male and female wild-type mice; at 72 h after I-R in male and female wild-type mice; and at 24 h after I-R in male and female Nox2-deficient mice.

Chapters 3 and 4 describe two components of one larger study that was performed over the course of this PhD. As mentioned above, Chapter 3 will discuss the effects of gender and

reperfusion on neurological function, and infarct and oedema volume, whereas Chapter 4 will discuss data relevant to the mechanisms underlying those results.

3.2 MATERIALS AND METHODS

3.2.1 Animals

This study was conducted in accordance with the National Health and Medical Research Council of Australia guidelines for the care and use of animals in research.

In Chapters 3 and 4, a total of 263 mice were studied, consisting of: 126 male (weight, 23.3±0.2 g) and 111 female (18.1±0.1 g) 6-8 week old C57Bl6/J mice, and 15 male (22.5±0.9 g) and 11 female (17.5±0.3 g) 6-8 week old Nox2-deficient ($Nox2^{-/-}$) mice. The actual number of mice used per experiment is indicated throughout Chapters 3 and 4. $Nox2^{-/-}$ (AKA gp91*phox*$^{-/-}$) mice were originally generated in the laboratory of Professor Mary Dinauer and bred at Ozgene (Bentley DC, WA, Australia) before a colony was established at Monash University. The mice had free access to water and food pellets before and after surgery. Thirty-one mice were excluded from the study if during the surgical procedure to induce MCAO: a) a significant volume of blood (>0.2 ml) was lost (n = 2); b) the filament did not stay in place for the entire 30 min of ischaemia (n = 1); c) the regional cerebral blood flow (rCBF) did not remain above ischaemic levels during the 30 min recorded reperfusion period (n = 1); d) the occluding clamp was in place for ≥5 min (n = 3); or e) they died prior to the specified time for euthanasia (at 23.5 h or 71.5 h reperfusion) (n = 24).

3.2.2 Tail cuffing

Systolic blood pressure (BP) was measured via tail cuffing, using a MC4000 Blood Pressure Analysis System (Hatteras Instruments; Cary, NC, USA), as described in section 2.6 of General Methods.

3.2.3 Evaluation of brain weight

In order to compare the brain size between genders, a number of naïve male and female wild-type mice were killed and their brains removed as described in section 2.5 of General Methods. These brains were then immediately weighed using a sensitive scale.

3.2.4 Focal cerebral ischaemia

Focal cerebral ischaemia was induced by transient or permanent intraluminal filament occlusion of the right middle cerebral artery (MCA) as described in section 2.3 of General Methods. In this study, we also measured regional cerebral blood flow (rCBF) at 24 h, in mice whose endpoint was 24 h. The laser Doppler probe holder was kept in place following surgery, and the head wound was closed around it. Just prior to 24 h, mice were re-anaesthetised with a mixture of ketamine (80 mg/kg, i.p.) and xylazine (10 mg/kg, i.p.). The laser Dopper probe was inserted into the probe holder, and the average rCBF measured over 1 min was recorded. We chose not to test this in mice whose endpoint was 72 h, to avoid having a probe holder glued to the skull for more than 24 h, in order to minimise the chance of infection.

3.2.5 Evaluation of neurological function

At the end of the experiment (either 24 or 72 h), neurological function was evaluated using a five-point scoring system, and the hanging wire test. Please refer to section 2.4 of General Methods for details.

3.2.6 Evaluation of cerebral infarct and oedema volume

Mice were killed, brains removed and cerebral infarct and oedema volume evaluated as described in section 2.5 of General Methods.

3.2.7 Drugs and chemicals

As per section 2.14 of General Methods.

3.2.8 Statistical analysis

Data are typically presented as mean ± standard error. Statistical analyses were performed using GraphPad Prism version 5 (GraphPad Software Inc., San Diego, CA, USA). Between-group comparisons were analysed as described in section 2.15 of General Methods. Group numbers are shown in parentheses. Statistical significance was accepted when $P < 0.05$.

3.3 RESULTS

3.3.1 Effect of gender on systolic blood pressure and brain weight in naïve wild-type and Nox2-deficient mice

There tended to be higher systolic blood pressure measured by tail cuffing in male (122±4 mmHg, $n = 11$) versus female (111±5 mmHg, $n = 8$) wild-type mice although this did not reach statistical significance (Figure 3.1A). There was no difference in brain weight between 6-8 week old male and female wild-type mice (males=0.47±0.01 g, females=0.46±0.01 g; $n = 5$-7; Figure 3.1B). There was also no difference in systolic blood pressure measured by tail cuffing between male (119±6 mmHg, $n = 8$) and female (122±3 mmHg, $n = 12$) Nox2-deficient mice (Figure 3.1C).

3.3.2 Effect of reperfusion and gender on outcome 24 h after middle cerebral artery occlusion (MCAO) in wild-type mice

3.3.2.1 Regional cerebral blood flow

Firstly, cerebral ischaemia-reperfusion (I-R) was produced by 30 min MCAO and 23.5 h reperfusion. Regional cerebral blood flow (rCBF) decreased to ~25 % of the pre-ischaemic level

for the duration of MCAO (Figure 3.2A). rCBF then increased initially to ~85 % upon removal of the monofilament, and then stabilised at ~60 % after 30 min of reperfusion, and remained at a similar level at 24 h (Figure 3.2A). Secondly, in mice subjected to permanent MCAO (i.e. no reperfusion; I-NR), rCBF remained at 25-30 % of the pre-ischaemic level for 60 min and reduced to ~15 % at 24 h (Figure 3.2B). No differences in rCBF profiles were observed between male and female mice in either protocol.

3.3.2.2 Mortality and neurological function

At 24 h, mortality rates were similar in male and female mice following I-R (6/57: 11 % in males; 5/41: 12 % in females; Figure 3.2C) or I-NR (5/34: 15 % in both males and females; Figure 3.2D). Similarly, neither gender nor reperfusion had any effect on neurological score; the mice in the stroked groups were generally given a score of 3 or 4, except for the occasional 0 or 1 (Figure 3.3A); or hanging wire times (I-R: males=22±5 s, females=24±7 s; I-NR: males=25±5 s, females=19±6 s; Figure 3.3B). Not surprisingly, neurological score was significantly higher and hanging wire time significantly lower in both genders, following both I-R and I-NR, compared to the matched sham-operated group (Neuro: all sham-operated mice were given a score of 0; Hanging wire: males=53±3 s, females=55±2 s; $P < 0.05$; Figures 3.3A & B).

3.3.2.3 Brain infarct and oedema volume measured as mm^3

Representative coronal sections of infarcted brain of male and female mice 24 h after I-R and 24 h after I-NR are shown in Figures 3.4A and B, respectively. Twenty-four h after I-R, significantly larger total and subcortical infarct volumes were produced in male mice compared with female mice (total: 55±11 vs. 24±6 mm^3; subcortical: 32±6 vs. 14±3 mm^3; $P < 0.05$; n = 7-8; Figures 3.4C & E). There was no significant gender difference in cortical infarct volume (23±7 vs. 10±4 mm^3; $P = 0.12$; Figure 3.4E). In both male and female mice, cortical infarct volume accounted for ~40 % of the total infarct volume (Figure 3.4E). Surprisingly, there was

no gender difference in oedema volume at 24 h following I-R (34±6 vs. 30±5 mm^3; P = 0.60; Figure 3.5A).

Following 24 h of I-NR, infarct volumes were larger than in mice subjected to I-R (Figures 3.4D & F vs. 3.4C & E). Moreover, there was no gender difference produced in these mice, in either total (88±11 vs. 88±9 mm^3; P = 1.00; n = 8-9; Figure 3.4D), cortical (43±5 vs. 45±3 mm^3; P = 0.67; Figure 3.4F) or subcortical infarct volume (45±7 vs. 43±6 mm^3; P = 0.81; Figure 3.4F). Cortical and subcortical infarct each accounted for approximately half of the total infarct in both male and female mice (Figure 3.4F). There was also no gender difference in oedema volume (63±6 vs. 54±5 mm^3; P = 0.28; Figure 3.5B).

3.3.2.4 Brain infarct volume measured as % of non-ischaemic hemisphere

Infarct volumes were also estimated as a percentage of the non-ischaemic hemisphere. The general profiles and the statistical significance achieved between groups for the total, cortical and subcortical infarcts following both I-R and I-NR were very similar to and in agreement with when the infarct was measured in mm^3 (Figure 3.6A-D).

3.3.2.5 Brain infarct area distribution

The distribution of the infarct area throughout the brain was also plotted. Twenty-four h after I-R, similar shaped distribution profiles were observed in male and female mice, with the peak infarct area observed in the rostral region of the hippocampus (-0.92 to -1.76 mm from bregma) in both the total and subcortical infarcts (Figures 3.7A & E). Both total and subcortical infarct areas were larger in male mice than female mice at all points in the brain. These were significantly larger in the region spanning from bregma +0.76 mm to bregma -1.76 mm in the total infarct (Figure 3.7A), and at two points in the subcortical infarct; approximately bregma (-0.08 mm) and bregma -0.92 mm (Figure 3.7E). No clear peak was seen in the cortical infarct

distribution, as it showed a flatter, more constant profile (Figure 3.7C). In the cortex, male mice also had larger infarct areas compared to female mice at most points (all except at bregma -4.28 mm), although this was only significant at bregma -0.92 mm and bregma -2.6 mm (Figure 3.7C).

The distribution of infarct area 24 h after I-NR, followed a similar profile to that of 24 h after I-R, however, the infarct area 24 h after I-NR was more widespread, both in the anterior and posterior parts of the forebrain. The only difference observed in the total (Figure 3.7B), cortical (Figure 3.7D) and subcortical (Figure 3.7F) distributions between male and female mice, was a significantly larger cortical infarct in females at one point (bregma +0.76 mm), supporting the conclusion that no overall gender difference exists following I-NR.

3.3.3 Effect of gender on outcome 72 h after MCAO in wild-type mice

3.3.3.1 Regional cerebral blood flow

72 h cerebral I-R was produced by 30 min MCAO and 71.5 h reperfusion. rCBF decreased to ~20 % of the pre-ischaemic level for the duration of MCAO (Figure 3.8A). rCBF then increased initially to ~115 % upon removal of the monofilament, and then stabilised at ~65 % after 30 min of reperfusion (Figure 3.8A). No differences in rCBF profiles were observed between male and female mice.

3.3.3.2 Mortality and neurological function

Mortality rates in the 72 h I-R studies were similar as for the 24 h I-R protocol, and not statistically different between genders (2/12: 17 % in males; 1/12: 8 % in females; $P = 0.55$; Figure 3.8B). Also, neurological score was not different between male and female mice following I-R; 6/8 males and 7/9 females were given a score of 3, and the remaining two male mice were given a score of 4, and the remaining two female mice were given a score of 1 (Figure 3.8C). However, hanging wire times by female mice were significantly longer than by male mice 72 h

after I-R (males=15±5 s, females=35±7 s; $P < 0.05$; Figure 3.8D). Furthermore, in both neurological score and hanging wire time 72 h after I-R, male mice were significantly different from control males studied 72 h post-sham surgery, whereas female mice were not different from sham-operated females (Figures 3.8C & D). No gender difference was observed following sham surgery in neurological score (all mice were given a score of 0; Figure 3.8C) or in hanging wire time (males=60±0 s, females=56±4 s; Figure 3.8D).

3.3.3.3 Brain infarct and oedema volume measured as mm^3

Representative coronal sections of infarcted brain of male and female mice 72 h after I-R are shown in Figures 3.9A and B. Seventy-two h after I-R, mean total infarct volume was ~70 % larger in males (40±8 mm^3, $n = 8$) versus females (24±5 mm^3, $n = 9$; Figure 3.9C) although this difference did not reach statistical significance ($P = 0.11$). Importantly, infarct volumes at 72 h were no larger in either gender than at 24 h (i.e. males=55±11 mm^3, females=24±6 mm^3; see Figure 3.4C for comparison). There was no statistically significant gender difference in cortical (12±4 vs. 5±2 mm^3; $P = 0.08$; Figure 3.9D) or subcortical (27±5 vs. 19±4 mm^3; $P = 0.24$; Figure 3.9D) infarct volumes 72 h after I-R, although infarct volumes in male mice tended to be larger than female mice. Cortical infarct accounted for approximately 30 % of the total infarct in male mice, and ~20 % in female mice 72 h after I-R (see Figure 3.9D). Oedema volumes 72 h after I-R also tended to be larger in males compared to females (males=32±12 mm^3, females=14±4 mm^3; $P = 0.14$; Figure 3.9E).

3.3.3.4 Brain infarct volume measured as % of non-ischaemic hemisphere

When estimated as a percentage of the non-ischaemic hemisphere, total ($P = 0.11$; males vs. females), cortical ($P = 0.11$) and subcortical ($P = 0.21$) infarcts 72 h after I-R had very similar profiles as when measured in mm^3 (Figure 3.10A-B). Again, although, there was no significant gender difference, infarct volumes tended to be larger in male mice compared to female mice.

3.3.3.5 Brain infarct area distribution

The distribution of infarct area 72 h after I-R followed a similar profile to that of 24 h after I-R, with the peak at bregma -0.92 mm, in both male and female mice in the total and subcortical infarct areas (Figures 3.11A & C). Male mice again tended to have larger infarcts than female mice throughout the total and subcortical infarcts, although there were no statistically significant differences between genders (Figures 3.11A & C). In the cortical infarct, male mice had a significantly larger infarct than female mice at bregma +1.6 mm, though they were very similar at all other points (Figure 3.11B).

3.3.4 Effect of gender on outcome 24 h after MCAO in Nox2-deficient mice

3.3.4.1 Regional cerebral blood flow

Cerebral I-R in Nox2-deficient mice was produced by 30 min MCAO and 23.5 h reperfusion. rCBF decreased to ~15 % of the pre-ischaemic level for the duration of MCAO (Figure 3.12A). rCBF increased initially to ~110 % upon removal of the monofilament, and then stabilised at ~65 % after 30 min of reperfusion. At 24 h after I-R, rCBF in male mice remained at a similar level to 30 min after the induction of reperfusion, and rCBF reduced to 46 % in female mice (Figure 3.12A). There was no difference in rCBF profile between genders of Nox2-deficient mice during MCAO and the initial 30 min of reperfusion, or at the 24 h time-point (Figure 3.12A).

3.3.4.2 Mortality and neurological function

No deaths occurred in male or female Nox2-deficient mice 24 h after I-R (both n = 10). Neurological score and hanging wire times were not statistically different between genders, although male mice tended to have a lower score (ie. less impairment); the majority of males were given a score of 3, and the majority of females were given a score of 4 (Figure 3.12B), and male

mice also tended to hold onto the wire for longer (males=25±5 s, females=16±6 s; P = 0.22; Figure 3.12C).

3.3.4.3 Brain infarct and oedema volume measured as mm^3

Representative coronal sections of infarcted brain of male and female Nox2-deficient mice 24 h after I-R are shown in Figures 3.13A and B. There was no significant difference between genders of Nox2-deficient mice in the total (males=30±9 mm^3, females=43±6 mm^3; P = 0.24; Figure 3.13C), cortical (males=6±4 mm^3, females=10±2 mm^3; P = 0.47; Figure 3.13D) or subcortical (males=24±6 mm^3, females=34±6 mm^3; P = 0.21; Figure 3.13D) infarct volume produced by I-R, although there was a trend for female mice to have larger infarcts than male mice. Cortical infarct accounted for approximately 20 % of the total infarct following I-R in both male and female Nox2-deficient mice (see Figure 3.13D). Oedema volumes were similar between genders (males=23±6 mm^3, females=31±5 mm^3; P = 0.32; Figure 3.13E).

3.3.4.4 Brain infarct volume measured as % of non-ischaemic hemisphere

Very similar profiles were seen in total (P = 0.29; males vs. females), cortical (P = 0.31), and subcortical (P = 0.35) infarct volumes when measured as a percentage of the non-ischaemic hemisphere, compared with when measured as mm^3 (Figures 3.14A-B).

3.3.4.5 Brain infarct area distribution

The distribution of infarct area in Nox2-deficient mice followed a similar profile to that in wild-type mice following I-R, with the peak in total and subcortical infarct area in both males and females at bregma -1.76 mm (Figures 3.15A & C). Interestingly, infarct areas were very similar between male and female Nox2-deficient mice from the anterior part of the brain until bregma (-0.08 mm) (Figures 3.15A-C). However, posterior to bregma, female mice had larger infarcts than male mice at each point, and these were significantly different at bregma -2.6 mm, -3.44

mm, and -4.28 mm in the total infarct (Figure 3.15A), at bregma -3.44 mm and -4.28 mm in the cortical infarct (Figure 3.15B), and at bregma -0.92 mm in the subcortical infarct (Figure 3.15C).

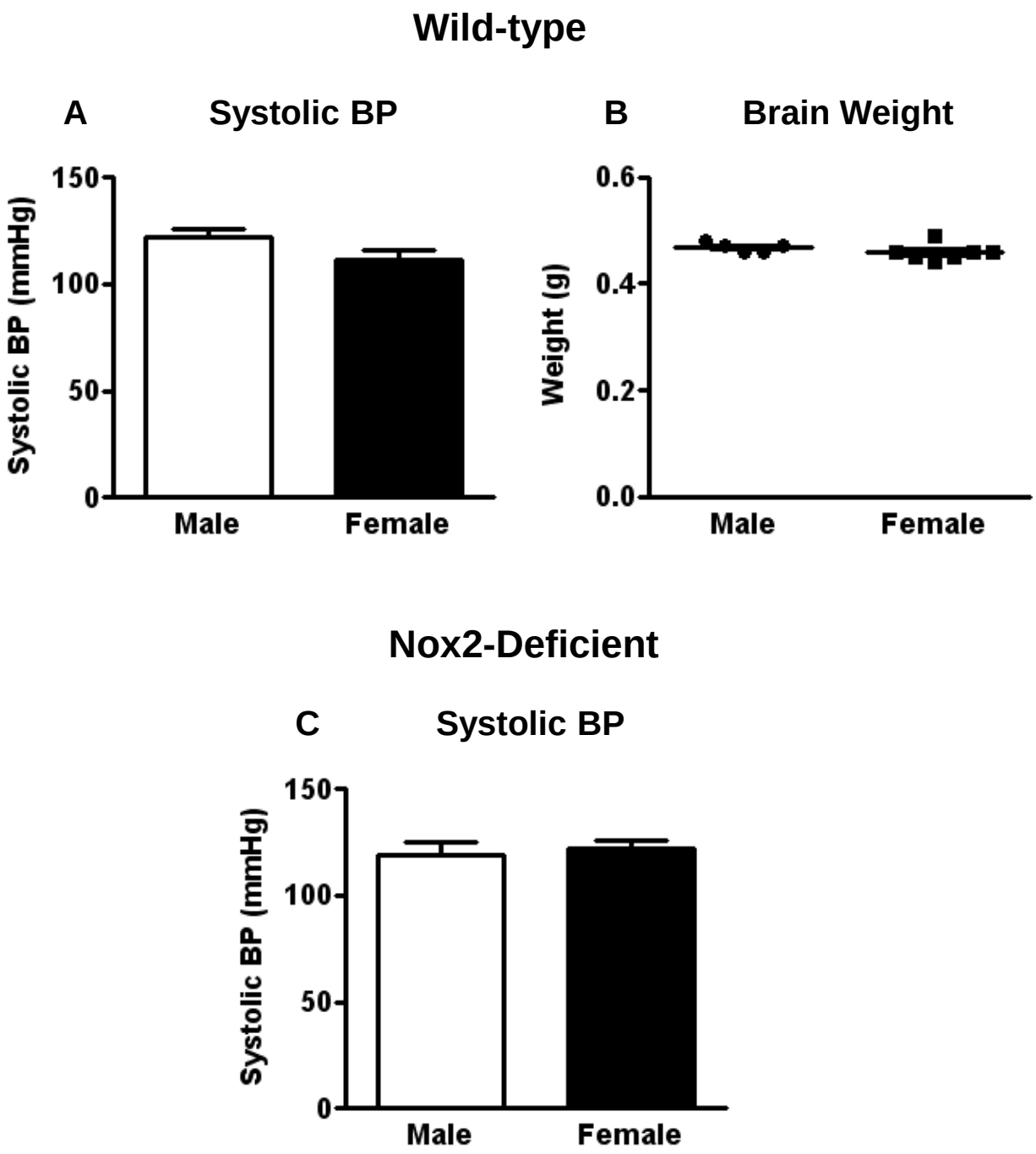

Figure 3.1. Systolic blood pressure in naïve wild-type and Nox2-deficient mice, and brain weight in naïve wild-type mice.

Systolic blood pressure was measured in naive wild-type mice (**A;** males, *n* = 11; females, *n* = 8) and naive Nox2-deficient mice (**C;** males, *n* = 8; females, *n* = 12). **B:** The brains of male and female naive wild-type mice were weighed (males, *n* = 5; females, *n* = 7). Systolic BP data are presented as mean ± SEM and brain weight data are presented as mean.

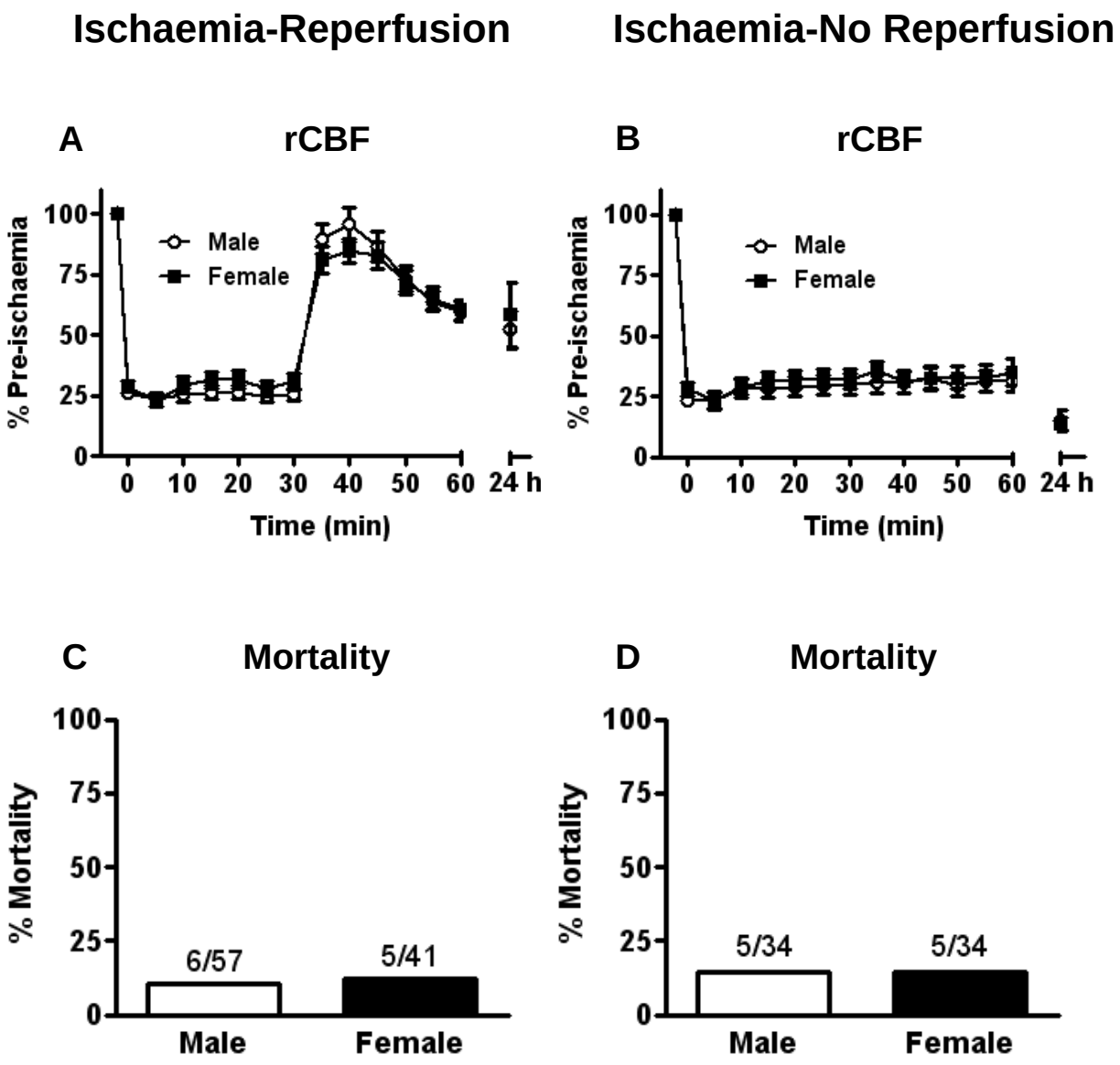

Figure 3.2. Regional cerebral blood flow (rCBF) and mortality at 24 h in wild-type mice. rCBF was recorded during and after 30 min MCAO, as well as at 24 h after MCAO, with (**A;** males, *n* = 39; females, *n* = 28; I-R) or without (**B;** males, *n* = 25; females, *n* = 25; I-NR) reperfusion. Mortality at 24 h after MCAO was measured in I-R (**C**) and I-NR (**D**). rCBF data are presented as mean ± SEM. Mortality data are presented as a percentage, with numbers above the bars representing the number of animals who didn't survive 24 h over the total number.

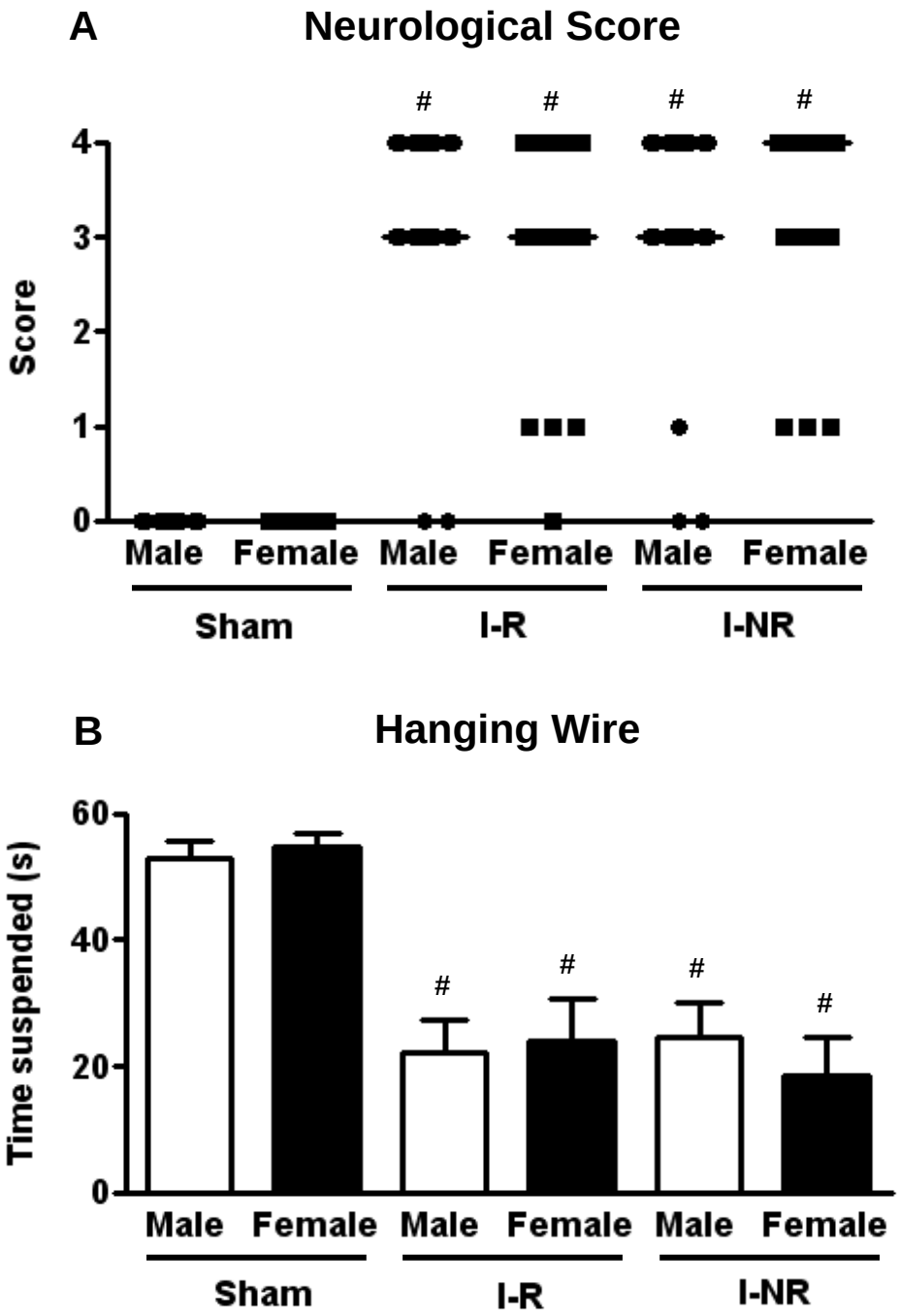

Figure 3.3. Neurological score and hanging wire at 24 h in wild-type mice.

A: Neurological score 24 h following sham surgery (males, n = 18; females, n = 19), I-R (males, n = 38; females, n = 27), and I-NR (males, n = 25; females, n = 25; $^{\#}P < 0.05$ vs. gender matched sham group, Kruskal-Wallis test with Dunn's *post-hoc* test). **B:** Hanging wire data 24 h following sham surgery (males, n = 10; females, n = 11), I-R (males, n = 18; females, n = 12), and I-NR (males, n = 13; females, n = 12; $^{\#}P < 0.05$ vs. gender matched sham group, ANOVA with Bonferroni's *post-hoc* test). Neurological score data are presented as median, and hanging wire data are presented as mean ± SEM.

Figure 3.4. Cerebral infarct volume at 24 h in wild-type mice (measured as mm^3).
Representative coronal brain sections are shown from male and female mice after I-R (**A**) or I-NR (**B**) with the infarct area outlined in white. Total cerebral infarct volume measured in male and female mice 24 h after I-R (**C;** males, $n = 8$; females, $n = 7$; $^*P < 0.05$, unpaired t test) or I-NR (**D;** males, $n = 8$; females, $n = 9$) are shown, as are cortical and subcortical cerebral infarct volumes 24 h after I-R (**E;** males, $n = 8$; females, $n = 7$; $^*P < 0.05$, unpaired t test) or I-NR (**F;** males, $n = 8$; females, $n = 9$). Infarct volume data are presented as mean ± SEM.

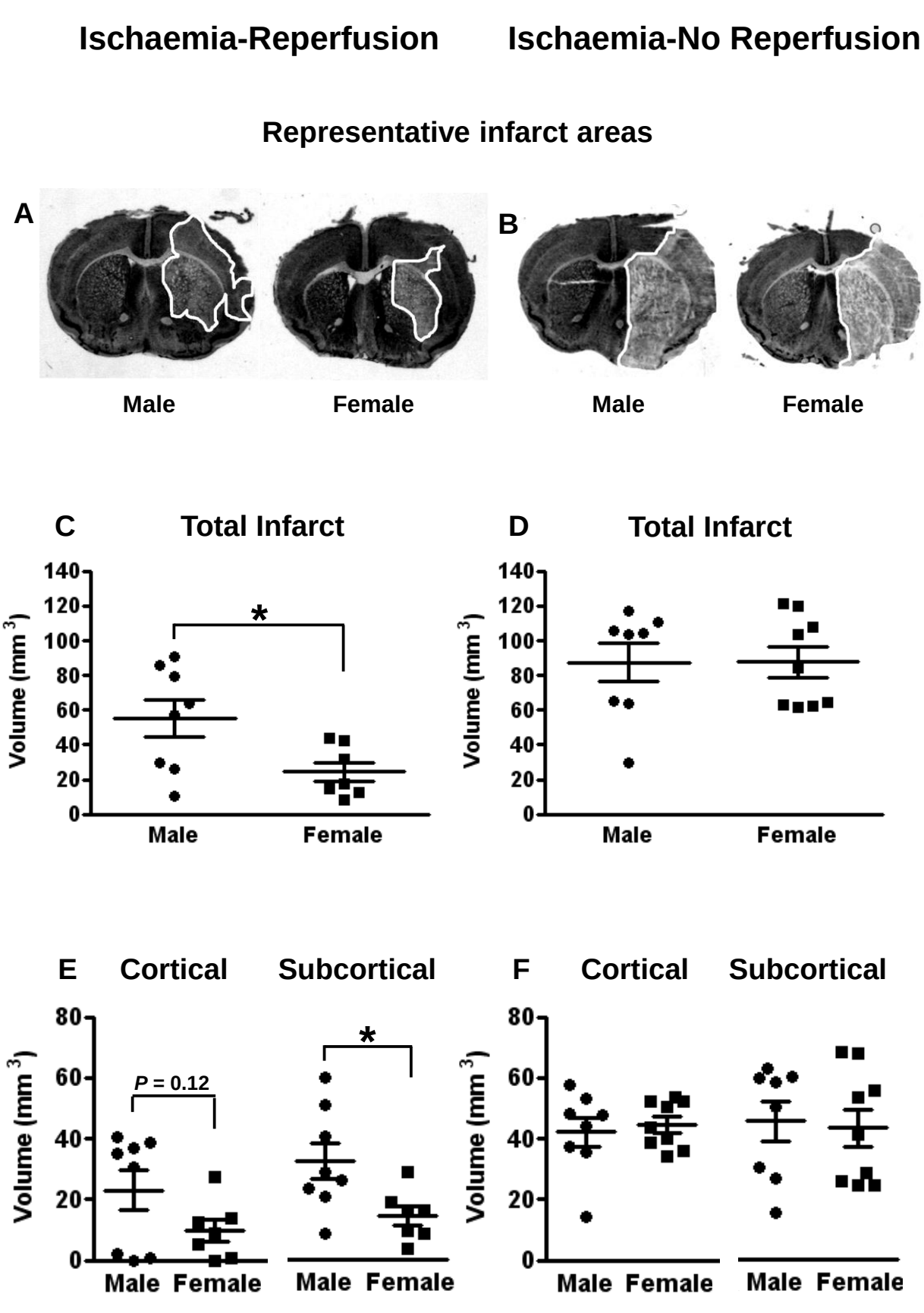
Ischaemia-Reperfusion
Ischaemia-No Reperfusion
Representative infarct areas
A
B
Male
Female
Male
Female
C
Total Infarct
D
Total Infarct
Volume (mm 3)
140
120
100
80
60
40
20
0
*
Male
Female
E
Cortical
Subcortical
F
Cortical
Subcortical
P = 0.12
Male Female

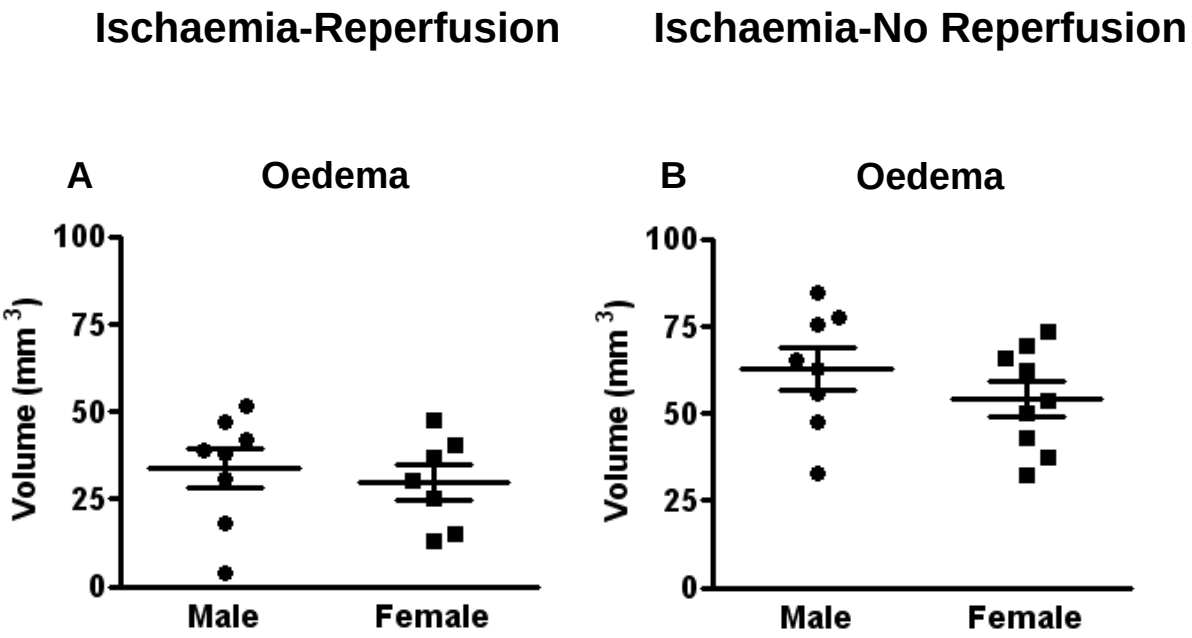

Figure 3.5. Cerebral oedema volume at 24 h in wild-type mice.

Cerebral oedema volume is shown 24 h after I-R (**A;** males, *n* = 8; females, *n* = 7) or I-NR (**B;** males, *n* = 8; females, *n* = 9). Data are presented as mean ± SEM.

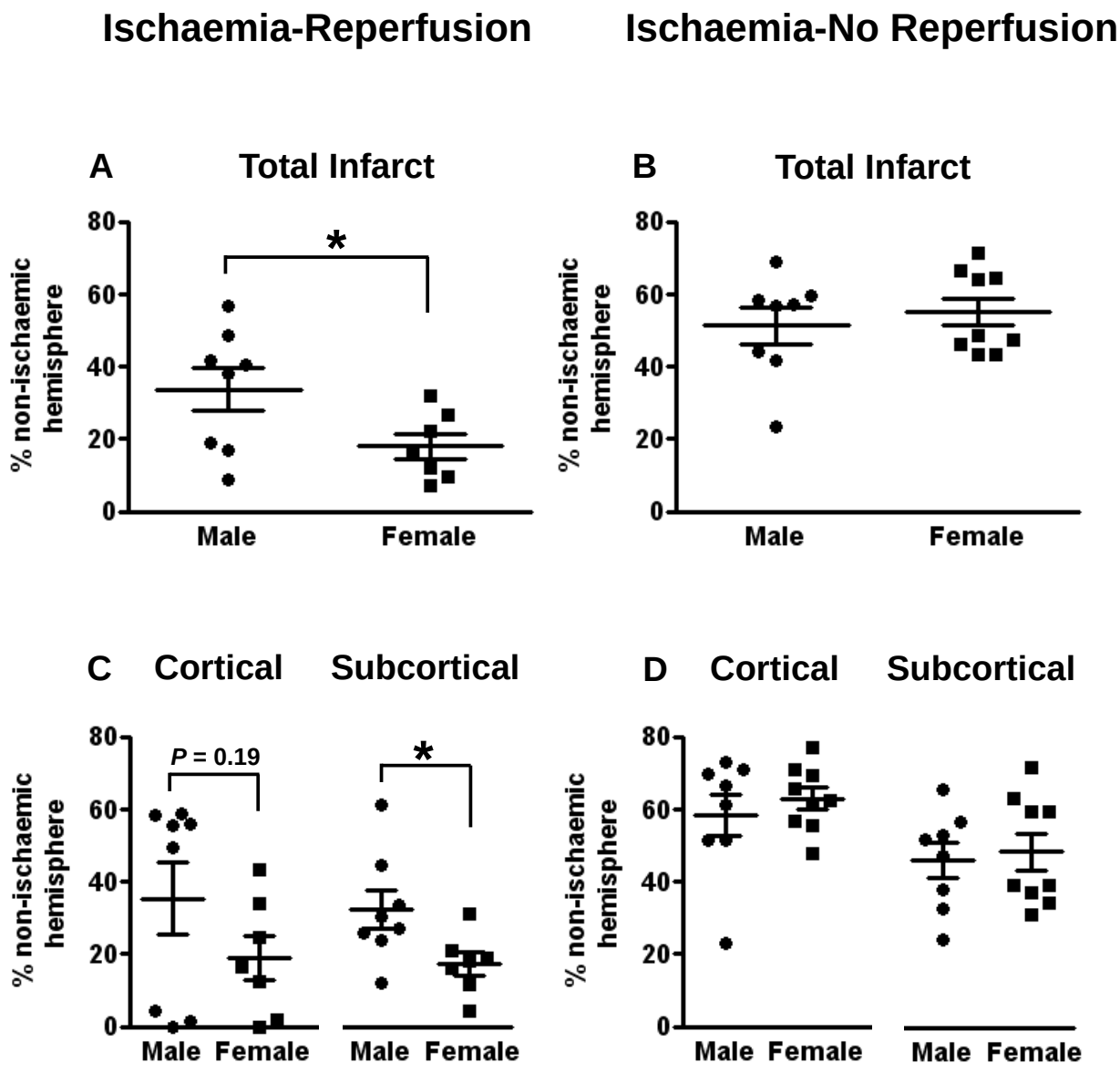

Figure 3.6. Cerebral infarct volume at 24 h in wild-type mice (measured as % of non-ischaemic hemisphere).

Total cerebral infarct volume measured in male and female mice 24 h after I-R (**A;** males, $n = 8$; females, $n = 7$; $^*P < 0.05$, unpaired t test) or I-NR (**B;** males, $n = 8$; females, $n = 9$) are shown, as are cortical and subcortical cerebral infarct volumes 24 h after I-R (**C;** males, $n = 8$; females, $n = 7$; $^*P < 0.05$, unpaired t test) or I-NR (**D;** males, $n = 8$; females, $n = 9$). Infarct volume data are presented as mean ± SEM.

Figure 3.7. Cerebral infarct area distribution at 24 h in wild-type mice.

Total (**A-B**), cortical (**C-D**) and subcortical (**E-F**) cerebral infarct area distributions were measured in male and female mice 24 h after I-R (**A,C,E**; males, $n = 8$; females, $n = 7$; $^*P < 0.05$ at each point, unpaired t test) or I-NR (**B,D,F;** males, $n = 8$; females, $n = 9$; $^*P < 0.05$ at each point, unpaired t test). Infarct area data are presented as mean ± SEM.

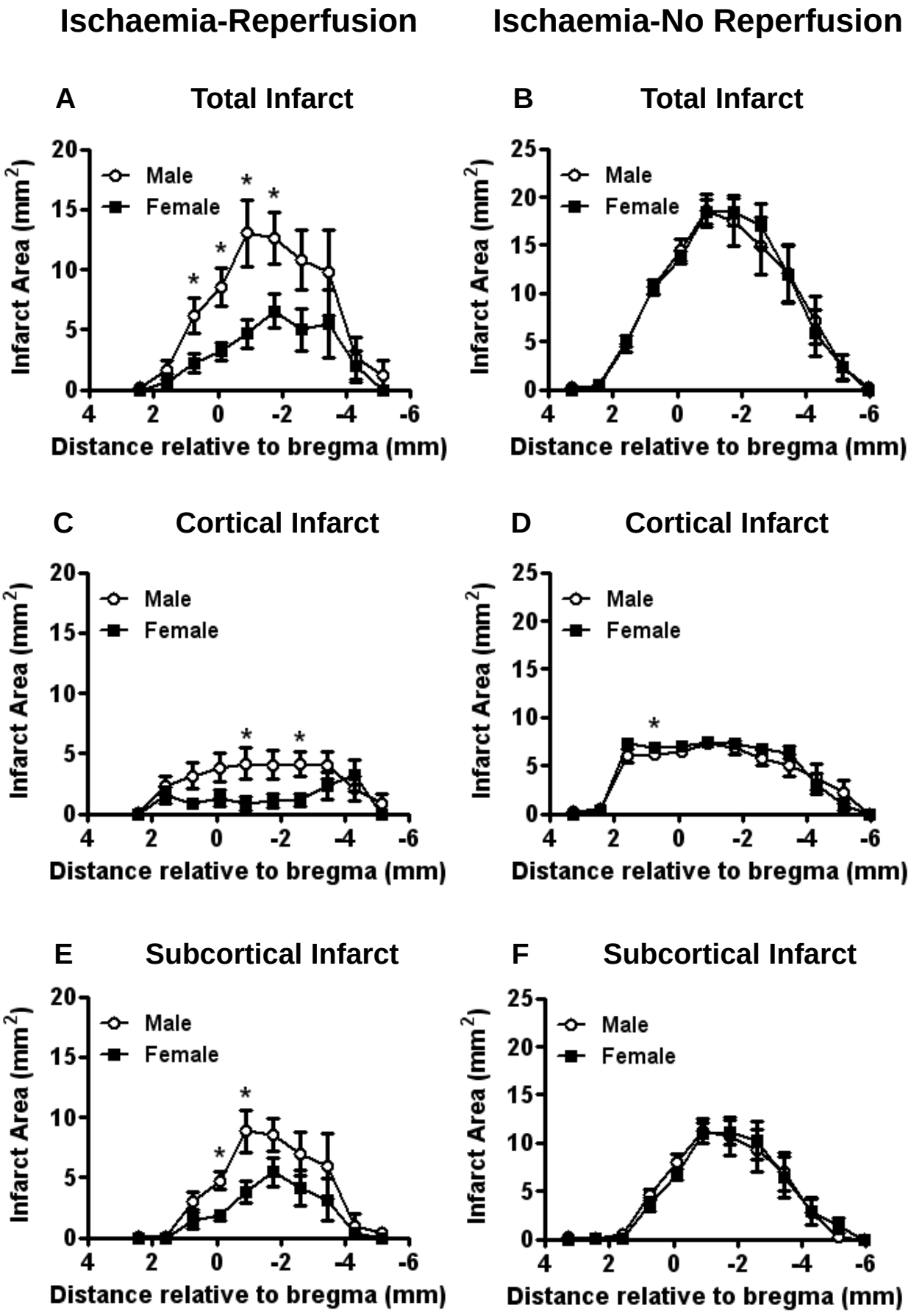
Ischaemia-Reperfusion
Ischaemia-No Reperfusion
A
Total Infarct
B
Total Infarct
C
Cortical Infarct
D
Cortical Infarct
E
Subcortical Infarct
F
Subcortical Infarct
Male
Female
Infarct Area (mm2)
Distance relative to bregma (mm)
20
15
10
5
0
25
4
2
0
-2
-4
-6
*

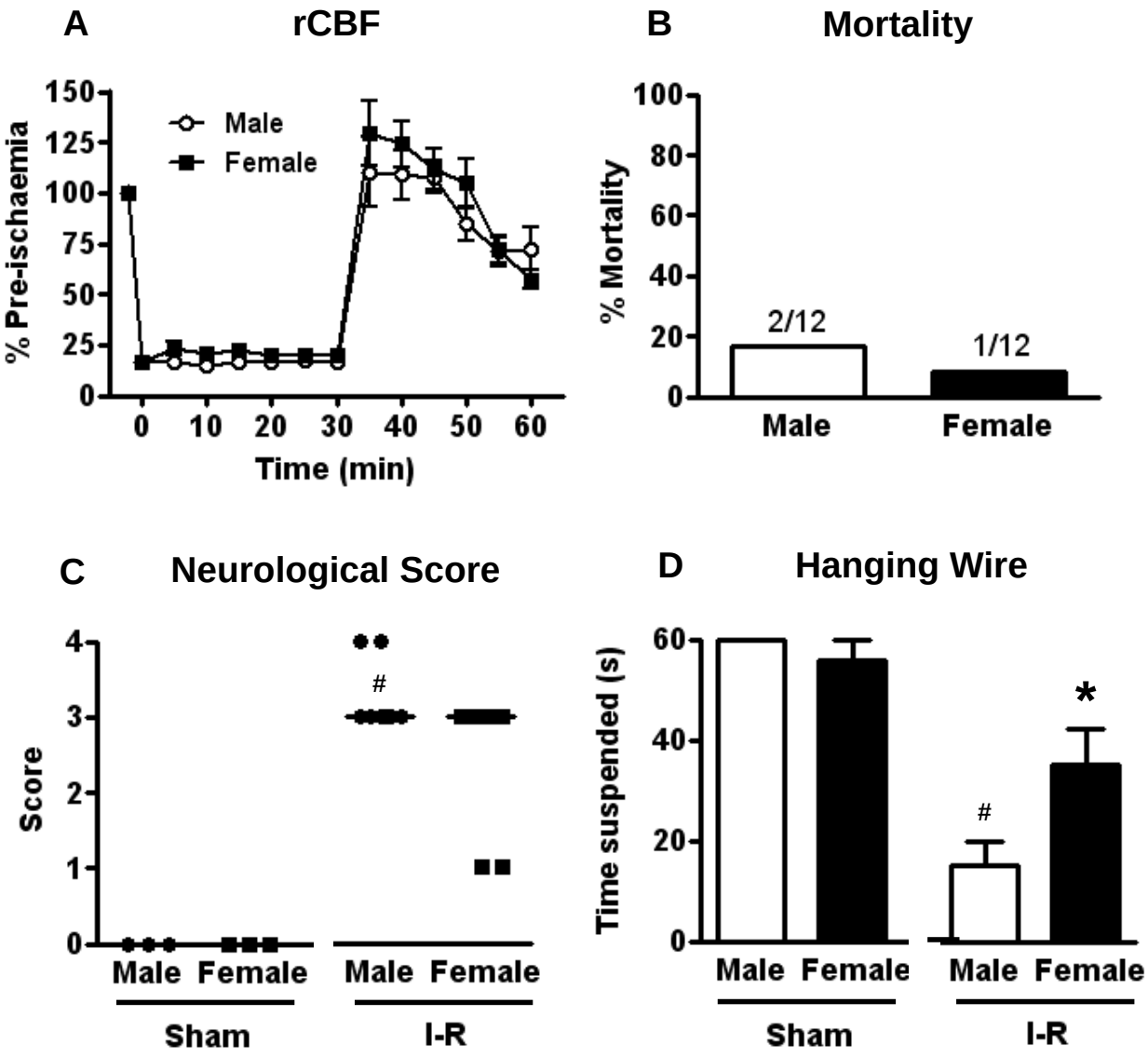

Figure 3.8. Regional cerebral blood flow (rCBF), mortality, neurological score and hanging wire at 72 h after I-R in wild-type mice.

rCBF was recorded during and after 30 min MCAO (**A;** males, n = 8; females, n = 9). **B:** Mortality at 72 h after MCAO. **C:** Neurological score 72 h following sham surgery (males, n = 3; females, n = 3), and I-R (males, n = 8; females, n = 9; $^{\#}P < 0.05$ vs. matched sham group, Kruskal-Wallis test with Dunn's *post-hoc* test). **D:** Hanging wire data 72 h following sham surgery (males, n = 3; females, n = 3), and I-R (males, n = 8; females, n = 9; $^{*}P < 0.05$ vs. matched male group, unpaired t test; $^{\#}P < 0.05$ vs. matched sham group, ANOVA with Bonferroni's *post-hoc* test). Mortality data are presented as a percentage, with numbers above the bars representing the number of animals who didn't survive 72 h over the total number, neurological score data are presented as median, and rCBF and hanging wire data are presented as mean ± SEM.

Figure 3.9. Cerebral infarct and oedema volume at 72 h after I-R in wild-type mice (measured as mm^3).

Representative coronal brain sections are shown from male (**A**) and female (**B**) mice 72 h after I-R with the infarct area outlined in white. Total (**C**), and cortical and subcortical (**D**) cerebral infarct volumes were measured in male and female mice 72 h after I-R (males, n = 8; females, n = 9; unpaired t test). **E:** Oedema volume measured at 72 h after I-R in male and female mice (males, n = 8; females, n = 9; unpaired t test). Data are presented as mean ± SEM.

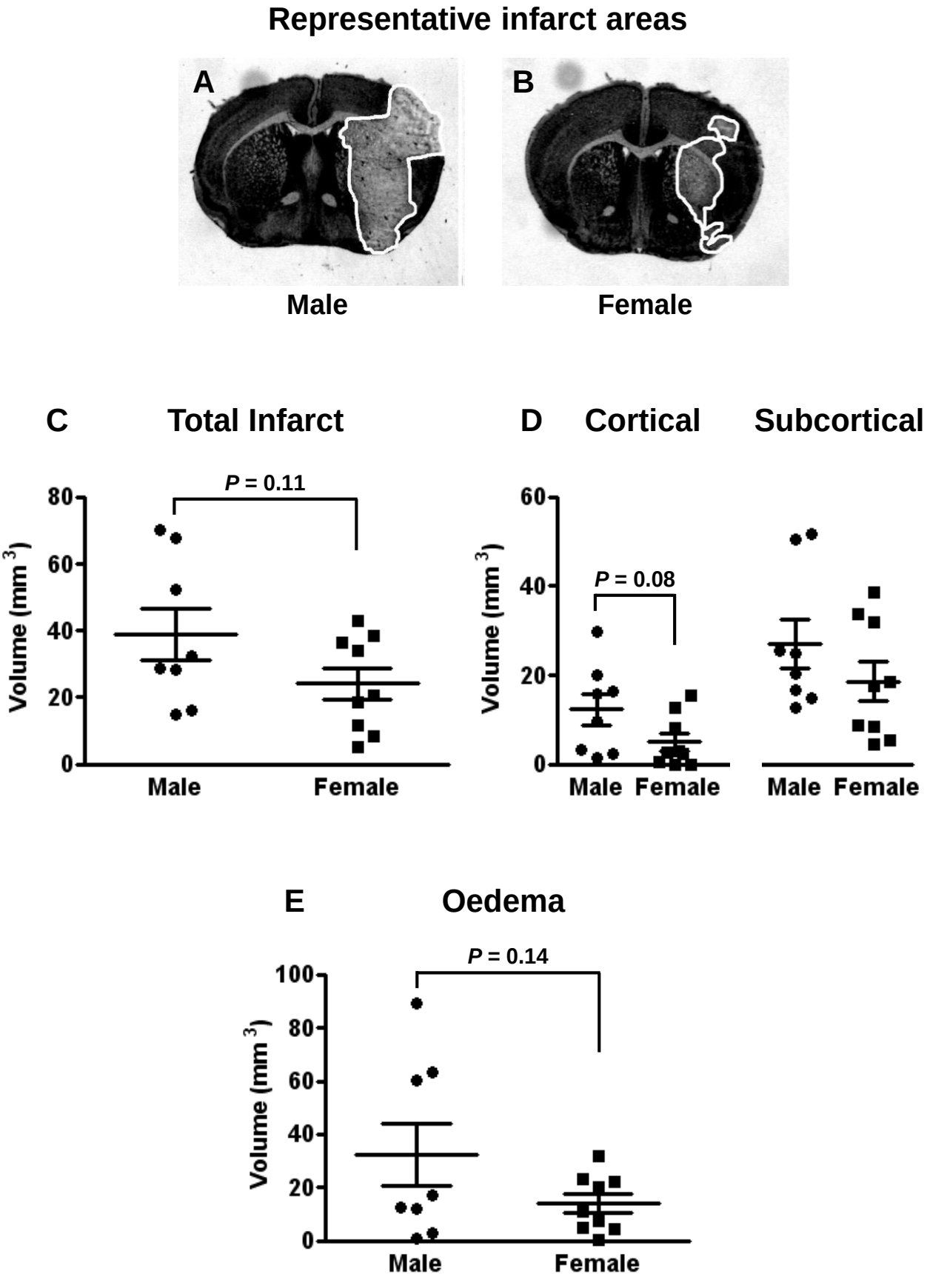
Representative infarct areas
A
B
Male
Female
C
Total Infarct
P = 0.11
Volume (mm 3)
80
60
40
20
0
Male
Female
D
Cortical
Subcortical
P = 0.08
Volume (mm 3)
60
40
20
0
Male
Female
Male
Female
E
Oedema
P = 0.14
Volume (mm 3)
100
80
60
40
20
0
Male
Female

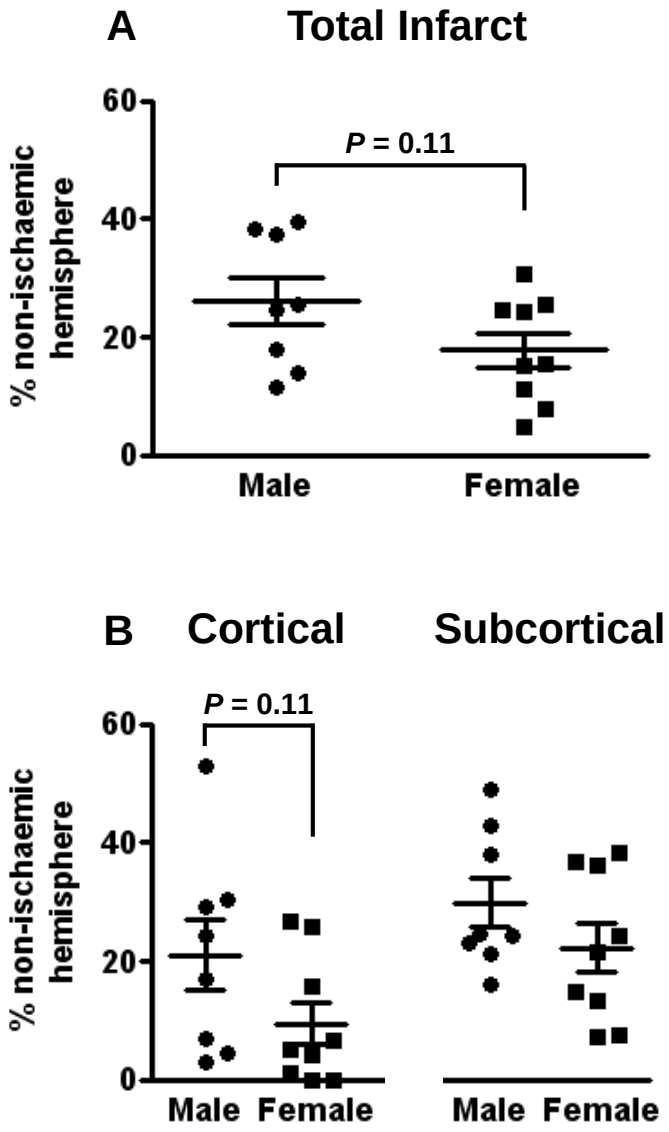

Figure 3.10. Cerebral infarct volume at 72 h after I-R in wild-type mice (measured as % of non-ischaemic hemisphere).

Total (**A**), and cortical and subcortical (**B**) cerebral infarct volumes were measured in male and female mice 72 h after I-R (males, $n = 8$; females, $n = 9$; unpaired t test). Infarct volume data are presented as mean ± SEM.

Figure 3.11. Cerebral infarct area distribution at 72 h after I-R in wild-type mice.

Total (**A**), cortical (**B**) and subcortical (**C**) cerebral infarct area distributions were measured in male and female mice 72 h after I-R (males, $n = 8$; females, $n = 9$; $^*P < 0.05$ at each point, unpaired t test). Infarct area data are presented as mean ± SEM.

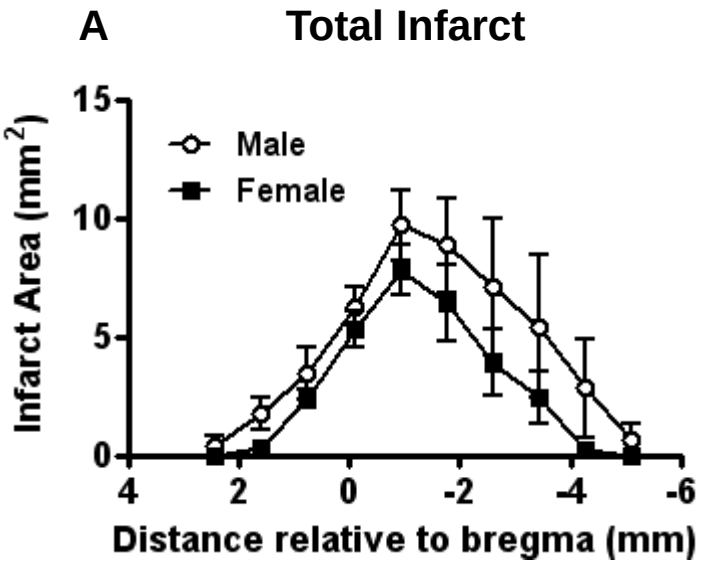
A
Total Infarct
Male
Female
Infarct Area (mm2)
15
10
5
0
4
2
0
-2
-4
-6
Distance relative to bregma (mm)

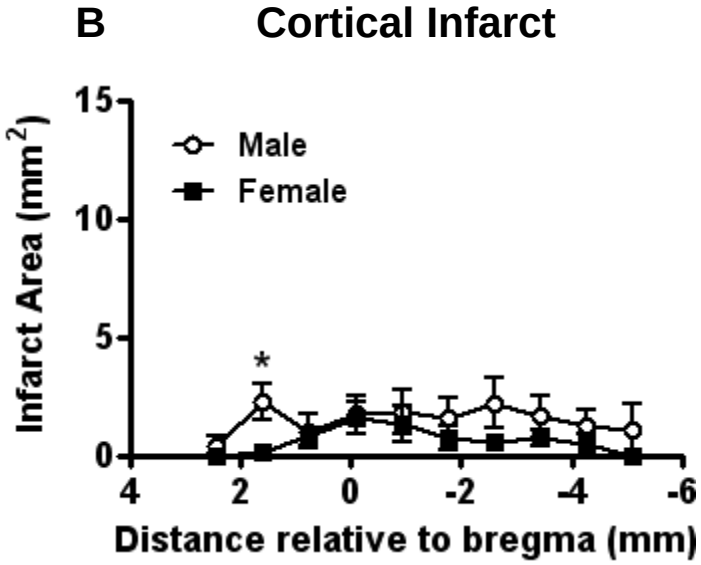
B
Cortical Infarct
Male
Female
Infarct Area (mm2)
*
15
10
5
0
4
2
0
-2
-4
-6
Distance relative to bregma (mm)

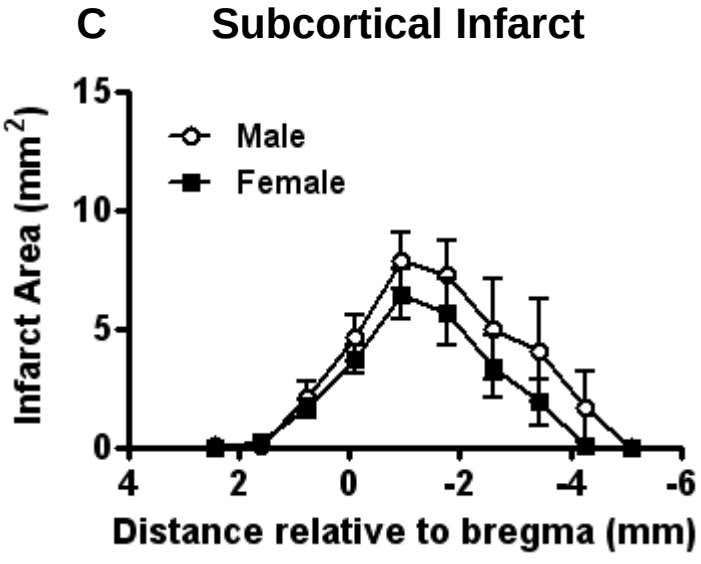
C
Subcortical Infarct
Male
Female
Infarct Area (mm2)
15
10
5
0
4
2
0
-2
-4
-6
Distance relative to bregma (mm)

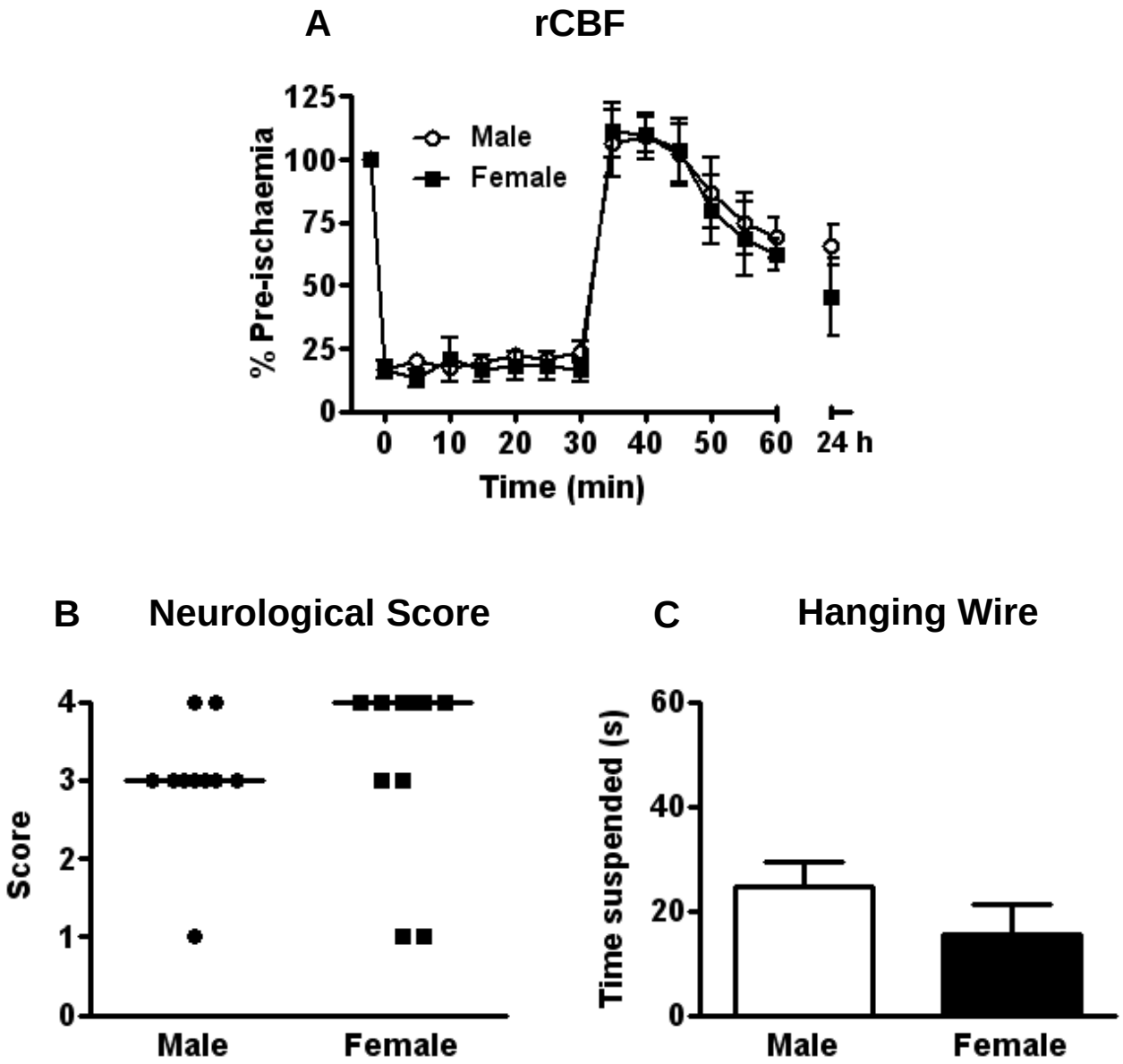

Figure 3.12. Regional cerebral blood flow (rCBF), neurological score and hanging wire at 24 h after I-R in Nox2-deficient mice.

rCBF was recorded in Nox2-deficient mice during and after 30 min MCAO, as well as at 24 h after MCAO (**A;** males, *n* = 10; females, *n* = 10). **B:** Neurological score 24 h after I-R (males, *n* = 10; females, *n* = 10). **C:** Hanging wire data 24 h following I-R (males, *n* = 10; females, *n* = 10). Neurological score data are presented as median, and rCBF and hanging wire data are presented as mean ± SEM.

Figure 3.13. Cerebral infarct and oedema volume at 24 h after I-R in Nox2-deficient mice (measured as mm^3).

Representative coronal brain sections are shown from a male (**A**) and a female (**B**) Nox2-deficient mouse 24 h after I-R with the infarct area outlined in white. Total (**C**), and cortical and subcortical (**D**) cerebral infarct volumes were measured in male and female Nox2-deficient mice 24 h after I-R (males, $n = 10$; females, $n = 10$). **E:** Oedema volume measured at 24 h in male and female Nox2-deficient mice (males, $n = 10$; females, $n = 10$). Data are presented as mean ± SEM.

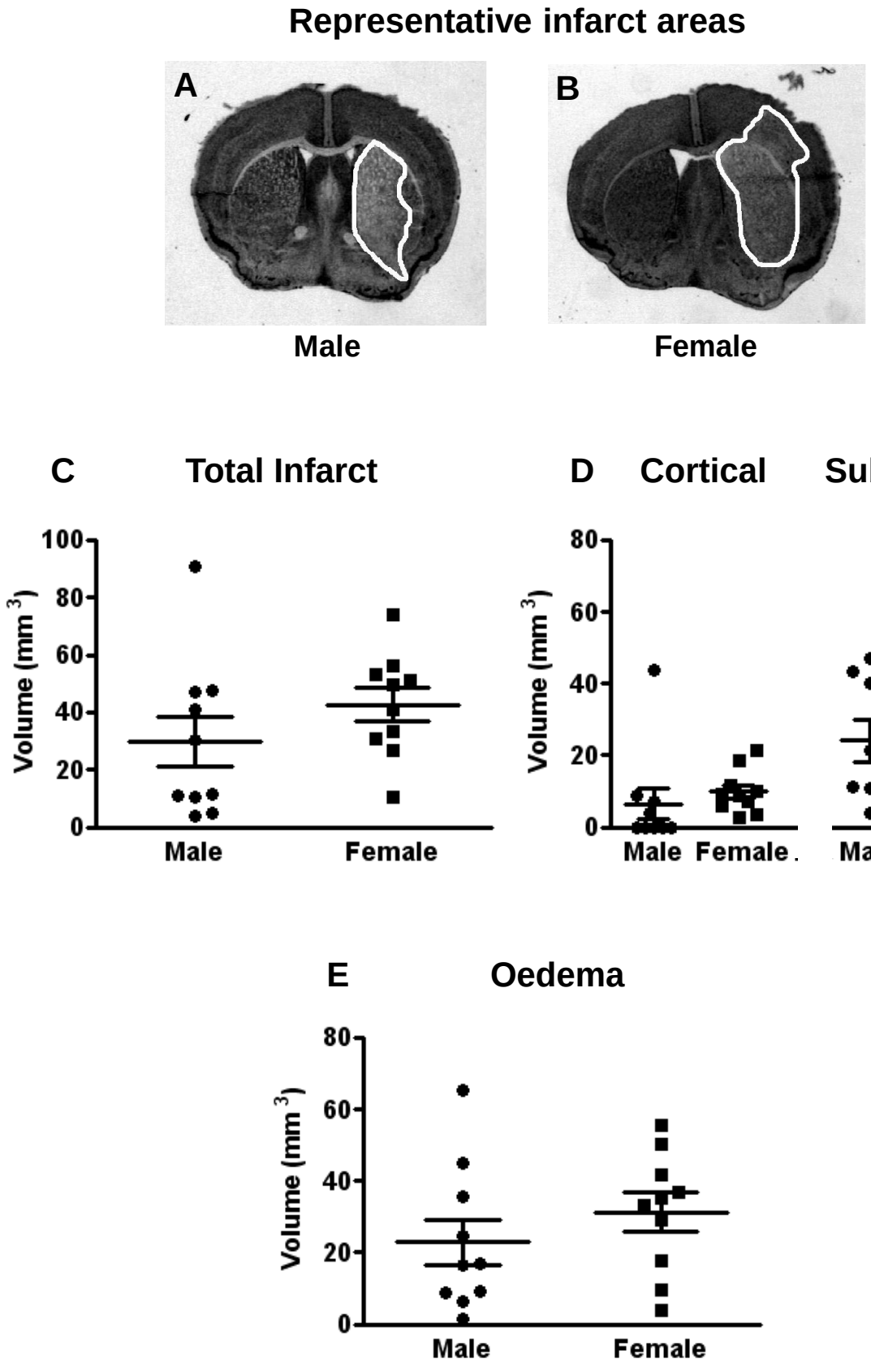
Representative infarct areas
A
B
Male
Female
C
Total Infarct
Volume (mm 3)
100
80
60
40
20
0
Male
Female
D
Cortical
Subcortical
Volume (mm 3)
80
60
40
20
0
Male
Female
Male
Female
E
Oedema
Volume (mm 3)
80
60
40
20
0
Male
Female

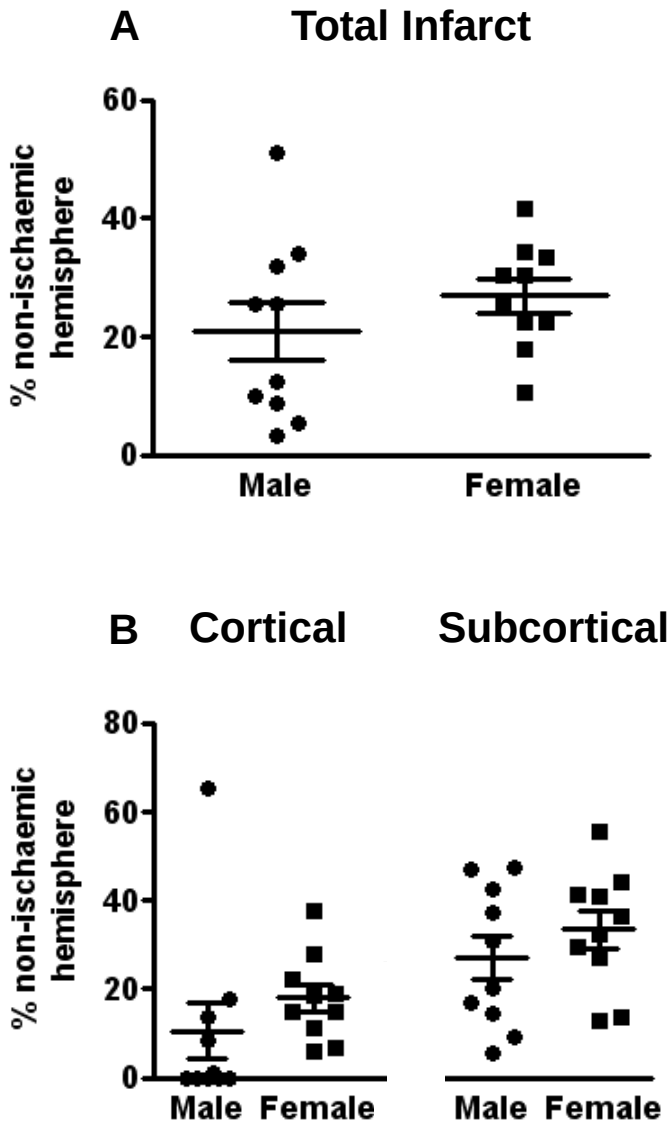

Figure 3.14. Cerebral infarct volume at 24 h after I-R in Nox2-deficient mice (measured as % of non-ischaemic hemisphere).

Total (**A**), and cortical and subcortical (**B**) cerebral infarct volumes were measured in male and female mice 24 h after I-R (males, $n = 10$; females, $n = 10$). Infarct volume data are presented as mean ± SEM.

Figure 3.15. Cerebral infarct area distribution at 24 h after I-R in Nox2-deficient mice.
Total (**A**), cortical (**B**) and subcortical (**C**) cerebral infarct area distributions were measured in male and female Nox2-deficient mice 24 h after I-R (males, $n = 10$; females, $n = 10$; $^*P < 0.05$ at each point, unpaired t test). Data are presented as mean ± SEM.

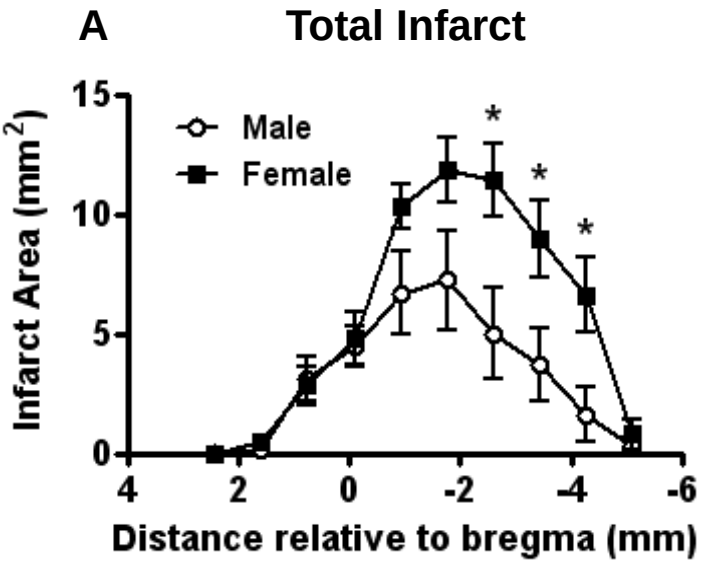
A
Total Infarct
Male
Female
Infarct Area (mm2)
15
10
5
0
4
2
0
-2
-4
-6
Distance relative to bregma (mm)
*
*
*

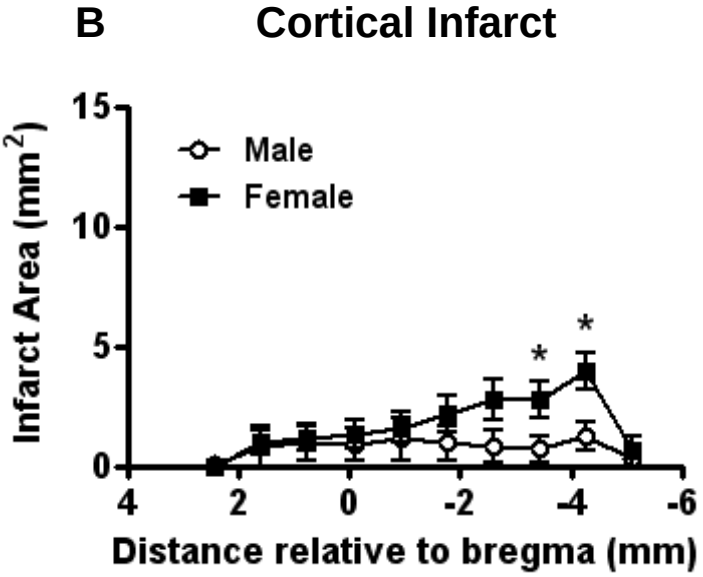
B
Cortical Infarct
Male
Female
Infarct Area (mm2)
15
10
5
0
4
2
0
-2
-4
-6
Distance relative to bregma (mm)
*
*

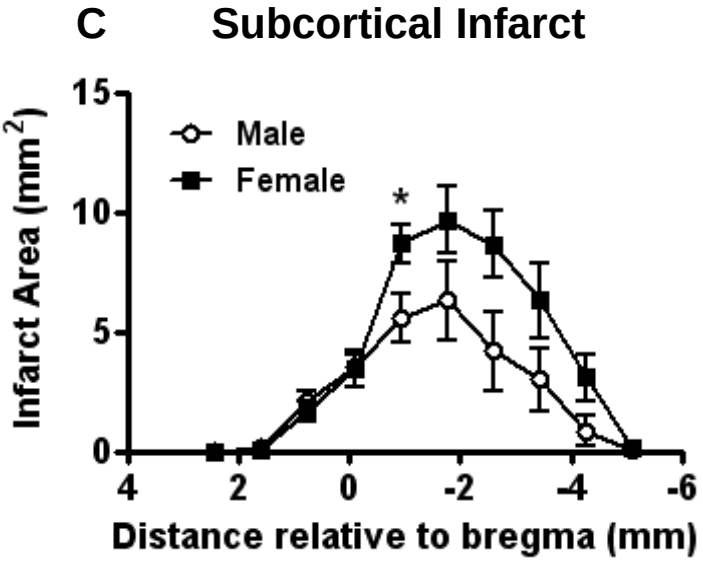
C
Subcortical Infarct
Male
Female
Infarct Area (mm2)
15
10
5
0
4
2
0
-2
-4
-6
Distance relative to bregma (mm)
*

3.4 DISCUSSION

This study has primarily assessed the effect of gender on the infarct volume which develops within 24 h following cerebral ischaemia in adult mice with or without reperfusion. We have provided evidence for the first time that the larger infarct volume present in males following ischaemia-reperfusion (I-R) is both reperfusion- and Nox2-dependent. Importantly, the magnitude of mean infarct volume was no greater at 72 h than at 24 h after I-R in either gender, and neurological function was significantly greater in females versus males at 72 h.

This is the first study to compare the effects of both gender and reperfusion on cerebral infarct volume produced after focal cerebral ischaemia. The data clearly indicate that whilst smaller infarcts develop in females than males within 24 h after I-R, there is no such gender difference in outcome if reperfusion is not instituted. It is clear that early (0.5 h) reperfusion leads to a reduced infarct volume in both genders, but the degree of salvage achieved by reperfusion was equivalent to only ~35 % in males whereas it was ~75 % in females. The smaller infarct volume in females after I-R is thought to be either due to the anti-inflammatory effects of oestrogen (Park *et al.*, 2006; Santizo *et al.*, 2000; Wen *et al.*, 2004), which will be discussed in more detail in Chapter 4, or its vasodilatory effects (Duckles and Krause, 2007). However, in our study, the neuroprotection observed in females is less likely to be due to different reductions in regional cerebral blood flow, as both genders were exposed to a similar relative ischaemic insult and underwent a similar relative level of reperfusion.

Importantly, our data also indicate that protection against infarct development in females is largely maintained for at least 72 h, suggesting that females ultimately do have smaller infarct volumes than males, rather than merely a delayed infarct progression.

It is possible that at 24 hours post-stroke, anaesthesia and surgery could still be affecting the mice, influencing behavioural scores, and consequently not representing an accurate assessment of differences between groups. Oedema may also be playing a role, as oedema volume is maximal at around 24 to 48 h after MCAO, and greatly reduced by 72 h. Moreover, in the present study at 72 h after I-R, female mice tended to have a smaller oedema volume than male mice, whereas there was no such trend at 24 h. For that reason, we also measured neurological deficits at 72 h, and in contrast to 24 h, where there was no difference between male and female mice; we found females to have a significantly longer hanging wire time compared to males at 72 h. This demonstrates a positive correlation between sensorimotor function and infarct volume, and strongly suggests that female mice have an improved outcome in both infarct size and function compared to male mice, following I-R.

Our laboratory and others have found that Nox2-containing NADPH oxidase contributes to infarct development in the male brain after stroke (Chen *et al.*, 2009; Jackman *et al.*, 2009a; Kahles *et al.*, 2007; Kunz *et al.*, 2007; Walder *et al.*, 1997). The cellular source(s) of the enzyme responsible for this brain damage is not well defined but may include circulating, bone-marrow-derived cells (Walder *et al.*, 1997), and we will develop this idea further in the following chapter. No previous study has examined the role of Nox2 in females after stroke. Unlike in wild-type mice, we found that cerebral infarct volume following I-R was not smaller in female versus male Nox2-deficient mice, and some of the potential mechanisms behind this will be discussed at length in the following chapter. It is unclear from the present data what role, if any, is played by Nox2 in females after stroke. Although not statistically significant, the tendency for a worsened stroke outcome in females versus males lacking Nox2 raises the intriguing possibility that this protein could in some way be beneficial in females after cerebral I-R.

Interestingly, infarcts were comprised of different proportions of cortical and subcortical tissue, depending on whether reperfusion was instituted, the length of reperfusion (23.5 or 71.5 h), and whether Nox2 was expressed. Reperfusion has been shown to reduce infarct development in the cortex (Heiss *et al.*, 2001). The main reason for this is that within 2 hours of reperfusion after a 30 min MCA occlusion, there is a full recovery of CBF in cortical regions, although striatal CBF still remains ~50 % lower than in the contralateral hemisphere (Takagi *et al.*, 1995). This is consistent with our findings that following 24 h I-NR in wild-type mice, approximately 50 % of the infarct comprised of cortical and subcortical tissue, whereas following I-R (whether 24 or 72 h in wild-type, or 24 h in Nox2-deficient mice), the cortical infarct accounted for less than the subcortical infarct. This strongly suggests that in a 30 min MCA occlusion, the cortex represents the potentially rescuable penumbral region. Furthermore, the proportion of infarct that comprised cortical tissue was lower in Nox2-deficient mice than wild-type mice, suggesting that Nox2 may be involved in producing reperfusion injury, which will be further discussed in Chapter 4.

The distribution of total, cortical and subcortical infarct areas showed very similar profiles after 24 or 72 h I-R or 24 h I-NR, with the peak infarct occurring in the middle of the hippocampal region in the total and subcortical infarcts. In wild-type mice, a similar profile between genders was observed. Interestingly, in Nox2-deficient mice, female mice had larger infarcts only posterior to bregma, towards the caudal extent of the infarct region. This could suggest that if Nox2 is in fact beneficial in females, then perhaps Nox2 is expressed more in the posterior regions of the forebrain, or that more Nox2 is entering the posterior regions of the forebrain, possibly via infiltrating immune cells. The infiltration of Nox2-expressing immune cells will be discussed further in the following chapter.

Given that female mice have a smaller body size than male mice, we considered that female mice may have a smaller brain. If this was the case, our measurements of infarct volume as mm^3 would be confounded when comparing the genders. We therefore weighed brains from naive male and female wild-type mice (ie. not subjected to stroke surgery), and found no difference. In addition to this, we also measured infarct volume as a percentage of the non-ischaemic hemisphere, as an alternative means of comparing genders which was independent of actual brain size. We found very concordant results in all groups comparing total, cortical and subcortical infarct volume measured as mm^3 or as a percentage of the non-ischaemic hemisphere. Even in Nox2-deficient mice, whose brains were not weighed, we found similar comparative data regardless of method of calculation.

In the present study, as well as in Chapter 4, we chose to focus on the model of cerebral I-R, rather than I-NR, because we found a gender difference following I-R, and wanted to investigate the mechanisms further. As mentioned in the introduction, reperfusion does not often occur in the clinic, however, revascularisation success rates are improving. rt-PA is becoming more utilised, since the therapeutic time window increased to 4.5 hours after stroke onset. In addition, new technologies, such as using rt-PA in combination with ultrasound (Alexandrov *et al.*, 2004; Tsivgoulis *et al.*, 2010), or using intra-arterial revascularisation techniques in patients that are ineligible for rt-PA or who don't achieve recanalisation through the use of i.v. rt-PA (Smith *et al.*, 2008) are increasing the number of successful revascularisations. Therefore, it is very important to fully understand both the beneficial and detrimental consequences of reperfusion.

In summary, our study provides the first evidence that the smaller infarct volume that develops in adult females versus males following cerebral ischaemia is reperfusion-dependent, and moreover, this gender difference is dependent on Nox2 expression in males.

Chapter 4:

Mechanisms Underlying the Effects of Gender and Reperfusion on Cerebral Infarct Size after Stroke

4.1 INTRODUCTION

Experimental cerebral ischaemia-reperfusion (I-R) studies, as well as our own findings from Chapter 3, report that stroke outcomes are better in female rodents compared to male rodents; and this is known to be oestrogen-dependent (Alkayed *et al.*, 1998; Park *et al.*, 2006; Zhang *et al.*, 1998b). In Chapter 3, we also found that females do not have a smaller infarct volume following ischaemia with no reperfusion (I-NR); when the occlusion remains in place. Reperfusion typically results in an increase in inflammation. The anti-inflammatory effects of oestrogen are believed to provide females protection from post-ischaemic cerebral injury via several mechanisms which may include reductions in leukocyte adhesion (Santizo *et al.*, 2000), nuclear factor-κB (NF-κB) activation (Wen *et al.*, 2004) and/or inducible nitric oxide synthase (iNOS) expression (Park *et al.*, 2006; Wen *et al.*, 2004). Thus, it is perhaps not surprising that female gender (or oestrogen treatment) is protective in the setting of cerebral I-R. However, these anti-inflammatory properties of oestrogen may be less beneficial and less relevant to outcome in the continued absence of blood flow to the ischaemic core (eg. in I-NR), where inflammation may play less of a crucial role.

Increased expression of the key pro-inflammatory proteins, the NADPH oxidase catalytic subunit Nox2 (gp91*phox*) (Kusaka *et al.*, 2004; McCann *et al.*, 2008), cyclo-oxygenase-2 (Cox-2) (Miettinen *et al.*, 1997; Nogawa *et al.*, 1997; Planas *et al.*, 1995), and the vascular cell adhesion molecule-1 (VCAM-1) (Justicia *et al.*, 2006), have been reported to occur in the brains of male rodents following I-R, but expression of these proteins have not yet been examined in females following I-R. Furthermore, increased expression of the Cox-2 protein has been reported to occur in the ischaemic hemisphere of male rats following I-NR (Yokota *et al.*, 2004), but this has not yet been examined in females, nor have Nox2 or VCAM-1 protein expression been examined in either gender following I-NR. In addition, recent work in our laboratory found that the deletion of the NADPH oxidase catalytic subunit Nox1 in male mice produced a slightly larger

cortical infarct, but had no effect on total infarct volume (Jackman *et al.*, 2009b). The effect of stroke on protein expression of Nox1 has not been investigated in either male or female rodents.

It is well established that local and systemic inflammatory responses occur following cerebral ischaemia, and contribute to infarct damage (For reviews see Amantea *et al.,* 2009; Huang *et al.,* 2006). However, it was only recently recognised that changes in the immune system occur following stroke. A generalised immunodepression in the spleen, thymus, lymph nodes and the circulation occurs over the several days following cerebral ischaemia (Haeusler *et al.*, 2008; Liesz *et al.*, 2009a; Offner *et al.*, 2006b; Prass *et al.*, 2003), which then increases the risk of infection, and consequently, mortality (Chamorro *et al.*, 2007). However, in rodents, this systemic immunodepression has only been confirmed in males or a combination of males and females (Liesz *et al.*, 2009a; Offner *et al.*, 2006b; Prass *et al.*, 2003), and the levels of specific leukocytes have not yet been studied in female rodents or in a filament model of I-NR. The extent to which the various leukocytes, including lymphocytes, are reduced, appears to reflect the degree of the ischaemic insult (Liesz *et al.*, 2009a; Offner *et al.*, 2006b; Prass *et al.*, 2003), and the duration of reperfusion (Offner *et al.*, 2006b). The immunodepression is largely due to increased apoptosis of these cells in the spleen and the thymus (Liesz *et al.*, 2009a; Offner *et al.*, 2006b; Prass *et al.*, 2003). However, another possible reason for the reduced circulating leukocyte levels is the infiltration of these cells into the brain (Campanella *et al.*, 2002; Stevens *et al.*, 2002).

Recent studies suggest that T lymphocytes contribute to the brain damage caused by cerebral I-R (Hurn *et al.*, 2007; Kleinschnitz *et al.*, 2010b; Shichita *et al.*, 2009; Yilmaz *et al.*, 2006). T lymphocytes are believed to enter the brain parenchyma within 24 h after stroke (Jander *et al.*, 1995), and to produce damage via the generation of pro-inflammatory mediators (Arumugam *et al.*, 2005). Interestingly, impaired T lymphocyte proliferation has been observed following ischaemic stroke in both male rodents (Gendron *et al.*, 2002; Offner *et al.*, 2006b) and male

humans (Czlonkowska *et al.*, 1979), which reflects a reduced function of this cell type, but has not yet been looked at in female rodents. The degree of impaired proliferation of T lymphocytes could thus be an important factor in the smaller infarct volume observed in female mice in Chapter 3.

T lymphocytes express a functional NADPH oxidase containing Nox2 (Jackson *et al.*, 2004; Purushothaman and Sarin, 2009), and superoxide produced by this isoform of NADPH oxidase is now established to play a detrimental role in the brain following stroke (Jackman *et al.*, 2009a; Kahles *et al.*, 2007; Walder *et al.*, 1997), which appears to involve an effect of circulating leukocytes (Walder *et al.*, 1997). Molecular mechanisms mediating the post-ischaemic brain damage caused by infiltrating T lymphocytes are largely unknown, including whether their generation of Nox2-derived superoxide is altered following stroke in males or females.

Hence, we first investigated whether expression of key pro-inflammatory proteins was correlated with the gender-related degree of salvage achieved by reperfusion shown in Chapter 3. Secondly, we examined whether gender had an effect on the infiltration and localisation of T lymphocytes and Nox2 protein in brain sections. Thirdly, we tested the effect of gender, ischaemia and reperfusion on the levels of various immune cells in the spleen and the blood. Fourthly, we assessed the effect of gender and I-R on proliferation of T lymphocytes. Lastly, we tested whether Nox2-derived superoxide generation by T lymphocytes is altered after I-R in males and/or females.

4.2 MATERIALS AND METHODS

4.2.1 Animals

Please refer to section 3.2.1.

4.2.2 Focal cerebral ischaemia

Focal cerebral ischaemia was induced by transient or permanent intraluminal filament occlusion of the right middle cerebral artery (MCA) as described in section 2.3 of General Methods. At 24 h, mice were killed, and brains removed and frozen as described in section 2.5 of General Methods.

4.2.3 Measurement of protein expression of Cox-2, Nox1, Nox2 and VCAM-1

Expression of the pro-inflammatory proteins cyclo-oxygenase-2 (Cox-2), NADPH oxidase catalytic subunits Nox1 and Nox2, and the vascular cell adhesion molecule-1 (VCAM-1) were measured in homogenates of the ischaemic (right) hemisphere using Western blotting. Please refer to section 2.7 of General Methods for details. Anti-mouse Cox-2 and anti-mouse Nox2 monoclonal antibodies (mAbs) were purchased from BD Biosciences (North Ryde, NSW, Australia), anti-human Nox1 polyclonal antibodies were purchased from Antagene (Mountain View, CA, USA), anti-mouse VCAM-1 mAbs were purchased from Santa Cruz (Santa Cruz, CA, USA) and anti-rabbit β-actin polyclonal antibodies were purchased from Cell Signaling Technology (Danvers, MA, USA). The 1 mm thick gels onto which the proteins were loaded were 7.5 % polyacrylamide (for Cox-2, Nox1 and Nox2) and 10 % (for VCAM-1). The optimal dilutions for each primary antibody were as follows: 1:500 for Cox-2, 1:1000 for Nox2, 1:250 for VCAM-1, and 1:2000 for Nox1 and β-actin. The membranes were then incubated with a horseradish peroxidase–conjugated anti-mouse (Cox-2 and Nox2; purchased from ImmunoResearch; West Grove, PA, USA), anti-rat (VCAM-1; purchased from Santa Cruz) or anti-rabbit (Nox1 and β-actin; purchased from Dako; Glostrup, Denmark) antibody. Relative intensities were normalised to the intensity of corresponding bands for β-actin and, within a single gel, bands of samples from male sham-operated and female sham-operated mice were taken to be equal to 1, and all other bands were normalised relative to their corresponding gender sham.

4.2.4 Localisation of T lymphocytes and Nox2

The localisation of $CD3^+$ cells (T lymphocytes) and Nox2-expressing cells in brain sections of sham-operated mice and mice 24 h after I-R was performed by immunohistochemistry and immunofluorescence, as described in section 2.9 of General Methods.

Firstly, for the localisation of $CD3^+$ cells, multiple serial coronal sections of 30 μm were taken at the paraventricular nucleus (bregma -0.58 mm) and the mid hippocampus (bregma -1.82 mm), and thaw-mounted onto poly-L-lysine coated glass slides (0.1 % poly-L-lysine in dH_2O). Tissue sections were fixed in acetone for 15 min and washed in 50 mM tris-buffered saline (TBS; pH 8.4; 3 x 5 min) before incubation in a humid chamber in 10 % goat serum (Abcam; Cambridge, MA, USA) in TBS for 2 h to block non-specific binding. Sections were then incubated for 1 h in anti-rabbit CD3 polyclonal antibody (1:250; Abcam). Sections were washed in TBS (3 x 5 min), blocked with a peroxidase blocking agent (Dako) for 15 min and stained using the DAKO EnVision+ system (Dako). Sections were then incubated for 45 min with a peroxidase-labelled polymer conjugated to a goat anti-rabbit antibody (Invitrogen; Carlsbad, CA, USA), washed in TBS (3 x 5 min), and followed by incubation with diaminobenzidine (Dako) for 5 min. Sections were then washed in TBS (3 x 5 min), mounted in aquatex (Merck; Darmstadt, Germany) and cover-slipped. Staining was analysed on an Olympus light microscope (Olympus; Hamburg, Germany) by two observers blinded to the identity of experimental groups, who counted $CD3^+$ cells within five high-power (200x) fields within the infarct and peri-infarct zones of the ipsilateral striatum and cortex. Infarct and peri-infarct zones were verified from thionin-stained adjacent sections (see section 2.5 of General Methods for details on thionin staining).

To determine whether $CD3^+$ cells were co-localised with Nox2 protein in the infarct core of the striatum, sections were simultaneously incubated with two primary antibodies raised in different species. Coronal tissue sections were fixed in 4 % paraformaldehyde (PFA) for 15 min and

washed in phosphate buffered saline (PBS; pH 7.4; 3 x 10 min). The tissue sections were then incubated overnight in anti-mouse Nox2 mAb (1:1000; BD Biosciences) and anti-rabbit CD3 polyclonal antibody (1:50; Abcam) in a humid chamber. The following day, tissues were washed in PBS (3 x 10 min) to remove any excess antibody, and incubated in a fluorescein isothiocyanate (FITC)-conjugated goat anti-mouse antibody (1:200; Zymed Labratories; South San Francisco, CA, USA) and Texas Red-labelled goat anti-rabbit antibody (1:200; Zymed Laboratories) for 3-4 h in a humid chamber. The sections were then washed in PBS (3 x 10 min), mounted in VECTASHIELD mounting medium (Vector laboratories; Burlingame, CA, USA) and cover-slipped. Tissue mounted slides were viewed and photographed on a Leica confocal scanning laser system (Leica Microsystems; Wetzlar, Germany). The appropriate control experiments were performed to ensure that no cross-reactivity occurred. This involved incubating brain sections following stroke with all of the possible combinations of primary and secondary antibodies. Our control experiments showed that FITC fluorescence was not visible using the Texas Red filter set and vice versa. Thus, the Nox2 and $CD3^+$ immunoreactivity were both concluded to be specific. Staining was analysed by counting the number of Nox2-expressing $CD3^+$ cells in the infarct core of each section, and expressing this number as a percentage of the total number of Nox2-expressing cells.

4.2.5 Isolation of leukocytes from spleen and blood

Mice were killed at 24 h by isofluorane inhalation and exsanguination, and leukocytes were isolated from spleen and blood as described in section 2.10 of General Methods.

4.2.6 Analysis of cell populations

Fluorescence flow cytometric analyses were performed to determine the numbers of T lymphocytes, B lymphocytes, monocytes and neutrophils in spleen and blood, as described in section 2.11 of General Methods. Primary antibodies conjugated with fluorophores were: the

FITC-conjugated Armenian hamster anti-mouse CD3 (clone 145-2C11; 1:100), phycoerythrine (PE)-conjugated anti-GR1 (clone RB6-8C5; 1:100), allophycocyanin (APC)-conjugated anti-B220 (clone RA3-6B2; 1:100) (eBioscience; San Diego, CA, USA), APC.Cy7-conjugated anti-CD4 (clone GK1.5; 1:300), PE–conjugated anti-CD8 (clone 53-6.7; 1:100), and FITC-conjugated anti-CD11b (clone M1/70; 1:200) (BD Biosciences). All antibodies were rat anti-mouse unless specified. Isotype control antibodies were: the PE-conjugated anti-IgG2a (clone eBR2a; eBioscience), FITC-conjugated anti-IgG2a-κ (clone R35-95; BD Biosciences) and APC.Cy7-conjugated anti-IgG2a-κ (clone G155-178; BD Biosciences).

4.2.7 T lymphocyte proliferation assay

T lymphocytes isolated from naïve mice and mice 24 h after I-R, were stimulated for 24, 48 and 72 h by exposure to the anti-mouse CD28 mAb (clone 37.51) in combination with the immobilised anti-mouse CD3 mAb (clone 145-2C11; eBioscience). Three standard 96-well flat-bottom tissue-culture plates were coated with anti-CD3 antibody (3 μg/ml in sterile PBS) at 50 μl/well and left overnight at 4 °C. Triplicate wells were used for each sample. Mice were culled, the spleen aseptically removed and single-cell suspensions were prepared as described in section 2.10 of General Methods. Once a suspension of leukocytes was prepared, it was resuspended in RPMI 1640, supplemented with 10 % foetal calf serum (FCS), 1 % Penicillin/Streptomycin, 1 % L-Glutamate and 0.1 % β-mercaptoethanol. The cells were then counted with trypan blue dye exclusion and $2x10^5$ cells were placed into each well. $2x10^5$ cells in triplicate were also collected in an eppendorf tube and stored at -20 °C for baseline Day 0 data. RPMI media was added to each well, to make the volume up to 100 μl, and then 100 μl of 4 μg/ml anti-CD28 antibody in RPMI media was added to all the wells. These tissue-culture plates were then incubated at 37 °C and 5 % CO_2 in air. Each day one of the plates was removed and 170 μl taken out of each well, making sure not to touch the bottom, so as not to disturb the cells. This solution was discarded, leaving ~30 μl in each well to run the assay. The plate was then

stored at -20 °C and the level of proliferation was determined using a CyQUANT kit (Invitrogen), as per the manufacturer's instructions. This assay displays a linear correlation (r^2 = 0.999) between cell number and fluorescence. Briefly, cells were lysed, green fluorescent dye was added, and each sample was transferred to a black 96-well plate. Cell number was quantified as fluorescence using a plate reader (BMG Fluostar Optima; BMG LABTECH; Offenburg, Germany), with excitation set at 480 nm and emission detection set at 520 nm, as the dye fluoresces when bound to nucleic acids. In all experiments, the triplicates were averaged, and the results were calculated by normalising the average fluorescence signal to the baseline Day 0 T lymphocyte number.

4.2.8 Measurement of superoxide production by T lymphocytes

After isolation of leukocytes, a purified suspension of T lymphocytes was obtained using the Dynal® Mouse T Cell Negative Isolation Kit (Invitrogen). Please refer to section 2.12 of General Methods for details. Basal and phorbol 12,13-dibutyrate (PDB; 1 μM)-stimulated superoxide production by T lymphocytes from blood and spleens of mice following I-R was then measured by 100 μmol/L L-012-enhanced chemiluminescence, as described in section 2.13 of General Methods.

4.2.9 Drugs and chemicals

As per section 2.14 of General Methods.

4.2.10 Statistical analysis

All data are presented as mean ± standard error. Statistical analyses were performed using GraphPad Prism version 5 (GraphPad Software Inc., San Diego, CA, USA). Between-group comparisons were analysed as described in section 2.15 of General Methods. Immunohistochemistry data was compared using a Student's unpaired *t* test. T lymphocyte

proliferation was compared using a one-way analysis of variance (ANOVA) with Bonferroni *post-hoc* test. Group numbers are shown in parentheses. Statistical significance was accepted when $P < 0.05$.

4.3 RESULTS

4.3.1 Effect of gender, ischaemia and reperfusion on pro-inflammatory protein expression

To investigate molecular mechanisms underlying the gender difference in infarct volume that occurred as a result of reperfusion, shown in Chapter 3, we examined expression of several pro-inflammatory proteins including Cox-2, the NADPH oxidase catalytic subunits Nox1 and Nox2, and VCAM-1, in the ischaemic hemisphere 24 h after I-R and I-NR.

Representative Western blots for Nox2 in male and female mice following sham surgery or I-R are shown in Figure 4.1A. Densitometric analyses of the immunoreactive band intensities are shown in Figures 4.1B and C. In male mice following I-R, Nox2 protein was expressed in the ischaemic hemisphere at a significantly greater level compared with sham-operated mice ($P < 0.05$, $n = 9$). In contrast, we found no significant change in Nox2 expression in the ischaemic hemisphere of female mice following I-R ($n = 6$-7; Figure 4.1B). Following I-NR, both male and female mice expressed significantly greater levels of Nox2 protein in the ischaemic hemisphere compared with sham-operated mice ($P < 0.05$, $n = 7$-10; Figure 4.1C). There was no significant difference between genders following I-NR (Figure 4.1C).

Representative Western blots for Cox-2 in male and female mice following sham surgery or I-R are shown in Figure 4.1D. Densitometric analyses of the immunoreactive band intensities are shown in Figures 4.1E and F. In male mice following I-R, Cox-2 protein was expressed at a significantly greater level compared with sham-operated mice ($P < 0.05$, $n = 11$). In contrast, we found no significant change in Cox-2 expression in female mice following I-R ($n = 8$; Figure

4.1E). Following I-NR, both male and female mice expressed significantly greater levels of Cox-2 protein in the ischaemic hemisphere compared with sham-operated mice ($P < 0.05$, $n = 8$-9; Figure 4.1F). There tended to be a greater Cox-2 expression in male mice compared to female mice following I-NR, although this did not reach statistical significance ($P = 0.13$; Figure 4.1F).

Representative Western blots for VCAM-1 in male and female mice following sham surgery or I-R are shown in Figure 4.2A. Densitometric analyses of the immunoreactive band intensities are shown in Figures 4.2B and C. In male mice following I-R, VCAM-1 protein was expressed at a significantly greater level compared with sham-operated mice ($P < 0.05$, $n = 9$). In contrast, we found no significant change in VCAM-1 expression in female mice following I-R ($n = 9$; Figure 4.2B). Following I-NR, both male and female mice expressed significantly greater levels of VCAM-1 protein in the ischaemic hemisphere compared with sham-operated mice ($P < 0.05$, $n = 8$-9; Figure 4.2C). There was no significant difference between genders following I-NR (Figure 4.2C).

Representative Western blots for Nox1 in male and female mice following sham surgery or I-R are shown in Figure 4.2D. Densitometric analyses of the immunoreactive band intensities are shown in Figures 4.2E and F. Neither I-R ($n = 3$-4) nor I-NR ($n = 5$) had any effect on protein expression levels of Nox1 in the ischaemic hemisphere (Figures 4.2D-F).

4.3.2 Localisation of T lymphocytes and Nox2

Twenty-four h after I-R, $CD3^+$ cells (i.e. T lymphocytes) were found to be present within cerebral infarct and also in peri-infarct areas at a frequency that was ~7-fold greater in males than in females (70±21 versus 10±5 cells per high power field; $P = 0.01$; $n = 15$ fields from 3 mice per group). Immunofluorescence studies confirmed the presence of Nox2-containing cells (Figures

4.3A-B) and also $CD3^+$ cells (Figures 4.3C-D) within the striatal infarct core of males and females 24 h following I-R. When these images were overlayed, it was apparent that, at 24 h in the infarcted core tissue of both genders, Nox2 was frequently co-localised with CD3 (Figures 4.3E-F). The frequency of Nox2-expressing cells in the infarct core that also expressed CD3 was similarly high in males (95 % - 99 %, $n = 3$) and females (94 % - 100 %, $n = 3$) and overall was estimated to be 97.5±1.1 % ($n = 6$).

4.3.3 Effect of gender, ischaemia and reperfusion on immune cell numbers in spleen and blood

4.3.3.1 Spleen

In the spleen, 24 h after I-R or I-NR ($n = 6$-9), a similar profile was observed, showing reduced levels in stroked mice of either protocol compared to sham-operated mice in all the immune cells analysed (i.e. T lymphocytes, B lymphocytes and neutrophils), except for $CD11b^+$ cells (monocytes), which showed a non-significant increase in the female group following I-NR (Figure 4.4A-F). There were significantly fewer $CD3^+$ and $CD4^+$ cells (total and helper T lymphocytes, respectively), and $B220^+$ cells (B lymphocytes) in the spleen 24 h after I-R and I-NR in male mice in comparison to sham-operated mice ($P < 0.05$, Figure 4.4A, B & D). The only statistically significant difference in female mice was a reduction in B lymphocytes following I-R ($P < 0.05$, Figure 4.4D).

4.3.3.2 Blood

In the blood, no consistent profile was observed between the levels of various immune cells following I-R and I-NR ($n = 5$-7; Figures 4.5A-F). Apart from a significant reduction in B lymphocytes in male mice after I-R (Figure 4.5D), circulating levels of immune cells were not significantly altered at 24 h following I-R or I-NR, in either male or female mice (Figures 4.5A-F).

4.3.4 Effect of gender and I-R on T lymphocyte proliferation

Twenty-four h after stimulation by anti-CD3 and anti-CD28 antibodies, T lymphocytes isolated from the spleens of naive male and female mice, and male and female mice 24 h after I-R, increased in number (n = 4 per group; Figure 4.6). However, neither gender nor I-R had any statistically significant effect on T lymphocyte proliferation levels at 24 h. Compared to T lymphocyte levels at 24 h, T lymphocyte levels in naive male and female mice increased by ~84 and ~94 % respectively, at 48 h, and by ~114 and ~128 % at 72 h respectively. Naive female mice tended to have higher T lymphocyte proliferation levels at 48 h and 72 h compared to naive male mice, although this difference did not reach statistical significance (Figure 4.6). After 48 and 72 h of stimulation, although not significantly different, there was a trend for I-R to reduce T lymphocyte proliferation in both male and female mice. After 48 h, male and female mice had ~30 and ~42 % less T lymphocyte proliferation than male and female naive mice, respectively, and after 72 h, male and female mice had ~24 and ~40 % less T lymphocyte proliferation, respectively (Figure 4.6).

4.3.5 Effect of I-R on the generation of Nox2-derived superoxide by T lymphocytes

Superoxide generation by T lymphocytes ($CD3^+$ cells) isolated from the blood of control male wild-type mice was slightly augmented (by ~4-fold above basal) by incubation with the Nox2 activator, PDB (n = 5; Figure 4.7A). However, PDB-stimulated superoxide release was profoundly greater (a further ~15-fold) from T lymphocytes isolated from the blood of male wild-type mice 24 h after I-R ($P < 0.05$ vs. PDB-stimulated control; n = 5; Figure 4.7A). Moreover, in separate experiments we found that PDB-stimulated superoxide production after I-R was markedly greater (~7-fold) in circulating T lymphocytes from males versus females ($P < 0.05$; n = 6 per group; Figure 4.7C). The effect of PDB to stimulate superoxide release from circulating T lymphocytes was subsequently found to be Nox2-dependent, as neither PDB nor I-R had any significant effect on superoxide release from T lymphocytes isolated from the blood

of Nox2-deficient mice (n = 3-5; Figure 4.7D). After stroke, PDB-induced superoxide generation was up to ~1,000-fold higher in T lymphocytes from blood versus spleen (see Figures 4.7A and 4.7B). However, neither stroke nor PDB had any significant effect on superoxide generation from spleen-derived T lymphocytes from wild-type male mice (n = 5; Figure 4.7B).

Figure 4.1. Nox2 and Cox-2 protein expression.

Representative Western blots and densitometric analyses of immunoreactive band intensities showing expression of the NADPH-oxidase catalytic subunit Nox2 (**A-C**), and cyclo-oxygenase-2 (Cox-2; **D-F**) in ischaemic hemispheres of male and female mice subjected to sham surgery or ischaemia-reperfusion (I-R; **A-B** & **C-D**) or ischaemia-no reperfusion (I-NR; **C** & **F**). The dotted line in **C** & **F** represents the expression level observed in the sham group of each gender. Values are expressed as relative intensity normalised to β-actin intensity, and then normalised relative to gender-matched control, and are presented as mean ± SEM (n = 6-11; $^*P < 0.05$ vs. matched sham group, unpaired t test).

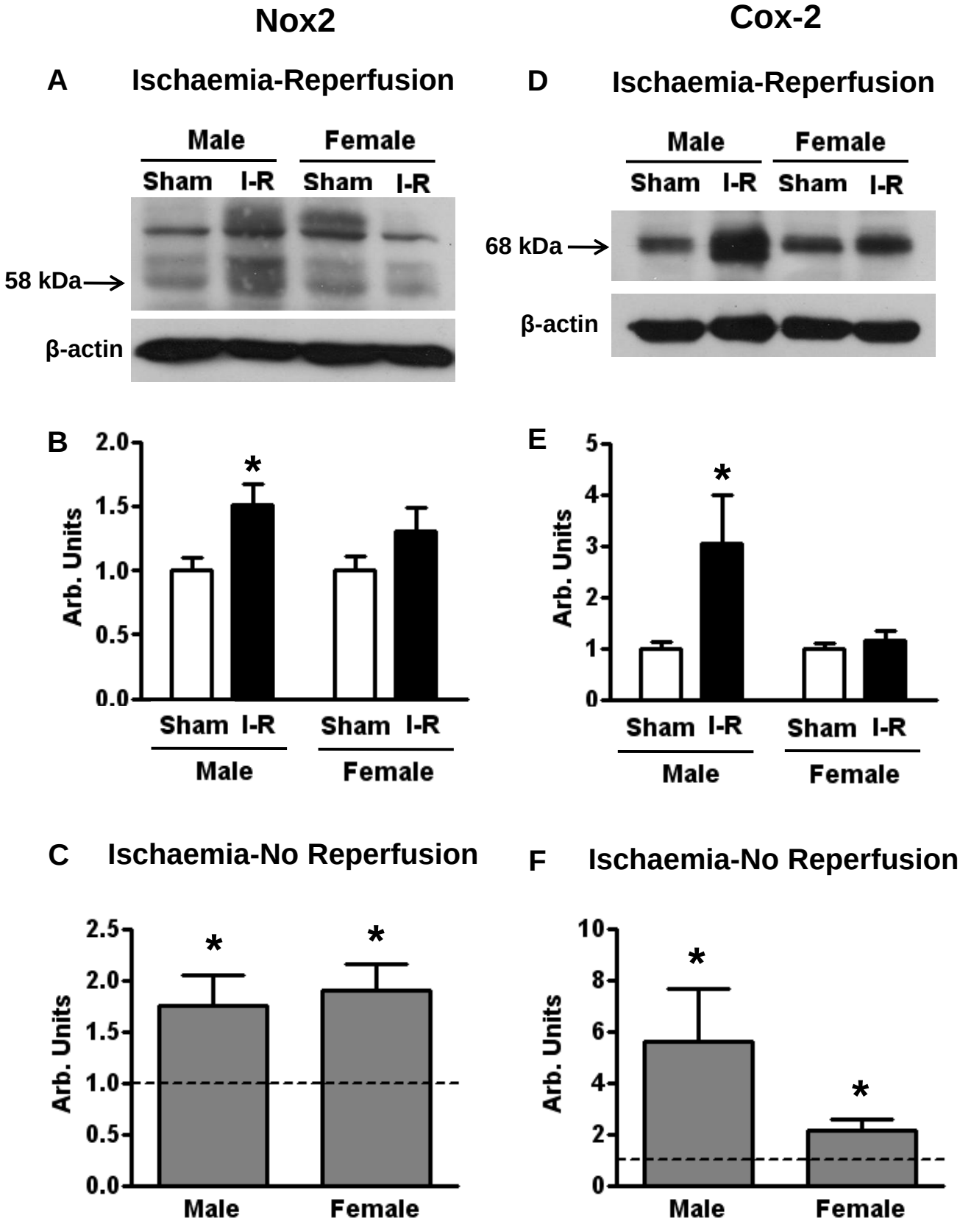
Nox2
A
Ischaemia-Reperfusion
Male
Female
Sham
I-R
Sham
I-R
58 kDa
β-actin
B
Arb. Units
2.0
1.5
1.0
0.5
0.0
*
Sham
I-R
Sham
I-R
Male
Female
C
Ischaemia-No Reperfusion
Arb. Units
2.5
2.0
1.5
1.0
0.5
0.0
*
*
Male
Female
Cox-2
D
Ischaemia-Reperfusion
Male
Female
Sham
I-R
Sham
I-R
68 kDa
β-actin
E
Arb. Units
5
4
3
2
1
0
*
Sham
I-R
Sham
I-R
Male
Female
F
Ischaemia-No Reperfusion
Arb. Units
10
8
6
4
2
0
*
*
Male
Female

Figure 4.2. VCAM-1 and Nox1 protein expression.

Representative Western blots and densitometric analyses of immunoreactive band intensities showing expression of the vascular cell adhesion molecule-1 (VCAM-1; **A-C**), and the NADPH-oxidase catalytic subunit Nox1 (**D-F**) in ischaemic hemispheres of male and female mice subjected to sham surgery or ischaemia-reperfusion (I-R; **A-B** & **C-D**) or ischaemia-no reperfusion (I-NR; **C** & **F**). The dotted line in **C** & **F** represents the expression level observed in the sham group of each gender. Values are expressed as relative intensity normalised to β-actin intensity, and then normalised relative to gender-matched control, and are presented as mean ± SEM (n = 3-9; *P < 0.05 vs. matched sham group, unpaired t test).

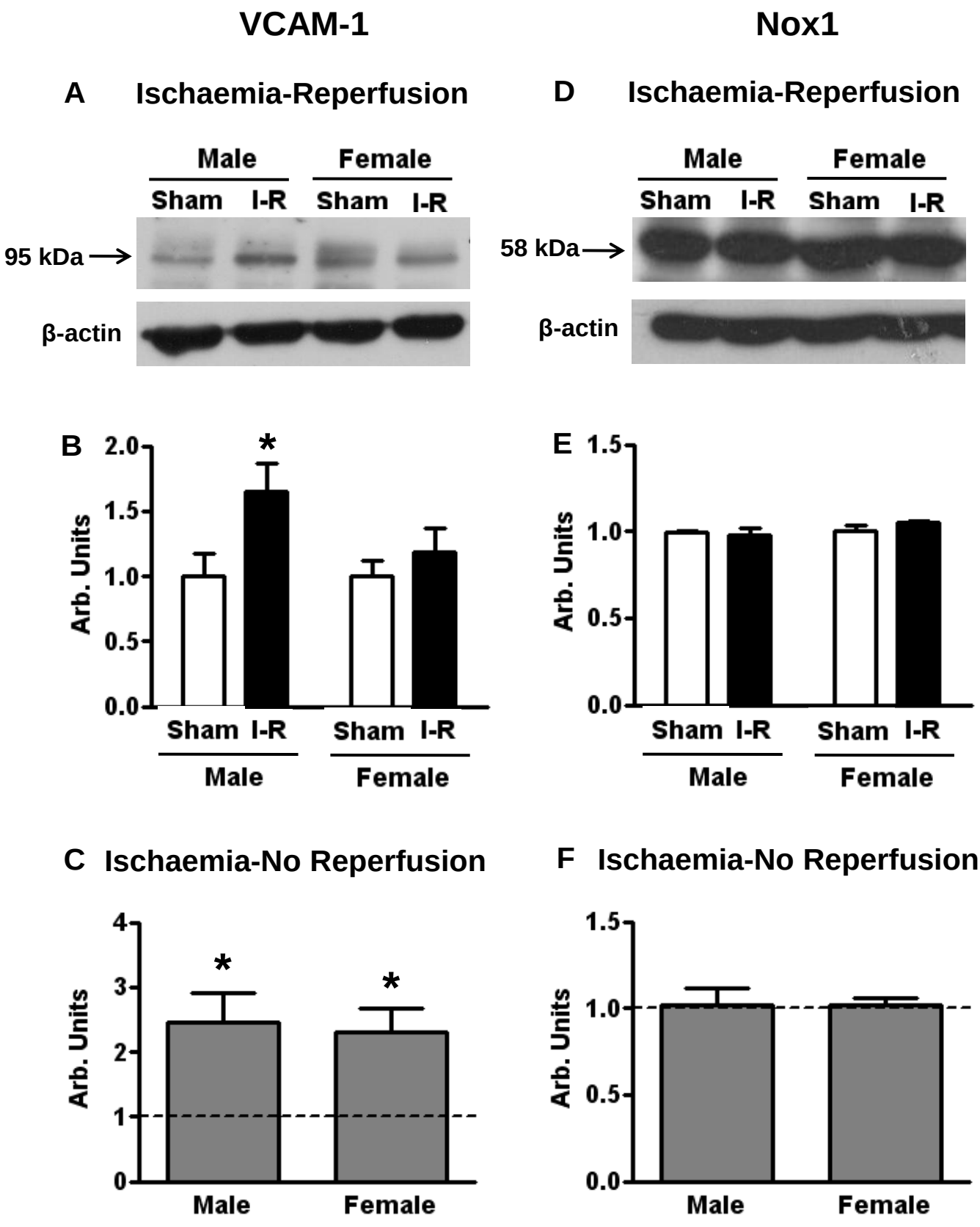
VCAM-1
Nox1
A
Ischaemia-Reperfusion
Male
Female
Sham
I-R
Sham
I-R
95 kDa
β-actin
D
Ischaemia-Reperfusion
Male
Female
Sham
I-R
Sham
I-R
58 kDa
β-actin
B
Arb. Units
2.0
1.5
1.0
0.5
0.0
*
Sham
I-R
Sham
I-R
Male
Female
E
Arb. Units
1.5
1.0
0.5
0.0
Sham
I-R
Sham
I-R
Male
Female
C
Ischaemia-No Reperfusion
Arb. Units
4
3
2
1
0
*
*
Male
Female
F
Ischaemia-No Reperfusion
Arb. Units
1.5
1.0
0.5
0.0
Male
Female

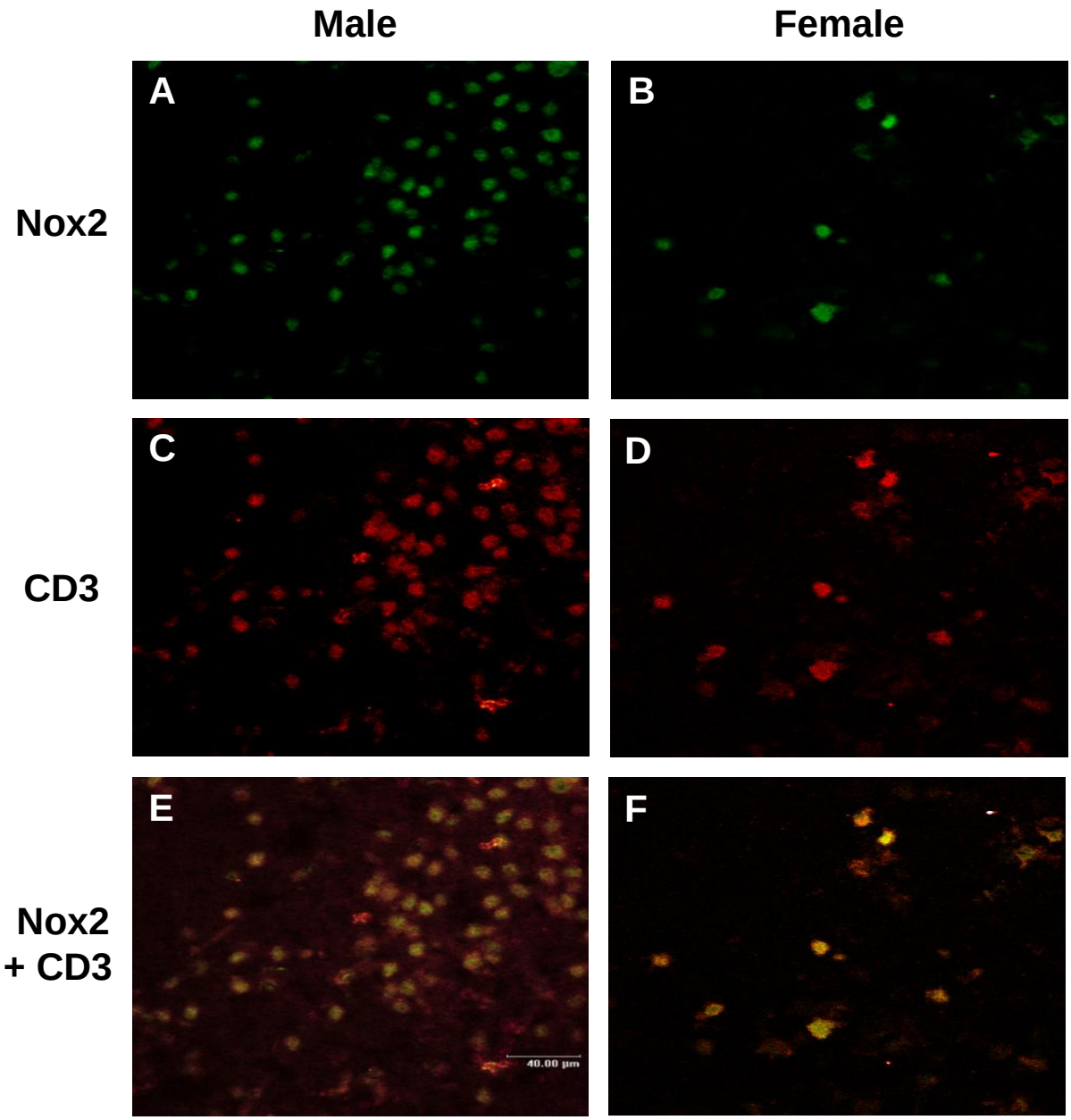

Figure 4.3. Localisation of T lymphocytes and Nox2 expressing cells.

Representative photomicrographs showing immunofluorescent staining within the core of striatal infarcts of a male and a female mouse following ischaemia-reperfusion (I-R). Approximately 7-fold more $Nox2^+$ and $CD3^+$ cells (i.e. T lymphocytes) were observed in infarcted brains of males (**A** and **C**, respectively) than females (**B** and **D**, respectively). Overlayed images revealed substantial co-localisation of Nox2 and CD3 (**E** and **F**). The scale bar represents 40 µm.

Figure 4.4. Immune cell counts in the spleen.

Flow cytometric analyses are shown for $CD3^+$ (**A;** total T lymphocytes), $CD4^+$ (**B;** T helper cells), $CD8^+$ (**C;** cytotoxic T cells), $B220^+$ (**D;** B lymphocytes), $CD11b^+$ (**E;** monocytes) and $Gr1^+$ (**F;** neutrophils) cells isolated from the spleen following sham surgery (white bars), I-R (black bars) and I-NR (grey bars; n = 6-9; $^*P < 0.05$ vs. matched sham group, ANOVA with Bonferroni *post-hoc* test). Data are presented as mean ± SEM.

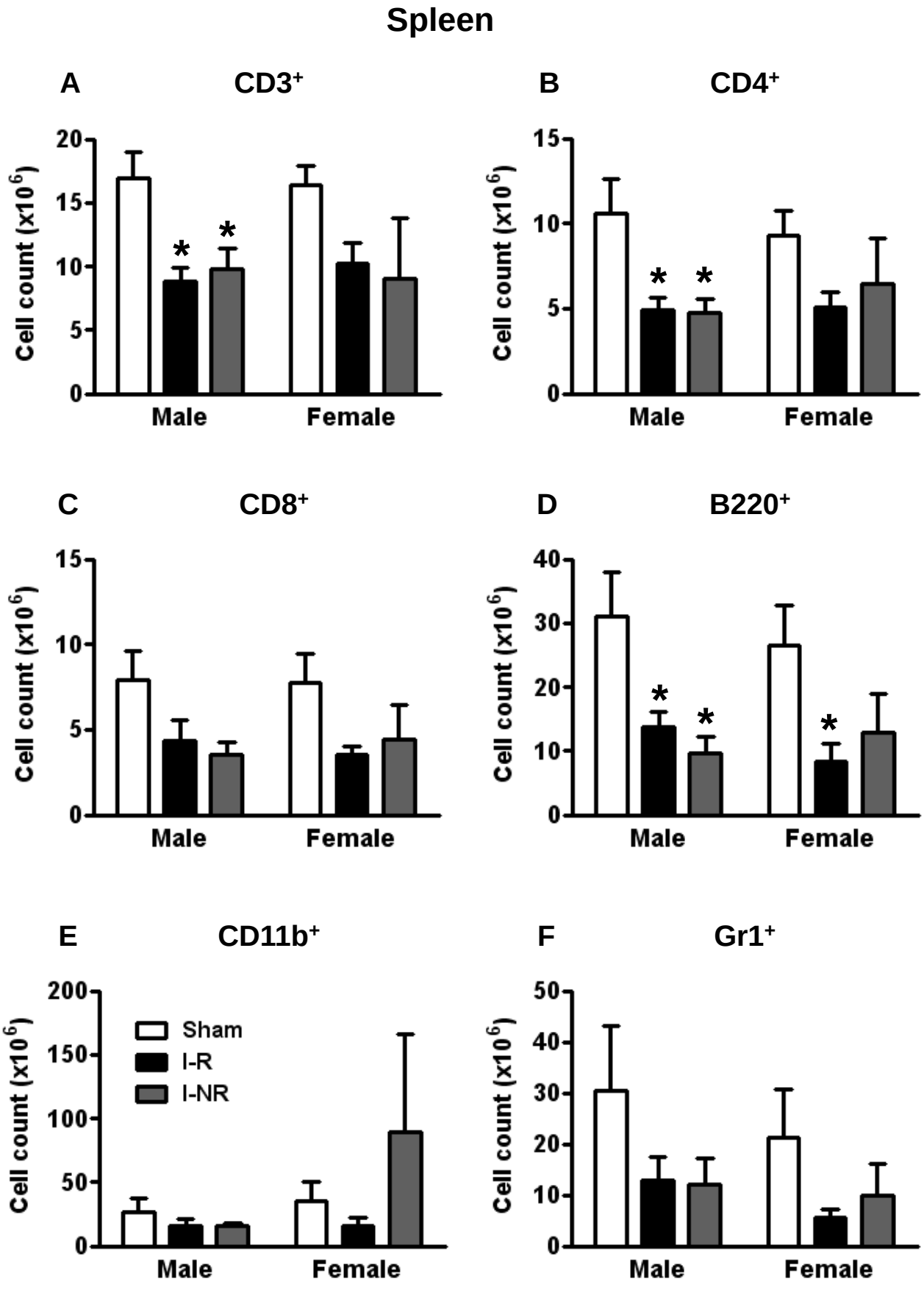
Spleen
A
CD3+
B
CD4+
C
CD8+
D
B220+
E
CD11b+
F
Gr1+
Cell count (x10^6)
Male
Female
Sham
I-R
I-NR
*

Figure 4.5. Immune cell counts in the blood.

Flow cytometric analyses are shown for $CD3^+$ (**A;** total T lymphocytes), $CD4^+$ (**B;** T helper cells), $CD8^+$ (**C;** cytotoxic T cells), $B220^+$ (**D;** B lymphocytes), $CD11b^+$ (**E;** monocytes) and $Gr1^+$ (**F;** neutrophils) cells isolated from the blood following sham surgery (white bars), I-R (black bars) and I-NR (grey bars; n = 5-7; $^*P < 0.05$ vs. matched sham group, ANOVA with Bonferroni *post-hoc* test). Data are presented as mean ± SEM.

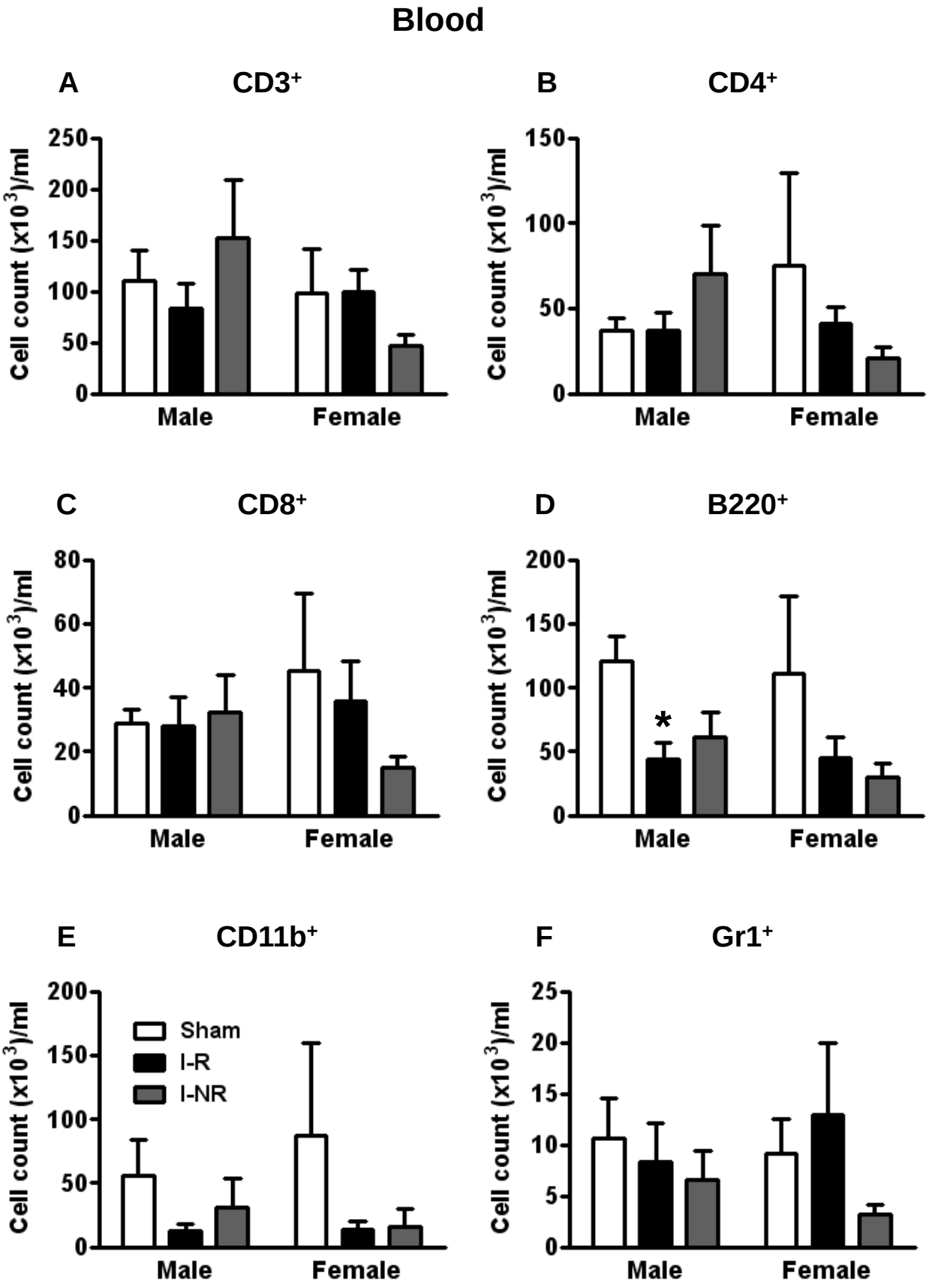
Blood
A
CD3+
B
CD4+
C
CD8+
D
B220+
E
CD11b+
F
Gr1+
Cell count (x10^3)/ml
Male
Female
Sham
I-R
I-NR
*

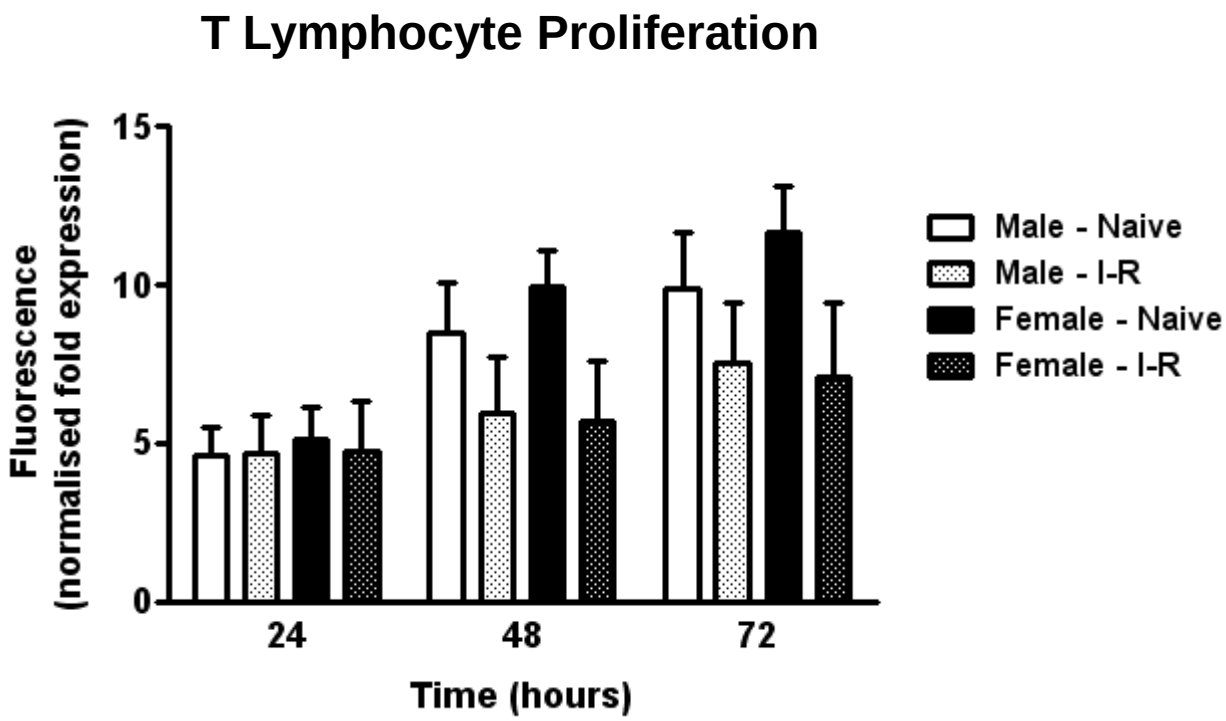

Figure 4.6. T lymphocyte proliferation.

T lymphocyte proliferation is shown for cells isolated from the spleen of naive mice and following I-R in male and female mice, 24, 48 and 72 hours after stimulation with anti-CD3 and anti-CD28 antibodies (n = 4 per group). Data are presented as mean ± SEM.

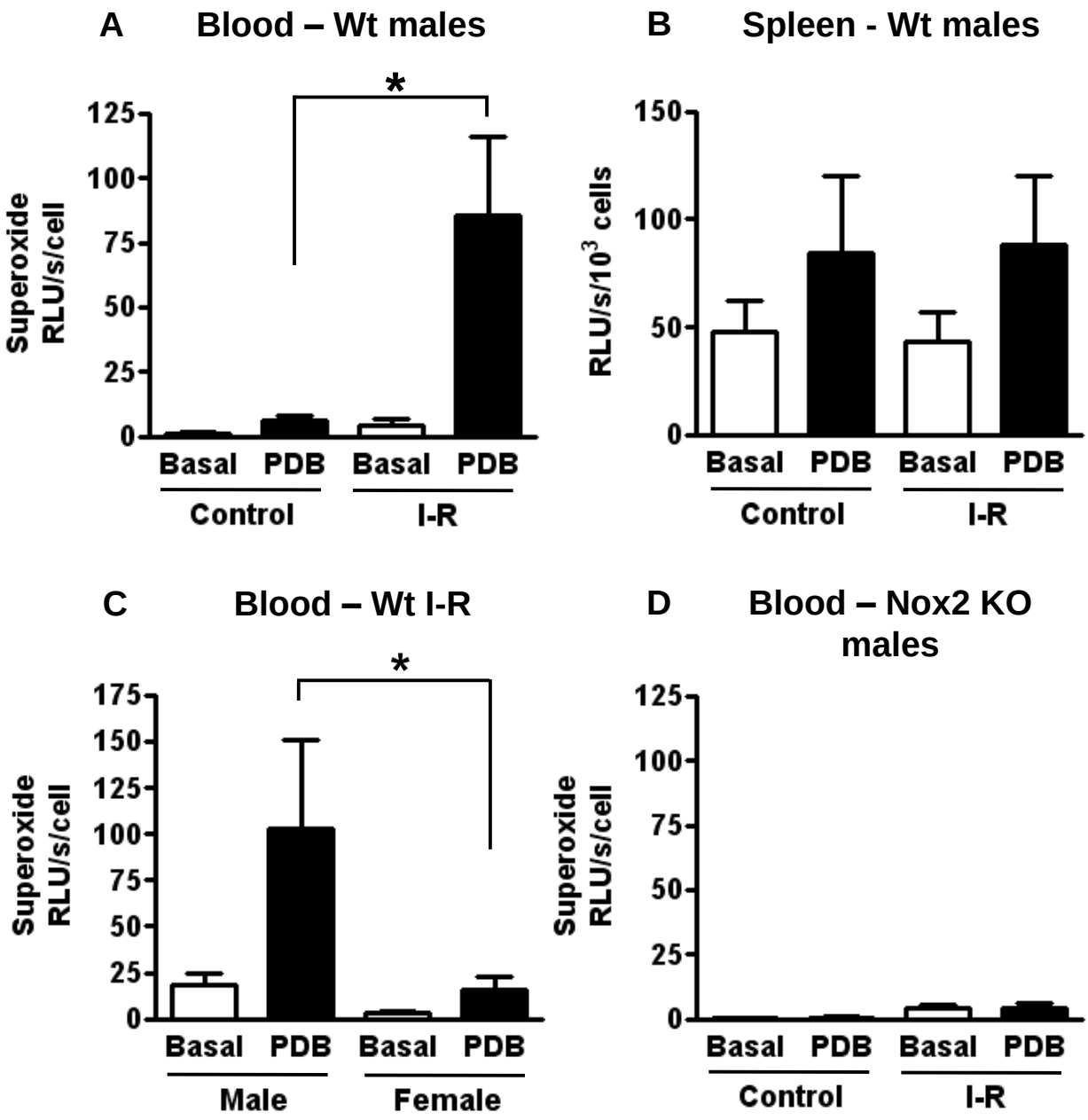

Figure 4.7. Superoxide generation by T lymphocytes.

Basal and PDB-stimulated superoxide generation by T lymphocytes from control mice and from mice 24 h after I-R. Data are shown for cells isolated from blood (**A**) and spleen (**B**) of wild-type male mice (n = 5 per group; $^*P < 0.05$, ANOVA with Bonferroni *post-hoc* test). Note the different Y-axis scales used in **A** and **B**. **C:** Superoxide generation by T lymphocytes isolated from blood of male and female wild-type mice 24 h after I-R (n = 6 per group; $^*P < 0.05$, ANOVA with Bonferroni *post-hoc* test). **D:** Basal and PDB-stimulated superoxide generation by T lymphocytes isolated from the blood of male Nox2-deficient mice (control, n = 3; I-R, n = 5). Data are presented as mean ± SEM.

4.4 DISCUSSION

This study has primarily assessed the molecular and cellular changes associated with the smaller infarct volume in female mice 24 h after I-R, established in Chapter 3. Following I-R, in the ischaemic hemisphere of male mice, we found an increased expression of the pro-inflammatory proteins, Nox2, Cox-2, and VCAM-1, and an infiltration of T lymphocytes, whereas there was little or no change in these parameters in female mice. A significant reduction in $CD3^+$ and $CD4^+$ T lymphocyte levels in the spleen occurred in male mice following I-R, as well as a significant reduction in B lymphocyte levels in the spleen in both males and females following I-R. In the blood, the only significant reduction was found in B lymphocyte levels following I-R in male mice. Interestingly, Nox2 protein was largely co-localised with T lymphocytes ($CD3^+$ cells) within the infarct core after I-R. Neither gender nor I-R significantly altered T lymphocyte proliferation. Moreover, we found circulating T lymphocytes to be a potentially important source of Nox2-derived superoxide after cerebral I-R especially in males, with Nox2-dependent superoxide production by these cells ~15-fold greater 24 h after I-R versus controls. Superoxide production by circulating T lymphocytes after stroke was substantially greater in male mice than in female mice. Our findings are compatible with the concept that salvage of brain tissue during post-ischaemic reperfusion is limited in males at least in part due to generation of Nox2-derived superoxide from T lymphocytes infiltrating the inflamed brain after stroke.

Increased expression of Nox2 (Kusaka *et al.*, 2004; McCann *et al.*, 2008), Cox-2 (Miettinen *et al.*, 1997; Nogawa *et al.*, 1997; Planas *et al.*, 1995), and VCAM-1 (Justicia *et al.*, 2006) have been reported to occur in the brain following I-R in male mice and rats. Moreover, the inhibition or genetic deletion of Nox2 and Cox-2 confers protection after focal cerebral I-R (Iadecola *et al.*, 2001a; Jackman *et al.*, 2009a; Kahles *et al.*, 2007; Nogawa *et al.*, 1997; Walder *et al.*, 1997), indicating their detrimental roles after stroke in males. We confirmed that protein expression of Nox2, Cox-2 and VCAM-1 are all increased in the ischaemic hemispheres of males following

cerebral I-R, and to our knowledge for the first time these key pro-inflammatory molecules were also examined after cerebral I-R in females. In contrast to males, compared with sham-operated female mice, none of these proteins were expressed at higher levels after I-R in females, consistent with the smaller infarct volume and with a protective, anti-inflammatory action of oestrogen. We also, for the first time, examined Nox1 protein expression in male and female mice following I-R, and found that neither ischaemia nor gender affected its expression in the ischaemic hemisphere.

The present study has also examined these proteins in both male and female mice after I-NR. Increased expression of Cox-2 had been reported to occur in the brain following I-NR in male rats (Yokota *et al.*, 2004). We confirmed that Cox-2 protein expression was increased in male mice, and also found Cox-2 protein expression to be significantly increased in the ischaemic hemisphere of female mice after I-NR. We also found for the first time, that protein expression of both Nox2 and VCAM-1 were significantly increased after I-NR in both males and females. This is consistent with there being no difference in infarct volume between male and female mice following I-NR. The increase in Nox2 expression following I-NR relative to the Nox2 expression after I-R in male mice was not as large as the increase observed from I-R to I-NR in female mice. This is again consistent with the relative difference in infarct volume, as infarct volume in female mice increased ~270 % from its infarct size after I-R to its infarct size after I-NR, whilst infarct volume in male mice only increased ~60 % (see Figures 3.4C & D). However, the increased Nox2 expression following I-NR is inconsistent with the concept that expression increases in the ischaemic hemisphere due to the infiltration of Nox2-expressing T lymphocytes, given that our immunofluorescence studies showed no infiltration of T lymphocytes following I-NR (data not shown; this will be discussed in more detail later). On the other hand, our immunofluorescence studies only focussed on the infarct core region, so it remains possible that Nox2-expressing T lymphocytes do infiltrate the periphery of the infarct

following I-NR, but do not penetrate to the core regions. Moreover, the expression of VCAM-1 protein, which promotes adhesion and consequently, infiltration of leukocytes (discussed in more detail in the following paragraph), similarly to Nox2, is increased more in female mice relative to male mice following I-NR from its I-R levels. Therefore, this idea that T lymphocytes still enter the brain when no reperfusion is instituted (i.e. I-NR) is further strengthened. However, it is also conceivable, that different processes are important in producing damage during I-NR than I-R, and perhaps local processes become more important, such as an increased expression of Nox2 and Cox-2 in resident brain cells (Green *et al.*, 2001; Yokota *et al.*, 2004). In contrast to Nox2 and VCAM-1, where there was no gender-difference in expression following I-NR, there tended to be a greater level of Cox-2 expression in male mice compared to female mice following I-NR, although this did not reach statistical significance. Cox-2 therefore, seems more 'gender-dependent' even following I-NR, which suggests that perhaps Cox-2 is not tightly linked to infarct volume. In contrast to the other 3 proteins examined, Nox1 protein expression in male or female mice, did not change after I-NR, compared with sham-operated mice.

In order to better understand the inflammatory consequences of stroke to the brain, we were interested to explore further our finding of increased VCAM-1 expression. VCAM-1 promotes adhesion of leukocytes, including lymphocytes, and is strongly expressed on activated vascular endothelial cells in response to pro-inflammatory cytokines (Marui *et al.*, 1993; Stins *et al.*, 1997), oxidative stress (Marui *et al.*, 1993), and following I-R (Justicia *et al.*, 2006). VCAM-1 expression is critical for infiltration of T lymphocytes into the brain (Baron *et al.*, 1993; Engelhardt *et al.*, 1995). Recent studies in T lymphocyte-deficient mice have revealed that these cells of the adaptive immune system are surprisingly important contributors to the acute brain infarction following cerebral I-R (Hurn *et al.*, 2007; Kleinschnitz *et al.*, 2010b; Shichita *et al.*, 2009; Yilmaz *et al.*, 2006). However, although it was recently discovered that the detrimental effects were not related to adaptive immunity (Kleinschnitz *et al.*, 2010b), the precise actions of T lymphocytes in

the brain after stroke are not well understood and are likely to be complex and somewhat specific for the different T lymphocyte subpopulations. After migration into the ischaemic brain, certain subsets of T lymphocytes may either directly elicit cell necrosis or apoptosis (i.e. cytotoxic T lymphocytes; $CD8^+$) (For review see Barry and Bleackley, 2002), or release pro-inflammatory cytokines and chemokines that propagate the cellular immune response by activating resident cells and up-regulating the expression of adhesion molecules, thus promoting further brain injury (i.e. T helper lymphocytes; $CD4^+$) (Arumugam *et al.*, 2005). By contrast, the regulatory T lymphocyte subpopulation (T_{reg} cells; $CD4^+CD25^+Foxp3^+$) was very recently found to play a protective role in the brain after stroke which includes secretion of the anti-inflammatory cytokine interleukin-10 (Liesz *et al.*, 2009b).

Using immunohistochemistry and immunofluorescence we documented the presence of T lymphocytes throughout the infarcted male mouse brain following I-R, as previously reported in male rats (Jander *et al.*, 1995). We noted that there were ~7-fold more T lymphocytes in infarct and peri-infarct brain areas of males than females, consistent with the gender-dependent expression of pro-inflammatory proteins after stroke, including the T lymphocyte adhesion molecule VCAM-1. We found little or no evidence of T lymphocytes in brains of sham-operated mice or within the core of ischaemic, but non-reperfused infarcts (I-NR; data not shown), indicating that these cells do not normally reside in the brain and that their infiltration into the infarct core occurred as a consequence of post-ischaemic reperfusion.

T lymphocytes express a functional Nox2-containing NADPH oxidase (Jackson *et al.*, 2004; Purushothaman and Sarin, 2009), and interestingly, superoxide generated by the activity of this enzyme in T lymphocytes was recently reported to contribute to angiotensin II-induced hypertension (Guzik *et al.*, 2007). We and others have found that Nox2-containing NADPH oxidase contributes to infarct development in the male brain after stroke (Chen *et al.*, 2009;

Jackman *et al.*, 2009a; Kahles *et al.*, 2007; Kunz *et al.*, 2007; Walder *et al.*, 1997). The cellular source(s) of the enzyme responsible for this brain damage is not well defined but may include circulating, bone-marrow-derived cells (Walder *et al.*, 1997). Having confirmed by Western blotting that Nox2 expression was increased in male brains after I-R, we next explored whether Nox2 in infiltrating T lymphocytes might be relevant to post-ischaemic changes in the brain. Using immunofluorescence we found that, at least in the infarct core within the striatum, Nox2 was mostly localised in $CD3^+$ cells (i.e. infiltrated T lymphocytes), suggesting that T lymphocytes may be an important source of Nox2-derived superoxide in the infarcted brain after I-R. We cannot exclude the possibility that other cell types also contributed to the increased Nox2 expression, but our observations suggest that in mice, T lymphocytes may be an important source of Nox2 within brain infarcts 24 h after I-R (see below for further discussion of the role of various Nox2-containing circulating cells).

The flow cytometric analyses showed no change in $CD8^+$ T lymphocyte, monocyte and neutrophil levels in the spleen in either male or female mice following I-R or I-NR compared to sham-operated mice. There were however, significant reductions in $CD3^+$ and $CD4^+$ T lymphocytes and B lymphocytes following I-R and I-NR in male mice, and also a significant reduction in female mice of B lymphocytes after I-R in the spleen. In the blood, there were no changes in any of the immune cells analysed, except for a significant reduction in B lymphocytes following I-R in male mice. Twenty-four h after a 30 min ischaemic period may be too early to see significant reductions, especially in the blood, as the extent of immunodepression is very dependent on the degree and length of the ischaemic insult (Liesz *et al.*, 2009a) and the length of reperfusion (Offner *et al.*, 2006b). The extent of immunodepression also has a positive relationship with infarct size (Liesz *et al.*, 2009a). This is consistent with female mice not experiencing as severe an immunodepression as do male mice following I-R, in association with the smaller infarct volume (see Figure 3.4C). However, this does not explain why female mice do

not also have significantly reduced levels following I-NR, which produced the same sized infarct volume as male mice (see Figure 3.4D); or why the degree of immunodepression was not greater following I-NR in both genders compared to I-R. Although perhaps, given that longer periods of reperfusion produce greater degrees of immunodepression (Offner *et al.*, 2006b), I-NR may not produce a large immunodepression, due to the lack of reperfusion, even though it produces a large infarct volume. It is also possible that the increased number of infiltrating T lymphocytes in the male brain compared to females could account for part of the reduction in $CD3^+$ (and $CD4^+$) T lymphocytes in the spleen in male mice following I-R. Importantly, although the largest changes were observed in B lymphocytes, these cells reportedly do not contribute to stroke-induced inflammation, neurological impairment or infarct volume (Yilmaz *et al.*, 2006), and therefore, we chose not to focus on B lymphocytes.

We next examined the *in vitro* proliferation ability of splenic T lymphocytes following I-R. T lymphocyte proliferation 3 days after stimulation was found previously to be significantly reduced in cells isolated from the spleen 22 h after a 90 min MCAO in mice, and more profoundly reduced when they were isolated 96 h after I-R (Offner *et al.*, 2006b). Although we did not find significantly reduced levels from T lymphocytes isolated 24 h after I-R at either 1, 2 or 3 days of stimulation, which could be due to the fact that the ischaemic period we used was one third the time Offner and colleagues used, or the fact that we had very small group sizes, there was a trend for less proliferation when these T lymphocytes were isolated from mice following I-R compared to naïve mice. However, importantly, as no gender difference was observed in proliferation levels, this data cannot account for the difference in $CD3^+$ and $CD4^+$ T lymphocyte counts in the spleen. Nor can it account for the difference in infarct volume following I-R.

Next, we determined whether superoxide production could be elicited in isolated T lymphocytes in response to a stimulus of Nox2-containing NADPH oxidase (i.e. PDB), and whether a previous (24 h) stroke had any effect on such release. We thus used L-012-enhanced chemiluminescence to detect superoxide generation from T lymphocytes isolated from the blood and spleens of control and post-stroke mice. The most profound finding was the ~15-fold increase in superoxide generation from T lymphocytes isolated from the blood of post-stroke males versus control mice. This increase in superoxide production by circulating T lymphocytes after I-R also occurred in cells from females, but to a much lesser degree. Importantly, PDB did not elicit superoxide production from T lymphocytes isolated from control or post-stroke Nox2-deficient mice, confirming that the source of superoxide generated in wild-type mice was a Nox2-containing NADPH oxidase. Furthermore, we found that neither PDB nor stroke had any effect on superoxide production by T lymphocytes isolated from the spleen, suggesting that only when these cells reach the circulation are they able to generate much larger amounts of Nox2-derived superoxide, and that this ability increases markedly after stroke. Such findings are consistent with the novel possibility of an acute detrimental effect in brain of infiltrating T lymphocytes after I-R, especially in males. Further studies are required to identify the precise stimuli and molecular signalling leading to increased Nox2-derived superoxide generation by circulating T lymphocytes after I-R.

In Chapter 3, when cerebral infarct volume was examined following I-R in male and female Nox2-deficient mice, we found that in contrast to wild-type mice, infarct volume was not smaller in female versus male Nox2-deficient mice. We speculate that the salvage of ischaemic brain by reperfusion is limited by inflammation, including Nox2-derived superoxide generated by infiltrating T lymphocytes. Moreover, we further speculate that the reduced infarct volume and infiltration of Nox2-containing T lymphocytes in females reflects an inhibitory effect(s) of oestrogen on these processes.

It might be suggested that neutrophils and monocytes/macrophages – blood cells involved in innate immunity that are well known to express Nox2 (Selemidis *et al.*, 2008) – are more likely candidates than T lymphocytes as sources of oxidative and inflammatory damage following cerebral I-R. However, there is evidence against a detrimental role of neutrophils in the brain following acute stroke, in that neutrophil depletion does not reduce infarct volume (Beray-Berthat *et al.*, 2003; Harris *et al.*, 2005; Yilmaz *et al.*, 2006). Neutrophils instead appear to enter the brain as a result of damage rather than being a cause of it (Emerich *et al.*, 2002), and this is reported to not occur to a significant degree for at least 3 days after stroke (Gelderblom *et al.*, 2009). We did detect a reduction of both monocytes and neutrophils in the spleen after I-R, although no gender difference was present, and this did not reach significance (please note that Chapter 6 will address some mechanisms relevant to the role of neutrophils following cerebral I-R). Although we cannot completely exclude a role for neutrophils or circulating monocytes in the post-stroke Nox2-dependent brain damage, our data indicate that at 24 h Nox2 appears to be predominantly co-localised with T lymphocytes at least in the infarct core, and Nox2-dependent superoxide production is markedly augmented in these cells present in the circulation. It is also possible that activated microglia could be Nox2-positive in the brain after I-R, including outside of the infarct core. However, our co-localisation studies here were only performed in regions of the striatal infarct core and therefore might not be representative of cell types expressing Nox2 around and beyond the infarct. Overall, we suggest that a possible scenario is that the damaging Nox2-derived superoxide production in the male brain in the first 24 h after cerebral I-R originates to some degree from T lymphocytes that infiltrate the brain. Furthermore, because Nox2-deficient females do not have a smaller infarct volume than Nox2-deficient males following cerebral I-R, Nox2-derived superoxide generated by infiltrating T lymphocytes could account for the limited salvage achieved by reperfusion in male versus female wild-type mice.

Here we have studied the effect of a 30 min ischaemic duration which produces a moderate infarct volume. Further studies will be necessary to assess whether similar findings are evident after other clinically relevant ischaemic durations that are either shorter (as in transient ischaemic attack patients) or longer (as in patients treated with recombinant tissue plasminogen activator [rt-PA] after up to 4.5 h ischaemia) than 30 min.

In summary, our data suggest that the salvage obtained by reperfusion may be greater in females because of limited expression of pro-inflammatory proteins, including VCAM-1, resulting in markedly less damage caused by superoxide from infiltrating Nox2-containing T lymphocytes. These circulating immune cells could represent a major source of superoxide in the ischaemic and reperfused brain. Viable new therapies for acute stroke are desperately needed. Our findings raise the possibility that short-term therapies to reduce T lymphocyte infiltration into the brain after transient ischaemic attack, or in acute ischaemic stroke patients who receive rt-PA, might be useful for reducing reperfusion injury, not only in younger males but potentially in aged patients of both genders.

Chapter 5:

Generation of Superoxide by T Lymphocytes after Cerebral Ischaemia-Reperfusion

5.1 INTRODUCTION

It is well established that Nox2 is detrimental in experimental models of stroke (Kahles *et al.*, 2007; Kunz *et al.*, 2007; Walder *et al.*, 1997). More recently, T lymphocytes have also been reported to contribute to damage during ischaemic stroke (Hurn *et al.*, 2007; Kleinschnitz *et al.*, 2010b; Shichita *et al.*, 2009; Yilmaz *et al.*, 2006). Studies in mice that lack functional T lymphocytes have reported improved outcome, including smaller infarct volumes (Hurn *et al.*, 2007; Kleinschnitz *et al.*, 2010b; Shichita *et al.*, 2009; Yilmaz *et al.*, 2006), and when wild-type $CD3^+$ T lymphocytes were transplanted back into these mice, this protection was lost (Kleinschnitz *et al.*, 2010b; Shichita *et al.*, 2009; Yilmaz *et al.*, 2006). T lymphocytes express a Nox2-containing NADPH oxidase (Jackson *et al.*, 2004; Purushothaman and Sarin, 2009), and we in Chapter 4, as well as others (Jander *et al.*, 1995), reported that they enter the brain within 24 h after ischaemia-reperfusion (I-R).

In Chapter 4, we found evidence that following cerebral I-R in male mice, circulating $CD3^+$ T lymphocytes, when stimulated by the Nox2 activator, phorbol 12,13-dibutyrate (PDB), produce greater amounts of superoxide (~15-fold greater) than PDB-stimulated $CD3^+$ T lymphocytes isolated from the blood of control male mice (see Figure 4.7A). Then, in studies using Nox2-deficient mice subjected to experimental stroke, we found no such increase in superoxide (see Figure 4.7D), suggesting that circulating T lymphocytes may be a major source of Nox2-derived superoxide following cerebral I-R. It is unclear which subset(s) of $CD3^+$ T lymphocytes contribute to this augmented superoxide production. Identification of the specific T lymphocyte subset responsible is fundamental for potentially targeting the source in order to minimise side effects. This is especially crucial given that the immunodepression that occurs after stroke (Haeusler *et al.*, 2008; Liesz *et al.*, 2009a; Offner *et al.*, 2006b; Prass *et al.*, 2003), facilitates infections, which are the most common cause of death in the post-acute phases of stroke (Heuschmann *et al.*, 2004; Vernino *et al.*, 2003).

There are many types of T lymphocytes that each plays a slightly different role in immunity. T lymphocyte subsets are differentiated by the expression of certain co-receptor proteins on their surface (eg. CD3 is expressed on the cell surface of 95 % of all mature T lymphocytes – all except γδ T lymphocytes). The two main types of mature T lymphocytes are the T helper lymphocytes (T_H lymphocytes; also known as $CD4^+$ T lymphocytes, because they express the CD4 protein on their cell surface) and cytotoxic T lymphocytes (also known as $CD8^+$ T lymphocytes, because they express the cell surface protein CD8) (Harrison *et al.*, 2008; Seder and Ahmed, 2003). T_H lymphocytes do not kill cells directly, but help to activate other members of the immune system. They can be further differentiated into three major types, defined by the different cytokines they secrete (Korn *et al.*, 2009; Santana and Rosenstein, 2003). They can either promote cell-mediated or inflammatory immunity (T_H1 lymphocytes), promote humoral and allergic responses (T_H2) (Abbas *et al.*, 1996; Glimcher and Murphy, 2000; Santana and Rosenstein, 2003), or promote inflammatory immunity to clear pathogens distinct from those handled by T_H1 or T_H2 lymphocytes, including fungi (T_H17) (Korn *et al.*, 2009). Cytotoxic T lymphocytes directly kill intracellular pathogens, such as cells infected with viruses, through the release of the cytotoxins perforin and various granzymes, or by the Fas-FasL pathway (Barry and Bleackley, 2002; Russell and Ley, 2002). Cytotoxic T lymphocytes also produce cytokines such as interferon-γ (IFN-γ) and interleukin-2 (IL-2) (Theodorou *et al.*, 2008). Unconventional T lymphocytes include the γδ T lymphocytes (accounting for ~5 %) and the natural killer T (NKT) cells. However these have previously been shown not to contribute to stroke injury (Kleinschnitz *et al.*, 2010b).

Few studies have investigated the roles of the different $CD3^+$ subsets of T lymphocytes in stroke. However, one very important study, in addition to examining the effect of lymphocyte deficiency (using recombination-activating gene 1-deficient; $Rag1^{-/-}$ mice) on stroke outcome, investigated the effects of deficiency in either $CD4^+$ or $CD8^+$ T lymphocytes after I-R. Yilmaz and colleagues reported that mice deficient in either $CD4^+$ or $CD8^+$ T lymphocytes had smaller infarct volumes

and reduced neurological deficit (Yilmaz *et al.*, 2006), suggesting that both T lymphocyte subsets contribute to stroke pathology. However, with the exception of reporting reduced leukocyte and platelet adhesion in these mice, the mechanism(s) of damage were not investigated, and could therefore be different between the two subsets.

The aim of this study was to investigate which subset(s) of $CD3^+$ T lymphocytes ($CD4^+$ and/or $CD8^+$ T lymphocytes) might be involved in producing the increased PDB-stimulated superoxide levels 24 h after I-R.

5.2 MATERIALS AND METHODS

5.2.1 Animals

This study was conducted in accordance with the National Health and Medical Research Council of Australia guidelines for the care and use of animals in research.

A total of 97 male 8-10 week old C57Bl6/J mice were studied (weight, 25.4±0.2 g). The mice had free access to water and food pellets before and after surgery. Two mice were excluded from the study after receiving MCAO, as they died prior to the specified time for euthanasia (at 23.5 h reperfusion).

5.2.2 Focal cerebral ischaemia

Focal cerebral ischaemia was induced by transient intraluminal filament occlusion of the right middle cerebral artery (MCA) as described in section 2.3 of General Methods.

5.2.3 Isolation of leukocytes from blood

Mice were killed at 24 h by isofluorane inhalation and exsanguination, and leukocytes were isolated from the blood as described in section 2.10 of General Methods.

5.2.4 Measurement of superoxide production by T lymphocytes

After isolation of leukocytes, a purified suspension of T lymphocytes (either $CD3^+$, $CD4^+$ or $CD8^+$) was obtained using the Dynal® Mouse T Cell Negative Isolation Kit (Invitrogen; Carlsbad, CA, USA). Please refer to section 2.12 of General Methods for details. Basal and phorbol 12,13-dibutyrate (PDB; 1 μM)-stimulated superoxide production by T lymphocytes from blood of control mice (a combination of sham-operated mice, n = 13; and naïve mice, n = 31) and mice 24 h after I-R (n = 39) was measured by 100 μmol/L L-012-enhanced chemiluminescence, as described in section 2.13 of General Methods. In addition to results being analysed and expressed as an average of the 30 measurement cycles, they were also expressed per cycle, and their superoxide production at cycle 30 was analysed.

5.2.5 Analysis of cell populations

Fluorescence flow cytometric preliminary analyses were performed in blood isolated from naive male mice to determine the purity of T lymphocyte subset isolation, following the use of the Dynal® negative isolation kits, as described in section 2.11 of General Methods. However, in the present study, to estimate the number of cells in each sample, cells were counted using a Coulter Counter (Beckman Coulter; Brea, CA, USA), and labelled for cytofluorimetry with antibodies for 20 min at 4 °C in PBS containing 1 % bovine serum albumin (BSA), 3.076 mM sodium azide and 5 mM EDTA. Primary antibodies conjugated with fluorophores were: the Alexa Fluor 488-conjugated anti-NK1.1 (clone PK136; 1:500), allophycocyanin (APC)-conjugated anti-TCRβ (clone H57-597; 1:800), Pacific Blue-conjugated anti-CD8 (clone 53-6.7; 1:1000) (BioLegend; San Diego, CA, USA), phycoerythrine (PE)-conjugated anti-MHC Class II (clone M5/114.15.2; 1:2000), PE-conjugated anti-CD19 (clone 1D3; 1:1000), PE-conjugated CD49b (clone DX5; 1:2000) (BD Biosciences; North Ryde, NSW, Australia), PE-conjugated anti-GR1 (clone RB6-8C5; 1:1000; eBioscience; San Diego, CA, USA), and Pacific Orange-conjugated anti-CD4 (clone RM4-5; 1:400; Invitrogen). All antibodies were rat anti-mouse. To exclude dead cells

from analysis, cells were stained with 1 mM 7-amino actinomycin D (7-AAD; Invitrogen) 1 min prior to FACS processing. Isotype control antibodies were: the FITC-conjugated anti-IgG2a-κ (clone HK1.4), PE-conjugated Armenian hamster anti-mouse IgG (clone HL3), APC-conjugated Armenian hamster anti-mouse IgG2-λ (clone H57-597), Pacific Blue-conjugated anti-IgG2a (clone 53-6.7) (Biolegend), PE-conjugated anti-IgG2a-κ (clone RA3-6B2; BD Biosciences) and Pacific Orange-conjugated anti-IgG2a (clone RM4-5; Invitrogen). The isotype controls were used at the same concentrations as the antibodies, and were all rat anti-mouse, unless specified.

5.2.6 Drugs and chemicals

As per section 2.14 of General Methods.

5.2.7 Statistical analysis

All data are presented as mean ± standard error. Statistical analyses were performed using GraphPad Prism version 5 (GraphPad Software Inc., San Diego, CA, USA). Between-group comparisons were analysed as described in section 2.15 of General Methods. Superoxide produced per cycle was compared between groups at cycle 30 (this point was chosen as the superoxide produced had typically reached a plateau) using a one-way ANOVA with Bonferroni *post-hoc* test. Group numbers are shown in parentheses. Statistical significance was accepted when $P < 0.05$.

5.3 RESULTS

5.3.1 Effect of cerebral I-R on the generation of superoxide by T lymphocyte subsets

5.3.1.1 $CD3^+$ T lymphocytes

To confirm that circulating $CD3^+$ T lymphocyte-derived superoxide is increased after cerebral I-R in the presence of the Nox2 activator PDB (our finding from Chapter 4; see Figure 4.7A), we

again isolated $CD3^+$ T lymphocytes from the blood of control male mice and mice after cerebral I-R, and observed a very similar profile to that of Chapter 4. We found that superoxide generated by purified $CD3^+$ T lymphocytes isolated from the blood of control mice was slightly augmented (by ~3.5-fold above basal) after incubation with PDB (n = 18; Figure 5.1A). When $CD3^+$ T lymphocytes from 24 h post-stroke mice were stimulated with PDB, superoxide release was increased by a further ~2-fold ($P < 0.05$ vs. PDB-stimulated control; n = 14; Figure 5.1A).

When superoxide generated at cycle 30 was analysed, a greater amount of PDB-stimulated superoxide was produced by $CD3^+$ T lymphocytes after cerebral I-R versus control mice ($P < 0.05$; Figure 5.1B).

5.3.1.2 $CD4^+$ T lymphocytes

We also investigated whether the superoxide produced by $CD3^+$ T lymphocytes was generated by the $CD4^+$ T lymphocyte subset. We isolated $CD4^+$ T lymphocytes from the blood of separate control and post-stroke mice, and found a similar profile to that of $CD3^+$ cells. Superoxide release from $CD4^+$ T lymphocytes isolated from the blood of control male mice was greatly augmented (by ~10-fold above basal) after incubation with PDB (n = 11; Figure 5.2A). When circulating $CD4^+$ T lymphocytes from post-stroke mice were stimulated with PDB, superoxide release was increased by a further ~2-fold, although this effect did not reach statistical significance (n = 10; Figure 5.2A).

Similar to what was observed with the mean superoxide production over 30 cycles, there was no statistically significant difference in the amount of PDB-stimulated superoxide generated by circulating $CD4^+$ T lymphocytes after cerebral I-R at cycle 30 compared to control mice, although there was a clear trend for $CD4^+$ T lymphocytes to generate greater amounts after I-R (Figure 5.2B).

5.3.1.3 $CD8^+$ T lymphocytes

We also investigated whether the superoxide produced by $CD3^+$ T lymphocytes was generated by the $CD8^+$ T lymphocyte subset. We isolated $CD8^+$ T lymphocytes from the blood of separate control and post-stroke mice, and found a similar profile to that of $CD3^+$ cells. Superoxide generation by $CD8^+$ T lymphocytes isolated from the blood of control male mice was slightly augmented (by ~2-fold above basal) by incubation with PDB (n = 15; Figure 5.3A). By contrast, in $CD8^+$ T lymphocytes isolated 24 h after cerebral I-R, PDB-stimulated superoxide release was significantly augmented by a further ~6.5-fold ($P < 0.05$ vs. PDB-stimulated control; n = 15; Figure 5.3A).

When superoxide generated at cycle 30 was analysed, PDB-stimulated superoxide produced by circulating $CD8^+$ T lymphocytes was greater in mice after cerebral I-R versus control mice ($P < 0.05$; Figure 5.3B).

5.3.2 Purity of isolated samples

The purity of T lymphocyte subset isolation following the use of Dynal® negative isolation kits was tested in blood samples from naive male mice using fluorescence flow cytometry. The results are shown in Table 5.1 (below). When purified suspensions of $CD3^+$, $CD4^+$ and $CD8^+$ T lymphocytes were each analysed, 55 %, 31 % and 17 % of all live cells in the suspensions were $CD3^+$, $CD4^+$ and $CD8^+$ T lymphocytes, respectively (n = 4 per group). These findings were much lower than expected. The other cells in the suspensions were natural killer T (NKT) cells, natural killer (NK) cells and others, comprising of B lymphocytes, dendritic cells, neutrophils, monocytes and others that were not identified.

Isolated T lymphocyte subset	% of Specific T lymphocyte subset	% NKT Cells	% NK Cells	% Other
$CD3^+$	55 %	9 %	5 %	31 %
$CD4^+$	31 %	13 %	24 %	32 %
$CD8^+$	17 %	16 %	16 %	51 %

Table 5.1. Purity of isolated samples.

The distribution of cell types within purified suspensions of $CD3^+$, $CD4^+$ and $CD8^+$ T lymphocytes (n = 4 per group), isolated from the blood of naive male mice, using Dynal® negative isolation kits (Invitrogen).

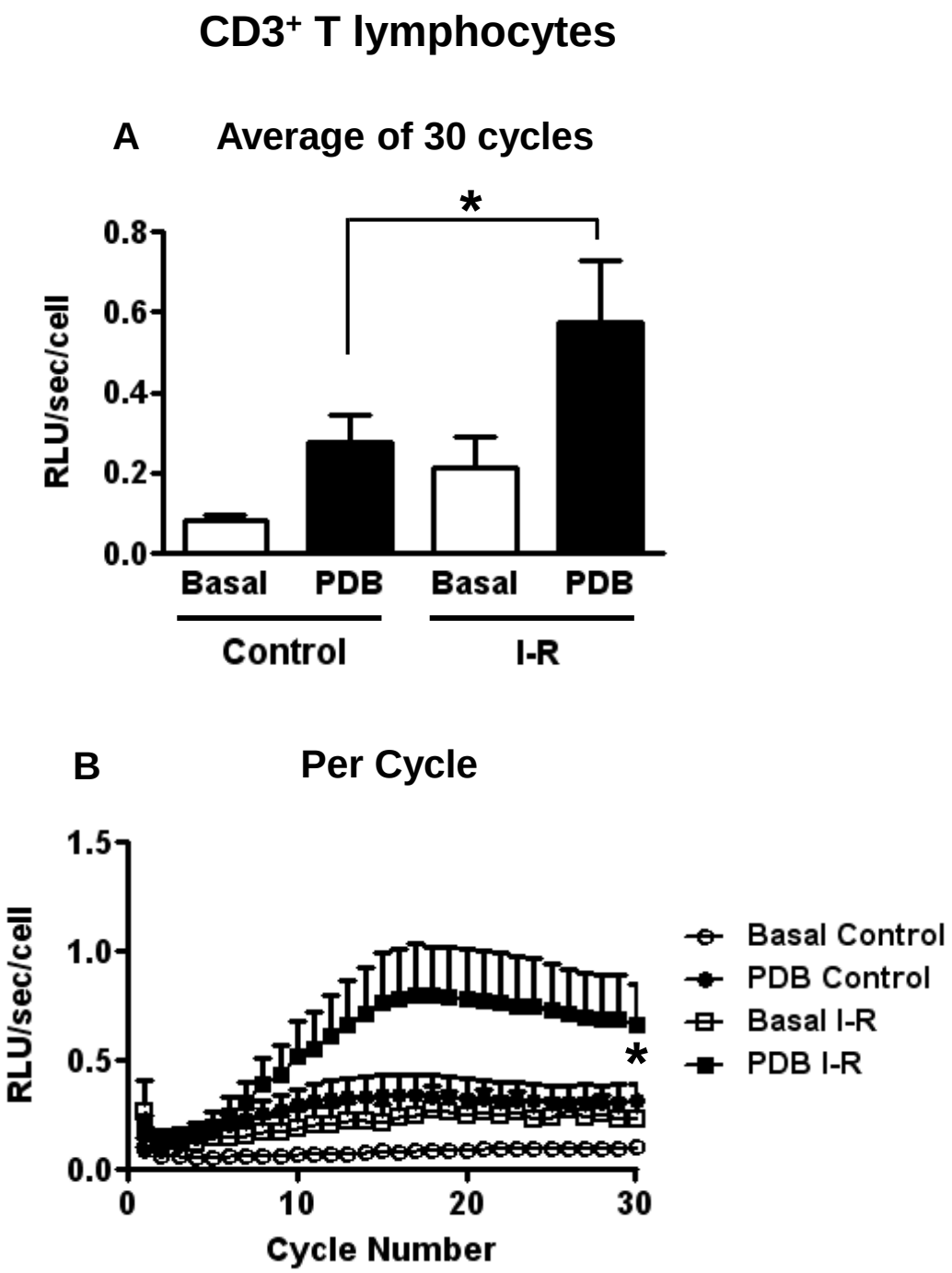

Figure 5.1. Superoxide generation by CD3$^+$ T lymphocytes.

Basal and PDB-stimulated superoxide generation by CD3$^+$ T lymphocytes isolated from the blood of male control mice and male mice 24 h after I-R. **A:** Average superoxide produced over the 30 measurement cycles (control, n = 18; I-R, n = 14; *P < 0.05, ANOVA with Bonferroni *post-hoc* test). **B:** Superoxide produced per cycle (control, n = 18; I-R, n = 14; *P < 0.05 vs. matched control group at cycle 30, ANOVA with Bonferroni *post-hoc* test). Data are presented as mean ± SEM.

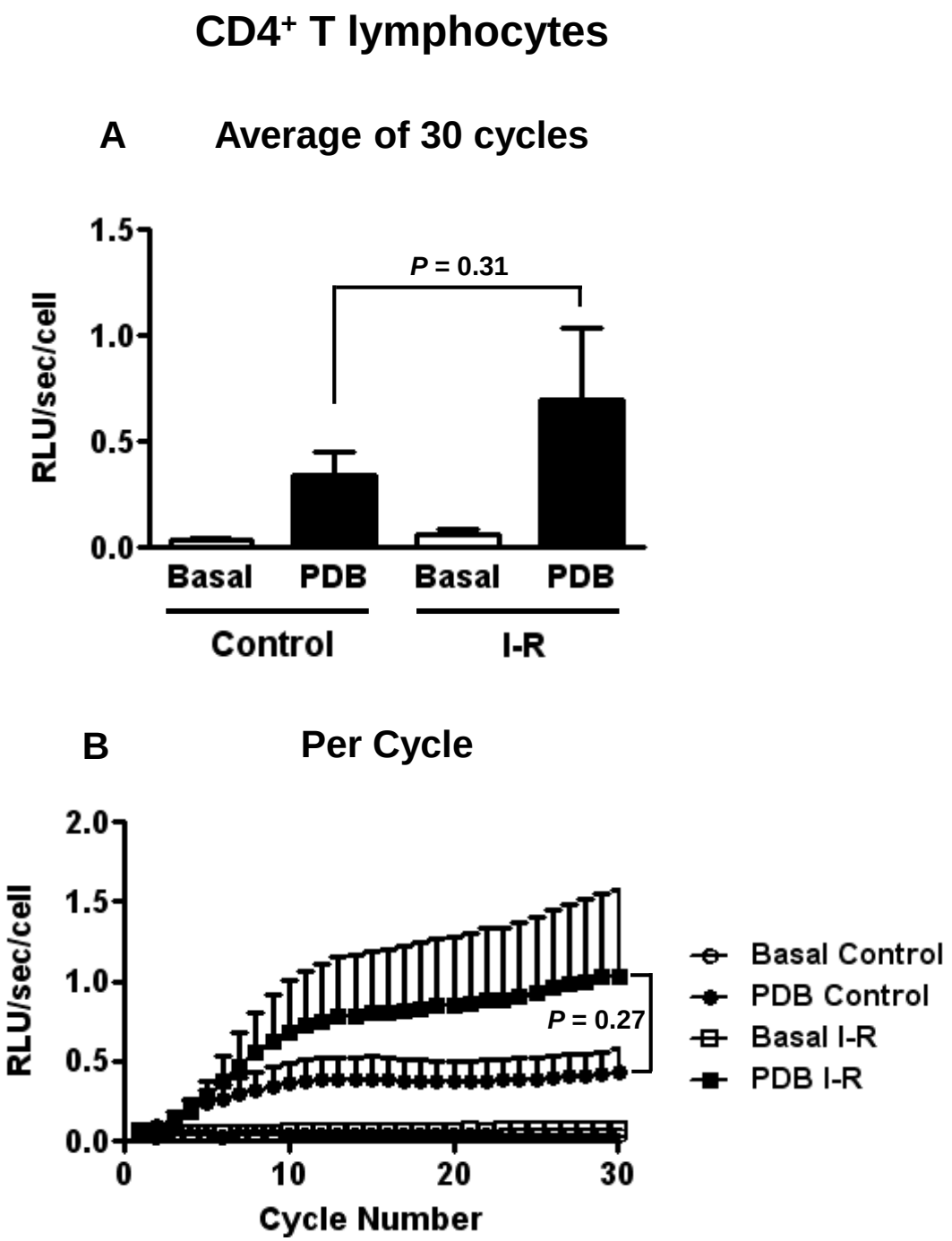

Figure 5.2. Superoxide generation by CD4$^+$ T lymphocytes.

Basal and PDB-stimulated superoxide generation by CD4$^+$ T lymphocytes isolated from the blood of male control mice and male mice 24 h after I-R. **A:** Average superoxide produced over the 30 measurement cycles (control, n = 11; I-R, n = 10; ANOVA with Bonferroni *post-hoc* test). **B:** Superoxide produced per cycle (control, n = 11; I-R, n = 10; ANOVA with Bonferroni *post-hoc* test). Data are presented as mean ± SEM.

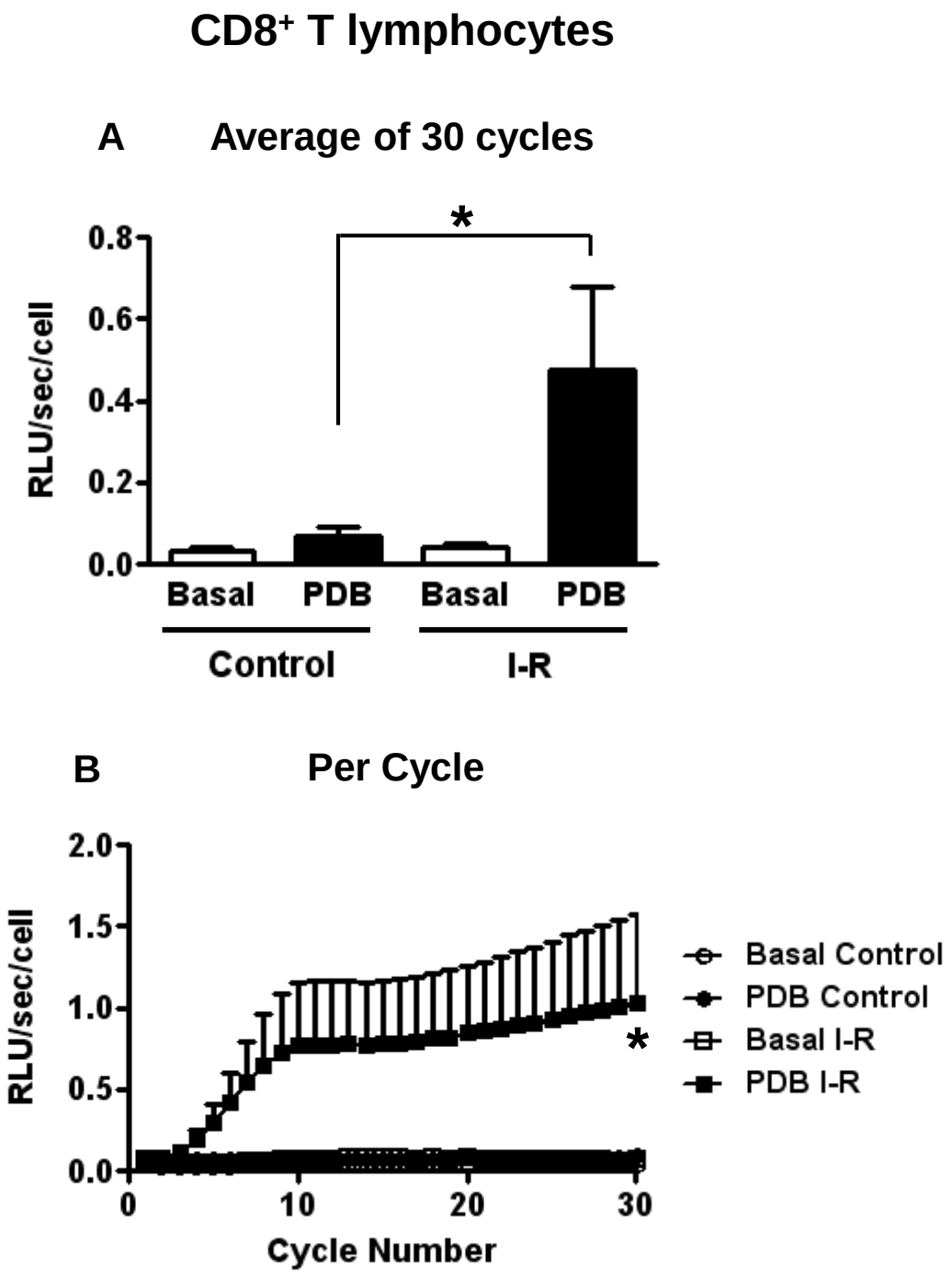

Figure 5.3. Superoxide generation by CD8$^+$ T lymphocytes.

Basal and PDB-stimulated superoxide generation by CD8$^+$ T lymphocytes isolated from the blood of male control mice and male mice 24 h after I-R. **A:** Average superoxide produced over the 30 measurement cycles (n = 15 per group; *P < 0.05, ANOVA with Bonferroni *post-hoc* test). **B:** Superoxide produced per cycle (n = 15 per group; *P < 0.05 vs. matched control group at cycle 30, ANOVA with Bonferroni *post-hoc* test). Data are presented as mean ± SEM.

5.4 DISCUSSION

This study confirmed our Chapter 4 finding that circulating $CD3^+$ T lymphocytes generate superoxide basally, and release greater amounts of superoxide after Nox2 is activated by PDB. We also confirmed the exciting finding that more PDB-stimulated superoxide is produced by circulating $CD3^+$ T lymphocytes after cerebral I-R. In addition, the present preliminary data indicate the tentative new finding that both circulating $CD4^+$ and $CD8^+$ T lymphocytes may produce superoxide basally, and produce greater levels of superoxide after stimulation by PDB. However, the most important finding of this study may be that following cerebral I-R, PDB-stimulated superoxide production from both $CD4^+$ and $CD8^+$ T lymphocytes is possibly enhanced compared to $CD4^+$ and $CD8^+$ T lymphocytes isolated from control mice.

The generation of reactive oxygen species (ROS), including superoxide, is increased in the brain following stroke (especially after cerebral I-R) and is well established to contribute to infarct damage (Chan, 2001; Crack and Taylor, 2005). ROS generation after stroke has been shown to occur in neurons, microglia, endothelial cells, as well as infiltrating neutrophils and macrophages (Chan, 2001). However, this is the first data to suggest that $CD4^+$ and $CD8^+$ T lymphocyte subsets each produce Nox2-depedent superoxide, and more importantly, produce a greater amount of superoxide following stroke.

T lymphocytes play an important role in the adaptive immune system. In response to an infection, T lymphocytes recognise 'non-self' antigens, proliferate into effector cells and then produce cytokines and cytotoxins to help eliminate the antigen (For reviews see Barry and Bleackley, 2002; Harrison *et al.*, 2008; Santana and Rosenstein, 2003). T lymphocytes, as well as many other cells, are known to release pro- and anti-inflammatory cytokines in the circulation and the brain following stroke (Arumugam *et al.*, 2005; Hurn *et al.*, 2007; Liesz *et al.*, 2009b; Loihl *et al.*, 1999; Offner *et al.*, 2006a; Vila *et al.*, 2000). These pro-inflammatory cytokines are known to

be deleterious in stroke (Liesz *et al.*, 2009b; Nawashiro *et al.*, 1997; Relton *et al.*, 1996), whereas the anti-inflammatory cytokines are protective (Liesz *et al.*, 2009b). Early after stroke, there is generally more of a pro-inflammatory T lymphocyte response, which shifts to an anti-inflammatory response in the post-acute phase (Offner *et al.*, 2006b; Theodorou *et al.*, 2008). Brain infiltration of T lymphocytes occurs early after I-R, and infiltration of both $CD4^+$ and $CD8^+$ T lymphocytes has been reported (Gelderblom *et al.*, 2009; Jander *et al.*, 1995). Although we have only examined circulating T lymphocytes here, we speculate that these early infiltrated T lymphocytes are likely to release large amounts of superoxide as well as various pro-inflammatory cytokines. Therefore, the inhibition of both $CD4^+$ and $CD8^+$ T lymphocyte brain infiltration, as early as possible after reperfusion, could be a potential therapeutic target. Moreover, a recent study found that ROS produced by Nox2 caused endothelial cells to contract through the activation of Rho-kinase, which subsequently produced increased permeability of the blood brain barrier (BBB) (Kahles *et al.*, 2007). This finding suggests that the inhibition of Nox2-dependent ROS production in circulating T lymphocytes may also be protective, and will consequently reduce infiltration of other damaging immune cells via the compromised BBB. However, a delicate balance between immunosuppression to reduce damage and an immune response to reduce infections after stroke needs to be achieved.

In Chapter 4, when we utilised Nox2-deficient mice and observed no increase in the amount of superoxide generated by $CD3^+$ T lymphocytes when in the presence of PDB, we verified that the increase in superoxide release by PDB-stimulated wild-type T lymphocytes was Nox2-dependent (see Figure 4.7D). These findings suggest than an increase in PDB-stimulated superoxide results from an increased Nox2 expression and/or activity in these T lymphocytes. The present relatively preliminary study found a statistically significant higher level of PDB-stimulated superoxide production after cerebral I-R compared with control mice by circulating $CD3^+$ and $CD8^+$ T lymphocytes, with a tendency for the same to occur in $CD4^+$ T lymphocytes. Since

PDB-stimulated superoxide production from $CD4^+$ T lymphocytes increased the least after I-R compared to control levels, perhaps the amount of Nox2 expression in the $CD4^+$ T lymphocyte subset is the least affected by cerebral I-R. Moreover, given that the greatest fold-change in PDB-stimulated superoxide production after cerebral I-R was observed in $CD8^+$ T lymphocytes, perhaps there is a greater increase in Nox2 protein expression in the $CD8^+$ T lymphocyte subset following cerebral I-R. However further Western blotting studies in these T lymphocyte subsets after stroke in purer suspensions need to be conducted to confirm this.

$CD4^+$ T lymphocytes were the only subset that produced an increase in PDB-stimulated superoxide release after stroke that did not reach statistical significance. If this difference is real, a closer look into the composition of T_H lymphocytes suggests two possible explanations. One of the main subsets of $CD4^+$ T lymphocytes, the T_H2 subset, is known to generally produce anti-inflammatory cytokines and part of its role is to suppress the pro-inflammatory immune response. However, T_H2 lymphocytes are more likely to appear later in immune responses (Abbas *et al.*, 1996), and therefore may not play as important a role as other subsets early after stroke. However, regulatory T (T_{reg}; $CD4^+CD25^+Foxp3^+$) cells account for ~10 % of all $CD4^+$ T lymphocytes (Zouggari *et al.*, 2009), and are crucial in limiting T lymphocyte responses and preventing autoimmune disorders (Sakaguchi *et al.*, 2006). Importantly, T_{reg} cell depletion in mice has been reported to increase infarct volume and augment neurological deficit 7 days after both 30 min ischaemia with reperfusion (I-R) and I-NR, suggesting a neuroprotective role after stroke (Liesz *et al.*, 2009b). T_{reg} cell depletion was also found to elevate blood and brain pro-inflammatory cytokine mRNA expression (TNF-α and IFN-γ) after stroke, as well as increase IFN-γ production in brain infiltrating $CD3^+$ T lymphocytes (Liesz *et al.*, 2009b). This suggests that T_{reg} cells do not produce pro-inflammatory cytokines, but that they may in fact play a role in inhibiting the activation and cytokine production of the other T lymphocytes. From this, it can be hypothesised that T_{reg} cells also do not produce damaging superoxide, but may in fact suppress

the release of superoxide by other $CD4^+$ T lymphocytes (and possibly $CD8^+$ T lymphocytes when they are both present), thus, dampening the overall effect. This is consistent with the finding that mice deficient in $CD8^+$ T lymphocytes undergo smaller infarct volumes than mice deficient in $CD4^+$ T lymphocytes (~73% and ~55% smaller than wild-type mice, respectively) (Yilmaz *et al.*, 2006), as it is likely that when T_{reg} cells were deleted together with the other $CD4^+$ T lymphocytes, it counteracted the protective effects.

In this study, as well as in Chapter 4, we utilised the Nox2 activator, PDB, in T lymphocytes. As mentioned above, we found evidence in Chapter 4 that the effect of PDB was Nox2-dependent. This Nox2 activation is not to be confused with conventional T lymphocyte activation. Jackson and colleagues reported that Nox2-containing NADPH oxidase in T lymphocytes was activated when the T cell receptor (TCR) was cross-linked (Jackson *et al.*, 2004), which occurs during antigen recognition, and is the first of two signals required to activate T lymphocytes (Murphy *et al.*, 2008). Intriguingly however, superoxide production after TCR stimulation did not require the expression of Nox2 (Jackson *et al.*, 2004). A very recent study reported that neither antigen recognition nor co-stimulation, the first and second steps vital for T lymphocyte activation, respectively (Murphy *et al.*, 2008), were required to produce the detrimental effects caused by T lymphocytes during the early stages of cerebral I-R (Kleinschnitz *et al.*, 2010b). Therefore we hypothesise that as there is a greater amount of superoxide being produced by T lymphocytes with PDB stimulation, this may be due to a greater expression and/or activity of Nox2 in the T lymphocytes. Given that stroke itself causes an increase in ROS production of which the Nox2-containing NADPH oxidase is a major source (Jackman *et al.*, 2009a; Kunz *et al.*, 2007), a greater production of superoxide from these circulating T lymphocytes most likely occurs following stroke in vivo. Moreover, we postulate that the increased generation of superoxide by T lymphocytes may account for part of the detrimental effects of T lymphocytes in stroke, and

further speculate that this increased superoxide production also occurs after the T lymphocytes have infiltrated the brain, thus promoting neuronal damage when inside the parenchyma.

In the present study, the apparent measured values of superoxide produced by T lymphocytes are much lower than that found in Chapter 4 (see Figures 4.7A & 5.1A-C). The reason for this is that here, we counted T lymphocyte number in each sample to normalise the chemiluminescence signal at a magnification of 40x rather than 10x. Counting cells at a magnification of 40x is more accurate, and therefore, the amount of superoxide produced per cell in the present study is likely to be more reliable. Nonetheless, it is important to note that the increased effect of stroke on superoxide generation was maintained and that the general profile remained.

A major limitation of this study is that the purity of the T lymphocyte suspensions was unfortunately found to be somewhat low. As a result, it is difficult at present to exclude the possibility that the samples prepared throughout these studies were commonly contaminated with significant numbers of neutrophils, monocytes, B lymphocytes, dendritic cells, NKT cells and/or NK cells. Moreover, many of these possible contaminating cell types are known to express Nox2 protein and produce superoxide (Jackson *et al.*, 2004; Selemidis *et al.*, 2008). In Chapter 4, we also performed FACS on some samples after T lymphocyte isolation (data not shown) and found >80 % purity in each sample. However, this was only performed for $CD3^+$ T lymphocyte isolation (as this was the only T lymphocyte subset we analysed), and was also performed following I-R, not in naive mice, as is the case in the present study. It is possible that the Dynal® bead kits are more efficient and selective when used on blood samples after I-R given that 24 h after I-R there was a slight trend for some immune cells in the blood to be reduced (see Figures 4.5A-F), leading to less cells available for the beads to bind to. If this were the case, it may be possible that the stroke samples used in the superoxide assays were purer and less contaminated than the naive samples we performed FACS analysis on, although we would need

to perform further routine FACS analysis on suspensions isolated from naive mice and mice after I-R to confirm this. The low level of purity may also account for the large variability observed in the PDB-stimulated groups, and this will need to be addressed in future work so as to clarify and advance the current data. As such, this study remains somewhat incomplete, mainly due to the time constraints in completing this PhD.

The preliminary findings of the present study suggest for the first time, a possible mechanism of T lymphocyte-mediated stroke injury other than through the more traditional role of the production of cytokines or cytotoxins, or the accumulation of these cells in the circulation. However, the present studies need to be repeated using a more reliable cell sorting method to increase purity, to confirm these findings. In addition, the isolation of $CD4^+$ T lymphocytes with the exclusion of T_{reg} cells to observe whether superoxide generated levels are higher would also be of interest.

Chapter 6:

The Role of Chemokines in Cerebral Ischaemia-Reperfusion

6.1 INTRODUCTION

Inflammatory processes are now well established to contribute to the pathophysiology of cerebral ischaemia, especially when the brain is reperfused (ischaemia-reperfusion; I-R). A characteristic feature of this neuro-inflammation is the attraction and brain infiltration of inflammatory cells, and many experimental cerebral I-R studies, as well as post-mortem studies, found evidence of neutrophils, monocytes, lymphocytes, natural killer (NK) cells and dendritic cells in the infarcted brain (Campanella *et al.*, 2002; Gelderblom *et al.*, 2009; Schwab *et al.*, 2001; Stevens *et al.*, 2002; Wang *et al.*, 1993). The majority of studies have focussed on neutrophils, monocytes and T lymphocytes, and the infiltration of these immune cells has been reported to be detrimental in stroke (Arumugam *et al.*, 2004; Wang *et al.*, 2002).

Chemokines are chemotactic cytokines, and they and their receptors play a crucial role in the migration of leukocytes under basal and inflammatory conditions (Gerard and Rollins, 2001; Mackay, 2001; Rossi and Zlotnik, 2000; Semple *et al.*, 2010; Zlotnik and Yoshie, 2000). In fact, in mammals, chemokines are the major mediators of leukocyte migration, and are essential for the trafficking of most cell types from the blood stream (Mackay, 2001). Chemokines are produced by many cells including neutrophils, monocytes, macrophages, platelets, mast cells, T lymphocytes, NK cells, fibroblasts, smooth muscle cells and endothelial cells (Armstrong *et al.*, 2004; Call *et al.*, 2001; Strieter *et al.*, 1996), and they mainly act on bone marrow-derived cells (Gerard and Rollins, 2001; Strieter *et al.*, 1996; Zlotnik and Yoshie, 2000). There are different classes of chemokines differentiated by their structures. The two main classes are 'CXC and CC'. These 'C's denote the two N-terminal cysteine residues, and the classes are divided depending on whether there is an amino acid between them (CXC), or whether they lie adjacently (CC) (Rollins, 1997; Rossi and Zlotnik, 2000; Strieter *et al.*, 1996; Zlotnik and Yoshie, 2000). The CXC subfamily can be further split into two groups: the better known ELR^+, or ELR^-, based on whether the glutamate-leucine-arginine motif is present between the N-terminus and the first

cysteine (Bizzarri *et al.*, 2006; Rollins, 1997; Rossi and Zlotnik, 2000). The ELR^+ CXC chemokine subfamily are mainly neutrophil chemoattractants (Di Cioccio *et al.*, 2004; Kielian *et al.*, 2001; Tani *et al.*, 1996), whereas the CC chemokines generally act on monocytes, T lymphocytes and dendritic cells (Rollins, 1997). However, members of the chemokine superfamily are very promiscuous, and a chemokine ligand may bind to several receptors, while a chemokine receptor may bind multiple ligands (Gerard and Rollins, 2001; Rollins, 1997; Zlotnik and Yoshie, 2000).

Chemokines and their receptors have been shown to be important in various inflammatory pathologies such as I-R injury, vascular diseases including atherosclerosis, and other diseases of the CNS (Bizzarri *et al.*, 2006; Gerard and Rollins, 2001; Semple *et al.*, 2010; Strieter *et al.*, 1996). Furthermore, the blockade or deficiency of one or more chemokine has been reported to improve a number of these pathologies (Gerard and Rollins, 2001; Strieter *et al.*, 1996). Several chemokines are reported to be increased in stroke, and also to contribute to the pathogenesis (Semple *et al.*, 2010), as they recruit leukocytes into the brain, inducing a higher expression of these or other chemokines as well as cytokines, which then recruit more leukocytes, ultimately resulting in a very damaging and ongoing cycle (Gerard and Rollins, 2001). It is therefore reasonable to predict that inhibition of this inflammatory cycle may reduce stroke damage, and for this reason, chemokine ligands and receptors are potential drug targets. Each chemokine ligand and receptor typically engages selective leukocyte subsets, and therefore, their inhibition is likely to produce a limited side effect profile (Gerard and Rollins, 2001). The specificity of an immunomodulatory drug is an especially desirable property for treatment following stroke, as the chance of inhibiting other important functions of the immune system, and consequently increasing the incidence of infection - the most common cause of death in the post-acute phase of stroke (Heuschmann *et al.*, 2004; Vernino *et al.*, 2003) - would be reduced.

The aims of this study were firstly, to examine the mRNA expression profiles of a large number of chemokines and their receptors in the ischaemic and non-ischaemic brain hemispheres 4, 24 and 72 h after I-R. From this array, we sought to identify a family of chemokines that were significantly up-regulated in the brain over 4 to 72 h following I-R, and to pharmacologically target them in an experimental model of stroke. This time frame is a major focus for development of new therapies for acute stroke because the only existing approved treatment (rt-PA) must be given within 4.5 h of stroke onset, whereas it is known that neuronal injury and death continues for up to several days to a few weeks (Dereski *et al.*, 1993; Kunz *et al.*, 2007; Li *et al.*, 2000; Li *et al.*, 1995).

6.2 MATERIALS AND METHODS

6.2.1 Animals

This study was conducted in accordance with the National Health and Medical Research Council of Australia guidelines for the care and use of animals in research.

A total of 57 male 8-10 week old C57Bl6/J mice were studied (weight, 24.9±0.3 g). The mice had free access to water and food pellets before and after surgery. Fourteen mice were excluded from the study as they died after MCAO but prior to the specified time for euthanasia (at 71.5 h reperfusion).

6.2.2 Focal cerebral ischaemia

Focal cerebral ischaemia was induced by transient intraluminal filament occlusion of the right middle cerebral artery (MCA) as described in section 2.3 of General Methods. In this study, some mice were killed at 4 h after sham surgery and I-R, in addition to the 24 and 72 h endpoints.

Mice were treated i.p. with vehicle (1 % dimethyl sulfoxide; DMSO) or SB 225002 (1 mg/kg) commencing at reperfusion, and then twice every 24 h, for either 24 h (i.e. a total of 2 mg/kg) or 72 h (i.e. a total of 6 mg/kg). Mice were randomly assigned a treatment group by coin toss, once the filament was inserted. DMSO has been reported to reduce infarct volume following I-R (Laha *et al.*, 1978) and I-NR (Bardutzky *et al.*, 2005; Shimizu *et al.*, 1997), however these studies only observed significant neuroprotection when DMSO was used at a minimum of 10 %, ten times higher than concentrations used in this study. Twenty-one mice were used to examine the mRNA expression levels in the ischaemic hemisphere following cerebral I-R, and were untreated.

6.2.3 Evaluation of neurological function

At the end of the experiment (72 h), neurological function was evaluated using a five-point scoring system, and the hanging wire test. Please refer to section 2.4 of General Methods for details.

6.2.4 Evaluation of cerebral infarct and oedema volume

Cerebral infarct and oedema volume were evaluated as described in section 2.5 of General Methods.

6.2.5 Measurement of mRNA in brain hemispheres

Brains from untreated sham-operated and stroked mice killed at 4, 24 and 72 h, as well as vehicle- or SB 225002-treated stroked mice killed at 24 h after I-R, were used to measure mRNA expression levels using real-time PCR. In the ischaemic (right) and non-ischaemic (left) hemispheres, a large number of chemokine and chemokine receptor genes were examined in a PCR array, and Taqman gene expression assays were used to specifically measure CXCR2, CXCL1 and CXCL2 mRNA levels. Please refer to section 2.8 of General Methods for details.

We first used the Mouse Chemokines & Receptors PCR Array with Sybr Green (SABiosciences; Frederick, MD, USA) to examine the expression of a large range of chemokines and their receptors after stroke. After RNA extraction (see section 2.8 of General Methods), the RNA was converted into cDNA, using the RT^2 First Strand Kit, which is part of the PCR array. First, the volume of RNA per sample needed for 1 μg of RNA was calculated. This volume was placed into a sterile PCR tube with 2 μl Genomic DNA (gDNA) Elimination mixture, and then RNase-free water was added to make up the final volume to 10 μl. The contents were then mixed gently with a pipette followed by brief centrifugation. This was then incubated at 42 °C for 5 min using a heat block, and immediately placed on ice for at least 1 min. On ice, the reverse transcriptase mix was made up, which per sample included 4 μl RT buffer (5x), 1 μl Primer and external control mix, 2 μl RT Enzyme mix and 3 μl H_2O. This was then added to each sample in the PCR tubes. The contents were then gently mixed with a pipette and incubated at 42 °C for exactly 15 min, and then immediately incubated at 95 °C for 5 min to inactivate the reverse transcriptase. 91 μl H_2O was added to each tube and mixed well. Each tube of Diluted First Strand cDNA was then placed on ice until the next step or stored at -20 °C until ready for use.

To carry out the real-time PCR, first the Experimental Cocktail was prepared in a 5 ml tube, containing 1350 μl 2x SABiosciences RT^2 qPCR Master Mix, 102 μl Diluted First Strand cDNA Synthesis Reaction and 1248 μl H_2O, and was mixed well. Next, the PCR array plate was carefully removed from its sealed bag and 25 μl of the Experimental Cocktail was added into each well. The PCR array plate was then tightly sealed with adhesive topseal and centrifuged (1000 g; 1 min at room temperature) to remove bubbles. Next, the plate was inspected from underneath to ensure that there were no bubbles, and then it was placed into the Bio-Rad CFX96™ Real-Time PCR Detection System (Bio-Rad; Hercules, CA, USA). The real-time PCR was then run for 40 cycles, using the following thermal-cycling parameters:

Stage	Temperature	Time
Hold	95 °C	10 min
Cycle	95 °C 55 °C 72 °C	15 s 30 s 30 s
Hold	95 °C	10 s
Melting Curve	65 → 95 °C (in 0.5 °C increments)	5 s each increment

From the findings of the PCR array experiment, we then selected 2 chemokine ligands and their receptor for further investigation. To confirm the changes we observed in the mRNA expression of these chemokines and their receptor using the PCR array, we separately purchased pre-designed Taqman® gene expression assays for CXCR2 (NCBI Reference Sequence; RefSeq NM_009909.3), CXCL1 (RefSeq NM_008176.3) and CXCL2 (RefSeq NM_009140.2), as well as β-actin (RefSeq NM_007393.1; Applied Biosystems; Carlsbad, CA, USA) for the house-keeping gene. The same RNA samples were used, as for the PCR array. The RNA was converted into cDNA using the Qiagen Quantitect Reverse transcription kit (Qiagen; Hilden, Germany). First, the volume of RNA per sample needed for 1 μg of RNA was calculated and placed into an RNase-free Eppendorf tube. Next, 2 μl gDNA wipeout buffer was added, as well as RNase-free water to make up the final volume to 14 μl. This was then incubated at 42 °C for 2 min using a heat block, and immediately placed on ice. On ice, the reverse transcriptase mix per sample was made up, which included 1 μl Quantiscript Reverse Transcriptase, 4 μl Quantiscript RT buffer (5x) and 1 μl RT Primer mix. This was then added to each sample. The samples were then incubated at 42 °C for exactly 15 min, and then immediately incubated at 95 °C for 3 min to inactivate the reverse transcriptase. Each tube of cDNA was then placed on ice until the next step or stored at -20 °C until ready for use.

To carry out the real-time PCR, first the PCR mixture was prepared, containing 3.5 μl 20x Taqman gene expression assay (Applied Biosystems), 35 μl 2x Taqman PCR Universal Master

Mix (Applied Biosystems), 14 µl cDNA (50 ng for CXCR2, CXCL1 and CXCL2 and 10 ng for β-actin) and 17.5 µl Nuclease-free water (Applied Biosystems). Each PCR reaction tube was mixed and centrifuged briefly. Each sample was run in triplicate, so 20 µl of the 70 µl PCR mixture (10 µl extra was made up to allow for pipetting errors) was pipetted into each well of a 96-well PCR plate (3 times per sample) and carefully covered with an adhesive topseal. The plate was then briefly centrifuged and placed into the Bio-Rad CFX96™ Real-Time PCR Detection System (Bio-Rad). The real-time PCR was then run for 40 cycles, using the following thermal-cycling parameters:

Stage	Temperature	Time
Hold	50 °C	2 min
Hold	95 °C	10 min
Cycle	95 °C 60 °C	15 s 1 min

6.2.6 Localisation of neutrophils

The localisation of myeloperoxidase-positive (MPO) cells in untreated brain sections following sham surgery, or brain sections treated with either vehicle or SB 225002 following cerebral I-R was performed by immunohistochemistry as described in section 2.9 of General Methods. Multiple serial coronal sections of 30 µm were taken at 6 levels: bregma +1.6 mm, +1.0 mm, +0.4 mm, -0.2 mm, -0.8 mm and -1.82 mm (the mid hippocampus), and were thaw-mounted onto poly-L-lysine coated glass slides (0.1 % poly-L-lysine in dH_2O). Four of these tissue sections per sham-operated brain, and five to six of these tissue sections per stroked brain were fixed in acetone for 15 min and washed in 50 mM tris-buffered saline (TBS; pH 8.4; 3 x 5 min) before incubation in a humid chamber in 10 % goat serum (Abcam; Cambridge, MA, USA) in TBS for 2 h to block non-specific binding. Sections were then incubated for 1 h in anti-rabbit MPO polyclonal antibody (1:100; Abcam). Sections were washed in TBS (3 x 5 min), blocked with a peroxidase blocking agent (Dako; Glostrup, Denmark) for 15 min and stained using the

DAKO EnVision+ system (Dako). Sections were then incubated for 45 min with a peroxidase-labelled polymer conjugated to a goat anti-rabbit antibody (Invitrogen; Carlsbad, CA, USA), washed in TBS (3 x 5 min), and followed by incubation with diaminobenzidine (Dako) for 5 min. Sections were then washed in TBS (3 x 5 min), mounted in aquatex (Merck; Darmstadt, Germany) and cover-slipped. Staining was analysed on an Olympus light microscope (Olympus; Hamburg, Germany) by two observers blinded to the identity of experimental groups, who counted MPO^+ cells in the ischaemic (right) hemisphere. Number of MPO^+ cells in the ischaemic hemisphere were normalised to the number of sections analysed per brain.

6.2.7 Drugs and chemicals

As per section 2.14 of General Methods. SB 225002 (Sapphire Bioscience; Redfern, NSW, Australia) was dissolved in DMSO (Merck) and diluted with 0.9 % saline (Baxter Healthcare; Old Toongabbie, NSW, Australia), achieving a final concentration of 1 % DMSO.

6.2.8 Statistical analysis

All data are presented as mean ± standard error. Statistical analyses were performed using GraphPad Prism version 5 (GraphPad Software Inc., San Diego, CA, USA). Between-group comparisons were analysed as described in section 2.15 of General Methods. Group numbers are shown in parentheses. Statistical significance was accepted when $P < 0.05$.

6.3 RESULTS

6.3.1 Effect of I-R on a wide range of chemokine and chemokine receptor mRNA expression levels in the brain

Firstly, we used a PCR array with Sybr Green, to acquire a general understanding of which chemokine and chemokine receptor expressions were changed at different time-points following

cerebral I-R in the brain. We used the Mouse Chemokines and Receptors PCR array (SABiosciences), which profiles the expression of 84 genes that encode mainly chemokine ligands and receptors from the CC and CXC families, as well as other chemokine ligands and receptors, and other related genes. Overall, I-R affected the mRNA expression of a large number of chemokine and chemokine related genes. The highest 10 changes at each time-point are shown in Table 6.1 (see below). Please note that there are only 16 different genes included here, as some genes formed part of the 10 highest changing genes at more than one time-point.

	Normalised mRNA fold expression in the ischaemic hemisphere		
Genes	**4 h after I-R**	**24 h after I-R**	**72 h after I-R**
CCL2	3	18	19
CCL4	32	34	4
CCL7	3	7	6
CCL11	3	5	12
CCL12	2	1	11
CCR4	1	24	0
CXCL1	1	37	14
CXCL2	3	303	8
CXCL10	3	12	35
CXCR2	2	6	13
Gdf5	5	5	1
IL-1a	11	3	3
IL-16	3	1	1
Lif	3	5	11
TNF-α	16	37	12
Trem1	1	13	13

Gdf5=growth differentiation factor 5; Lif=leukaemia inhibitory factor; Trem=triggering receptor expressed on myeloid cells 1

Table 6.1. The mRNA expression at 4, 24 and 72 h after I-R of the genes that changed the most (the top 10) at each time-point in the PCR array.

The mRNA expression of various chemokine, chemokine receptor and chemokine related genes in the ischaemic (right) hemisphere at 4, 24 and 72 h after I-R, normalised to the expression in the left hemisphere of sham-operated mice. The listed genes formed part of the top 10 changed expressions at each time-point after I-R.

Based on the findings from the PCR array, we chose to focus on the CXCR2 receptor (formerly named interleukin receptor 8 type b; IL8Rb), and its ligands, CXCL1 (also named keratinocyte-derived chemokine; KC) and CXCL2 (macrophage inflammatory protein-2; MIP-2) (Lee *et al.*, 1995). This subfamily was selected due to the high changes in mRNA expression of all 3 members after I-R, especially at the later time-points (24 and 72 h), because this is a desirable time-frame for novel effective therapeutic intervention after stroke. Furthermore, although not many commercially available chemokine antagonists are functional in mice, SB 225002, an inhibitor of human CXCR2 (White *et al.*, 1998) has previously been shown to reduce experimental colitis in mice, through a reduction in neutrophil infiltration and CXCL1 and CXCL2 expression (Bento *et al.*, 2008), suggesting that it is also able to inhibit mouse CXCR2. Therefore, we focussed on this chemokine subfamily and later treated mice with SB 225002 after stroke (see sections 6.3.3, 6.3.4 and 6.3.5).

At 4, 24 and 72 h after I-R, CXCR2 mRNA expression in the ischaemic (right) hemisphere was increased by 2-, 6- and 13-fold, respectively, when compared to the left hemisphere of sham-operated mice (n = 3; Figure 6.1A). There was a very small change in the non-ischaemic hemisphere 4, 24 and 72 h after I-R (no change, 2- and 2-fold increases, respectively; Figure 6.1A). CXCR2 mRNA expression in the right hemisphere of sham-operated mice did not differ from the left hemisphere (Figure 6.1A).

At 24 and 72 h after I-R, CXCL1 mRNA expression in the ischaemic (right) hemisphere was increased by 37- and 14-fold, respectively, but it was unchanged at 4 h, when compared to the left hemisphere of sham-operated mice (n = 3; Figure 6.1B). CXCL1 mRNA expression in the non-ischaemic hemisphere of mice 4, 24 and 72 h after I-R showed a similar profile to the ischaemic hemisphere, although the changes were smaller (no change, 15- and 4-fold increases, respectively;

Figure 6.1B). There was no difference in expression in the right hemisphere of sham-operated mice compared to the left (Figure 6.1B).

At 4, 24 and 72 h after I-R, CXCL2 mRNA expression in the ischaemic (right) hemisphere was increased by 3-, 303- and 8-fold, respectively, when compared to the left hemisphere of sham-operated mice (n = 3; Figure 6.1C). CXCL2 mRNA expression in the non-ischaemic hemisphere of mice 4, 24 and 72 h after I-R showed a similar profile to the ischaemic hemisphere, although the increases in expression were smaller (2-, 110- and 2-fold increases, respectively; Figure 6.1C). Furthermore, CXCL2 mRNA expression in the right hemisphere of sham-operated mice also slightly increased at 4 and 24 h after sham surgery by 2- and 4-fold, respectively, but was unchanged at 72 h, compared to the left hemisphere (Figure 6.1C).

6.3.2 Effect of I-R on CXCR2, CXCL1 and CXCL2 mRNA expression levels in the brain

To confirm the changes we observed in CXCR2, CXCL1 and CXCL2 mRNA expression using the PCR array, we measured the mRNA expression of these 3 genes in the ischaemic (right) and non-ischaemic (left) hemisphere 4, 24 and 72 h after sham surgery or I-R, using specific pre-designed Taqman® gene expression assays.

CXCR2 mRNA expression showed a very similar profile to that observed using the PCR array. mRNA expression at 4, 24 and 72 h after I-R was increased by 4-, 3- and 12-fold, respectively in the ischaemic (right) hemisphere when compared to the left hemisphere of sham-operated mice (n = 3; Figure 6.2A). There was also a small increase in the non-ischaemic hemisphere after I-R by 2-, 2- and 4-fold at 4, 24 and 72 h after I-R, respectively (Figure 6.2A). In contrast, CXCR2 mRNA expression in the right hemisphere of sham-operated mice did not differ from the left hemisphere (Figure 6.2A).

A similar profile in CXCL1 mRNA expression at 4, 24 and 72 h after I-R was observed as for the PCR array, although changes were not as great (expression increased by 6-, 29- and 7-fold, respectively; n = 3; Figure 6.2B). CXCL1 mRNA expression in the non-ischaemic hemisphere of mice at each time-point after I-R showed a similar profile, although these increases were lower than in the ischaemic hemisphere (6-, 18- and 4-fold increase, respectively; Figure 6.2B). There was no difference in expression in the right hemisphere of sham-operated mice compared to the left (Figure 6.2B).

At 4, 24 and 72 h after I-R, CXCL2 mRNA expression in the ischaemic hemisphere was increased by 17-, 101- and 77-fold, respectively (n = 3; Figure 6.2C). Expression in the non-ischaemic hemisphere of mice 4, 24 and 72 h after I-R showed a similar profile, although these increases were smaller than the changes observed in the ischaemic hemisphere (17-, 62- and 10-fold, respectively; Figure 6.2C). Furthermore, CXCL2 mRNA expression in the right hemisphere of sham-operated mice also slightly increased at 4 and 24 h after sham surgery by 6- and 2-fold, respectively, but was unchanged at 72 h, compared to the left hemisphere (Figure 6.2C).

6.3.3 Effect of CXCR2 antagonist SB 225002 on CXCR2, CXCL1 and CXCL2 mRNA expression levels in the brain 24 h after I-R

We next treated mice with vehicle (1 % DMSO) or the CXCR2 antagonist, SB 225002 (1 mg/kg i.p.) commencing at reperfusion, and then administered twice every 24 h. SB 225002 [*N*-(2-hydroxy-4-nitrophenyl)-*N*9-(2-bromophenyl)urea] is a potent selective non-peptide inhibitor of human CXCR2, reported to reduce neutrophil migration mediated by the human and rabbit CXCL1 and CXCL2 homologue, CXCL8 (also named IL-8), both in vitro and in vivo (White *et al.*, 1998). Following treatment with SB 225002, expression levels of CXCR2 mRNA in the ischaemic hemisphere 24 h after I-R were reduced to 9 % of the levels in

vehicle-treated mice (veh=11.6±7.5, SB=1.1±0.4; n = 3; P = 0.23; Figure 6.3A). CXCL1 mRNA expression levels in the ischaemic hemisphere 24 h after I-R in SB 225002-treated mice were reduced to 12 % of the levels in vehicle-treated mice (veh=5.8±0.9, SB=0.5±0.1; n = 3; P = 0.15; Figure 6.3B). Following treatment with SB 225002, CXCL2 mRNA expression levels in the ischaemic hemisphere 24 h after I-R were reduced to 13 % of the levels in vehicle-treated mice (veh=6.6±3.4, SB=0.9±0.4; n = 3; P = 0.17; Figure 6.3C). These results suggest that SB 225002 does in fact antagonise mouse CXCR2.

6.3.4 Effect of CXCR2 antagonist SB 225002 on outcome 72 h after I-R

6.3.4.1 Regional cerebral blood flow

72 h cerebral I-R was produced by 30 min MCAO and 71.5 h reperfusion. Regional cerebral blood flow (rCBF) initially decreased to ~16 % of the pre-ischaemic level when the filament was inserted (Figure 6.4A). In the vehicle-treated group, rCBF remained at this level for the duration of MCAO, whereas rCBF increased to ~26 % of the pre-ischaemic level in the SB 225002-treated group during MCAO. The rCBF curve during the 30 min of ischaemia (i.e. prior to SB 225002 administration) was slightly but significantly higher in the SB 225002-treated group versus the vehicle-treated group (P < 0.05; Figure 6.4A). However, this occurred by chance and was not related to the specific treatment, as a coin was flipped to assign treatment after insertion of the filament, and the treatment was first administered at reperfusion (immediately after the 30 min time-point). At this time-point, upon removal of the monofilament, rCBF increased initially to ~117 %, and then stabilised at ~77 % after 30 min of reperfusion (Figure 6.4A).

6.3.4.2 Mortality and neurological function

Mortality rates at 72 h after I-R were somewhat high in both the vehicle- and the SB 225002-treated groups, however, they were not statistically different (vehicle, 6/13: 46 %; SB 225002, 5/14: 36 %; P = 0.59; Figure 6.4B). In addition, vehicle- and SB 225002-treated mice had a

similar level of functional impairment. Neurological score was not significantly different between vehicle- and SB 225002-treated mice following I-R, although there was a trend for SB 225002-treated mice to be worse off, as 4/9 SB 225002-treated mice had no spontaneous movement (were given a score of 4), whereas no vehicle-treated mice were given a score of 4 (Figure 6.4C). Similarly, vehicle- and SB 225002-treated mice had similar hanging wire times (veh=34±7 s, SB=27±8 s; P = 0.50; n = 7-9; Figure 6.4D).

6.3.4.3 Brain infarct and oedema volume measured as mm^3

Representative coronal sections of infarcted brain of vehicle- and SB 225002-treated mice 72 h after I-R are shown in Figures 6.5A and B, respectively. Seventy-two h after I-R, vehicle- and SB 225002-treated mice had very similar total (veh=18±5 mm^3, SB=23±8 mm^3; P = 0.63; n = 7-9; Figure 6.5C), cortical (veh=3±1 mm^3, SB=5±3 mm^3; P = 0.49; Figure 6.5D), and subcortical (veh=15±5 mm^3, SB=17±6 mm^3; P = 0.81; Figure 6.5D) infarct volumes. Oedema volumes 72 h after I-R were also very similar between treatment groups (veh=14±7 mm^3, SB=16±4 mm^3; P = 0.77; n = 7-9; Figure 6.5E).

6.3.4.4 Brain infarct volume measured as % of non-ischaemic hemisphere

Infarct volumes were also estimated as a percentage of the non-ischaemic hemisphere. The general profiles between treatment groups for the total, cortical and subcortical infarcts following I-R were very similar to when the infarct was measured in mm^3 (Figures 6.6A-B).

6.3.4.5 Brain infarct area distribution

The distribution of the infarct area throughout the brain was also plotted. Seventy-two h after I-R, similar shaped distribution profiles of the total, cortical and subcortical infarcts were observed in vehicle- and SB 225002-treated mice (Figures 6.7A-C).

6.3.5 Effect of CXCR2 antagonist SB 225002 on neutrophil infiltration 72 h after I-R

The number and localisation of infiltrated neutrophils in the ischaemic hemisphere was determined using immunohistochemistry with an anti-myeloperoxidase (MPO) antibody. MPO is abundantly expressed in neutrophils, although it is also found in monocytes and some macrophages (Lau and Baldus, 2006). We took coronal sections at 6 levels of the forebrain: bregma +1.6 mm, +1.0 mm, +0.4 mm, -0.2 mm, -0.8 mm and -1.82 mm (the mid hippocampus), and counted MPO^+ cells in the ischaemic (right) hemisphere of 4 of these sections in the brain of each sham-operated mouse, and 5 to 6 of these sections in the brain of each stroked mouse. At 72 h after sham surgery, MPO^+ cells were found to be present in the right hemisphere (4.3±0.8 cells per section; Figures 6.8A & D). Cerebral I-R produced a 2-3-fold increase in MPO^+ cells present in the ischaemic hemisphere (vehicle, 11.3±2.3 cells per section; Figures 6.8B & D). MPO^+ staining was significantly lower in SB 225002-treated mice (5.3±1.3 cells per section; Figures 6.8B & D) and did not differ from the sham-operated mice. In both stroked groups, MPO^+ cells were present in all 5 or 6 regions throughout the forebrain (data not shown).

Figure 6.1. CXCR2, CXCL1 and CXCL2 mRNA expression 4, 24 and 72 h after sham surgery or I-R using the PCR array.

CXCR2 (**A**), CXCL1 (**B**) and CXCL2 (**C**) mRNA expression was measured in ischaemic (right; R) and non-ischaemic (left; L) brain hemispheres 4, 24 and 72 h after sham surgery or I-R, using a PCR array with Sybr Green (n = 3 per group). Data are presented as mean ± SEM.

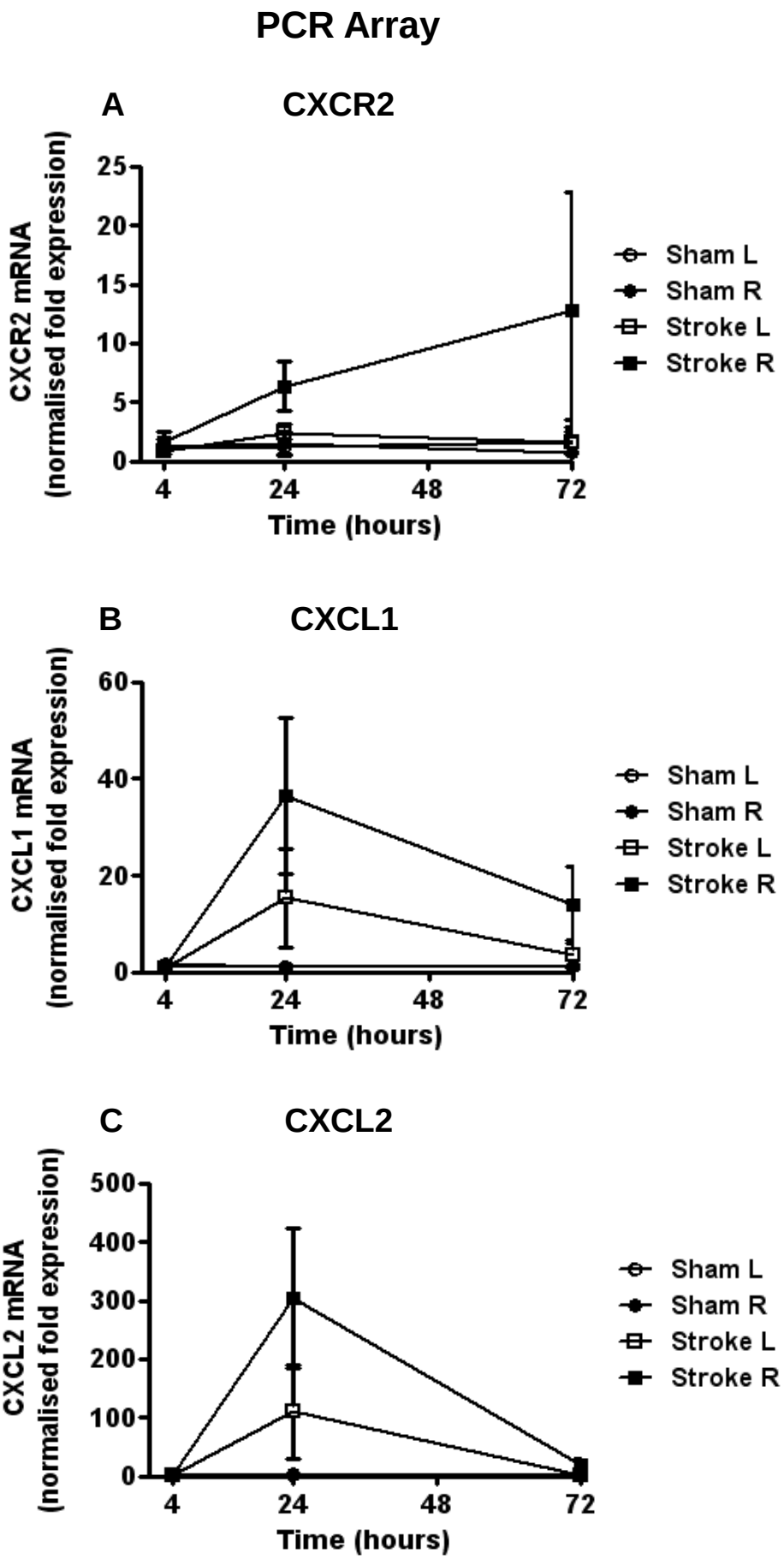
PCR Array
A
CXCR2
CXCR2 mRNA (normalised fold expression)
25
20
15
10
5
0
4
24
48
72
Time (hours)
Sham L
Sham R
Stroke L
Stroke R
B
CXCL1
CXCL1 mRNA (normalised fold expression)
60
40
20
0
4
24
48
72
Time (hours)
Sham L
Sham R
Stroke L
Stroke R
C
CXCL2
CXCL2 mRNA (normalised fold expression)
500
400
300
200
100
0
4
24
48
72
Time (hours)
Sham L
Sham R
Stroke L
Stroke R

Figure 6.2. CXCR2, CXCL1 and CXCL2 mRNA expression 4, 24 and 72 h after sham surgery or I-R using Taqman gene expression assays.

CXCR2 (**A**), CXCL1 (**B**) and CXCL2 (**C**) mRNA expression was measured in ischaemic (right; R) and non-ischaemic (left; L) brain hemispheres 4, 24 and 72 h after sham surgery or I-R, using Taqman gene expression assays (n = 3 per group). Data are presented as mean ± SEM.

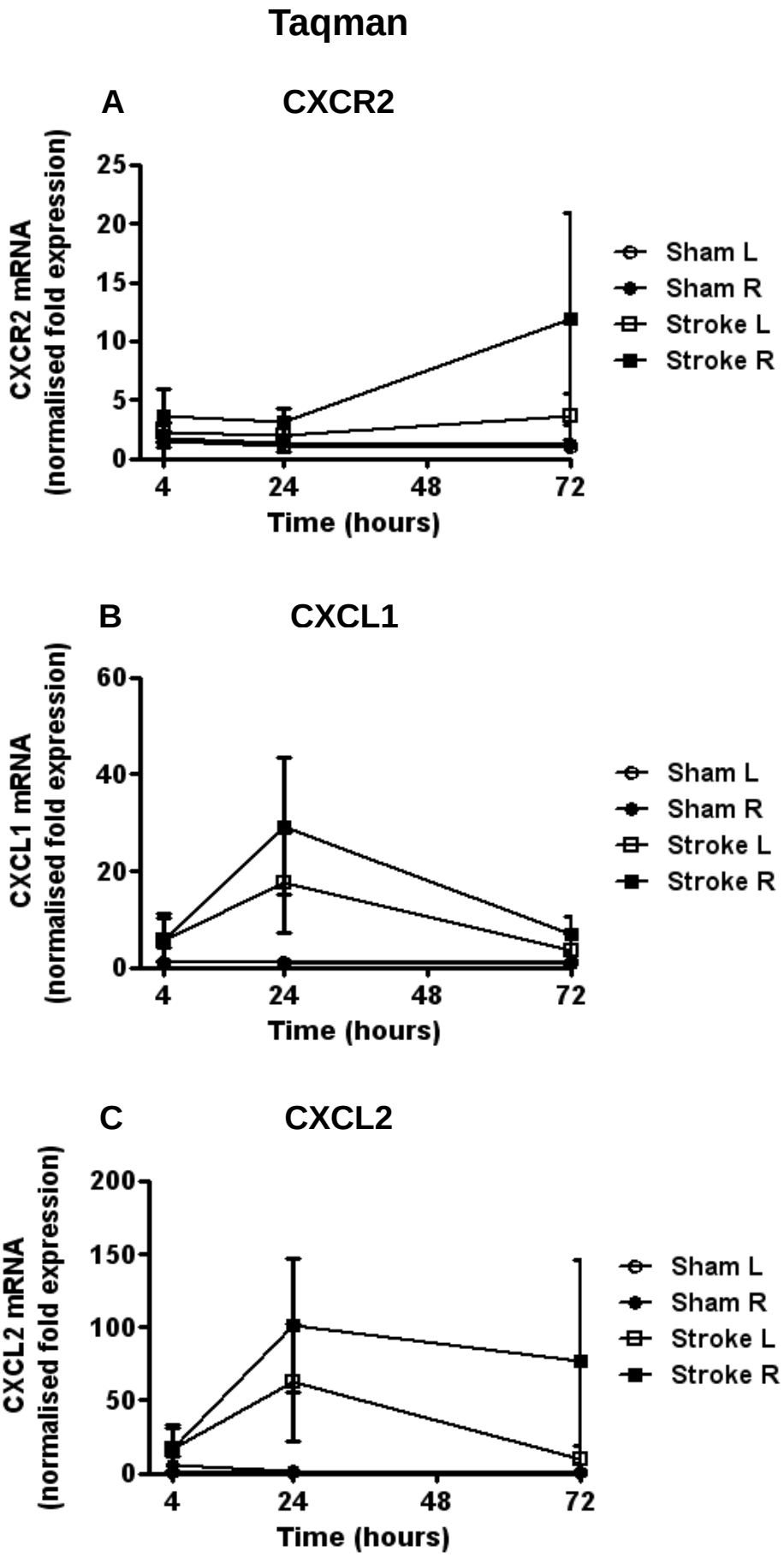
Taqman
A
CXCR2
CXCR2 mRNA
(normalised fold expression)
25
20
15
10
5
0
4
24
48
72
Time (hours)
Sham L
Sham R
Stroke L
Stroke R
B
CXCL1
CXCL1 mRNA
(normalised fold expression)
60
40
20
0
4
24
48
72
Time (hours)
Sham L
Sham R
Stroke L
Stroke R
C
CXCL2
CXCL2 mRNA
(normalised fold expression)
200
150
100
50
0
4
24
48
72
Time (hours)
Sham L
Sham R
Stroke L
Stroke R

Figure 6.3. CXCR2, CXCL1 and CXCL2 mRNA expression 24 h after I-R in vehicle- or SB 225002-treated mice.

CXCR2 (**A**), CXCL1 (**B**) and CXCL2 (**C**) mRNA expression was measured in ischaemic (right; R) and non-ischaemic (left; L) brain hemispheres 24 h after I-R in vehicle- (veh) or SB 225002-treated (SB) mice using Taqman gene expression assays (n = 3 per group). Data are presented as mean ± SEM.

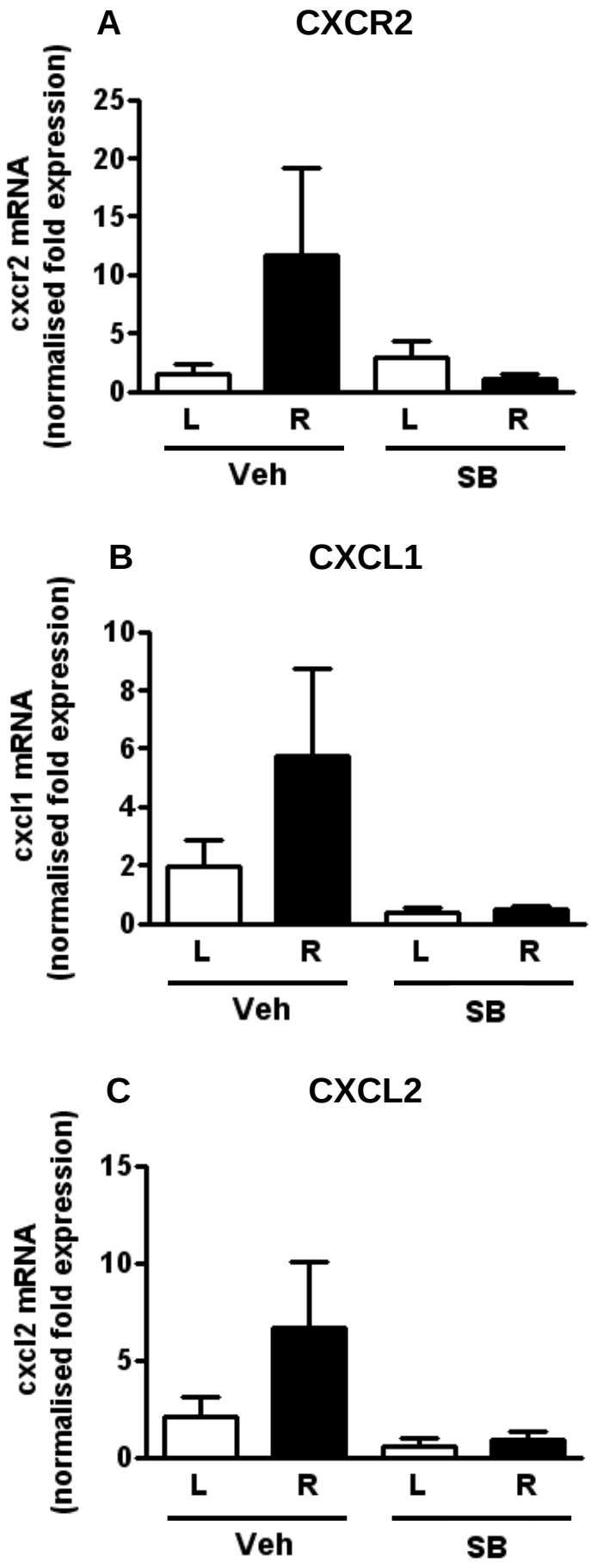
A
CXCR2
cxcr2 mRNA
(normalised fold expression)
25
20
15
10
5
0
L
R
L
R
Veh
SB
B
CXCL1
cxcl1 mRNA
(normalised fold expression)
10
8
6
4
2
0
L
R
L
R
Veh
SB
C
CXCL2
cxcl2 mRNA
(normalised fold expression)
15
10
5
0
L
R
L
R
Veh
SB

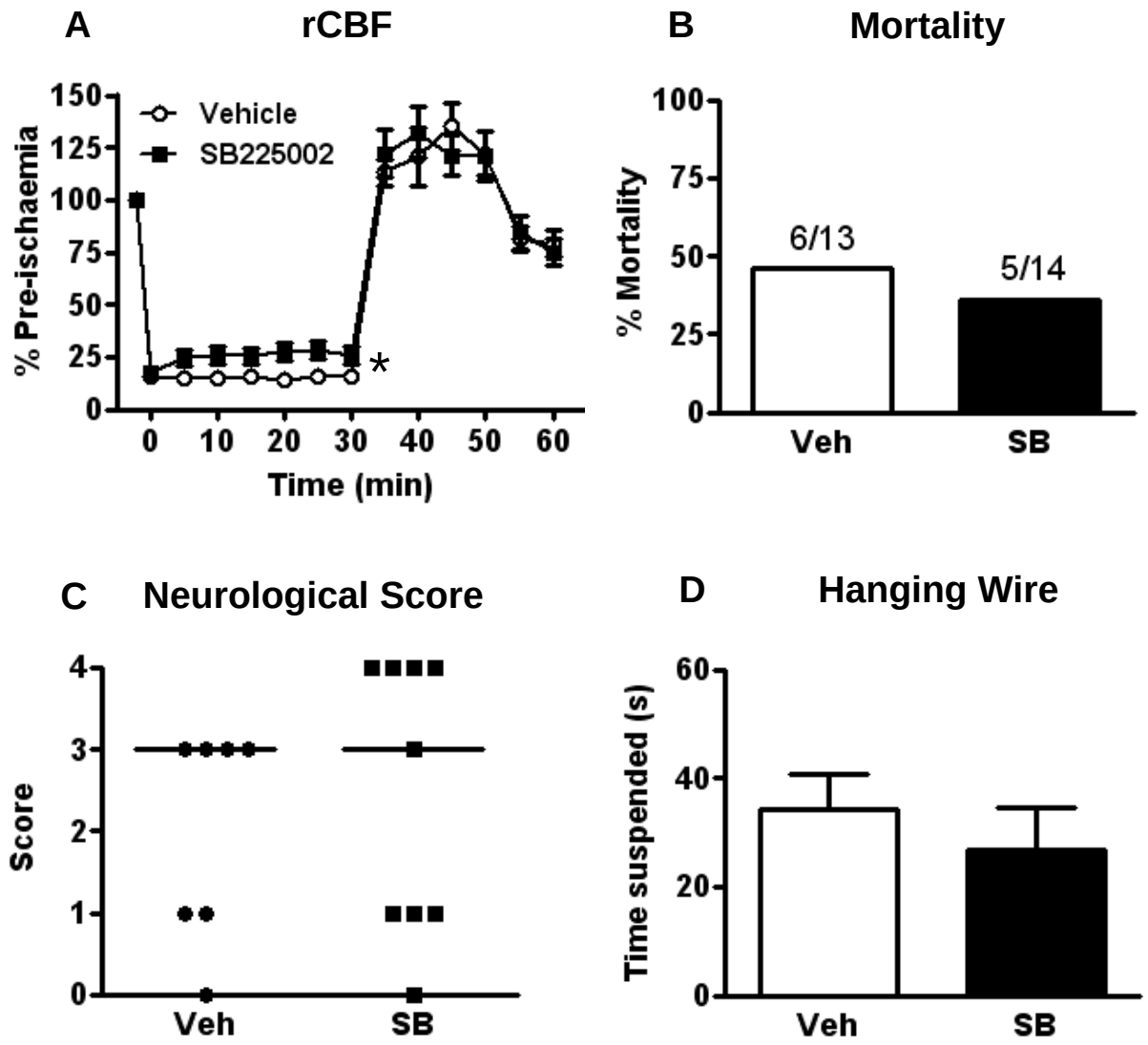

Figure 6.4. Regional cerebral blood flow (rCBF), mortality, neurological score and hanging wire at 72 h after I-R.

rCBF was recorded during and after 30 min MCAO (**A;** vehicle, n = 7; SB 225002, n = 9; *$P < 0.05$, 2-way ANOVA). **B:** Mortality at 72 h after MCAO. **C:** Neurological score 72 h after I-R (vehicle, n = 7; SB 225002, n = 9). **D:** Hanging wire data 72 h after I-R (vehicle, n = 7; SB 225002, n = 9). Mortality data are presented as a percentage; with numbers above the bars representing the number of animals who didn't survive 72 h over the total number, neurological score data are presented as median, and rCBF and hanging wire data are presented as mean ± SEM.

Figure 6.5. Cerebral infarct and oedema volume at 72 h after I-R (measured as mm^3). Representative coronal brain sections are shown from a vehicle- (**A**) and SB 225002-treated (**B**) mouse 72 h after I-R with the infarct area outlined in white. Total (**C**), and cortical and subcortical (**D**) cerebral infarct volumes were measured in vehicle- (veh; $n = 7$) and SB 225002-treated (SB; $n = 9$) mice 72 h after I-R. **E:** Oedema volume measured at 72 h in vehicle- ($n = 7$) and SB 225002-treated ($n = 9$) mice. Data are presented as mean ± SEM.

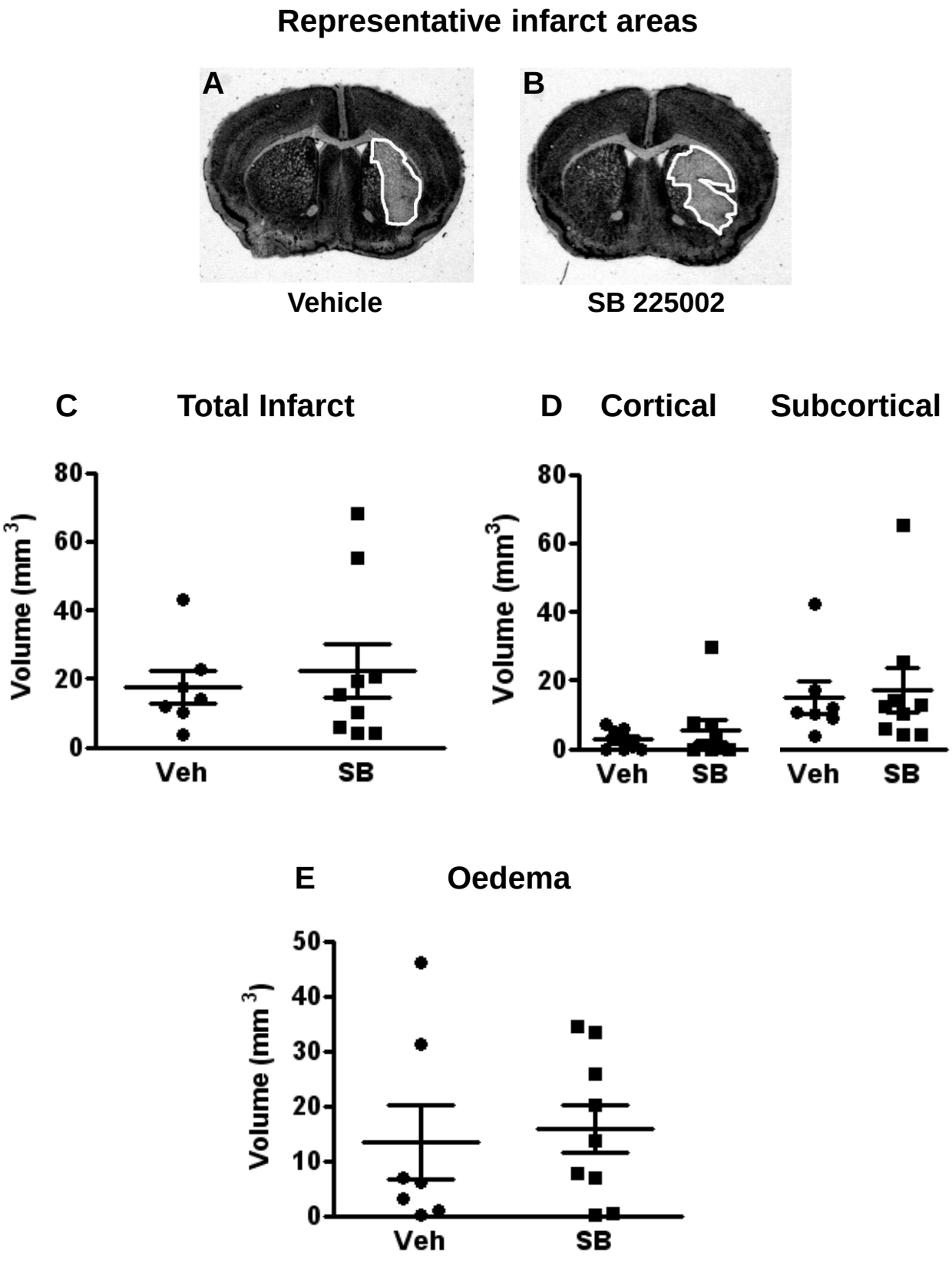
Representative infarct areas
A
B
Vehicle
SB 225002
C
Total Infarct
D
Cortical
Subcortical
Volume (mm3)
80
60
40
20
0
Veh
SB
E
Oedema
50
40
30
20
10
0

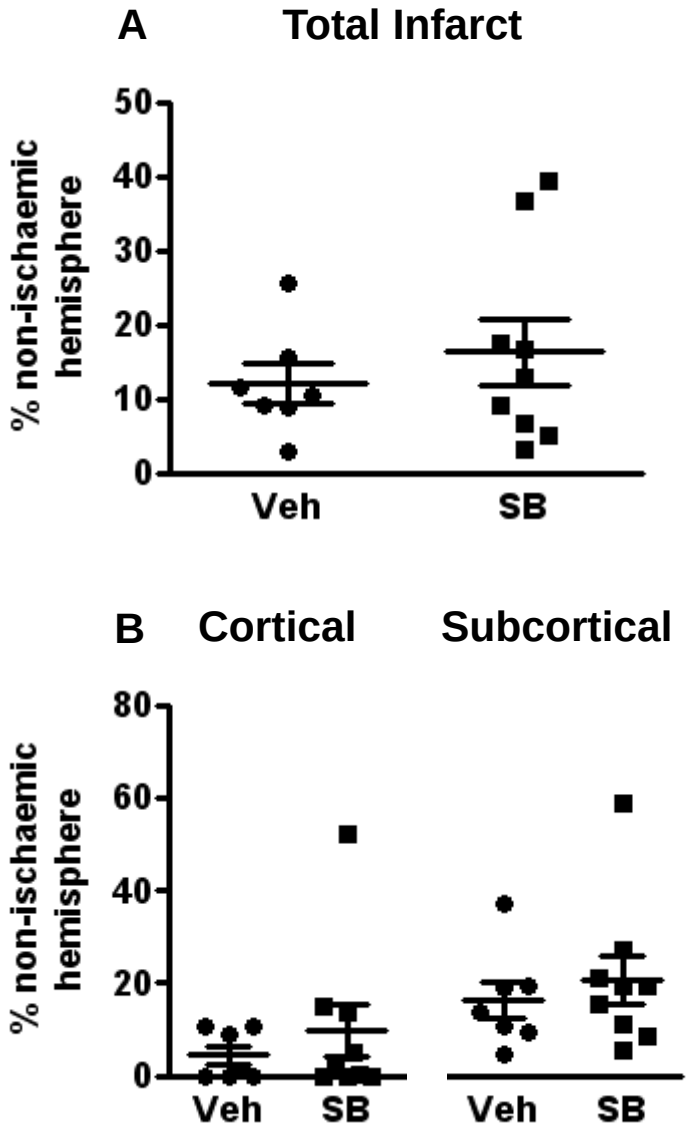

Figure 6.6. Cerebral infarct volume at 72 h after I-R (measured as % of non-ischaemic hemisphere).

Total (**A**), and cortical and subcortical (**B**) cerebral infarct volumes were measured in vehicle- (veh; n = 7) and SB 225002-treated (SB; n = 9) mice 72 h after I-R. Infarct volume data are presented as mean ± SEM.

Figure 6.7. Cerebral infarct area distribution at 72 h after I-R.

Total (**A**), cortical (**B**) and subcortical (**C**) cerebral infarct area distributions were measured in vehicle- (n = 7) and SB 225002-treated (n = 9) mice 72 h after I-R. Data are presented as mean ± SEM.

A Total Infarct

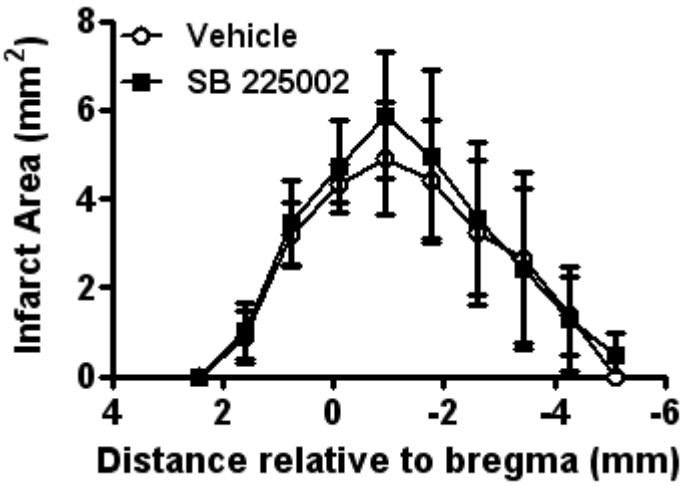

B Cortical Infarct

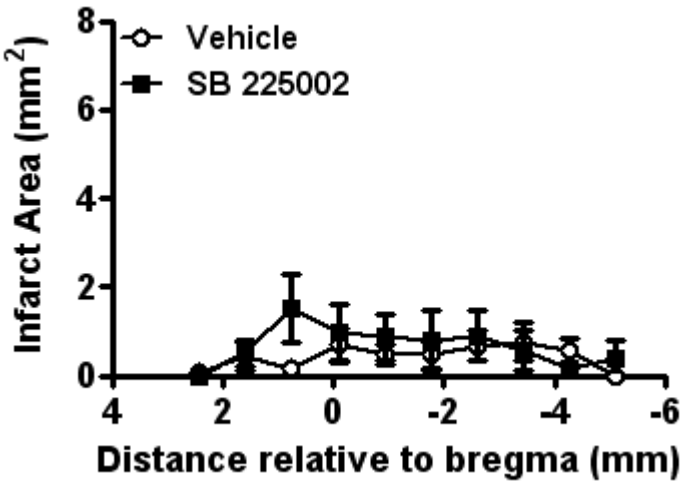

C Subcortical Infarct

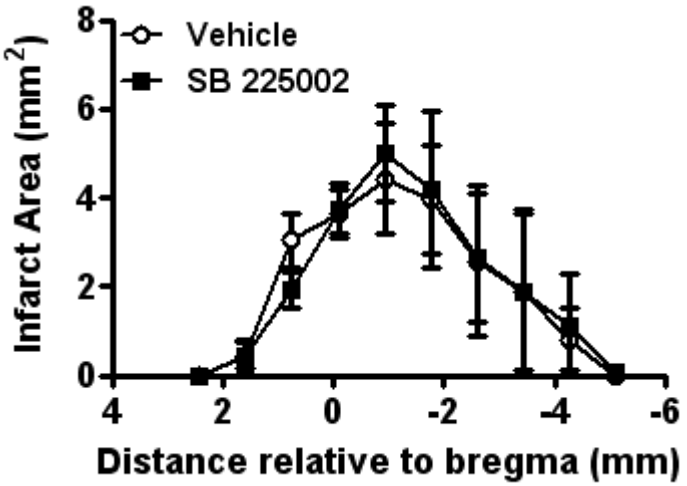

Figure 6.8. Neutrophil localisation and counts.

Representative photomicrographs showing MPO immunohistochemical staining (arrows) within the ischaemic (right) hemisphere of an untreated mouse 72 h after sham surgery (**A;** $n = 3$), and a vehicle- (**B;** $n = 5$) and SB 225002-treated (**C;** $n = 6$) mouse 72 h after I-R. The scale bar represents 100 μm. Quantitative analysis is shown in **D** (MPO^+ cells per section; $^*P < 0.05$ vs. vehicle-treated group, ANOVA with Bonferroni *post- hoc* test). Data are presented as mean ± SEM.

MPO+ Staining

Sham

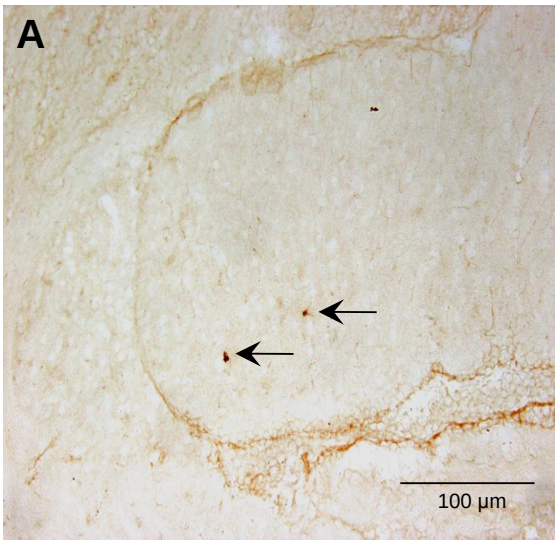

Vehicle

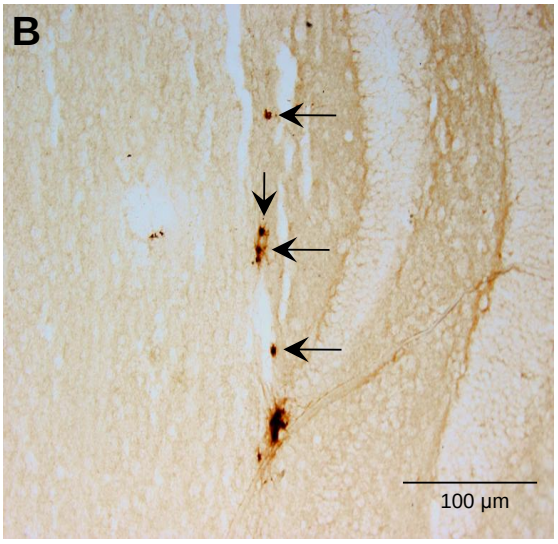

SB 225002

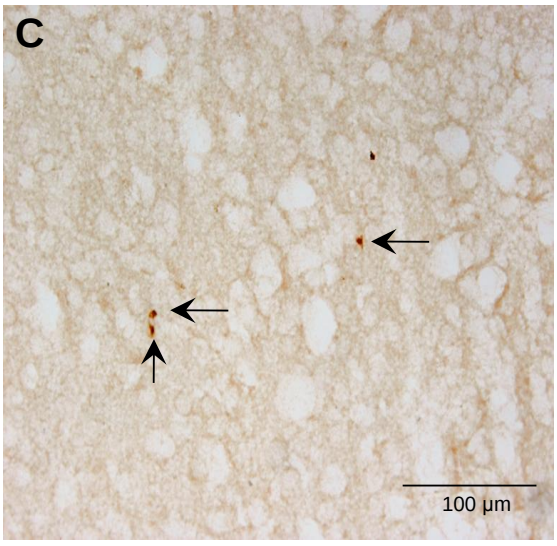

D MPO+ Cells per section

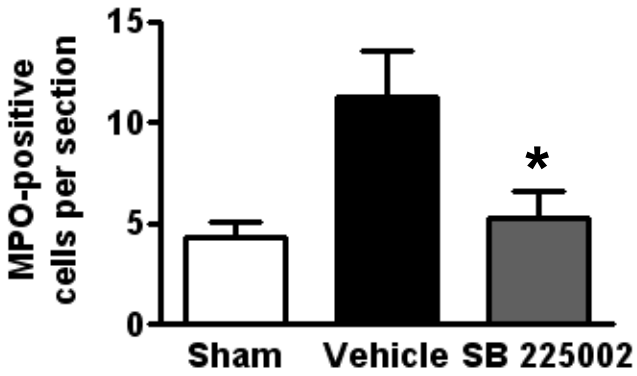

6.4 DISCUSSION

This study has shown that the mRNA expression of several chemokines and their receptors increases in the brain after cerebral I-R, with the largest changes occurring at 24 h. We also found that mRNA expression of important members of the ELR^+ CXC chemokine subfamily, CXCR2, CXCL1 and CXCL2, is increased in the ischaemic hemisphere at 4, 24 and 72 h after I-R. Next we administered vehicle or the CXCR2 antagonist SB 225002 to mice after I-R and found that treatment reduced CXCR2, CXCL1 and CXCL2 mRNA levels and neutrophil infiltration in the ischaemic hemisphere. Surprisingly, this treatment had no effect on functional outcome, infarct or oedema volume at 72 h after I-R.

No studies have previously examined CXCR2 mRNA or protein expression following focal cerebral ischaemia. However, several studies have reported increased mRNA expression of CXCL1 in the blood (Chapman *et al.*, 2009; McColl *et al.*, 2007) and brain (Chapman *et al.*, 2009; Schmerbach *et al.*, 2008), and CXCL2 in the blood (McColl *et al.*, 2007) and the MCA (Vikman *et al.*, 2007) following cerebral I-R in rodents. We have confirmed that mRNA expression of CXCL1 is increased in the brain following cerebral I-R, and for the first time, have reported that mRNA expression of both CXCR2 and CXCL2 are also increased in the brain after cerebral I-R.

One interpretation of the increase in CXCR2 mRNA expression after I-R may be that immune cells expressing the receptor, predominantly neutrophils (Ludwig *et al.*, 2000), but also mast cells and some T lymphocytes (Lippert *et al.*, 2004), infiltrate into the brain. This idea is consistent with studies showing not many infiltrated neutrophils at 24 h, but increased levels at 72 h after I-R (Gelderblom *et al.*, 2009), matching our CXCR2 expression data. Another interpretation is that neurons, cells that express CXCR2 under control conditions (Puma *et al.*, 2001; Valles *et al.*, 2006), increase their expression of CXCR2 after I-R, and/or that other resident cells that do not express CXCR2 under control conditions start expressing CXCR2 after cerebral I-R, such as

activated microglial cells, which were previously reported to express CXCR2 after global ischaemia in monkeys (Popivanova *et al.*, 2003) and traumatic brain injury in rats (Valles *et al.*, 2006). Both interpretations are consistent with previous findings, and therefore, it is likely that both immune cells and resident brain cells contribute to the increased CXCR2 expression.

When we examined mRNA levels after SB 225002 treatment, we observed drastically reduced mRNA expression levels of CXCR2, CXCL1 and CXCL2 in the brain. In contrast, previous studies reported that CXCR2-deficient mice exhibited increased CXCL1 mRNA levels in the blood (~17-fold) and the brain (~4-fold), compared to Wt littermates. Similarly, CXCL2 mRNA was up-regulated in the blood in CXCR2-deficient mice, although its expression in the brain was not examined (Cardona *et al.*, 2008; Kuboki *et al.*, 2008). This suggests that signalling through CXCR2 provides negative feedback for CXCL1 and CXCL2 production. In addition, it is believed that once a ligand has bound to CXCR2, it is internalised (Feniger-Barish *et al.*, 1999), resulting in an increased expression of ligands, when the receptor is no longer present. An important difference between the present study and the study by Cardona and colleagues, is that we have used a CXCR2 antagonist, and have not generated mice deficient in CXCR2. It is possible that in response to a complete deficiency of CXCR2, the body may increase the expression of CXCL1 and CXCL2 to attempt to counteract the lack of CXCR2 binding, whereas a 71.5 h inhibition of CXCR2 does not appear to induce this response. Therefore, we speculate that the reduction in CXCR2, CXCL1 and CXCL2 mRNA expression, represent a reduction in neutrophil infiltration (i.e. of CXCR2), as well as a reduction in resident brain cell expression (i.e. possibly of CXCR2, CXCL1 and CXCL2), suggesting that the dose of SB 225002 utilised in the present study was most likely sufficient to antagonise CXCR2.

Three previous studies have investigated the simultaneous inhibition of CXCR1 (formerly named interleukin receptor 8 type a; IL8Ra) and CXCR2 on outcome and neutrophil infiltration

following cerebral I-R, utilising either Reparixin (formally Repertaxin) (Garau *et al.*, 2005; Villa *et al.*, 2007), a specific non-competitive allosteric inhibitor of CXCR1 and CXCR2 (Bertini *et al.*, 2004; Casilli *et al.*, 2005), or DF2156Y, an optimised version of Reparixin (Garau *et al.*, 2006). These three studies found significant reductions in infarct volume as well as neutrophil infiltration 24 h after I-R, either when commencing treatment at the onset of ischaemia or at the time of reperfusion (Garau *et al.*, 2005; Garau *et al.*, 2006; Villa *et al.*, 2007). In the present study, although the administration of CXCR2 antagonist, SB 225002, probably antagonised the interaction between CXCR2 and its chemokine ligands in the ischaemic brain, evident by the reduced CXCR2, CXCL1 and CXCL2 mRNA expression at 24 h after I-R, and the complete abrogation of neutrophil infiltration at 72 h after I-R, it did not improve outcome at 72 h after I-R. There are a few possible explanations for this discrepancy. Firstly, these studies all used a 90 min MCA occlusion and only analysed infarct volume and neutrophil infiltration at 24 h after cerebral I-R. Depending on the period of ischaemia used, infarcts usually reach their maximum within 24 to 72 hours (Dirnagl, 2009). Thus, the inhibition of CXCR1 and CXCR2 may delay the progression of the infarct, but may not ultimately, reduce the final infarct volume. Furthermore, in a study of hepatic I-R in CXCR2-deficient mice, neutrophil infiltration into the liver was reduced compared to wild-type mice at 12 h, although by 24 h, neutrophil infiltration was similar in both groups of mice and this was sustained until at least 96 h (Kuboki *et al.*, 2008). Therefore, following a 90 min MCA occlusion, Reparixin or DF2156Y treatment may reduce neutrophil infiltration up to 24 h, but it is possible that after that time, neutrophil infiltration, and consequently infarct volume increase rapidly, to a similar level as in the wild-type mice. Secondly, perhaps the additional inhibition of CXCR1 by Reparixin and DF2156Y plays an important role in the protection these drugs achieved. Reparixin is much more potent at inhibiting CXCR1 than CXCR2 (Bertini *et al.*, 2004). It was previously believed that no functional mouse homologue of CXCR1 existed (Lee *et al.*, 1995), however, recently, one was identified (Fan *et al.*, 2007). Mouse CXCL6 (also named granulocyte chemotactic protein-2; GCP-2) was shown to bind to and

activate the novel mouse CXCR1, to stimulate chemotaxis and activation of neutrophils, whereas CXCL1 and CXCL2 did not (Fan *et al.*, 2007). Mouse CXCL6 was found to be more potent than mouse CXCL1 and CXCL2 in neutrophil recruitment (Wuyts *et al.*, 1996). However, CXCL6 was not in the PCR array we used, therefore we do not know whether it was affected by stroke or not. In any case, if the combination of CXCR1 and CXCL6 is important, this could explain why the inhibition of CXCR2 alone yielded no protection, while blocking both CXCR1 and CXCR2 simultaneously did.

Another possible reason to explain why the probably successful antagonism of CXCR2 did not reduce infarct volume or improve functional outcome, is that the contribution of neutrophils to cerebral I-R injury is controversial. CXCR2 and its ligands, CXCL1 and CXCL2 are very important in the adhesion and migration of neutrophils (Di Cioccio *et al.*, 2004; Kielian *et al.*, 2001; Tani *et al.*, 1996). Neutrophils can contribute to reperfusion injury by a number of mechanisms, including the physical plugging of microvessels resulting in the "no-reflow" phenomenon (del Zoppo *et al.*, 1991; Hatchell *et al.*, 1994), and the release of vasoconstrictors (Mugge *et al.*, 1991), reactive oxygen species (Matsuo *et al.*, 1995), proteolytic enzymes, such as elastase (Stowe *et al.*, 2009), and myeloperoxidase, which can react with hydrogen peroxide and chloride ions to produce the highly damaging hypochlorous acid (Malle *et al.,* 2007). Following cerebral I-R, they infiltrate the brain early in both experimental studies of stroke (Connolly *et al.*, 1996; Gelderblom *et al.*, 2009; Matsuo *et al.*, 1994) and in the clinic (Akopov *et al.*, 1996). However, although some studies have reported that protection from stroke injury occurs in neutropenic rodents or when neutrophil function is inhibited (Connolly *et al.*, 1996; Jiang *et al.*, 1998; Matsuo *et al.*, 1994; Petrault *et al.*, 2005), other studies found no such neuroprotection (Beray-Berthat *et al.*, 2003; Harris *et al.*, 2005; Yilmaz *et al.*, 2006). Given that SB 225002 treatment appears to have reduced neutrophil infiltration to similar levels as that observed in sham-operated mice, this study is consistent with the conclusion that neutrophil infiltration does

not adversely contribute to stroke pathology. This idea is in agreement with a review reporting that the existing evidence does not establish a clear cause-effect relationship between the infiltration of neutrophils and ischaemic injury (Emerich *et al.*, 2002). Furthermore, administration of CXCL1 and CXCL2 *in vitro*, have been found to provide neuroprotection against amyloid beta (Aβ) (Watson and Fan, 2005) or low K^+ (Limatola *et al.*, 2000) through the activation of AMPA receptors and ERK1/2 and Akt, respectively. Also, in a model of hepatic I-R, low concentrations of CXCL2 (<100 ng/ml) were found to increase hepatocyte survival, whereas high concentrations (>100 ng/ml) induced cell death. These effects were mediated by CXCR2 (Kuboki *et al.*, 2008), and it is therefore possible that the inhibition of CXCR2 can inhibit some protective pathways.

Cerebral I-R increased the mRNA expression of a number of other chemokines and chemokine-related genes in the ischaemic hemisphere. Out of the 10 genes that increased the most at each time-point measured, the vast majority were chemokines and their receptors. Most were of the CC class, CCL4, CCR4, CCL2, CCL7, CCL11 and CCL12, and one was from the CXC class, CXCL10. In general, these chemokines are involved in attracting monocytes, T lymphocytes, particularly $CD4^+$ cells, basophils and eosinophils (Abcam, 2009). CCL2 (also named MCP-1) has been reported, through the induction of MCAO in CCL2 transgenic and knock-out mice, to contribute to stroke injury (Chen *et al.*, 2003; Hughes *et al.*, 2002; Kumai *et al.*, 2004). CCL4 is up-regulated after stroke, and this increase is reduced in SOD1 over-expressed mice (Nishi *et al.*, 2005). CCL7 and CXCL10 expressions are increased after stroke (Wang *et al.*, 1998; Wang *et al.*, 1999), whereas no studies have previously examined the role of CCR4, CCL11 and CCL12 in stroke. Other genes that were up-regulated by cerebral I-R included TNF-α (tumour necrosis factor-alpha), an important pro-inflammatory cytokine that promotes the infiltration of leukocytes and the production of other pro-inflammatory cytokines (Tracey and Cerami, 1994), and is well established to contribute to I-R injury (Barone *et al.*, 1997), and IL-1α (interleukin-1

alpha), a pro-inflammatory cytokine produced by monocytes/macrophages, fibroblasts and dendritic cells, that when inhibited in combination with IL-1β reduces infarct volume (Boutin *et al.*, 2001; Garcia *et al.*, 1995; Loddick and Rothwell, 1996). Trem1 (triggering receptor expressed on myeloid cells 1) is expressed on neutrophils and monocytes/macrophages, and releases pro-inflammatory cytokines and chemokines when activated. It has not been examined in cerebral I-R, although it was reported to reduce intestinal I-R injury, via the attenuation of TNF-α and IL-6 expression, as well as NF-κB activity (Gibot *et al.*, 2008). IL-16 (interleukin-16) is a pro-inflammatory cytokine that was found to be expressed at higher levels on neutrophils, $CD8^+$ T lymphocytes and activated microglia/macrophages in the ischaemic regions in the brains of stroke patients compared to controls (Schwab *et al.*, 2001). Lif (leukaemia inhibitory factor) is a member of the IL-6 family, and its expression is shown to increase in the brain after stroke (Bond *et al.*, 2002; Slevin *et al.*, 2008), but it may have protective neurotrophic effects (Lemke *et al.*, 1996), and Gdf5 (growth differentiation factor 5) has never been looked at in stroke or any form of I-R, and may also play a role in increasing neuronal survival. The inhibition of any of these genes, perhaps except for Lif and Gdf5 therefore, may be an effective treatment in stroke.

As MPO is contained within some macrophages, it is possible that some of the infiltrated MPO^+ cells are macrophages. However, although CXCR2 and its ligands are known as neutrophil chemoattractants, they are also involved in monocyte recruitment (Zernecke *et al.*, 2001), so the antagonism of CXCR2 by SB 225002 may also have had an effect on monocyte brain infiltration.

In all of the end-points measured at 72 h after I-R, there is evidence that SB 225002 treatment worsens outcome. Moreover, as there was a higher rCBF level that occurred randomly during the ischaemic period in the group that were later treated with SB 225002 versus the vehicle-treated group, it might be expected that SB 225002-treated mice would have an improved outcome (Takagi *et al.*, 1993). This suggests that, perhaps if anything, SB 225002 treatment

caused an even worse outcome. The higher neurological scores and lower hanging wire time are consistent with this. In addition, mortality rates in both the vehicle- and SB 225002-treated groups were higher than in previous studies in this thesis. In contrast, the infarct volumes in the vehicle-treated mice were surprisingly small and hanging wire time was relatively high. The significance of these observations is unclear, but it is possible that the vehicle had a detrimental effect on health and survival in the 3 days following stroke.

In summary, administration of SB 225002, a CXCR2 antagonist, markedly reduces mRNA expression of CXCR2, CXCL1 and CXCL2 in the brain, as well as neutrophil brain infiltration following cerebral I-R. However, this reduced neutrophil-related inflammation does not improve outcome at 72 h after cerebral I-R, and therefore is not likely to be a potential therapeutic treatment after ischaemic stroke.

Chapter 7:

The Effect of Down Syndrome Candidate Region 1 (*DSCR1*) Gene Expression on Outcome Following Cerebral Ischaemia-Reperfusion

7.1 INTRODUCTION

Down syndrome results from the trisomy of all, or part of, chromosome 21. It has an incidence of 1 in 700 births and is the most frequent genetic cause of mental retardation (Rachidi and Lopes, 2008). Individuals with Down syndrome also have a multitude of immune system defects, including reduced T lymphocyte function (Ugazio *et al.*, 1990). By the age of 35 to 40 years, virtually all Down syndrome individuals develop the neuropathologic hallmarks of Alzheimer's disease (Wisniewski *et al.*, 1985). It is notable that there are a number of similar pathological features that occur in Alzheimer's disease and cerebrovascular disease, including the deposition of Aβ (Chow *et al.*, 2007; Iadecola, 2004; Zhang *et al.*, 1997). Interestingly, while cerebral ischaemia is known to contribute to the pathogenesis of Alzheimer's disease in the general population, and individuals with Alzheimer's disease are at increased risk for cerebral ischaemic events (For review see Koistinaho and Koistinaho, 2005), there is little or no information about stroke in individuals with Down syndrome.

One of the genes thought to be important in Down syndrome is Down syndrome candidate region 1 (*DSCR1*; also named Adapt78), found on Chromosome 21, in the sub-region of 21q22.1-q22.2 (Fuentes *et al.*, 1995). There are 2 isoforms of DSCR1, due to alternative first exons, termed isoform 1 (denoted DSCR1.1) and isoform 4 (DSCR1.4). Both of these isoforms are widely expressed throughout the body in similar expression patterns, however, isoform 1 is thought to be somewhat 'brain-specific', because it is present in the human brain, whereas isoform 4 is not (Fuentes *et al.*, 1997). Isoform 4 however, is expressed in the mouse brain and in the same regions as isoform 1, but at much lower levels (Porta *et al.*, 2007). In the adult mouse brain, strong anti-DSCR1 immunoreactivity has been detected in the olfactory bulb, the striatum, the CA1 and CA3 pyramidal cells of the hippocampus and the substantia nigra. Moderate-to-strong immunoreactivity was found in the pyramidal neurons of the cerebral cortex, especially in layer IV (Porta *et al.*, 2007). In addition to the brain, DSCR1 is also expressed in T lymphocytes

(although the isoform is not specified and the expression has only been investigated in $CD4^+$ T lymphocytes thus far) (Ryeom *et al.*, 2003).

DSCR1 mRNA and protein levels are elevated 1.9 fold (Fuentes *et al.*, 2000) and 2-3 fold, respectively, in the brains of individuals with Down syndrome compared with control brains (Ermak *et al.*, 2001). DSCR1 is also found to be increased in the brains of individuals with Alzheimer's disease (Cook *et al.*, 2005; Ermak *et al.*, 2002). It is induced by both calcium and hydrogen peroxide (Crawford *et al.*, 1997; Ermak *et al.*, 2002). Consistent with such a mechanism, a recent study examining DSCR1.4 mRNA and protein expression following ischaemia-reperfusion (I-R) in mice, found increased mRNA expression in the ischaemic hemisphere at 6 and 24 h, but no difference at 72 h after stroke, and increased protein immunoreactivity at 24 and 72 h, but no difference at 6 h after stroke, compared to the contralateral hemisphere (Cho *et al.*, 2008).

DSCR1 binds to calcineurin (Fuentes *et al.*, 2000; Rothermel *et al.*, 2000) and inhibits its activity (Rothermel *et al.*, 2000). As a result, it is also known as modulatory calcineurin-interacting protein 1 (MCIP1), calcipressin 1 (CSP1) and regulator of calcineurin 1 (RCAN1). Calcineurin is a Ca^{2+} and Ca^{2+}/calmodulin-dependent protein phosphatase abundant in the brain and expressed in neurons of rodents in the same brain regions as DSCR1 (Goto *et al.*, 1987; Porta *et al.*, 2007). Calcineurin links calcium signaling to transcriptional responses in several cell types of the immune and nervous systems, as well as others (Ryeom *et al.*, 2003). The best characterised target of calcineurin is the transcription factor; nuclear factor of activated T cells (NFAT). Once activated, calcineurin dephosphorylates NFAT, and activates the transcription of pro-inflammatory (eg. IL-2, IL-4, IFN-γ, TNF-α) and pro-apoptotic (eg. Fas ligand) genes, in the brain and T lymphocytes, as well as in other tissues (Crabtree, 1999; Hogan *et al.*, 2003; Santana *et al.*, 2000). There is limited information on the role of NFAT in stroke; however, calcineurin-

induced nuclear NFAT translocation has recently been suggested to mediate the delayed apoptotic neuronal cell death following brain ischaemia (Shioda *et al.*, 2007; Shioda *et al.*, 2006). Many reports have also implicated calcineurin in the activation of the important transcription factor, nuclear factor-kappa B (NF-κB), through the dephosphorylation and subsequent inactivation of its predominant inhibitory molecule, IκBα (Frantz *et al.*, 1994; Steffan *et al.*, 1995). This occurs in a variety of cells, including neurons and T lymphocytes (Frantz *et al.*, 1994; Lilienbaum and Israel, 2003; Steffan *et al.*, 1995; Trushin *et al.*, 1999). Furthermore, DSCR1 was also recently found to stabilise IκBα, and consequently attenuate the transcriptional activity of NF-κB (Kim *et al.*, 2006), through a calcineurin-independent pathway.

The expression and activation of NF-κB is increased in the brain after cerebral I-R (Gabriel *et al.*, 1999; Schneider *et al.*, 1999), and it promotes cell death following stroke (Schneider *et al.*, 1999; Zhang *et al.*, 2005). Inflammation is well established to contribute to cerebral damage after I-R, and thus, as might be expected, pharmacological inhibitors of calcineurin, such as cyclosporin A and FK506 (Tacrolimus), are reported to reduce neuronal cell death following cerebral I-R (Bochelen *et al.*, 1999; Sharkey and Butcher, 1994; Sharkey *et al.*, 1996; Uchino *et al.*, 1998; Vachon *et al.*, 2002; Yoshimoto and Siesjo, 1999). Therefore, through the increased inhibition of calcineurin in brain cells and/or in circulating T lymphocytes, we hypothesise that *DSCR1* transgenic (Tg) mice may be protected from stroke. Conversely, in *DSCR1* knock-out (KO) mice, stroke may be exacerbated.

Thus, using a *DSCR1* Tg mouse that over-expresses isoform 1 of the human *DSCR1* gene with the same temporal- and tissue-specific expression of the endogenous gene, we examined the effect of *DSCR1* over-expression on outcome following cerebral I-R, and investigated the possible mechanisms underlying this effect. In addition, we performed some similar studies in

DSCR1 KO mice, and examined the effect of *DSCR1*-deficiency on outcome following cerebral I-R.

7.2 MATERIALS AND METHODS

7.2.1 Animals

This study was conducted in accordance with the National Health and Medical Research Council of Australia guidelines for the care and use of animals in research.

A total of 94 male 8-14 week old mice were studied, consisting of: 39 *DSCR1* Transgenic (Tg) mice (weight, 22.4±0.4 g), and 39 *DSCR1* matched wild-type (Wt_{Tg}) mice (22.9±0.5 g), and 11 *DSCR1* knock-out (KO) mice (25.0±0.7 g) and 5 *DSCR1* matched Wt (Wt_{KO}) mice (28.2±0.7 g). *DSCR1* Tg and KO mice were generated in the laboratory of Dr. Melanie Pritchard (Department of Biochemistry and Molecular Biology, Monash University). The *DSCR1* over-expressing Tg mice were generated on a mixed genetic background of C57Bl6/J x CBA using human *DSCR1* cDNA encoding the exon 1 splice variant (isoform 1) (Refer to Keating *et al.*, 2008). The KO mice were generated on a mixed genetic background of C57Bl6/J x SV129. Thus, the appropriate Wt control strain was studied in each case. The mice had free access to water and food pellets before and after surgery. Fourteen mice were excluded from the study if during the surgical procedure to induce MCAO: a) the filament did not stay in place for the entire 30 min of ischaemia (n = 3); b) the occluding clamp was in place for ≥5 min (n = 1); c) the regional cerebral blood flow (rCBF) dropped to >90 % of pre-ischaemic levels (n = 8); or d) they died prior to the specified time for euthanasia (at 23.5 h reperfusion) (n = 2).

7.2.2 Tail cuffing

Systolic blood pressure (BP) was measured in mice prior to surgery via tail cuffing, using a MC4000 Blood Pressure Analysis System (Hatteras Instruments; Cary, NC, USA), as described in section 2.6 of General Methods.

7.2.3 Isolation of leukocytes from blood and spleen

Mice were killed at 24 h by isofluorane inhalation and exsanguination, and leukocytes were isolated from the blood as described in section 2.10 of General Methods.

7.2.4 Analysis of cell populations

Fluorescence flow cytometric analyses were performed to determine the numbers of circulating T lymphocytes ($CD3^+$, $CD4^+$ and $CD8^+$) and B lymphocytes as described in section 2.11 of General Methods. Primary antibodies conjugated with fluorophores were: the fluorescein isothiocyanate (FITC)-conjugated Armenian hamster anti-mouse CD3 (clone 145-2C11; 1:100), phycoerythrine (PE)-conjugated anti-CD8 (clone 53-6.7; 1:100), PE–conjugated anti-B220 (clone RA3-6B2; 1:100) (BD Biosciences; North Ryde, NSW, Australia), and allophycocyanin (APC)-conjugated anti-CD4 (clone RM4-5; 1:300) (eBioscience; San Diego, CA, USA). All antibodies were rat anti-mouse, unless specified.

7.2.5 Focal cerebral ischaemia

Focal cerebral ischaemia was induced by transient intraluminal filament occlusion of the right middle cerebral artery (MCA) as described in section 2.3 of General Methods. In the *DSCR1* Tg and Wt_{Tg} mice, regional cerebral blood flow (rCBF) at 24 h was also measured. The laser Doppler probe holder was kept in place following surgery, and the head wound was closed around it. Just prior to 24 h, mice were re-anaesthetised with a mixture of ketamine (80 mg/kg,

i.p.) and xylazine (10 mg/kg, i.p.). The laser Dopper probe was inserted into the probe holder, and the average rCBF measured over 1 min was recorded.

7.2.6 Evaluation of neurological function

At the end of the experiment (24 h), neurological function was evaluated using a five-point scoring system, and the hanging wire test. Please refer to section 2.4 of General Methods for details.

7.2.7 Evaluation of cerebral infarct and oedema volume

Mice were killed, brains removed and cerebral infarct and oedema volume evaluated as described in section 2.5 of General Methods.

7.2.8 Localisation of von Willebrand factor

The localisation of von Willebrand factor (vWF) in brain sections from naive Wt_{Tg} and Tg mice was performed by immunofluorescence as described in section 2.9 of General Methods. Multiple serial coronal sections of 20 μm were taken at 3 different levels: bregma -0.08 mm, -1.76 mm and -3.44 mm, and were thaw-mounted onto poly-L-lysine coated glass slides (0.1 % poly-L-lysine in dH_2O). Tissue sections were fixed in acetone for 15 min and washed in 0.01 M phosphate buffered saline (PBS, 0.01 M phosphate buffer and 0.15 M NaCl; pH 7.4) (3 x 10 min). Tissue mounted sections were incubated in an anti-rabbit vWF polyclonal antibody (1:500, Abcam; Cambridge, MA, USA) overnight in a humid box. The following day, the tissues were washed in 0.01 M PBS (3 x 10 min) to remove any excess antibody, and incubated in a Texas Red-conjugated goat anti-rabbit antibody (1:200; Zymed Labratories; South San Francisco, CA, USA) for 3-4 h in a humid box. The sections were then washed in 0.01 M PBS (3 x 10 min), mounted in VECTASHIELD mounting medium (Vector Laboratories; Burlingame, CA, USA) and cover-

slipped. Tissue mounted slides were viewed and photographed on an Olympus light microscope (Olympus; Hamburg, Germany).

7.2.9 Measurement of mRNA in brain hemispheres

The ischaemic (right) hemispheres from naive and stroked *DSCR1* Wt_{Tg} and Tg mice, killed at 6 and 24 h, were used to measure the mRNA expression of various inflammatory genes using real-time PCR, as described in section 2.8 of General Methods.

Ninety-six immune-related genes were examined using the Taqman® Mouse Immune Array (Applied Biosciences; Carlsbad, CA, USA), which included cytokines, chemokines, growth factors, immune regulators, apoptosis markers and ischaemia markers. We also separately purchased pre-designed Taqman® gene expression assays for DSCR1 isoform 1 (NCBI Reference Sequence; RefSeq NM_001081549.1), DSCR1 isoform 4 (RefSeq NM_019466.3), CXCL1 (RefSeq NM_008176.3), and matrix metalloproteinase-9 (MMP-9; RefSeq NM_013599.2), as well as GAPDH (RefSeq NM_008084.2; Applied Biosystems; Carlsbad, CA, USA) for the house-keeping gene.

The PCR was performed in Dr. Melanie Pritchard's laboratory by Katherine Martin (PhD student). Firstly, all RNA solutions were treated with 0.1 % diethyl pyrocarbonate (DEPC; Sigma Aldrich; St. Louis, MO, USA) overnight and autoclaved prior to use. After RNA extraction (see section 2.8 of General Methods), the total RNA (2 μg) was treated with DNase (Promega; Madison, WI, USA) for 45 min at 37 °C to remove any gDNA contamination. Half of the RNA (1 μg) was then converted into cDNA, using Superscript III Reverse Transcriptase (Invitrogen; Carlsbad, CA, USA) and random hexamers (Promega), according to the manufacturer's instructions. The remaining 1 μg of RNA was used in a reaction without the reverse transcriptase enzyme, which acted as a negative control to assess the levels of gDNA

contamination. A GAPDH PCR was used to confirm the successful generation of cDNA and to identify gDNA contamination. The PCRs were then carried out using the ABI 7900HT Fast Real-Time PCR System (Applied Biosystems).

7.2.10 Measurement of DSCR1 protein expression

In separate mice, expression of DSCR1 protein was measured in homogenates of the ischaemic (right) and non-ischaemic (left) hemispheres using Western blotting. Please refer to section 2.7 of General Methods for details. The Polyvinylidene Fluoride (PVDF) membranes were sent to Drs. Mariona Arbones and Maria Jose Barallobre (Centre de Regulació Genòmica, Barcelona, Spain), where they used the anti-DSCR1.1 and anti-DSCR1.4 antibodies they designed. To see bands in the DSCR1.4 blots, a longer exposure time was required. Relative intensities were normalised to the intensity of corresponding bands for Vinculin and, within a single gel, all bands were quantitated relative to the naive Wt_{Tg} mice.

7.2.11 Drugs and chemicals

As per section 2.14 of General Methods.

7.2.12 Statistical analysis

All data are presented as mean ± standard error. Statistical analyses were performed using GraphPad Prism version 5 (GraphPad Software Inc., San Diego, CA, USA). Between-group comparisons were analysed as described in section 2.15 of General Methods. Group numbers are shown in parentheses. Statistical significance was accepted when $P < 0.05$.

7.3 RESULTS

7.3.1 Effect of *DSCR1* over-expression on systolic blood pressure

No significant difference was observed in systolic blood pressure (BP) between naive *DSCR1* Wt_{Tg} and Tg mice (Wt_{Tg}, 121 ± 4 mmHg; Tg, 129 ± 3 mmHg; n = 10-13; P = 0.14; Figure 7.1).

7.3.2 Effect of *DSCR1* over-expression on circulating T and B lymphocyte levels

There were significantly fewer circulating $CD3^+$, $CD4^+$ and $CD8^+$ T lymphocytes in naive *DSCR1* Tg mice in comparison to naive Wt_{Tg} mice ($P < 0.05$; n = 3 per group; Figures 7.2A-C). There was a trend for fewer circulating B lymphocytes in *DSCR1* Tg mice compared to their Wt_{Tg} littermates, but this did not reach statistical significance (P = 0.15; n = 3; Figure 7.2D).

7.3.3 Effect of *DSCR1* over-expression on outcome following I-R

7.3.3.1 Regional cerebral blood flow

Cerebral I-R was produced by 30 min MCAO and 23.5 h reperfusion. rCBF decreased to ~25 % of the pre-ischaemic level following insertion of the monofilament for the duration of MCAO (Figure 7.3A). rCBF then increased initially to ~95 % of the pre-ischaemic level upon removal of the monofilament, and then stabilised at ~70 % after 30 min of reperfusion (n = 14 per group; Figure 7.3A). No difference in rCBF profile was observed between *DSCR1* Wt_{Tg} and Tg mice. However, rCBF levels at 24 h were significantly higher in Tg mice than Wt_{Tg} littermates (Wt_{Tg}=37±8 %, Tg=76±9 % pre-ischaemia; $P < 0.05$; n = 14 per group; Figure 7.3A).

7.3.3.2 Mortality and neurological function

Mortality rates at 24 h after cerebral I-R were lower in *DSCR1* Tg mice in which no deaths occurred (0/19; 0 %) compared to Wt_{Tg} mice (2/19; 10.5 %; Figure 7.3B), although this did not reach statistical significance. *DSCR1* Tg mice had less neurological impairment, with a

significantly lower neurological score ($P < 0.05$; Figure 7.3C) and a significantly longer hanging wire time (Wt_{Tg}=17±5 s, Tg=40±5 s; $P < 0.05$; Figure 7.3D) than Wt_{Tg} littermates.

7.3.3.3 Brain infarct and oedema volume measured as mm³

Representative coronal sections of infarcted brain of *DSCR1* Wt_{Tg} and Tg mice 24 h after I-R are shown in Figures 7.4A and B, respectively. Following I-R, significantly smaller total infarct volumes were produced in *DSCR1* Tg mice compared with Wt_{Tg} littermates (18±5 vs. 36±5 mm^3; $P < 0.05$; $n = 11$ per group; Figure 7.4C). This corresponded to a significantly smaller subcortical infarct volume (12±2 vs. 33±5 mm^3; $P < 0.05$; Figure 7.4D), but no difference in cortical infarct volume (6±3 vs. 3±1 mm^3; $P = 0.48$; Figure 7.4D). Cerebral oedema volume was also significantly smaller in *DSCR1* Tg mice compared to Wt_{Tg} littermates (11±2 vs. 23±4 mm^3; $P < 0.05$; Figure 7.4E).

Interestingly, none of the *DSCR1* Tg brains contained infarcts in the hippocampus. In the 11 *DSCR1* Tg mice, 0 out of 50 coronal sections comprising the hippocampus contained hippocampal lesions, whereas, in the 11 *DSCR1* WT_{Tg} mice, 37 out of 53 (69.8 %) coronal sections comprising the hippocampus contained hippocampal lesions.

7.3.3.4 Brain infarct volume measured as % of non-ischaemic hemisphere

Infarct volumes were also measured as a percentage of the non-ischaemic hemisphere. The general profiles and statistical significance achieved between *DSCR1* Wt_{Tg} and Tg mice for the total ($P < 0.05$), cortical ($P = 0.42$) and subcortical ($P < 0.05$) infarcts following I-R were very similar to when the infarct was measured in mm^3 (Figures 7.5A-B).

7.3.3.5 Brain infarct area distribution

The distribution of the infarct area throughout the brain was also plotted. I-R produced different cerebral infarct distributions in *DSCR1* Wt_{Tg} and Tg mice, with a more rostral infarct in Tg mice than Wt_{Tg} mice. In *DSCR1* Wt_{Tg} mice, peak infarct area was observed at bregma -1.76 mm, whereas in *DSCR1* Tg mice, the infarct was largest at bregma (-0.08 mm; Figure 7.6A). Representative coronal sections of infarcted brain at these two points, and at bregma -3.44 mm, where there is no longer an infarct in *DSCR1* Tg brains but still a large infarct in Wt_{Tg} mice, are shown in Figures 7.7A-F. *DSCR1* Wt_{Tg} and Tg mice had similar sized total infarcts at regions spanning bregma +1.60 mm to -0.08 mm, but posterior to bregma -0.08 mm, *DSCR1* Tg mice had significantly smaller infarcts (Figure 7.6A). The same profile is seen for subcortical infarct distribution (Figure 7.6C), whereas there is no significant difference in cortical infarct distributions (Figure 7.6B).

7.3.3.6 von Willebrand factor (vWF) immunofluorescence

To assess whether the difference in infarct distribution could have been due to increased vascularisation (and hence blood flow) in the brains of *DSCR1* Tg mice, von Willebrand factor (vWF, indicative of endothelium) immunofluorescence was performed on sections at bregma -0.08, -1.76 and -3.44 mm on naive *DSCR1* Wt_{Tg} and Tg mice. These 3 sections were chosen to assess a range throughout the brain that included a region where there was no difference in infarct area (bregma -0.08 mm), and regions with differences between infarct areas (bregma -1.76 mm and -3.44 mm; see Figures 7.6A & C). Representative coronal sections of infarcted brain of *DSCR1* Wt_{Tg} and Tg mice at these regions 24 h after I-R are shown in Figures 7.7A-F. No difference was observed in vWF immunofluorescent staining between naive *DSCR1* Wt_{Tg} and Tg mice in any of the sections examined (n = 2-3; Figure 7.7G-H).

7.3.4 Effect of I-R and *DSCR1* over-expression on DSCR1 mRNA and protein expression

7.3.4.1 mRNA

To investigate the effect of stroke on DSCR1.1 mRNA expression, and to test whether DSCR1.4 mRNA expression increases following I-R in our studies (c.f. Cho *et al.*, 2008), we performed real-time PCR on the ischaemic (right) hemispheres of naive Wt_{Tg} mice, as well as in Wt_{Tg} mice 6 and 24 h after cerebral I-R. DSCR1.1 mRNA expression was increased by 2- and 12-fold, 6 and 24 h after I-R, respectively, when compared to naive Wt_{Tg} mice (n = 3; Figure 7.8A). In contrast, DSCR1.4 mRNA was not altered by I-R at either 6 or 24 h (no change and 0.6-fold compared to naive Wt_{Tg} mice, respectively; Figure 7.8B).

To investigate the effect of human *DSCR1.1* over-expression on mouse DSCR1.1 and DSCR1.4 mRNA expression, we performed real-time PCR on the ischaemic (right) hemispheres of naive *DSCR1* Tg mice, as well as at 6 and 24 h after cerebral I-R. There was no change in DSCR1.1 mRNA expression in the naive Tg mice compared with the naive Wt_{Tg} mice. At 6 and 24 h after I-R, DSCR1.1 mRNA expression increased to a similar level to the Wt_{Tg} mice (2- and 11-fold increase, respectively compared to naive Wt_{Tg} mice; n = 3; Figure 7.8A). It is important to note that the DSCR1.1 primers only bind to mouse DSCR1.1. The *DSCR1* Tg mice over-express the human isoform 1, and have normal levels of mouse DSCR1.1. DSCR1.4 mRNA expression did not change either at 6 or 24 h after I-R in the Tg mice (naive, 0.6-fold; 6 h, 0.5-fold; 24 h, 0.4-fold compared to naive Wt_{Tg} mice; Figure 7.8B), however, it is important to note, that the DSCR1.4 mRNA was lower in the Tg mice compared to the Wt_{Tg} mice (Figure 7.8B).

7.3.4.2 Protein

To investigate the effect of stroke on DSCR1.1 protein expression, and to test whether DSCR1.4 protein expression increases following I-R in our studies (c.f. Cho *et al.*, 2008), Western blotting was performed on the ischaemic (right) hemisphere of naive Wt_{Tg} mice, in addition to the

ischaemic (right) and non-ischaemic (left) hemispheres of Wt_{Tg} mice 6 and 24 h after cerebral I-R. Representative Western blots for DSCR1.1 and DSCR1.4 in the right hemisphere of naive Wt_{Tg} and Tg mice, as well as at 6 and 24 h after cerebral I-R in both the ischaemic (right) and non-ischaemic (left) hemispheres are shown in Figure 7.8C. DSCR1.1 protein expression did not change either at 6 or 24 h after I-R (0.8- and 0.6-fold, respectively, compared to naive Wt_{Tg} mice; n = 3; Figure 7.8D). Similarly, DSCR1.4 protein was not altered by I-R at either 6 or 24 h (0.6- and 0.7-fold compared to naive Wt_{Tg} mice, respectively; Figure 7.8E). It is important to note that DSCR1.4 protein was expressed in the brain at a much lower level to DSCR1.1 protein (see Figure 7.8C, where the representative DSCR1.4 blot was exposed for a longer period of time).

To investigate the effect of human *DSCR1.1* over-expression on DSCR1.1 and DSCR1.4 protein expression, Western blotting was performed on the right hemisphere of naive *DSCR1* Tg mice, as well as the ischaemic (right) and non-ischaemic (left) hemispheres of *DSCR1* Tg mice at 6 and 24 h after cerebral I-R. It is important to note, that in contrast to the DSCR1.1 primers, the DSCR1.1 antibody detects both the endogenous mouse protein and the human transgene. There was a 6-fold increase in DSCR1.1 protein expression in the naive Tg mice compared with the naive Wt_{Tg} mice, confirming that *DSCR1.1* is over-expressed in these mice. DSCR1.1 expression was not affected by stroke in *DSCR1* Tg mice, which can further be seen in the blots for DSCR1.1 (see Figure 7.8C), where there was no difference between the expression in the left and right brain hemispheres at each time-point. At 6 and 24 h after I-R, DSCR1.1 protein expression was lower than in naive Tg mice, but was still 4-5-fold higher than in Wt_{Tg} mice at both time-points (n = 3; Figure 7.8D). DSCR1.4 protein expression did not change in naive Tg mice, or at 6 or 24 h after I-R (naive, 0.7-fold; 6 h, no change; 24 h, 2-fold compared to naive Wt_{Tg} mice), although it tended to be lower in naive mice and increase after I-R (n = 3; Figure 7.8E).

7.3.5 Effect of I-R and *DSCR1* over-expression on cerebral cytokine and chemokine mRNA expression

The mRNA expression of 61 cytokines, chemokines and immune-related genes were altered after cerebral I-R and/or *DSCR1* over-expression. Table 7.1 (below) shows the changes that occurred in 20 genes of interest.

	Normalised mRNA fold expression in the ischaemic hemisphere					
	Naive		**6 h after I-R**		**24 h after I-R**	
Genes	**Wt_{Tg}**	**Tg**	**Wt_{Tg}**	**Tg**	**Wt_{Tg}**	**Tg**
CCL2	1	2	45	22	77	136
CCL3	1	1	42	15	52	36
CCL5/RANTES	1	1	2	1	3	12
CD28	1	2	1	2	1	3
CD68	1	2	1	2	2	4
CD80	1	2	4	4	12	13
Cox-2	1	1	4	4	6	3
CXCL1	UD	UD	1	0	32	1
CXCL10	1	2	3	2	8	28
CXCL11	1	0	4	0	1	1
Endothelin-1	1	2	4	5	5	6
HMOX1	1	1	4	4	5	10
IL-1β	1	1	2	1	4	7
IL-6	1	3	5	3	11	64
MMP-9	UD	UD	1	1	5	6
NF-κB1	1	1	1	1	1	1
NF-κB2	1	1	2	2	2	3
TBX21	1	8	6	21	15	33
TGF-β	1	1	1	1	1	1
TNF-α	1	1	14	8	32	20

UD=undetected; HMOX1=heme-oxygenase-1; TBX21=T box transcription factor 21

Table 7.1. The mRNA expression of immune-related genes in naive *DSCR1* Wt_{Tg} and Tg mice, and at 6 and 24 h after cerebral I-R.

The mRNA expression of 20 cytokines, chemokines and immune-related genes in the ischaemic (right) hemisphere of naive *DSCR1* Wt_{Tg} and Tg mice, and at 6 and 24 h after I-R, normalised to the expression in the right hemisphere of naive Wt_{Tg} mice (however if expression was undetected in naive mice, expression was normalised to the right hemisphere of Wt_{Tg} mice at 6 h after I-R).

7.3.6 Effect of *DSCR1*-deficiency on outcome following I-R

7.3.6.1 Regional cerebral blood flow

Cerebral I-R was produced by 30 min MCAO and 23.5 h reperfusion. Regional cerebral blood flow (rCBF) in *DSCR1* Wt_{KO} mice initially decreased to ~22 % of the pre-ischaemic level and remained at 27-33 % of the pre-ischaemic level for the remainder of the ischaemic period (Figure 7.9A). rCBF then increased to ~100 % upon removal of the monofilament, and then stabilised at ~65 % after 30 min of reperfusion (Figure 7.9A). In *DSCR1* KO mice, rCBF initially decreased to ~20 % of the pre-ischaemic level and remained at 35-42 % of the pre-ischaemic level for the remainder of the ischaemic period (Figure 7.9A). rCBF then increased initially to ~90 % upon removal of the monofilament, and then stabilised at ~53 % after 30 min of reperfusion (Figure 7.9A). No differences in rCBF profiles were observed between *DSCR1* Wt_{KO} and KO mice.

In our other studies (Chapters 3, 5 and 6), mice that did not undergo a reduction of >70 % in rCBF when the filament was inserted, were excluded. With the *DSCR1* Wt_{KO} and KO mice, such a modest reduction in rCBF inexplicably accounted for a large proportion of the mice from each group (Wt_{KO}, n = 3, 60 % of all Wt_{KO} mice used in this study; KO, n = 7, 64 % of all KO mice used in this study). I had previously attempted to perform cerebral I-R on *DSCR1* KO mice without being able to achieve any drop in rCBF (n = 5; data not shown), suggesting that these mice were resistant to ischaemia performed using the 6-0 sized filament. It is possible that this could perhaps be due to a larger diameter in the MCA, although this has not been examined. However, the left and right posterior communicating arteries were found to be larger in SV129 mice compared to C57Bl6/J mice, although the basilar artery was smaller in SV129 mice compared to C57Bl6/J mice (Wellons *et al.*, 2000). For this reason, as well as other housing issues, the *DSCR1* Wt_{KO} and KO mice were re-generated. Therefore, these newly generated mice may still have larger cerebral blood vessels than C57Bl6/J mice, that could account for the larger proportion of <70 % reductions in rCBF. These mice were not excluded in this study, as we did

not have time to perform enough surgeries to achieve acceptable group numbers. Importantly however, I have also analysed total infarct volume separately in mice that achieved a <70 % reduction in rCBF and those that achieved an >70 % reduction in rCBF (see section 7.3.6.3 below).

7.3.6.2 Mortality and neurological function

No deaths occurred in *DSCR1* Wt_{KO} or KO mice 24 h after cerebral I-R (Wt_{KO}, n = 5; KO, n = 11). Neurological score and hanging wire times were not statistically different between groups (Figures 7.9B & C), although *DSCR1* KO mice tended to have a lower score (ie. less impairment) with the majority of KO mice given a score of 0, and the majority of Wt_{KO} mice given a score of 3 (P = 0.06; Figure 7.9B).

7.3.6.3 Brain infarct and oedema volume measured as mm^3

Representative coronal sections of infarcted brain of *DSCR1* Wt_{KO} and KO mice 24 h after I-R are shown in Figures 7.10A and B, respectively. Twenty-four h after I-R, significantly smaller total and subcortical infarct volumes were produced in *DSCR1* KO mice compared with their Wt_{KO} littermates (total: 19±5 vs. 49±10 mm^3; subcortical: 16±4 vs. 38±10 mm^3; $P < 0.05$; n = 5-11; Figures 7.10C & D). *DSCR1* KO mice also had smaller cortical infarct volumes compared to Wt_{KO} mice, although this did not reach statistical significance (3±1 vs. 11±7 mm^3; P = 0.11; Figure 7.10D). Oedema volume was also smaller in *DSCR1* KO mice compared to Wt_{KO} mice, however, this did not reach statistical significance (11±3 vs. 24±7 mm^3; P = 0.08; Figure 7.10E).

Importantly, when data from *DSCR1* Wt_{KO} and KO mice were separated into subsets that achieved a reduction in rCBF of <70 % (P = 0.06; Wt_{KO}, n = 3; KO, n = 7) or >70 % (P = 0.08; Wt_{KO}, n = 2; KO, n = 4), *DSCR1* KO mice still appeared to have smaller total infarct volumes

compared to their Wt_{KO} littermates, although of course these did not reach statistical significance with such low n values.

7.3.6.4 Brain infarct volume measured as % of non-ischaemic hemisphere

When measured as a percentage of the non-ischaemic hemisphere, total ($P < 0.05$; *DSCR1* Wt_{KO} vs. KO), cortical ($P = 0.13$) and subcortical ($P < 0.05$) infarcts 24 h after I-R had very similar profiles compared to when the infarct was measured in mm^3 (Figures 7.11A-B).

7.3.6.5 Brain infarct area distribution

Twenty-four h after cerebral I-R, similar shaped distribution profiles were observed in *DSCR1* Wt_{KO} and KO mice, with the peak in total and subcortical infarct area in both groups at bregma -0.92 mm (Figures 7.12A & C). Both total and subcortical infarct areas were significantly smaller in *DSCR1* KO mice than Wt_{KO} mice in the region spanning from bregma -0.08 mm to bregma -4.28 mm (Figures 7.12A & C). No significant difference was observed in the cortical infarct distribution, although *DSCR1* KO mice tended to have smaller cortical infarct areas throughout the lesion (Figure 7.12B).

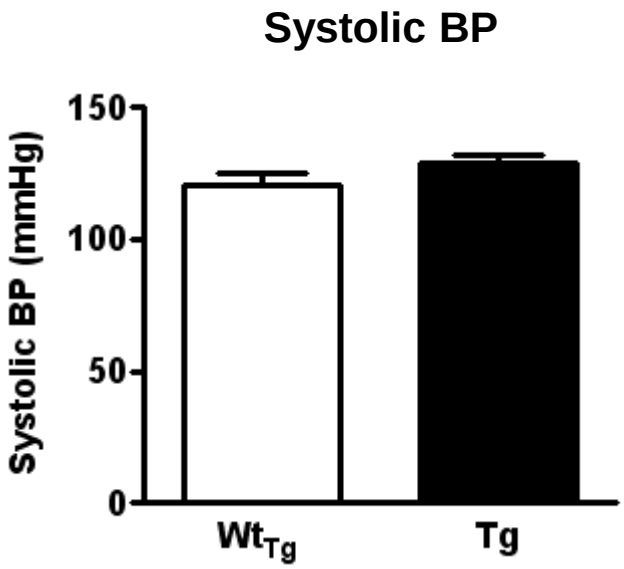

Figure 7.1. Systolic blood pressure in naïve DSCR1 Wt_{Tg} and Tg mice.

Systolic blood pressure was measured in naive DSCR1 Wt_{Tg} (n = 10) and Tg (n = 13) mice. Data are presented as mean ± SEM.

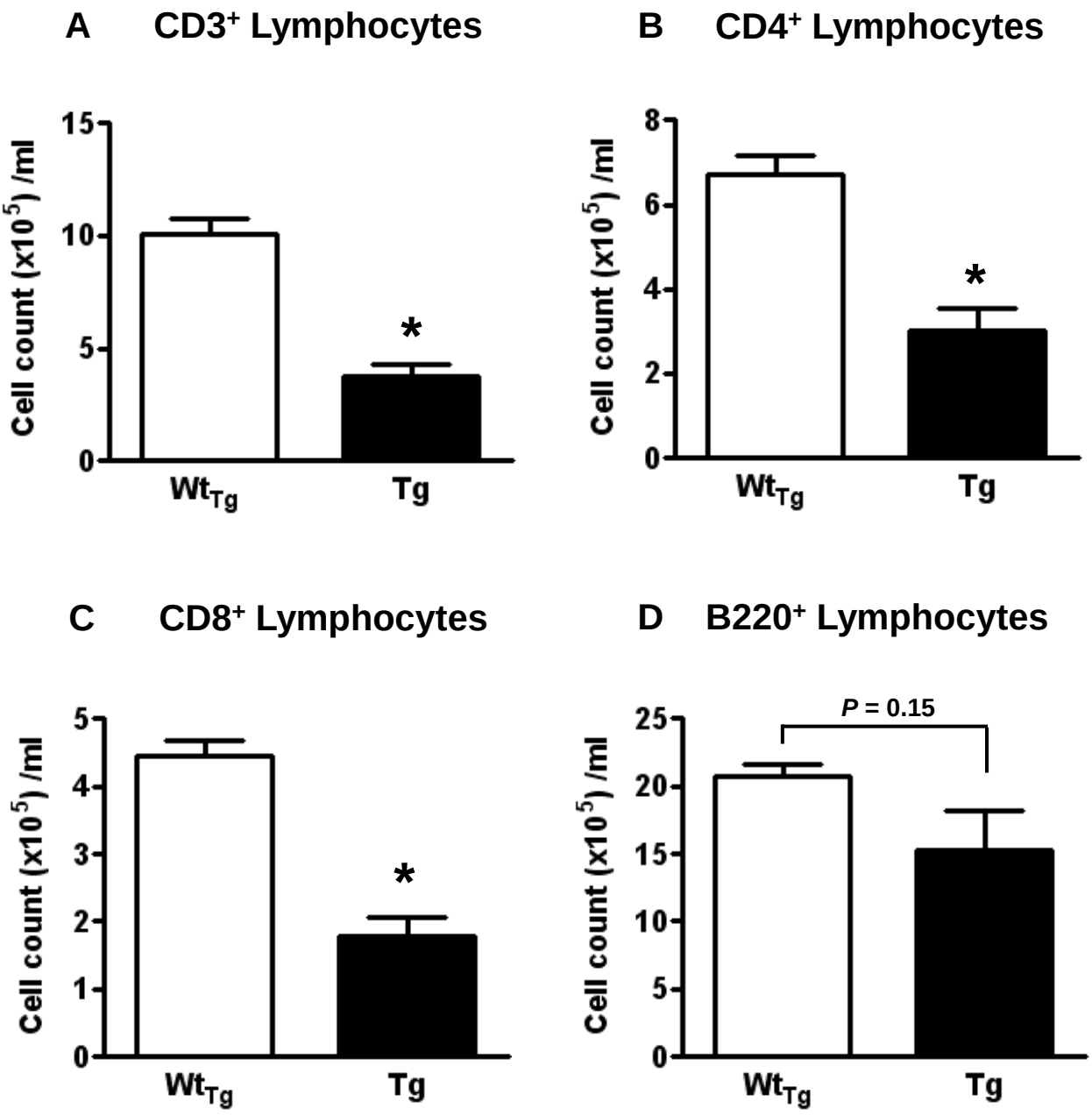

Figure 7.2. T and B lymphocyte counts in the blood of naive DSCR1 Wt_{Tg} and Tg mice. Flow cytometric analyses are shown for $CD3^+$ (**A**), $CD4^+$ (**B**), and $CD8^+$ (**C**) T lymphocytes, and $B220^+$ B lymphocytes (**D**) isolated from the blood of naive DSCR1 Wt_{Tg} and Tg mice (n = 3 per group; $^*P < 0.05$, unpaired t test). Data are presented as mean ± SEM.

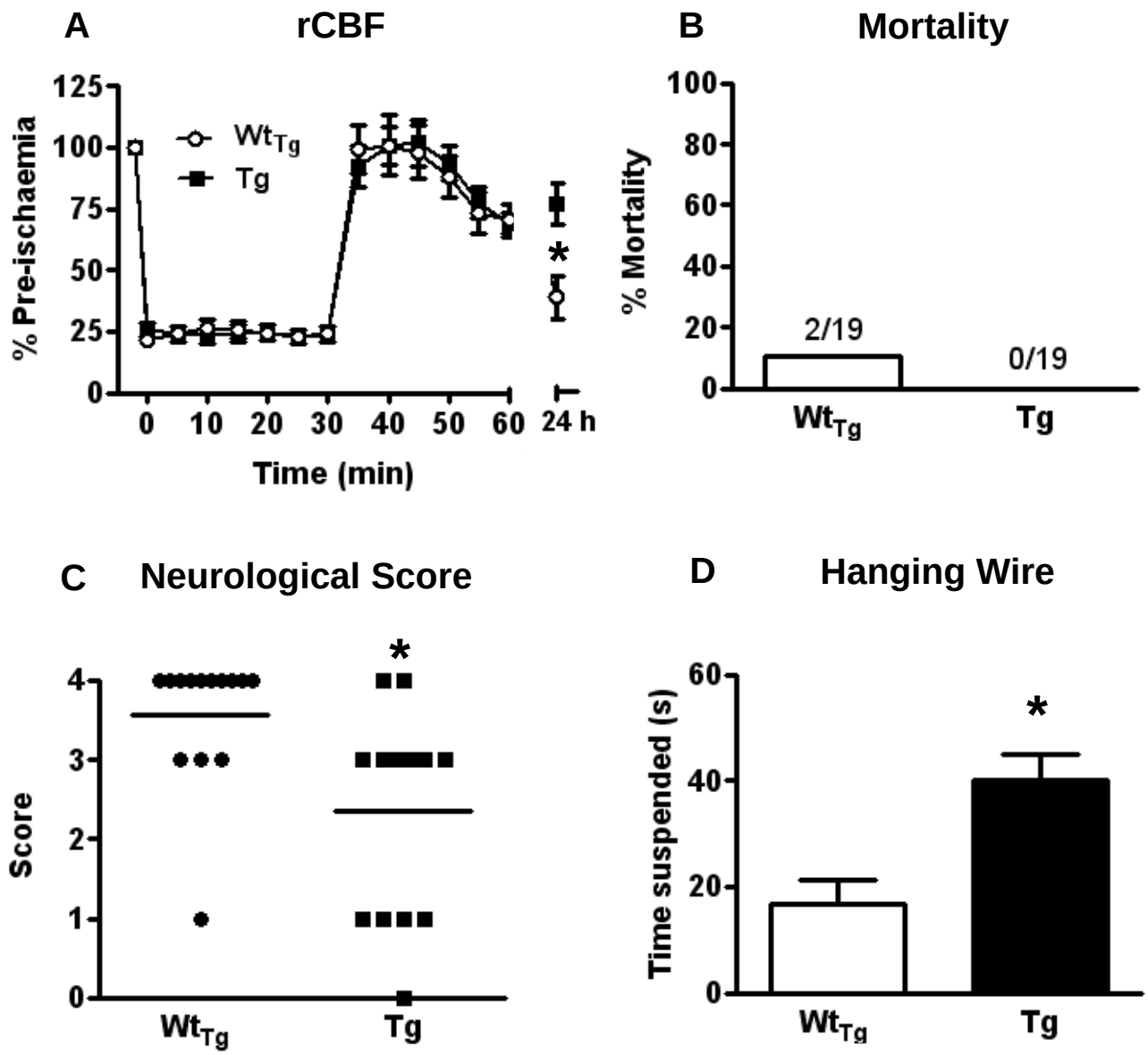

Figure 7.3. Regional cerebral blood flow (rCBF), mortality, neurological score and hanging wire at 24 h after I-R in DSCR1 Wt_{Tg} and Tg mice.

rCBF was recorded during and after 30 min MCAO, as well as at 24 h after MCAO (**A;** n = 14 per group; *P < 0.05 at 24 h after I-R, unpaired t test). **B:** Mortality at 24 h after MCAO. **C:** Neurological score 24 h following I-R (n = 14 per group; *P < 0.05, Mann-Whitney test). **D:** Hanging wire data 24 h following I-R (n = 14 per group; *P < 0.05, unpaired t test). Mortality data are presented as a percentage, with numbers above the bars representing the number of animals who didn't survive 24 h over the total number, neurological score data are presented as median, and rCBF and hanging wire data are presented as mean ± SEM.

Figure 7.4. Cerebral infarct and oedema volume at 24 h after I-R in *DSCR1* Wt_{Tg} and Tg mice (measured as mm^3).

Representative coronal brain sections are shown from a *DSCR1* Wt_{Tg} (**A**) and a *DSCR1* Tg (**B**) mouse 24 h after I-R with the infarct area outlined in white. Total (**C**), and cortical and subcortical (**D**) cerebral infarct volumes were measured in *DSCR1* Wt_{Tg} and Tg mice 24 h after I-R (Wt_{Tg}, $n = 11$; Tg, $n = 11$; $^*P < 0.05$, unpaired t test). **E:** Oedema volume measured at 24 h in *DSCR1* Wt_{Tg} and Tg mice (Wt_{Tg}, $n = 11$; Tg, $n = 11$; $^*P < 0.05$, unpaired t test). Data are presented as mean ± SEM.

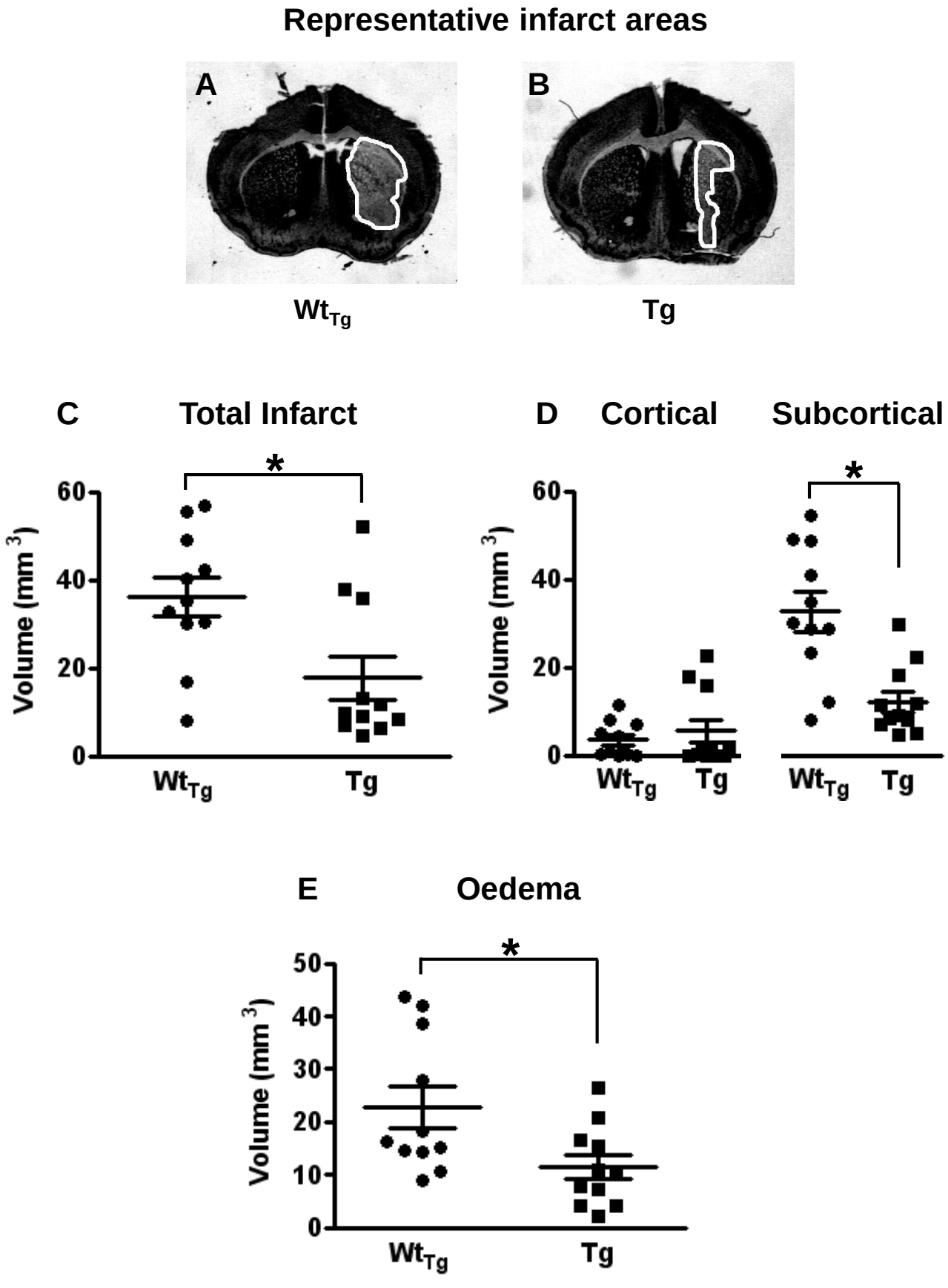
Representative infarct areas
A
B
Wt Tg
Tg
C
Total Infarct
D
Cortical
Subcortical
Volume (mm 3)
60
40
20
0
*
Wt Tg
Tg
E
Oedema
50
40
30
20
10
0

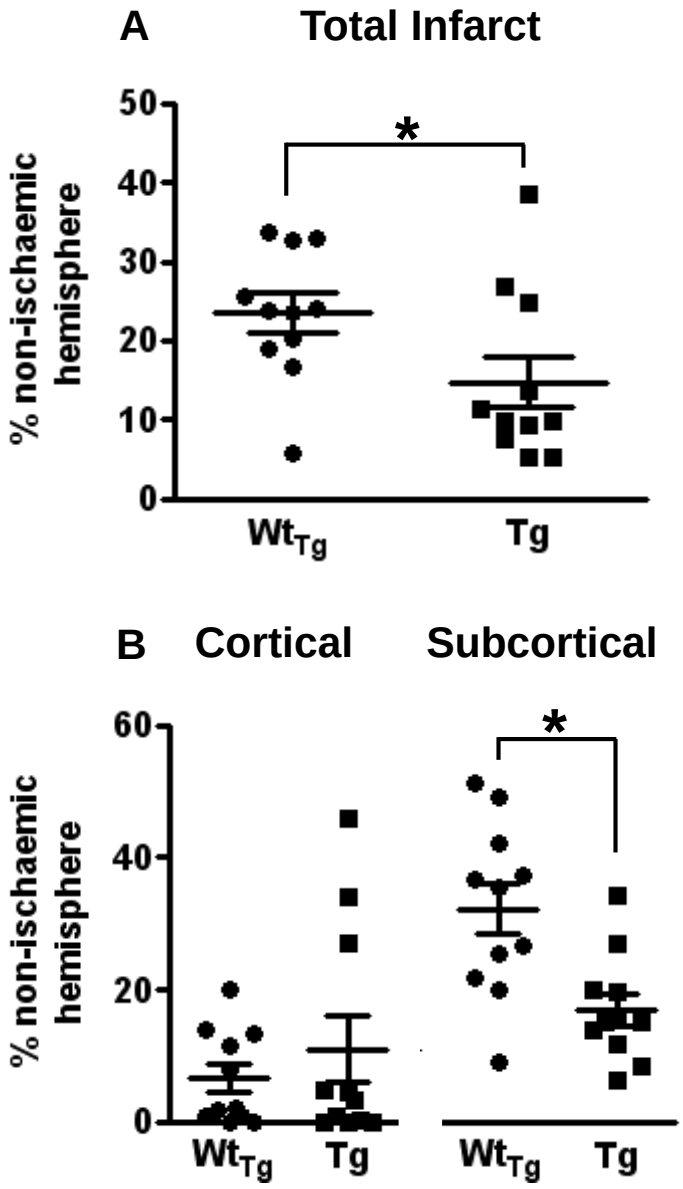

Figure 7.5. Cerebral infarct volume at 24 h after I-R in DSCR1 Wt_{Tg} and Tg mice (measured as % of non-ischaemic hemisphere).

Total (**A**), and cortical and subcortical (**B)** cerebral infarct volumes were measured in DSCR1 Wt_{Tg} and Tg mice 24 h after I-R (Wt_{Tg}, $n = 11$; Tg, $n = 11$; $^*P < 0.05$, unpaired t test). Infarct volume data are presented as mean ± SEM.

Figure 7.6. Cerebral infarct area distribution at 24 h after I-R in *DSCR1* Wt_{Tg} and Tg mice.

Total (**A**), cortical (**B**) and subcortical (**C**) cerebral infarct area distributions were measured in *DSCR1* Wt_{Tg} and Tg mice 24 h after I-R (Wt_{Tg}, $n = 11$; Tg, $n = 11$; $^*P < 0.05$ at each point, unpaired t test). Data are presented as mean ± SEM.

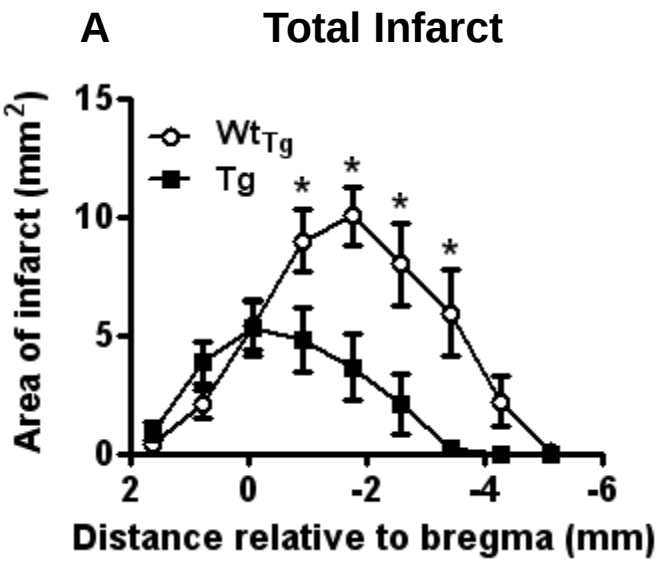
A
Total Infarct
Area of infarct (mm2)
15
10
5
0
Wt
Tg
Tg
*
*
*
*
2
0
-2
-4
-6
Distance relative to bregma (mm)

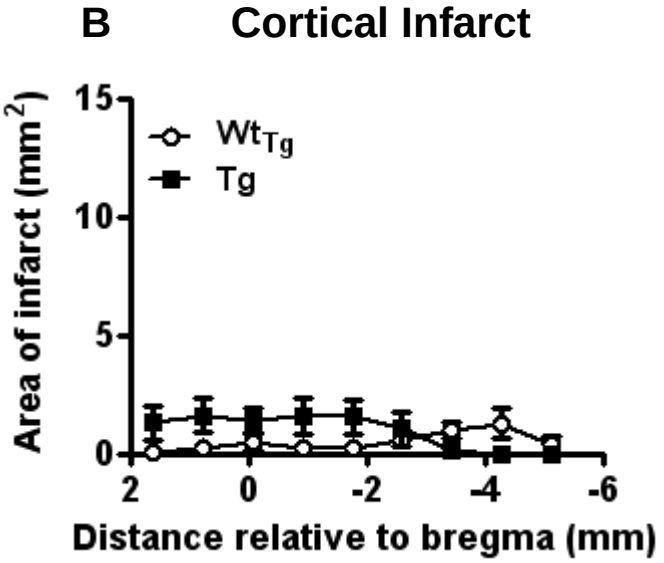
B
Cortical Infarct
Area of infarct (mm2)
15
10
5
0
Wt
Tg
Tg
2
0
-2
-4
-6
Distance relative to bregma (mm)

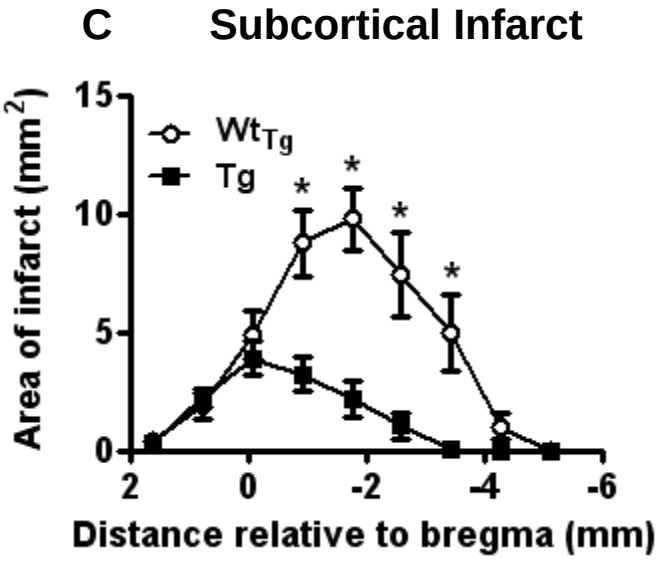
C
Subcortical Infarct
Area of infarct (mm2)
15
10
5
0
Wt
Tg
Tg
*
*
*
*
2
0
-2
-4
-6
Distance relative to bregma (mm)

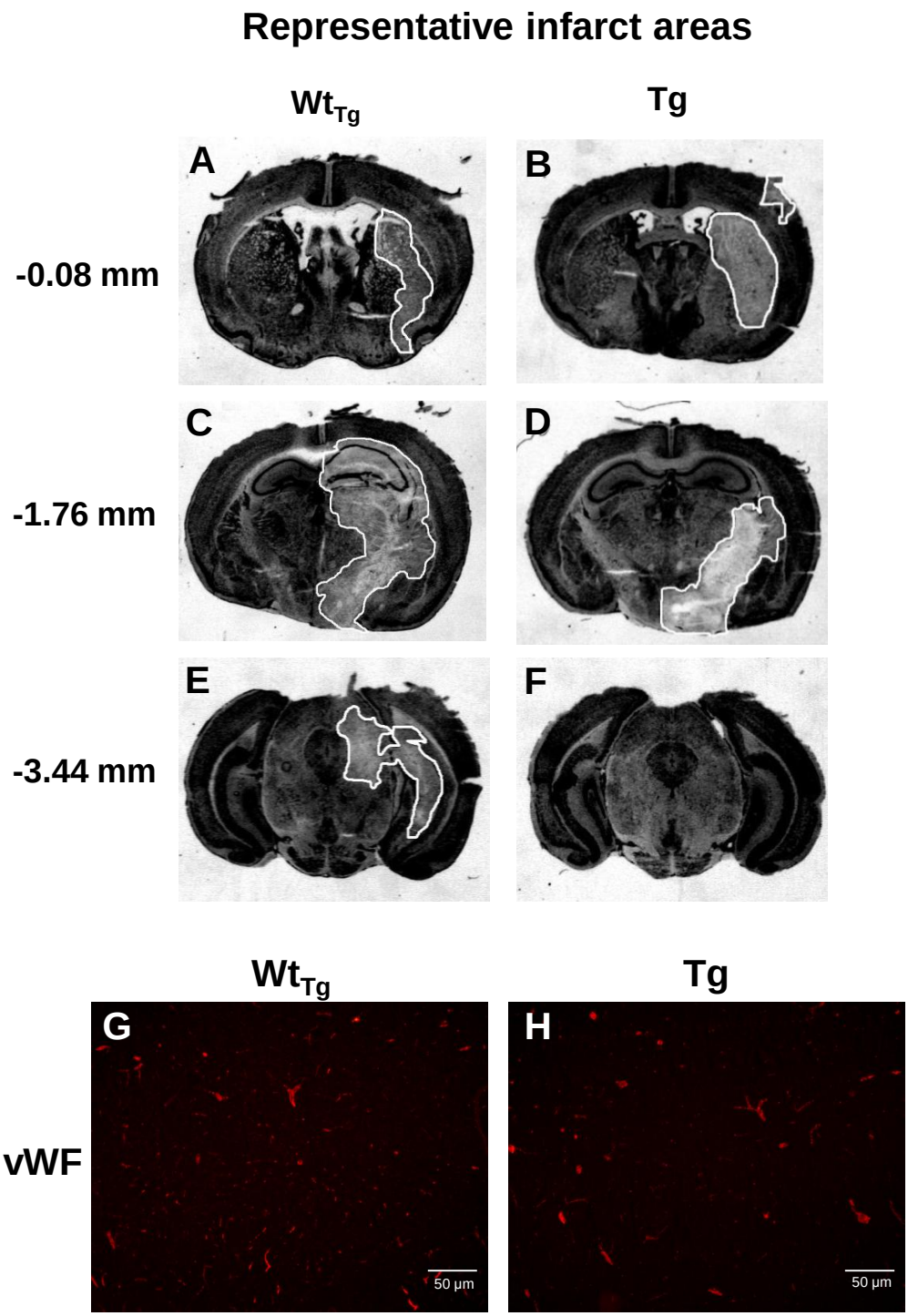

Figure 7.7. von Willebrand factor Immunofluorescence.

Representative coronal brain sections are shown from DSCR1 Wt_{Tg} and Tg mice after I-R at bregma -0.08 mm (**A-B**), -1.76 mm (**C-D**) and -3.44 mm (**E-F**), with the infarct area outlined in white (representative of Wt_{Tg}, n = 2; Tg, n = 3). Representative photomicrographs taken from bregma -1.76mm, showing vWF immunofluorescent staining within the right hemisphere of a naive DSCR1 Wt_{Tg} (**G**) and Tg (**H**) mouse. The scale bar represents 50 µm.

Figure 7.8. DSCR1 mRNA and protein expression in naïve *DSCR1* Wt_{Tg} and Tg mice, and at 6 and 24 h after I-R.

DSCR1.1 (**A**) and DSCR1.4 (**B**) mRNA expression was measured in the ischaemic (right) hemisphere of naïve *DSCR1* Wt_{Tg} and Tg mice, as well as at 6 and 24 h after I-R. Values are expressed as relative intensity normalised relative to naïve Wt_{Tg} control, and are presented as mean ± SEM (n = 3 per group; $^*P < 0.05$ vs. matched Wt_{Tg} group, unpaired t test). Representative Western blots of DSCR1.1 and DSCR1.4 protein measured in the ischaemic (right; R) and non-ischaemic (left; L) hemispheres are shown in **C**. Note that the DSCR1.4 blot had a longer exposure time compared to the DSCR1.1 and Vinculin. Densitometric analyses of immunoreactive band intensities of DSCR1.1 (**D**) and DSCR1.4 (**E**) protein expression was measured in the ischaemic (right) hemisphere of naïve *DSCR1* Wt_{Tg} and Tg mice, as well as at 6 and 24 h after I-R. Values are expressed as relative intensity normalised to Vinculin intensity, and then normalised relative to naïve Wt_{Tg} control, and are presented as mean ± SEM (n = 3 per group; $^*P < 0.05$ vs. matched Wt_{Tg} group, unpaired t test).

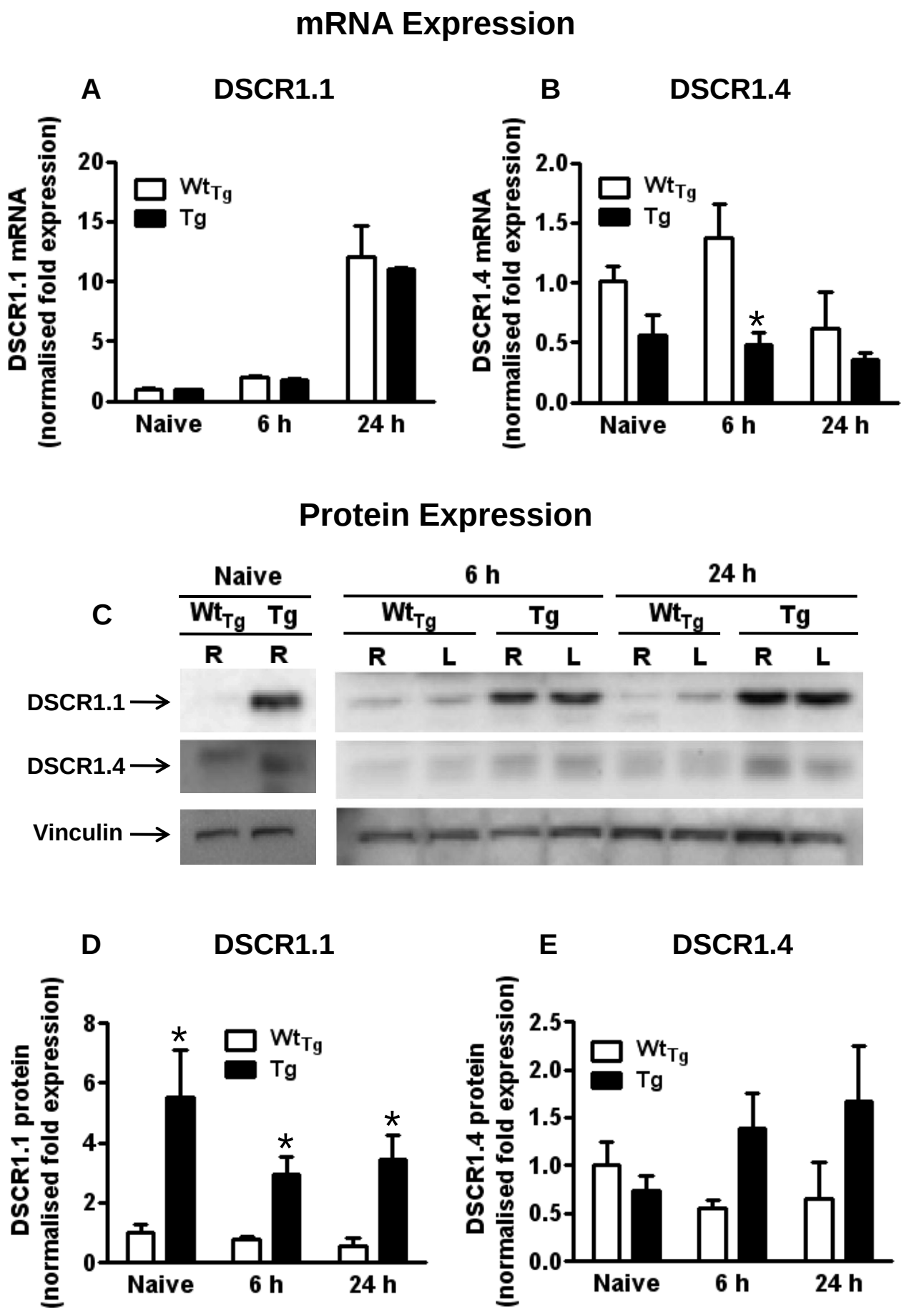
mRNA Expression
A
DSCR1.1
DSCR1.1 mRNA (normalised fold expression)
20
15
10
5
0
Wt Tg
Tg
Naive
6 h
24 h
B
DSCR1.4
DSCR1.4 mRNA (normalised fold expression)
2.0
1.5
1.0
0.5
0.0
*
Protein Expression
C
Naive
6 h
24 h
Wt Tg
Tg
R
L
DSCR1.1
DSCR1.4
Vinculin
D
DSCR1.1
DSCR1.1 protein (normalised fold expression)
8
6
4
2
0
*
E
DSCR1.4
DSCR1.4 protein (normalised fold expression)
2.5
2.0
1.5
1.0
0.5
0.0

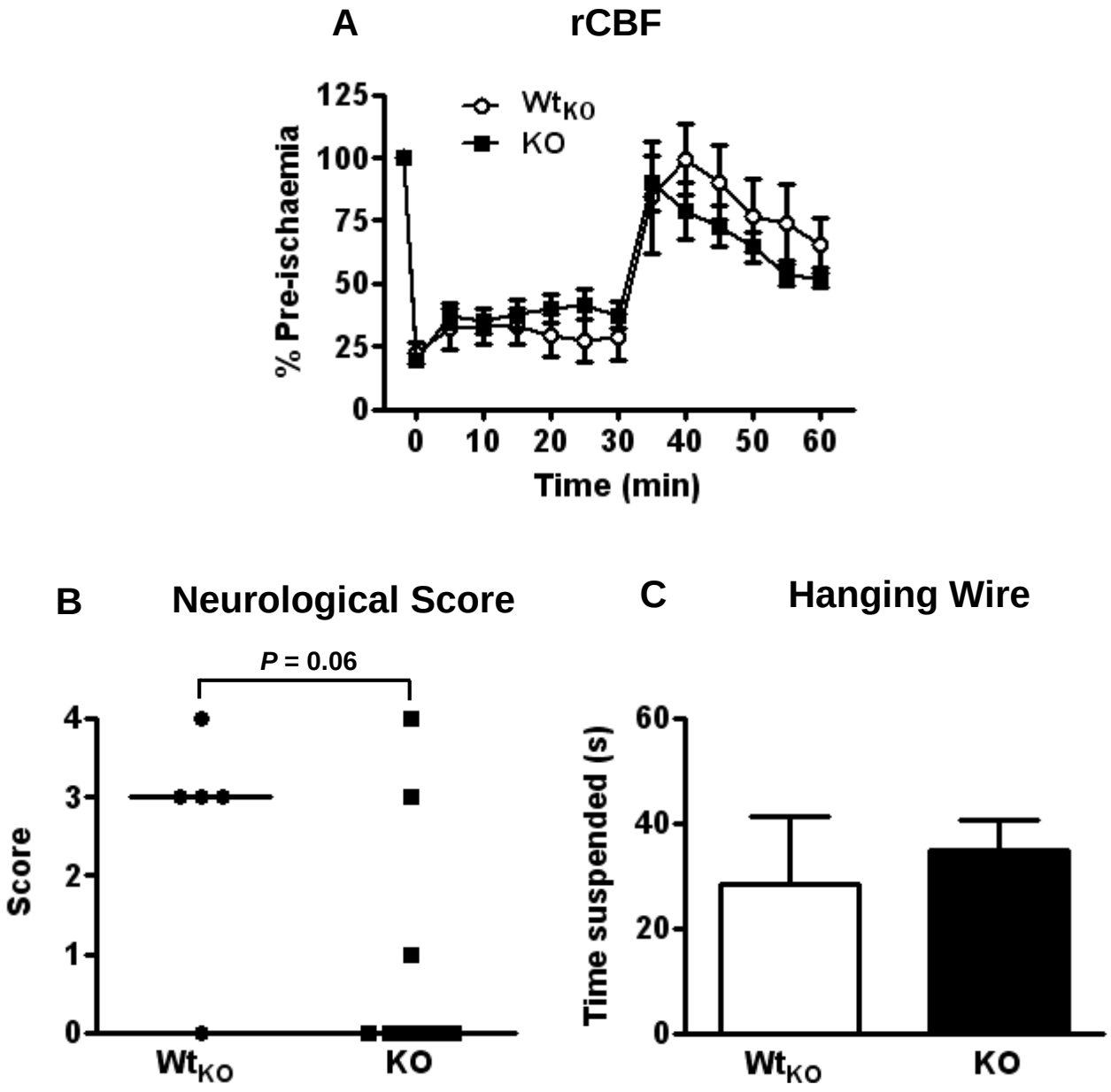

Figure 7.9. Regional cerebral blood flow (rCBF), neurological score and hanging wire at 24 h after I-R in DSCR1 Wt_{KO} and KO mice.

rCBF was recorded in DSCR1 Wt_{KO} and KO mice during and after 30 min MCAO (**A;** Wt_{KO}, n = 5; KO, n = 11). **B:** Neurological score 24 h after I-R (Wt_{KO}, n = 5; KO, n = 11; Kruskal-Wallis test with Dunn's *post-hoc* test). **C:** Hanging wire data 24 h after I-R (Wt_{KO}, n = 5; KO, n = 11). Neurological score data is presented as median, and rCBF and hanging wire data are presented as mean ± SEM.

Figure 7.10. Cerebral infarct and oedema volume at 24 h after I-R in *DSCR1* Wt_{KO} and KO mice (measured as mm^3).

Representative coronal brain sections are shown from a *DSCR1* Wt_{KO} (**A**) and a *DSCR1* KO (**B**) mouse 24 h after I-R with the infarct area outlined in white. Total (**C**), and cortical and subcortical (**D**) cerebral infarct volumes were measured in *DSCR1* Wt_{KO} and KO mice 24 h after I-R (Wt_{KO}, $n = 5$; KO, $n = 11$; $^*P < 0.05$, unpaired *t* test). **E:** Oedema volume measured at 24 h in *DSCR1* Wt_{KO} and KO mice (Wt_{KO}, $n = 5$; KO, $n = 11$; unpaired *t* test). Data are presented as mean ± SEM.

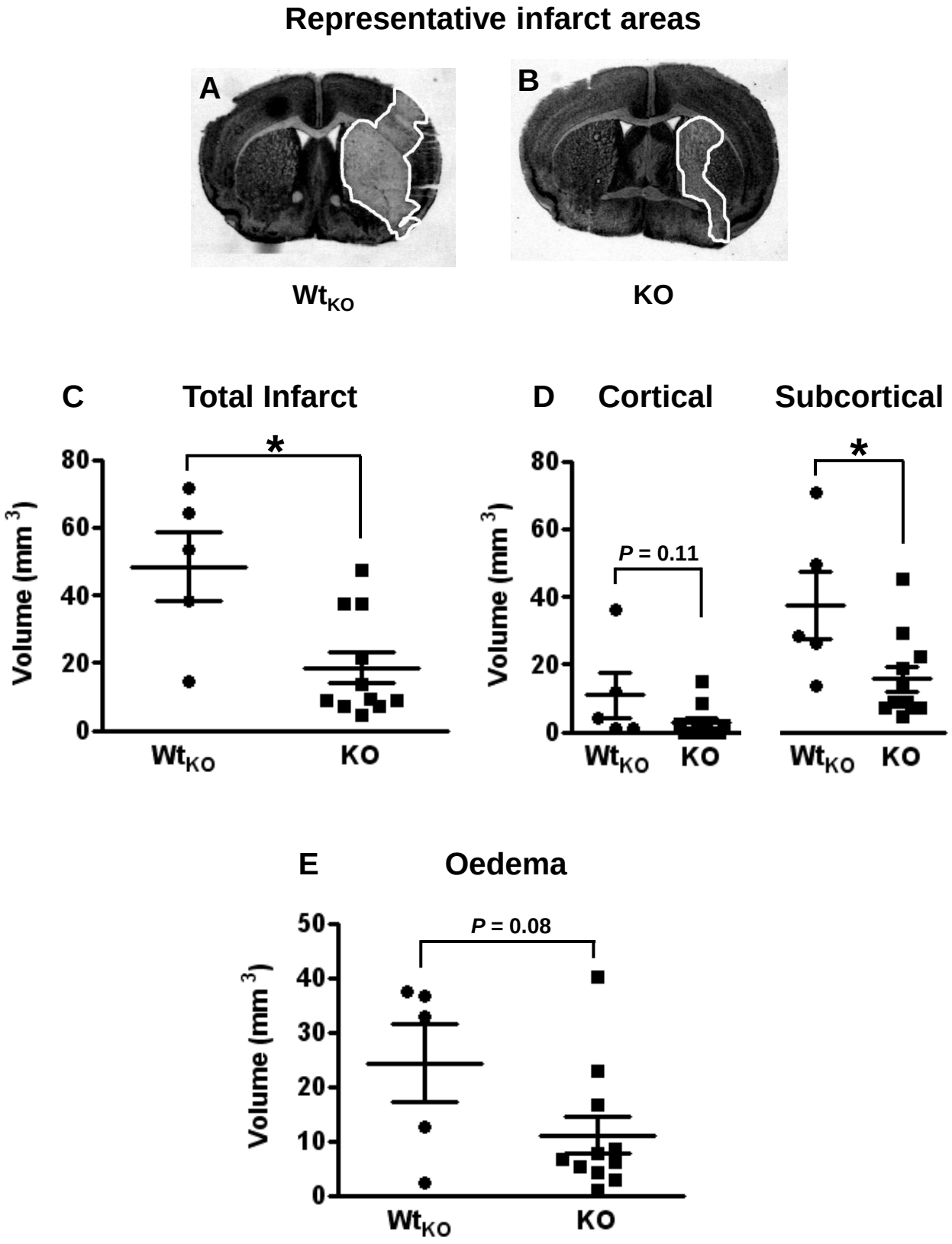
Representative infarct areas
A
B
Wt$_{KO}$
KO
C
Total Infarct
Volume (mm^3)
80
60
40
20
0
*
Wt$_{KO}$
KO
D
Cortical
P = 0.11
Subcortical
*
E
Oedema
50
40
30
20
10
0
P = 0.08

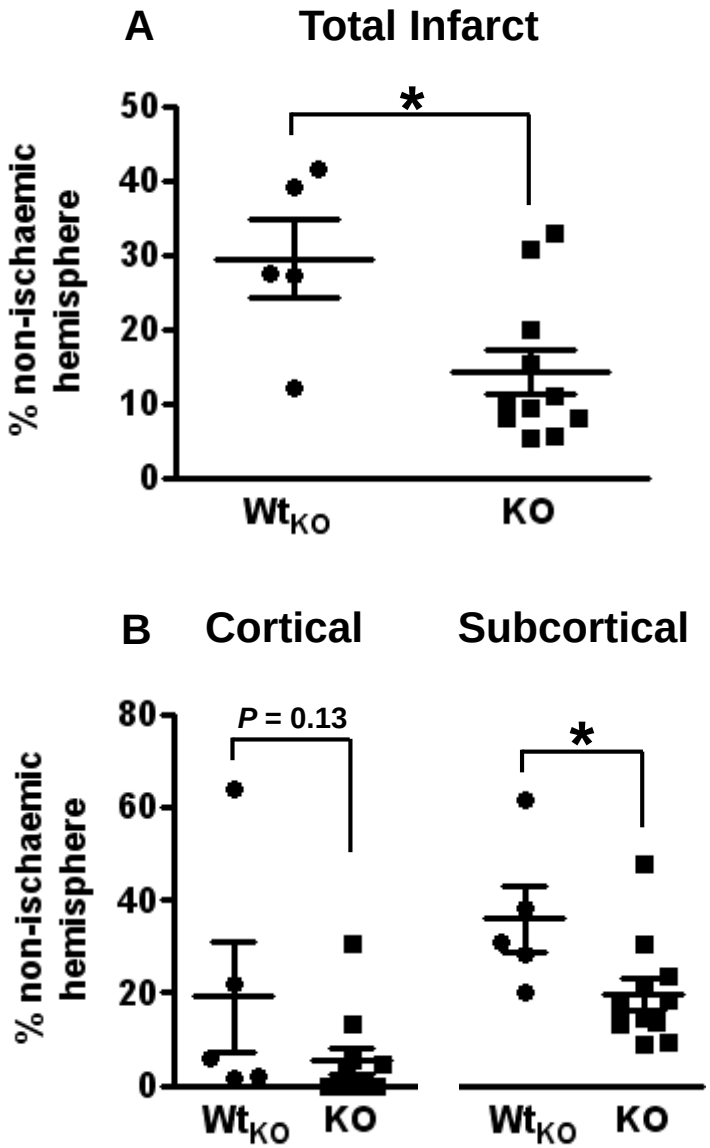

Figure 7.11. Cerebral infarct volume at 24 h after I-R in DSCR1 Wt_{KO} and KO mice (measured as % of non-ischaemic hemisphere).

Total (**A**), and cortical and subcortical (**B**) cerebral infarct volumes were measured in DSCR1 Wt_{KO} and KO mice 24 h after I-R (Wt_{KO}, $n = 5$; KO, $n = 11$; $^*P < 0.05$, unpaired t test). Infarct volume data are presented as mean ± SEM.

Figure 7.12. Cerebral infarct area distribution at 24 h after I-R in *DSCR1* Wt_{KO} and KO mice. Total (**A**), cortical (**B**) and subcortical (**C**) cerebral infarct area distributions were measured in *DSCR1* Wt_{KO} and KO mice 24 h after I-R (Wt_{KO}, $n = 5$; KO, $n = 11$; $^*P < 0.05$ at each point, unpaired t test). Data are presented as mean ± SEM.

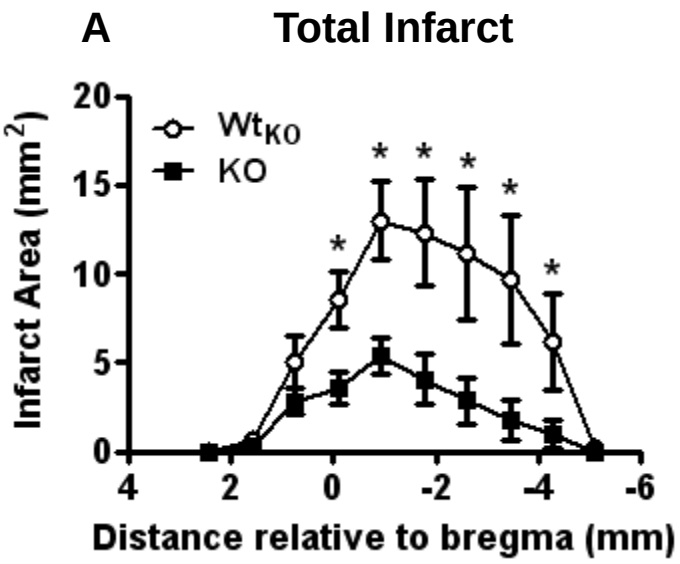
A
Total Infarct
Wt
KO
KO
Infarct Area (mm2)
20
15
10
5
0
4
2
0
-2
-4
-6
Distance relative to bregma (mm)

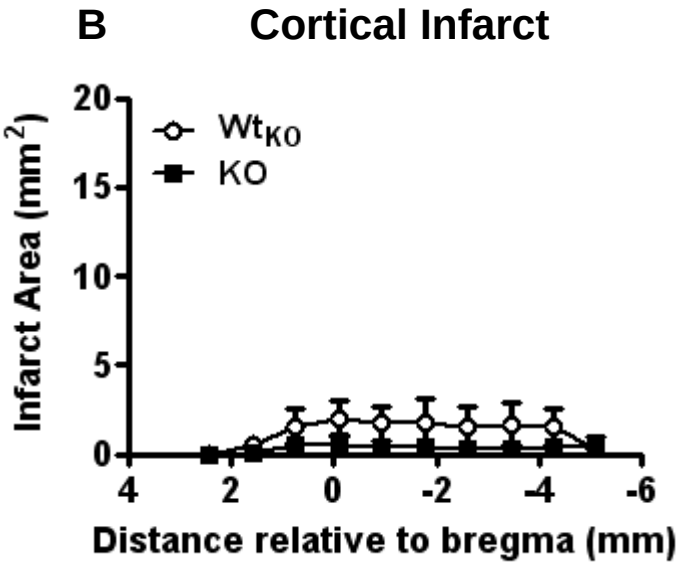
B
Cortical Infarct
Wt
KO
KO
Infarct Area (mm2)
20
15
10
5
0
4
2
0
-2
-4
-6
Distance relative to bregma (mm)

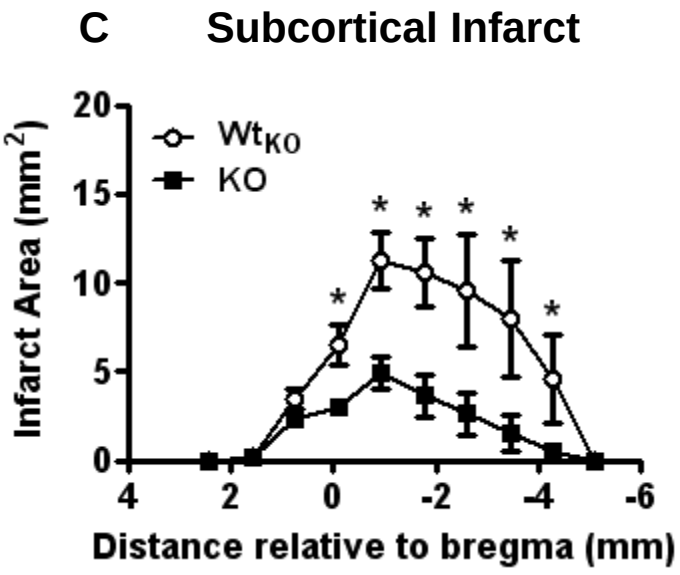
C
Subcortical Infarct
Wt
KO
KO
Infarct Area (mm2)
20
15
10
5
0
4
2
0
-2
-4
-6
Distance relative to bregma (mm)

7.4 DISCUSSION

This is the first study to investigate the contribution of the Down syndrome candidate region 1 (*DSCR1*) gene on outcome following stroke. We have provided evidence that the over-expression of *DSCR1* protects against cerebral ischaemia-reperfusion (I-R). In addition, somewhat surprisingly, preliminary findings suggest that *DSCR1* knock-out (KO) mice also may have an improved outcome following I-R.

Here, for the first time, we report that the over-expression of human *DSCR1* in mice improves neurological function, and reduces cerebral infarct and oedema volume following cerebral I-R. DSCR1 is a calcineurin inhibitor (Rothermel *et al.*, 2000), and previous studies that have administered pharmacological calcineurin inhibitors following cerebral I-R, such as cyclosporin A and FK506 (Tacrolimus), have reported reduced lesion size and neurological deficit (Bochelen *et al.*, 1999; Sharkey and Butcher, 1994; Sharkey *et al.*, 1996; Uchino *et al.*, 1998; Vachon *et al.*, 2002; Yoshimoto and Siesjo, 1999). These drugs are known as potent immunosuppressants that are used therapeutically in patients following organ transplantation to reduce rejection. Local inflammatory responses are well known to play an important role in the exacerbation of neuronal loss after stroke (Dirnagl *et al.*, 1999), so it is perhaps not surprising that these drugs, and the over-expression of *DSCR1*, are reported to improve outcome.

As DSCR1 is highly expressed in neuronal cells as well as circulating T lymphocytes, the improved outcome following stroke could be from the over-expression of DSCR1 in one or both of these cell types. The smaller total cerebral infarct volume correlated with a reduced subcortical, but not cortical infarct volume. This was unexpected, given that the cortex usually pertains to the penumbra in the mouse model of MCA occlusion. However, DSCR1 is highly expressed in the subcortical regions (Porta *et al.*, 2007), consistent with the possibility that neuronal cell over-expression of *DSCR1* contributed to the protection observed. DSCR1 is also

moderately expressed in the cortex (Porta *et al.*, 2007), and that expression is increased after I-R (Cho *et al.*, 2008). However, cortical infarct is very small in the Wt_{Tg} mice, and perhaps could not be reduced further. Furthermore, *DSCR1* Tg mice were found to have a more rostral spatial infarct profile than Wt_{Tg} mice. In the more caudal part of the forebrain, where *DSCR1* Tg mice have significantly smaller infarcts than Wt_{Tg} mice, strong DSCR1 immunoreactivity occurs in the striatum and the CA1 and CA3 pyramidal cells of the hippocampus, as well as in the cerebral cortex (Porta *et al.*, 2007), further strengthening this idea of neuronal over-expression of *DSCR1* contributing to the protection from ischaemic damage. Another important feature of this protection is the fact that there were no hippocampal lesions in the brains of *DSCR1* Tg mice. The hippocampus is normally especially sensitive to reductions in oxygen, and is therefore quite sensitive to damage by cerebral ischaemia (Kirino, 2000). Interestingly, calcineurin is most highly expressed in the regions of brain that are most susceptible to ischaemia, and high levels of calcineurin activity predispose neurons to apoptosis (Asai *et al.*, 1999). DSCR1 also has strong immunoreactivity in these regions, including the hippocampus. This again points to the plausibility of neuronal over-expression of *DSCR1* as being important for the smaller infarct volume observed in Tg mice.

Abnormal T lymphocyte function may also have played a role in the reduced infarct damage and improved neurological function. Recent studies utilising T lymphocyte-deficient mice have reported that T lymphocytes contribute to infarct size development (Hurn *et al.*, 2007; Kleinschnitz *et al.*, 2010b; Shichita *et al.*, 2009; Yilmaz *et al.*, 2006). This could be through the increased release of inflammatory cytokines and chemokines (Offner *et al.*, 2006a), the increased production of superoxide (see Chapters 4 and 5), or other mechanisms resulting in microvascular dysfunction (Arumugam *et al.*, 2004). We found fewer circulating $CD3^+$, $CD4^+$ and $CD8^+$ T lymphocytes in *DSCR1* Tg mice than Wt_{Tg} littermates. Therefore, reduced T lymphocyte numbers in the blood, and consequently, less brain infiltration, may be one way in which *DSCR1*

Tg mice were protected. However, less T lymphocyte infiltration probably cannot account for the dramatically different spatial infarct distribution. For that reason, we speculate that the main mechanism of protection was through the over-expression of *DSCR1* in neurons, especially in the forebrain structures posterior to bregma -0.92 mm, although lower circulating T lymphocyte levels may also have played a role. Future studies, including the generation of chimeras by bone marrow transplantation in gamma-irradiated *DSCR1* Tg and KO mice will help determine if the cellular source(s) of DSCR1 that affects stroke outcome is confined to neurons and/or involves circulating leukocytes.

DSCR1.4 mRNA expression was previously found to be increased in the ischaemic cortex of the brain at 6 h, and decreased afterwards, but was still elevated at 24 and 72 h after cerebral I-R in mice. Increased expression of DSCR1.4 protein was also previously found to be increased in the ischaemic cortex at 24 and 72 h after I-R in mice, whereas there was no change at 6 h (Cho *et al.*, 2008). In contrast, the present study found no significant change in DSCR1.4 mRNA or protein expression at either 6 or 24 h after I-R. Importantly, the Cho and colleagues study analysed the mRNA expression in the cortex, whereas we homogenised the entire hemisphere. Therefore, it is possible that the expression of DSCR1.4 increases in the cortex following I-R, but not in the much larger subcortex, such that the cortical signal was diluted in our samples. In addition, we also examined DSCR1.1 mRNA and protein expression in the ischaemic hemisphere, and found evidence for a small increase in mRNA expression at 6 h and a greater increase at 24 h after I-R. Protein expression however, did not change after stroke, although it was expressed at a much higher level compared to DSCR1.4 protein, consistent with a previous study (Porta *et al.*, 2007). This suggests that the increase in mRNA either precedes a later increase in protein expression, or occurs independently of any change in protein expression.

When using primers that only detect mouse DSCR1.1, we found that the over-expression of human *DSCR1.1* in these mice had no effect on mouse DSCR1.1 brain mRNA expression in either naïve mice, or at 6 or 24 h after cerebral I-R. DSCR1.1 protein expression in Tg mice was not affected by I-R, although DSCR1.1 protein expression was expressed at ~4-6-fold higher than in the Wt_{Tg} mice at all time-points measured, confirming the over-expression of this isoform in the Tg mice. DSCR1.4 mRNA and protein expression in Tg mice, was not greatly affected by stroke. Hence, the protective effects we see of *DSCR1.1* over-expression in Tg mice at 24 h after I-R is not dependent on the up-regulation of DSCR1 protein following stroke. It was however, interesting to note that there was less DSCR1.4 mRNA expression in the brains of Tg mice at all time-points measured, as well as a slightly lower expression of DSCR1.4 protein in naïve Tg mice, compared to their matched Wt_{Tg} mice. DSCR1 expression is induced by activated calcineurin (Yang *et al.*, 2000), and has therefore been proposed to function in a negative feedback loop to modulate calcineurin activity, suggesting that DSCR1 regulates its own expression. The lower expression of DSCR1.4 in naïve Tg mice compared to Wt_{Tg} mice, strongly suggests that DSCR1.1 negatively regulates the expression of DSCR1.4. Interestingly however, it does not appear to regulate its own expression.

Cerebral I-R increased the mRNA expression of many cytokines, chemokines and immune-related genes in the ischaemic hemisphere. The largest increases were observed in CCL2, CCL3, CXCL1, TBX21 (T-box 21) and TNF-α. CCL2 (also named MCP-1) and CCL3 (also named monocyte inflammatory protein-1; MIP-1α) are monocyte chemoattractants that have been previously reported to be increased after stroke (Minami and Satoh, 2003). CXCL1 (see Chapter 6) is a chemokine that attracts neutrophils (Rollins, 1997) and TBX21 is a T_H1 cell-specific transcription factor that is essential for the production of IFN-γ (interferon-gamma) (Kaminuma *et al.*, 2009). TNF-α (tumour necrosis factor-alpha) is an important inflammatory mediator that promotes the infiltration of leukocytes and triggers local production of other pro-inflammatory

cytokines (Tracey and Cerami, 1994), and is also well established to be increased after stroke (Gong *et al.*, 1998; Uno *et al.*, 1997; Wang *et al.*, 1994). The increased expression of these genes further supports the well established concept of stroke producing a pro-inflammatory response.

DSCR1 is known to inhibit calcineurin (Rothermel *et al.*, 2000), and consequently reduce activation of the transcription factors NFAT and NF-κB (Alzuherri and Chang, 2003; Arron *et al.*, 2006), resulting in less transcription of their target genes. The present study found that many cytokines, chemokines and immune-related genes, most of which are regulated by either NFAT, NF-κB or both (For reviews see Hogan *et al.*, 2003; Lee and Burckart, 1998; Pahl, 1999; Rao *et al.*, 1997), were affected by the over-expression of *DSCR1*. However, the majority were in fact increased more in the Tg mice than in the Wt_{Tg} mice. These findings indicate that either DSCR1 does not inhibit all genes regulated by NFAT and NF-κB, or perhaps the genes with increased expression are also target genes of other transcription factors that are induced after stroke, but are not affected by DSCR1. Interestingly, some of the changes caused by *DSCR1* over-expression appear contradictory. For example, we observed lower expression of monocyte, neutrophil and T lymphocyte chemoattractants (eg. CCL3, CXCL1 and CXCL11, respectively), but also reported increased expression of other monocyte and T lymphocyte chemoattractants (eg., CCL2 and CXCL10, respectively), and CCL2 has previously been shown to contribute to stroke damage (Chen *et al.*, 2003; Hughes *et al.*, 2002; Kumai *et al.*, 2004). The reason for these opposing findings is currently unclear, although after stroke, there is a release of both pro- and anti-inflammatory cytokines (Arumugam *et al.*, 2005; Hurn *et al.*, 2007; Liesz *et al.*, 2009b; Loihl *et al.*, 1999; Offner *et al.*, 2006a; Vila *et al.*, 2000), suggesting that the critical balance of inflammation is very complex. Furthermore, the mRNA expression of CD28 (a T lymphocyte cell surface receptor), CD68 (a monocyte/macrophage cell surface receptor) and CD80 (a B lymphocyte/monocyte cell surface receptor) can function as markers of infiltration of the respective immune cells. There were only small changes in expression of CD28 and CD68;

however, CD80 expression had a greater increase, 6 and 24 h after I-R, although it was still relatively small, and there were no real differences between *DSCR1* Wt_{Tg} and Tg mice. This is again surprising because previous studies have reported infiltration of T lymphocytes and macrophages 24 h after stroke (Gelderblom *et al.*, 2009; Jander *et al.*, 1995; and Chapter 4). Further immunohistochemistry studies are required to increase our understanding of the infiltration of these cells and to clarify whether the mRNA expression of cell surface markers or chemokines that attract these cells, correlate better with the infiltration of these cells.

The active NF-κB dimeric complex is either made up of NF-κB1 (formerly termed p50) or NF-κB2 (formerly termed p52), bound to a Rel protein. The most common form consists of NF-κB1 and RelA (formerly termed p65) (Lee & Burckart, 1998). In the present study, neither stroke nor *DSCR1* over-expression affected the mRNA expression of NF-κB1; however there was a very small increase in NF-κB2 after I-R. Although previous studies have shown that NF-κB expression and activity increase after stroke, they found increases in the expression of the RelA protein (Gabriel *et al.*, 1999; Schneider *et al.*, 1999), but did not find any changes in the protein expression levels of NF-κB1. This suggests that no new synthesis is induced, but rather, that existing NF-κB1 protein forms the dimer with newly synthesised RelA protein (Gabriel *et al.*, 1999). This indicates that stroke may still have increased NF-κB1/RelA expression and activity, and that *DSCR1* over-expression may still be acting through the inhibition of NF-κB.

It should be pointed out that the *DSCR1* Tg mice are not a model of Down syndrome. They do not have intellectual or physical disabilities, and they also do not display Alzheimer's disease-like pathology when aged. However, they do have impaired immune cell function, like individuals with Down syndrome. *DSCR1* is an important gene in Down syndrome but because an entire chromosome is usually replicated, *DSCR1* on its own is not sufficient to cause Down syndrome. Another difference between individuals with Down syndrome and the *DSCR1* Tg mice is that

DSCR1 protein is up-regulated by 2-3-fold in Down syndrome individuals, whereas it is up-regulated by ~6-fold in Tg mice. However, the present study is not examining Down syndrome and stroke as such, but is attempting to further enhance our understanding of the damaging inflammatory mechanisms in stroke, and find potential therapeutic targets, such as the DSCR1 signalling mechanism in key cell types.

The data from the *DSCR1* KO mice is somewhat preliminary, as we have low numbers of matched wild-type mice. Nonetheless, we have so far found that when *DSCR1* KO mice are subjected to cerebral I-R, they appear to also have a smaller infarct volume, and less neurological impairment, as indicated by the neurological score. Intriguingly, although the majority of *DSCR1* KO mice achieved a superior neurological score of 0 (i.e. normal), they did not hang onto the wire for longer than the Wt_{KO} mice. This is currently difficult to explain, but the Wt_{KO} group is still very small with only 5 mice. More substantial group sizes are required to see if these findings persist or change.

It is somewhat surprising that both *DSCR1* Tg and KO mice achieve similarly smaller infarct volumes following cerebral I-R. Given that DSCR1 suppresses calcineurin, it was hypothesised that calcineurin activity would be at its maximum in *DSCR1* KO mice, and hence these mice may suffer larger infarcts. In the heart, calcineurin activity leads to hypertrophy in response to pressure overload. However, in *DSCR1* KO mice, reduced hypertrophy after pressure overload was reported (Sanna *et al.*, 2006; Vega *et al.*, 2003), and calcineurin activity was found to be surprisingly ~45 % lower in the hearts of these mice (Vega *et al.*, 2003). Similarly, mice deficient in both *DSCR1* and *DSCR1L1* (DSCR1-like 1; another member of the DSCR1 family), were reported to have skeletal muscle and brain phenotypes similar to mice lacking calcineurin (Sanna *et al.*, 2006). Furthermore, mouse embryonic fibroblasts deficient in *DSCR1* were found to have lower levels of calcineurin-NFAT coupling (Sanna *et al.*, 2006), and deletion of *rcn1* in yeast (a

homologue of *DSCR1*) produced a phenotype that was similar to *rcn1* over-expression (Kingsbury and Cunningham, 2000). These data strongly suggest that DSCR1 expression is required for normal activation of calcineurin. Moreover, although no gross abnormalities in the immune system were reported in *DSCR1* KO mice (all immune organs appeared normal and there were normal numbers of T and B lymphocytes) (Ryeom *et al.*, 2003; Sanna *et al.*, 2006), one of these studies reported a 50 % reduction in $CD4^+$ T lymphocyte proliferation compared to in matched wild-type mice, and these mice were also found to have a defective T_H1 population with a decreased IFN-γ production when stimulated (Ryeom *et al.*, 2003). In contrast, the Sanna and colleagues study reported no difference in $CD4^+$ T lymphocyte proliferation or IFN-γ production (Sanna *et al.*, 2006). However, both studies found that these cells were undergoing premature cell death (Ryeom *et al.*, 2003; Sanna *et al.*, 2006), and this was found to be due to the premature expression of the Fas ligand (an NFAT target gene) (Ryeom *et al.*, 2003). This suggests that calcineurin can regulate expression of genes that control opposing actions such as T lymphocyte proliferation and death. It has been suggested that the genes involved in T lymphocyte proliferation have low calcineurin thresholds, whereas genes involved in T lymphocyte apoptosis have high thresholds. In T lymphocytes deficient of *DSCR1*, there is a shift in the calcineurin thresholds required, resulting in less calcineurin activity being necessary for their activation, leading to a faster proliferation, but more premature Fas ligand expression. This suggests that DSCR1, depending on its level of expression, may in fact modulate calcineurin activation rather than simply inhibiting it (Ryeom *et al.*, 2003). This idea is consistent with our PCR results demonstrating that the mRNA expression of many inflammatory cytokines and chemokines were increased in *DSCR1* Tg mice. Further studies into the mechanisms behind the protection in *DSCR1* KO mice are needed, but at present, it appears that *DSCR1*-deficiency may in fact result in reduced calcineurin activity, similar to that found when *DSCR1* is over-expressed.

This study strongly suggests that reduced calcineurin activity, whether through the over-expression of its inhibitor *DSCR1*, or intriguingly, through the deficiency of *DSCR1*, improves outcome after cerebral I-R. However, a large problem with global immunodepression is the increased risk of infection, which even without pharmacological intervention is already the greatest cause of death in the post-acute stages of ischaemic stroke (Heuschmann *et al.*, 2004; Vernino *et al.*, 2003). Importantly, lymphocytes have ~5,000 calcineurin molecules per cell whereas hippocampal neurons and cardiac muscle cells have ~200,000. Thus, it is interesting to speculate that it may be possible to inhibit calcineurin activity selectively in T lymphocytes by administering lower concentrations of calcineurin inhibitors (Crabtree, 1999). If further studies were to discover that *DSCR1* over-expression in T lymphocytes mediates the majority of the protection demonstrated in this study, low concentrations of calcineurin inhibitors could be administered to possibly reduce T lymphocyte-mediated damage without jeopardising the balance of the immune system.

In summary, our study provides the first evidence that *DSCR1* over-expression improves outcome following cerebral I-R. This protection was seen in all endpoints measured, including sensorimotor assessment and cerebral infarct and oedema volume. We speculate that the mechanism behind this protection from stroke comes from the inhibition of calcineurin by DSCR1 expressed in both neurons and T lymphocytes, thus reducing the transcription of some pro-inflammatory and pro-apoptotic cytokines, as well as reducing T lymphocyte infiltration through the lower numbers of circulating T lymphocytes; although further studies need to be undertaken to confirm this. The findings of the present study also suggest that the deficiency of *DSCR1* in mice may also lead to improved outcome following cerebral I-R. More studies are needed to confirm these findings and to understand the mechanisms involved. For now, we speculate that both *DSCR1*-deficiency in neurons and in T lymphocytes may play an important role in protection after stroke.

Chapter 8:

General Discussion

8.1 Summary of major findings

Overall, data presented in this thesis provides insight into the inflammatory processes that occur following focal cerebral ischaemia-reperfusion (I-R). We specifically examined the influence of gender on various mechanisms of inflammation occurring after I-R (Chapters 3 and 4), the role of superoxide generated by $CD3^+$, $CD4^+$ and $CD8^+$ T lymphocytes after I-R (Chapters 4 and 5), and the contributions of the CXCR2 chemokine subfamily (Chapter 6) and calcineurin (Chapter 7) to outcome after I-R. The major findings of this thesis are as follows:

1. a) Female mice have a smaller infarct volume if reperfusion is instituted (i.e. in the I-R protocol) when assessed at either 24 or 72 h after MCAO. By contrast, there is no difference in infarct volume between male and female mice following I-NR. Thus, the smaller infarct volume in females following stroke is strictly reperfusion-dependent.

   b) Male mice deficient in Nox2 have a reduced infarct volume following I-R versus their wild-type controls, which is comparable to the infarct volume in either wild-type or Nox2-deficient female mice. Therefore, the data suggest that Nox2 expression is detrimental for stroke outcome in male mice only, and the larger infarct volume in males following I-R is Nox2-dependent. Interestingly, unlike in wild-type mice, there tended to be a greater infarct volume in female versus male Nox2-deficient mice, suggesting that Nox2 may not have a detrimental role in female mice, but it could even play a beneficial role.

2. a) After I-R, protein expression of Nox2, Cox-2 and VCAM-1 increase in the ischaemic hemisphere of male mice, whereas female mice subjected to I-R do not have an increased expression of these proteins. In male mice there was significant infiltration of Nox2-containing T lymphocytes into the ischaemic hemisphere, whereas female mice had

less infiltration of these cells. This is consistent with a generally lower inflammatory response in female mice, most likely due to the well established anti-inflammatory effects of oestrogen. Within the infarct core, Nox2 protein was found to be solely co-localised with T lymphocytes.

b) Evidence of immunodepression was observed in male and female mice, in terms of immune cell number in the spleen after both I-R and I-NR. The reduced levels of immune cells were found to be statistically significant for $CD3^+$ and $CD4^+$ T lymphocytes and B lymphocytes in male mice after both I-R and I-NR, and for B lymphocytes after I-R in female mice. However, 24 h after I-R is likely to be too early for substantial reductions in circulating leukocyte levels to become evident.

c) Consistent with a developing depression of immune cell function, there tended to be lower levels of T lymphocyte proliferation after I-R in both male and female mice.

d) T lymphocytes generated superoxide under basal conditions, and produced greater amounts when Nox2 activity was stimulated with PDB. Following I-R, T lymphocytes generated markedly enhanced amounts of Nox2-derived superoxide, in both male and female mice. More superoxide was produced by T lymphocytes in male mice after stroke, when compared to female mice. Interestingly, this increase in superoxide generation only occurred in circulating T lymphocytes, and not from T lymphocytes isolated from the spleen of the same animals.

3. A significantly greater amount of Nox2-dependent, T lymphocyte-generated superoxide was produced after stroke by circulating $CD3^+$ and $CD8^+$ T lymphocytes isolated from male mice, when compared to control male mice, and there was also a trend for the same general profile to occur in circulating $CD4^+$ T lymphocytes after stroke. However, these

findings in T lymphocyte subsets are only preliminary and need to be repeated with a purer cell isolation method.

4. a) Chemokine and chemokine-related gene expression, including the potent neutrophil chemoattractant subfamily, CXCR2, CXCL1 and CXCL2, is increased in the ischaemic hemisphere following cerebral I-R, consistent with the concept that an initial pro-inflammatory response occurs in the brain after stroke.

   b) SB 225002, a CXCR2 antagonist, administered at the beginning of reperfusion markedly reduced both mRNA expression of CXCR2, CXCL1 and CXCL2 in the ischaemic hemisphere, and neutrophil infiltration following cerebral I-R, indicating successful antagonism of the receptor. However, this antagonism did not ultimately improve outcome following cerebral I-R, either in infarct volume or functional impairment, consistent with the possibility that neutrophil infiltration does not contribute to I-R injury.

5. a) Mice over-expressing *DSCR1* have improved outcome following cerebral I-R. This was seen in a lower neurological score, longer hanging wire time, and smaller cerebral infarct and oedema volumes. This protection was most likely through the inhibition of calcineurin in neurons, although the reduction in circulating levels of T lymphocytes may also have contributed.

   b) Preliminary data indicate that mice deficient in *DSCR1* also have improved outcome following cerebral I-R. The mechanism(s) underlying this protection is currently unclear.

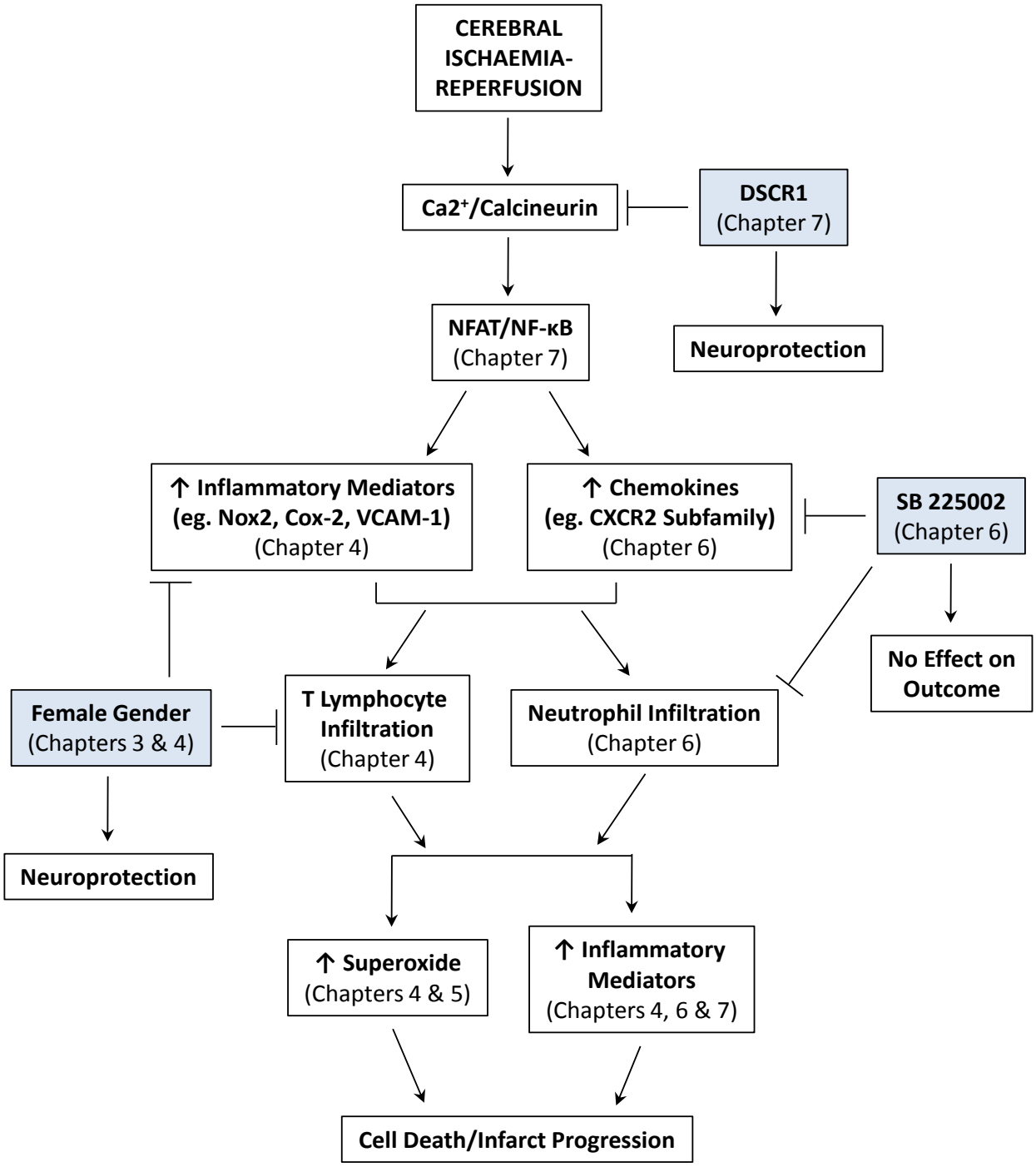

Figure 8.1. Flow chart of the inflammatory mechanisms and therapies tested in this thesis.

The coloured boxes represent protective mechanisms or potential therapies that were addressed in this thesis. NFAT, nuclear factor of activated T cells; NF-κB, nuclear factor-kappa B; Cox-2, cyclo-oxygenase-2; VCAM-1, vascular cell adhesion molecule-1.

8.2 Clinical implications of major findings

8.2.1 Influence of Gender

Our findings from Chapters 3 and 4, suggest that young adult females have a smaller infarct volume and a reduced inflammatory response after cerebral I-R, further reinforcing the concept that post-ischaemic inflammation contributes to ischaemic injury, especially in age-matched males. Reperfusion injury is mainly due to the influx of oxidative and inflammatory mediators, overwhelming already impaired antioxidant enzymes and increasing cytokine and chemokine production, and adhesion and infiltration of immune cells (For review see Schaller and Graf, 2004). Therefore, there may be less reperfusion injury (and thus, more salvaged brain) in pre-menopausal women when administered rt-PA, due to the anti-oxidative and anti-inflammatory effects of oestrogen. It therefore follows, that it may be possible to administer rt-PA at a later time-point (i.e. later than 4.5 h after stroke onset) in pre-menopausal women. However, the vast majority of females experiencing ischaemic strokes are post-menopausal (NHLBI, 2006), and thus no longer have high circulating levels of oestrogen. Therefore they are most likely to undergo similar mechanisms of damage to males, and the advantage of the suppressed inflammatory mechanisms and less reperfusion injury would not be relevant to many individuals experiencing stroke. Indeed, for this reason, the more severe consequences of stroke observed here in young adult males versus females are likely to apply to elderly men and women who suffer stroke. Thus, these findings can also be applied to the use of combination therapies (see section 8.2.3 below).

8.2.2 Role of T lymphocytes in cerebral ischaemia

T lymphocytes were previously shown to contribute to I-R injury (Hurn *et al.*, 2007; Kleinschnitz *et al.*, 2010b; Shichita *et al.*, 2009; Yilmaz *et al.*, 2006), although the exact mechanisms underlying this damage remain unknown. In Chapters 4 and 5, we reported an increase in Nox2-dependent superoxide generation by circulating T lymphocytes after cerebral I-R, and in Chapter 4, found

high levels of superoxide production in T lymphocytes isolated from male versus female mice, which had an association with larger infarct volumes, suggesting that the superoxide generated by circulating T lymphocytes after I-R may play a role in the progression of infarct volume. In light of the recent Kleinschnitz and colleagues study (2010b), which shows that the contribution of T lymphocytes to ischaemic injury does not depend on the activation of the adaptive immune system – i.e. no antigen recognition, nor co-stimulation of T lymphocytes are required for their detrimental effects after stroke – our novel findings, that circulating T lymphocytes generate more superoxide after cerebral I-R, could emerge as one of the main mechanisms by which T lymphocytes mediate post-stroke brain damage, as the generation of superoxide from Nox2-containing NADPH oxidase in T lymphocytes does not rely on T lymphocyte activation. The superoxide production from circulating T lymphocytes may also represent a major part of Nox2-mediated damage after stroke, which was previously reported to contribute to ischaemic injury in male mice (Chen *et al.*, 2009; Jackman *et al.*, 2009a; Kahles *et al.*, 2007; Kunz *et al.*, 2007; Walder *et al.*, 1997).

8.2.3 Potential therapies using anti-inflammatory drugs in combination with rt-PA

It seems that novel stroke therapies will be most realistic if administered together with, rather than instead of, rt-PA. Combination therapies thus represent a promising new concept for ischaemic stroke therapy. As mentioned above, inflammation is well established to contribute to ischaemic injury, as well as reperfusion-associated injury following stroke. Therefore, the administration of an anti-inflammatory drug with rt-PA, would be a valid combination, likely to reduce reperfusion injury, and hence further improve outcome following cerebral I-R. Our findings from Chapters 4 and 5 raise the possibility that the combination of rt-PA and a drug that reduces T lymphocyte infiltration into the brain or the production of superoxide from these cells may be a beneficial therapy. In Chapter 7, we have provided evidence that over-expression of *DSCR1*, an endogenous calcineurin inhibitor, reduces infarct volume, and improves functional

outcome. Intriguingly, *DSCR1* KO mice were also protected following stroke. This was initially surprising, but was actually compatible with other studies that have curiously found that the deficiency of *DSCR1* can reduce calcineurin activity (Vega *et al.*, 2003) or produce a phenotype of reduced calcineurin activity (Kingsbury and Cunningham, 2000; Sanna *et al.*, 2006). This suggests that targeting calcineurin pharmacologically, alongside rt-PA could be beneficial in stroke. Although in Chapter 6, our findings indicated that the successful antagonism of CXCR2 did not ameliorate infarct damage or improve functional outcome, the concept of a combination of anti-chemokine therapies with rt-PA remain a potential therapeutic. Our findings strongly suggest that neutrophils do not contribute to damage in I-R, however, we found that many chemokines and their receptors are increased in the brain after stroke, and some of these attract and activate other leukocytes, such as monocytes and T lymphocytes. Therefore, the administration of antagonists for appropriate key chemokine receptor targets, could possibly successfully reduce the infiltration of these cells, and ultimately reduce reperfusion injury, infarct volume and neurological impairment. However, severe immunodepression and infection are of great concern over the days following stroke, and need to be taken into account when investigating optimally timed and targeted immunomodulatory therapies.

8.3 Limitations of these studies

Outcome in some studies (Chapters 4, 5 and 7) is analysed at 24 h only, although infarcts may not reach their maximum until ~48 h after reperfusion (Kunz *et al.*, 2007; Li *et al.*, 2000). It should be noted however, that data in Chapter 3 indicated that infarct volume did not increase from 24 to 72 h in these studies. Furthermore, Chapters 4 and 5 do not analyse infarct volume, but examine mechanisms that may be activated and ultimately contribute to the cerebral infarct. For that reason, it can be argued that 24 h after I-R is a valid time-point.

The majority of patients that experience an ischaemic stroke are elderly (NHLBI, 2006; Senes, 2006), and also have co-morbidities. The most common is hypertension, but diabetes and cardiac related problems are also common in individuals that experience an ischaemic stroke (Fang and Alderman, 2001; Ostwald *et al.*, 2006; Shuaib *et al.*, 2007). Therefore, experimental stroke studies would be more relevant to the clinical situation if the rodents utilised in the studies were aged, and also had these diseases.

The intraluminal filament model of ischaemic stroke is versatile, as it can mimic I-NR by keeping the filament in place, but also, with the withdrawal of the filament, it can mimic I-R. The withdrawal of the filament however, produces a sudden reperfusion, whereas spontaneous or rt-PA-induced reperfusion is much slower progressing, as the clot is gradually broken down (Hossmann, 2008). In addition, many individuals who experience a stroke and are administered rt-PA, only achieve partial recanalisation (Alexandrov and Grotta, 2002; Alexandrov *et al.*, 2004; Saqqur *et al.*, 2007), which cannot be mimicked using this model. Therefore, potential therapeutics designed to be used in combination with rt-PA, should ideally be tested in animals using the thrombo-embolic model and rt-PA administration, as this best mimics the clinical situation.

Another limitation of the filament model of ischaemic stroke is that it requires the stroke to be induced under general anaesthetic. The anaesthetic utilised in these studies was a mixture of ketamine and xylazine. However, ketamine has been reported to reduce the number of circulating neutrophils, as well as suppress their release of superoxide (Zilberstein *et al.,* 2002). Another commonly used anaesthetic is isofluorane gas, but this has also been shown to have neuroprotective effects, resulting in smaller infarct volumes following ischaemia-reperfusion (Kapinya *et al.,* 2002). For these reasons, as well as the fact that people are generally conscious

when they suffer an ischaemic stroke, a model of ischaemic stroke that allows the induction of stroke to occur while the animal is conscious, such as the endothelin-1 model, would be superior.

8.4 Conclusion

Overall, this thesis presents important findings on the role of inflammation in ischaemic brain injury following cerebral I-R. Collectively, the work suggests that reductions in inflammation in the early stages after the induction of reperfusion, are associated with reduced infarct volume and possibly improved functional outcome. While the majority of neuroprotective drugs have failed in clinical trials, careful therapeutic strategies targeting specific aspects of inflammation in combination with rt-PA administration could prove to be successful.

References:

ABBAS, A. K., MURPHY, K. M. & SHER, A. (1996) Functional diversity of helper T lymphocytes. *Nature,* 383, 787-93.

ABCAM (2009) Chemokines and their receptors. Viewed 4 August 2010, <http://docs.abcam.com/pdf/immunology/chemokines_poster.pdf>

ABRAMOV, A. Y., JACOBSON, J., WIENTJES, F., HOTHERSALL, J., CANEVARI, L. & DUCHEN, M. R. (2005) Expression and Modulation of an NADPH Oxidase in Mammalian Astrocytes. *J. Neurosci.,* 25, 9176-9184.

AKOPOV, S. E., SIMONIAN, N. A. & GRIGORIAN, G. S. (1996) Dynamics of Polymorphonuclear Leukocyte Accumulation in Acute Cerebral Infarction and Their Correlation With Brain Tissue Damage. *Stroke,* 27, 1739-1743.

ALEXANDROV, A. V. & GROTTA, J. C. (2002) Arterial reocclusion in stroke patients treated with intravenous tissue plasminogen activator. *Neurology,* 59, 862-7.

ALEXANDROV, A. V., MOLINA, C. A., GROTTA, J. C., GARAMI, Z., FORD, S. R., ALVAREZ-SABIN, J., MONTANER, J., SAQQUR, M., DEMCHUK, A. M., MOYE, L. A., HILL, M. D. & WOJNER, A. W. (2004) Ultrasound-enhanced systemic thrombolysis for acute ischemic stroke. *N Engl J Med,* 351, 2170-8.

ALKAYED, N. J., HARUKUNI, I., KIMES, A. S., LONDON, E. D., TRAYSTMAN, R. J. & HURN, P. D. (1998) Gender-linked brain injury in experimental stroke. *Stroke,* 29, 159-65; discussion 166.

ALZUHERRI, H. & CHANG, K. C. (2003) Calcineurin activates NF-kappaB in skeletal muscle C2C12 cells. *Cell Signal,* 15, 471-8.

AMANTEA, D., NAPPI, G., BERNARDI, G., BAGETTA, G. & CORASANITI, M. T. (2009) Post-ischemic brain damage: pathophysiology and role of inflammatory mediators. *FEBS J,* 276, 13-26.

ANKARCRONA, M., DYPBUKT, J. M., BONFOCO, E., ZHIVOTOVSKY, B., ORRENIUS, S., LIPTON, S. A. & NICOTERA, P. (1995) Glutamate-induced neuronal death: a succession of necrosis or apoptosis depending on mitochondrial function. *Neuron,* 15, 961-73.

ARMSTRONG, D. A., MAJOR, J. A., CHUDYK, A. & HAMILTON, T. A. (2004) Neutrophil chemoattractant genes KC and MIP-2 are expressed in different cell populations at sites of surgical injury. *J Leukoc Biol,* 75, 641-648.

ARONOWSKI, J., STRONG, R. & GROTTA, J. C. (1997) Reperfusion Injury: Demonstration of Brain Damage Produced by Reperfusion After Transient Focal Ischemia in Rats. *J Cereb Blood Flow Metab,* 17, 1048-1056.

ARRON, J. R., WINSLOW, M. M., POLLERI, A., CHANG, C. P., WU, H., GAO, X., NEILSON, J. R., CHEN, L., HEIT, J. J., KIM, S. K., YAMASAKI, N., MIYAKAWA,

T., FRANCKE, U., GRAEF, I. A. & CRABTREE, G. R. (2006) NFAT dysregulation by increased dosage of DSCR1 and DYRK1A on chromosome 21. *Nature,* 441, 595-600.

ARUMUGAM, T. V., GRANGER, D. N. & MATTSON, M. P. (2005) Stroke and T-cells. *Neuromolecular Med,* 7, 229-42.

ARUMUGAM, T. V., SALTER, J. W., CHIDLOW, J. H., BALLANTYNE, C. M., KEVIL, C. G. & GRANGER, D. N. (2004) Contributions of LFA-1 and Mac-1 to brain injury and microvascular dysfunction induced by transient middle cerebral artery occlusion. *Am J Physiol Heart Circ Physiol,* 287, H2555-60.

ASAHI, M., ASAHI, K., JUNG, J.-C., DEL ZOPPO, G. J., FINI, E. M. & LO, E. H. (2000) Role for Matrix Metalloproteinase 9 After Focal Cerebral Ischemia: Effects of Gene Knockout and Enzyme Inhibition With BB-94. *Journal of Cerebral Blood Flow and Metabolism,* 20, 1681.

ASAI, A., QIU, J., NARITA, Y., CHI, S., SAITO, N., SHINOURA, N., HAMADA, H., KUCHINO, Y. & KIRINO, T. (1999) High level calcineurin activity predisposes neuronal cells to apoptosis. *J Biol Chem,* 274, 34450-8.

AUSTRALIAN INSTITUTE OF HEALTH AND WELFARE (AIHW). (2006) *Australia's Health 2006*.

AYATA, C. & ROPPER, A. H. (2002) Ischaemic brain oedema. *J Clin Neurosci,* 9, 113-24.

BACK, T., GINSBERG, M. D., DIETRICH, W. D. & WATSON, B. D. (1996) Induction of spreading depression in the ischemic hemisphere following experimental middle cerebral artery occlusion: effect on infarct morphology. *J Cereb Blood Flow Metab,* 16, 202-13.

BACK, T., KOHNO, K. & HOSSMANN, K. A. (1994) Cortical negative DC deflections following middle cerebral artery occlusion and KCl-induced spreading depression: effect on blood flow, tissue oxygenation, and electroencephalogram. *J Cereb Blood Flow Metab,* 14, 12-9.

BARBER, P. A., DAVIS, S. M., INFELD, B., BAIRD, A. E., DONNAN, G. A., JOLLEY, D. & LICHTENSTEIN, M. (1998) Spontaneous reperfusion after ischemic stroke is associated with improved outcome. *Stroke,* 29, 2522-8.

BARBER, P. A., ZHANG, J., DEMCHUK, A. M., HILL, M. D. & BUCHAN, A. M. (2001) Why are stroke patients excluded from TPA therapy? An analysis of patient eligibility. *Neurology,* 56, 1015-20.

BARDUTZKY, J., MENG, X., BOULEY, J., DUONG, T. Q., RATAN, R. & FISHER, M. (2005) Effects of intravenous dimethyl sulfoxide on ischemia evolution in a rat permanent occlusion model. *J Cereb Blood Flow Metab,* 25, 968-77.

BARON, J. L., MADRI, J. A., RUDDLE, N. H., HASHIM, G. & JANEWAY, C. A., JR. (1993) Surface expression of alpha 4 integrin by CD4 T cells is required for their entry into brain parenchyma. *J Exp Med,* 177, 57-68.

BARONE, F. C., ARVIN, B., WHITE, R. F., MILLER, A., WEBB, C. L., WILLETTE, R. N., LYSKO, P. G. & FEUERSTEIN, G. Z. (1997) Tumor necrosis factor-alpha. A mediator of focal ischemic brain injury. *Stroke,* 28, 1233-44.

BARRY, M. & BLEACKLEY, R. C. (2002) Cytotoxic T lymphocytes: all roads lead to death. *Nat Rev Immunol,* 2, 401-9.

BATMANIAN, J. J., LAM, M., MATTHEWS, C., FINCKH, A., DUFFY, M., WRIGHT, R., BREW, B. J. & MARKUS, R. (2007) A protocol-driven model for the rapid initiation of stroke thrombolysis in the emergency department. *Med J Aust,* 187, 567-70.

BEDERSON, J., PITTS, L., TSUJI, M., NISHIMURA, M., DAVIS, R. & BARTKOWSKI, H. (1986) Rat middle cerebral artery occlusion: evaluation of the model and development of a neurologic examination. *Stroke,* 17, 472-476.

BEHL, C., SKUTELLA, T., LEZOUALC'H, F., POST, A., WIDMANN, M., NEWTON, C. J. & HOLSBOER, F. (1997) Neuroprotection against oxidative stress by estrogens: structure-activity relationship. *Mol Pharmacol,* 51, 535-41.

BENTO, A. F., LEITE, D. F., CLAUDINO, R. F., HARA, D. B., LEAL, P. C. & CALIXTO, J. B. (2008) The selective nonpeptide CXCR2 antagonist SB225002 ameliorates acute experimental colitis in mice. *J Leukoc Biol,* 84, 1213-21.

BERAY-BERTHAT, V., PALMIER, B., PLOTKINE, M. & MARGAILL, I. (2003) Neutrophils do not contribute to infarction, oxidative stress, and NO synthase activity in severe brain ischemia. *Exp Neurol,* 182, 446-54.

BERTINI, R., ALLEGRETTI, M., BIZZARRI, C., MORICONI, A., LOCATI, M., ZAMPELLA, G., CERVELLERA, M. N., DI CIOCCIO, V., CESTA, M. C., GALLIERA, E., MARTINEZ, F. O., DI BITONDO, R., TROIANI, G., SABBATINI, V., D'ANNIBALLE, G., ANACARDIO, R., CUTRIN, J. C., CAVALIERI, B., MAINIERO, F., STRIPPOLI, R., VILLA, P., DI GIROLAMO, M., MARTIN, F., GENTILE, M., SANTONI, A., CORDA, D., POLI, G., MANTOVANI, A., GHEZZI, P. & COLOTTA, F. (2004) Noncompetitive allosteric inhibitors of the inflammatory chemokine receptors CXCR1 and CXCR2: prevention of reperfusion injury. *Proc Natl Acad Sci U S A,* 101, 11791-6.

BIZZARRI, C., BECCARI, A. R., BERTINI, R., CAVICCHIA, M. R., GIORGINI, S. & ALLEGRETTI, M. (2006) ELR+ CXC chemokines and their receptors (CXC chemokine receptor 1 and CXC chemokine receptor 2) as new therapeutic targets. *Pharmacol Ther,* 112, 139-49.

BLOUGH, N. V. & ZAFIRIOU, O. C. (1985) Reaction of superoxide with nitric oxide to form peroxonitrite in alkaline aqueous solution. *Inorg Chem,* 24, 3502–3504.

BOCHELEN, D., RUDIN, M. & SAUTER, A. (1999) Calcineurin Inhibitors FK506 and SDZ ASM 981 Alleviate the Outcome of Focal Cerebral Ischemic/Reperfusion Injury. *J Pharmacol Exp Ther,* 288, 653-659.

BOGOUSSLAVSKY, J., VAN MELLE, G. & REGLI, F. (1988) The Lausanne Stroke Registry: analysis of 1,000 consecutive patients with first stroke. *Stroke,* 19, 1083-1092.

BOND, B. C., VIRLEY, D. J., CAIRNS, N. J., HUNTER, A. J., MOORE, G. B. T., MOSS, S. J., MUDGE, A. W., WALSH, F. S., JAZIN, E. & PREECE, P. (2002) The quantification of gene expression in an animal model of brain ischaemia using TaqMan(TM) real-time RT-PCR. *Molecular Brain Research,* 106, 101-116.

BONFOCO, E., KRAINC, D., ANKARCRONA, M., NICOTERA, P. & LIPTON, S. A. (1995) Apoptosis and necrosis: two distinct events induced, respectively, by mild and intense insults with N-methyl-D-aspartate or nitric oxide/superoxide in cortical cell cultures. *Proc Natl Acad Sci U S A,* 92, 7162-6.

BOUTIN, H., LEFEUVRE, R. A., HORAI, R., ASANO, M., IWAKURA, Y. & ROTHWELL, N. J. (2001) Role of IL-1{alpha} and IL-1{beta} in Ischemic Brain Damage. *J. Neurosci.,* 21, 5528-5534.

BOWES, M. P., ROTHLEIN, R., FAGAN, S. C. & ZIVIN, J. A. (1995) Monoclonal antibodies preventing leukocyte activation reduce experimental neurologic injury and enhance efficacy of thrombolytic therapy. *Neurology,* 45, 815-9.

BOWLER, J. V., WADE, J. P., JONES, B. E., NIJRAN, K. S. & STEINER, T. J. (1998) Natural history of the spontaneous reperfusion of human cerebral infarcts as assessed by 99mTc HMPAO SPECT. *J Neurol Neurosurg Psychiatry,* 64, 90-7.

BROUGHTON, B. R., REUTENS, D. C. & SOBEY, C. G. (2009) Apoptotic mechanisms after cerebral ischemia. *Stroke,* 40, e331-9.

BUSCH, E., GYNGELL, M. L., EIS, M., HOEHN-BERLAGE, M. & HOSSMANN, K. A. (1996) Potassium-induced cortical spreading depressions during focal cerebral ischemia in rats: contribution to lesion growth assessed by diffusion-weighted NMR and biochemical imaging. *J Cereb Blood Flow Metab,* 16, 1090-9.

BUTTINI, M., SAUTER, A. & BODDEKE, H. W. (1994) Induction of interleukin-1 beta mRNA after focal cerebral ischaemia in the rat. *Brain Res Mol Brain Res,* 23, 126-34.

CAI, H., YAO, H., IBAYASHI, S., UCHIMURA, H. & FUJISHIMA, M. (1998) Photothrombotic middle cerebral artery occlusion in spontaneously hypertensive rats: influence of substrain, gender, and distal middle cerebral artery patterns on infarct size. *Stroke,* 29, 1982-6; discussion 1986-7.

CALL, D. R., NEMZEK, J. A., EBONG, S. J., BOLGOS, G. R., NEWCOMB, D. E., WOLLENBERG, G. K. & REMICK, D. G. (2001) Differential local and systemic regulation of the murine chemokines KC and MIP2. *Shock,* 15, 278-84.

CAMPANELLA, M., SCIORATI, C., TAROZZO, G. & BELTRAMO, M. (2002) Flow cytometric analysis of inflammatory cells in ischemic rat brain. *Stroke,* 33, 586-92.

CARDONA, A. E., SASSE, M. E., LIU, L., CARDONA, S. M., MIZUTANI, M., SAVARIN, C., HU, T. & RANSOHOFF, R. M. (2008) Scavenging roles of chemokine receptors: chemokine receptor deficiency is associated with increased levels of ligand in circulation and tissues. *Blood,* 112, 256-63.

CARSWELL, H. V., ANDERSON, N. H., CLARK, J. S., GRAHAM, D., JEFFS, B., DOMINICZAK, A. F. & MACRAE, I. M. (1999) Genetic and gender influences on sensitivity to focal cerebral ischemia in the stroke-prone spontaneously hypertensive rat. *Hypertension,* 33, 681-5.

CASILLI, F., BIANCHINI, A., GLOAGUEN, I., BIORDI, L., ALESSE, E., FESTUCCIA, C., CAVALIERI, B., STRIPPOLI, R., CERVELLERA, M. N., DI BITONDO, R., FERRETTI, E., MAINIERO, F., BIZZARRI, C., COLOTTA, F. & BERTINI, R. (2005) Inhibition of interleukin-8 (CXCL8/IL-8) responses by repertaxin, a new inhibitor of the chemokine receptors CXCR1 and CXCR2. *Biochem Pharmacol,* 69, 385-94.

CASTILLO, J., DAVALOS, A. & NOYA, M. (1997) Progression of ischaemic stroke and excitotoxic aminoacids. *Lancet,* 349, 79-83.

CHAMORRO, A., AMARO, S., VARGAS, M., OBACH, V., CERVERA, A., GOMEZ-CHOCO, M., TORRES, F. & PLANAS, A. M. (2007) Catecholamines, infection, and death in acute ischemic stroke. *J Neurol Sci,* 252, 29-35.

CHAN, P. H. (2001) Reactive oxygen radicals in signaling and damage in the ischemic brain. *J Cereb Blood Flow Metab,* 21, 2-14.

CHAPMAN, K. Z., DALE, V. Q., DENES, A., BENNETT, G., ROTHWELL, N. J., ALLAN, S. M. & MCCOLL, B. W. (2009) A rapid and transient peripheral inflammatory response precedes brain inflammation after experimental stroke. *J Cereb Blood Flow Metab,* 29, 1764-8.

CHEN, H., SONG, Y. S. & CHAN, P. H. (2009) Inhibition of NADPH oxidase is neuroprotective after ischemia-reperfusion. *J Cereb Blood Flow Metab,* 29, 1262-72.

CHEN, Y., HALLENBECK, J. M., RUETZLER, C., BOL, D., THOMAS, K., BERMAN, N. E. & VOGEL, S. N. (2003) Overexpression of monocyte chemoattractant protein 1 in the brain exacerbates ischemic brain injury and is associated with recruitment of inflammatory cells. *J Cereb Blood Flow Metab,* 23, 748-55.

CHEN, Z. L. & STRICKLAND, S. (1997) Neuronal death in the hippocampus is promoted by plasmin-catalyzed degradation of laminin. *Cell,* 91, 917-25.

CHENG, Y. D., AL-KHOURY, L. & ZIVIN, J. A. (2004) Neuroprotection for ischemic stroke: two decades of success and failure. *NeuroRx,* 1, 36-45.

CHERANOV, S. Y. & JAGGAR, J. H. (2006) TNF-alpha dilates cerebral arteries via NAD(P)H oxidase-dependent Ca2+ spark activation. *Am J Physiol Cell Physiol,* 290, C964-71.

CHERET, C., GERVAIS, A., LELLI, A., COLIN, C., AMAR, L., RAVASSARD, P., MALLET, J., CUMANO, A., KRAUSE, K.-H. & MALLAT, M. (2008) Neurotoxic Activation of Microglia Is Promoted by a Nox1-Dependent NADPH Oxidase. *J. Neurosci.,* 28, 12039-12051.

CHO, K. O., KIM, Y. S., CHO, Y. J. & KIM, S. Y. (2008) Upregulation of DSCR1 (RCAN1 or Adapt78) in the peri-infarct cortex after experimental stroke. *Exp Neurol,* 212, 85-92.

CHOW, N., BELL, R. D., DEANE, R., STREB, J. W., CHEN, J., BROOKS, A., VAN NOSTRAND, W., MIANO, J. M. & ZLOKOVIC, B. V. (2007) Serum response factor and myocardin mediate arterial hypercontractility and cerebral blood flow dysregulation in Alzheimer's phenotype. *Proc Natl Acad Sci U S A,* 104, 823-8.

CONNOLLY, E. S., JR., WINFREE, C. J., SPRINGER, T. A., NAKA, Y., LIAO, H., YAN, S. D., STERN, D. M., SOLOMON, R. A., GUTIERREZ-RAMOS, J. C. & PINSKY, D. J. (1996) Cerebral protection in homozygous null ICAM-1 mice after middle cerebral artery occlusion. Role of neutrophil adhesion in the pathogenesis of stroke. *J Clin Invest,* 97, 209-16.

COOK, C. N., HEJNA, M. J., MAGNUSON, D. J. & LEE, J. M. (2005) Expression of calcipressin1, an inhibitor of the phosphatase calcineurin, is altered with aging and Alzheimer's disease. *J Alzheimers Dis,* 8, 63-73.

COYOY, A., VALENCIA, A., GUEMEZ-GAMBOA, A. & MORÁN, J. (2008) Role of NADPH oxidase in the apoptotic death of cultured cerebellar granule neurons. *Free Radical Biology and Medicine,* 45, 1056-1064.

CRABTREE, G. R. (1999) Generic signals and specific outcomes: signaling through Ca2+, calcineurin, and NF-AT. *Cell,* 96, 611-4.

CRACK, P. J. & TAYLOR, J. M. (2005) Reactive oxygen species and the modulation of stroke. *Free Radic Biol Med,* 38, 1433-44.

CRACK, P. J., TAYLOR, J. M., FLENTJAR, N. J., DE HAAN, J., HERTZOG, P., IANNELLO, R. C. & KOLA, I. (2001) Increased infarct size and exacerbated apoptosis in the glutathione peroxidase-1 (Gpx-1) knockout mouse brain in response to ischemia/reperfusion injury. *Journal of Neurochemistry,* 78, 1389-1399.

CRAWFORD, D. R., LEAHY, K. P., ABRAMOVA, N., LAN, L., WANG, Y. & DAVIES, K. J. A. (1997) Hamster adapt78 mRNA Is a Down Syndrome Critical Region Homologue That Is Inducible by Oxidative Stress. *Archives of Biochemistry and Biophysics,* 342, 6-12.

CUI, K., LUO, X., XU, K. & VEN MURTHY, M. R. (2004) Role of oxidative stress in neurodegeneration: recent developments in assay methods for oxidative stress and nutraceutical antioxidants. *Progress in Neuro-Psychopharmacology and Biological Psychiatry,* 28, 771-799.

CZLONKOWSKA, A., CYRTA, B. & KORLAK, J. (1979) Immunological observations on patients with acute cerebral vascular disease. *J Neurol Sci,* 43, 455-64.

DAI, X., CAO, X. & KREULEN, D. L. (2006) Superoxide anion is elevated in sympathetic neurons in DOCA-salt hypertension via activation of NADPH oxidase. *Am J Physiol Heart Circ Physiol,* 290, H1019-1026.

DAIBER, A., AUGUST, M., BALDUS, S., WENDT, M., OELZE, M., SYDOW, K., KLESCHYOV, A. L. & MUNZEL, T. (2004) Measurement of NAD(P)H oxidase-derived superoxide with the luminol analogue L-012. *Free Radic Biol Med,* 36, 101-11.

DAVALOS, A., CASTILLO, J., SERENA, J. & NOYA, M. (1997) Duration of glutamate release after acute ischemic stroke. *Stroke,* 28, 708-10.

DAVIS, S. M., HAND, P. J. & DONNAN, G. A. (2007) Tissue plasminogen activator for ischaemic stroke: highly effective, reasonably safe and grossly underused. *Med J Aust,* 187, 548-9.

DE KEULENAER, G. W., ALEXANDER, R. W., USHIO-FUKAI, M., ISHIZAKA, N. & GRIENDLING, K. K. (1998) Tumour necrosis factor alpha activates a p22phox-based NADH oxidase in vascular smooth muscle. *Biochem J,* 329 (Pt 3), 653-7.

DEL ZOPPO, G. J., SAVER, J. L., JAUCH, E. C. & ADAMS JR, H. P. ON BEHALF OF THE AMERICAN HEART ASSOCIATION STROKE COUNCIL. (2009) Expansion of the time window for treatment of acute ischemic stroke with intravenous tissue plasminogen activator. *Stroke,* 40, 2945-48.

DEL ZOPPO, G. J., SCHMID-SCHONBEIN, G. W., MORI, E., COPELAND, B. R. & CHANG, C. M. (1991) Polymorphonuclear leukocytes occlude capillaries following middle cerebral artery occlusion and reperfusion in baboons. *Stroke,* 22, 1276-83.

DERESKI, M. O., CHOPP, M., KNIGHT, R. A., RODOLOSI, L. C. & GARCIA, J. H. (1993) The heterogeneous temporal evolution of focal ischemic neuronal damage in the rat. *Acta Neuropathol,* 85, 327-33.

DI CIOCCIO, V., STRIPPOLI, R., BIZZARRI, C., TROIANI, G., CERVELLERA, M. N., GLOAGUEN, I., COLAGRANDE, A., CATTOZZO, E. M., PAGLIEI, S., SANTONI, A., COLOTTA, F., MAINIERO, F. & BERTINI, R. (2004) Key role of proline-rich tyrosine kinase 2 in interleukin-8 (CXCL8/IL-8)-mediated human neutrophil chemotaxis. *Immunology,* 111, 407-15.

DIRNAGL, U. (2009) Experimental Design to Publication Course Material. *XXIVth International Symposium on Cerebral Blood Flow, Metabolism and Function.* Chicago.

DIRNAGL, U., IADECOLA, C. & MOSKOWITZ, M. A. (1999) Pathobiology of ischaemic stroke: an integrated view. *Trends Neurosci,* 22, 391-7.

DOHMEN, C., SAKOWITZ, O. W., FABRICIUS, M., BOSCHE, B., REITHMEIER, T., ERNESTUS, R. I., BRINKER, G., DREIER, J. P., WOITZIK, J., STRONG, A. J. & GRAF, R. (2008) Spreading depolarizations occur in human ischemic stroke with high incidence. *Annals of Neurology,* 63, 720-728.

DUCKLES, S. P. & KRAUSE, D. N. (2007) Cerebrovascular effects of oestrogen: multiplicity of action. *Clin Exp Pharmacol Physiol,* 34, 801-8.

DURUKAN, A., STRBIAN, D. & TATLISUMAK, T. (2008) Rodent models of ischemic stroke: a useful tool for stroke drug development. *Curr Pharm Des,* 14, 359-70.

DURUKAN, A. & TATLISUMAK, T. (2007) Acute ischemic stroke: overview of major experimental rodent models, pathophysiology, and therapy of focal cerebral ischemia. *Pharmacol Biochem Behav,* 87, 179-97.

EAKER, E. D., CHESEBRO, J. H., SACKS, F. M., WENGER, N. K., WHISNANT, J. P. & WINSTON, M. (1993) Cardiovascular disease in women. *Circulation,* 88, 1999-2009.

ELS, T., ROTHER, J., BEAULIEU, C., DE CRESPIGNY, A. & MOSELEY, M. (1997) Hyperglycemia delays terminal depolarization and enhances repolarization after peri-infarct spreading depression as measured by serial diffusion MR mapping. *J Cereb Blood Flow Metab,* 17, 591-5.

EMERICH, D. F., DEAN, R. L., 3RD & BARTUS, R. T. (2002) The role of leukocytes following cerebral ischemia: pathogenic variable or bystander reaction to emerging infarct? *Exp Neurol,* 173, 168-81.

ENGELHARDT, B., CONLEY, F. K., KILSHAW, P. J. & BUTCHER, E. C. (1995) Lymphocytes infiltrating the CNS during inflammation display a distinctive phenotype and bind to VCAM-1 but not to MAdCAM-1. *Int Immunol,* 7, 481-91.

ENGELHARDT, B. & RANSOHOFF, R. M. (2005) The ins and outs of T-lymphocyte trafficking to the CNS: anatomical sites and molecular mechanisms. *Trends Immunol,* 26, 485-95.

ERMAK, G., HARRIS, C. D. & DAVIES, K. J. (2002) The DSCR1 (Adapt78) isoform 1 protein calcipressin 1 inhibits calcineurin and protects against acute calcium-mediated stress damage, including transient oxidative stress. *FASEB J,* 16, 814-24.

ERMAK, G., MORGAN, T. E. & DAVIES, K. J. (2001) Chronic overexpression of the calcineurin inhibitory gene DSCR1 (Adapt78) is associated with Alzheimer's disease. *J Biol Chem,* 276, 38787-94.

FAN, X., PATERA, A. C., PONG-KENNEDY, A., DENO, G., GONSIOREK, W., MANFRA, D. J., VASSILEVA, G., ZENG, M., JACKSON, C., SULLIVAN, L., SHARIF-RODRIGUEZ, W., OPDENAKKER, G., VAN DAMME, J., HEDRICK, J. A., LUNDELL, D., LIRA, S. A. & HIPKIN, R. W. (2007) Murine CXCR1 is a functional receptor for GCP-2/CXCL6 and interleukin-8/CXCL8. *J Biol Chem,* 282, 11658-66.

FANG, J. & ALDERMAN, M. H. (2001) Trend of stroke hospitalization, United States, 1988-1997. *Stroke,* 32, 2221-6.

FENIGER-BARISH, R., RAN, M., ZASLAVER, A. & BEN-BARUCH, A. (1999) Differential modes of regulation of cxc chemokine-induced internalization and recycling of human CXCR1 and CXCR2. *Cytokine,* 11, 996-1009.

FIESCHI, C., ARGENTINO, C., LENZI, G. L., SACCHETTI, M. L., TONI, D. & BOZZAO, L. (1989) Clinical and instrumental evaluation of patients with ischemic stroke within the first six hours. *J Neurol Sci,* 91, 311-21.

FRANTZ, B., NORDBY, E. C., BREN, G., STEFFAN, N., PAYA, C. V., KINCAID, R. L., TOCCI, M. J., O'KEEFE, S. J. & O'NEILL, E. A. (1994) Calcineurin acts in synergy with PMA to inactivate I kappa B/MAD3, an inhibitor of NF-kappa B. *EMBO J,* 13, 861-70.

FUENTES, J.-J., PRITCHARD, M. A., PLANAS, A. M., BOSCH, A., FERRER, I. & ESTIVILL, X. (1995) A new human gene from the Down syndrome critical region encodes a proline-rich protein highly expressed in fetal brain and heart. *Hum. Mol. Genet.,* 4, 1935-1944.

FUENTES, J. J., GENESCA, L., KINGSBURY, T. J., CUNNINGHAM, K. W., PEREZ-RIBA, M., ESTIVILL, X. & LUNA, S. D. L. (2000) DSCR1, overexpressed in Down syndrome, is an inhibitor of calcineurin-mediated signaling pathways. *Hum. Mol. Genet.,* 9, 1681-1690.

FUENTES, J. J., PRITCHARD, M. A. & ESTIVILL, X. (1997) Genomic organization, alternative splicing, and expression patterns of the DSCR1 (Down syndrome candidate region 1) gene. *Genomics,* 44, 358-61.

FURUKAWA, K., FU, W., LI, Y., WITKE, W., KWIATKOWSKI, D. J. & MATTSON, M. P. (1997) The Actin-Severing Protein Gelsolin Modulates Calcium Channel and NMDA Receptor Activities and Vulnerability to Excitotoxicity in Hippocampal Neurons. *J. Neurosci.,* 17, 8178-8186.

GABRIEL, C., JUSTICIA, C., CAMINS, A. & PLANAS, A. M. (1999) Activation of nuclear factor-kappaB in the rat brain after transient focal ischemia. *Brain Res Mol Brain Res,* 65, 61-9.

GARAU, A., BERTINI, R., COLOTTA, F., CASILLI, F., BIGINI, P., CAGNOTTO, A., MENNINI, T., GHEZZI, P. & VILLA, P. (2005) Neuroprotection with the CXCL8 inhibitor repertaxin in transient brain ischemia. *Cytokine,* 30, 125-31.

GARAU, A., BERTINI, R., MOSCA, M., BIZZARRI, C., ANACARDIO, R., TRIULZI, S., ALLEGRETTI, M., GHEZZI, P. & VILLA, P. (2006) Development of a systemically-active dual CXCR1/CXCR2 allosteric inhibitor and its efficacy in a model of transient cerebral ischemia in the rat. *Eur Cytokine Netw,* 17, 35-41.

GARCIA, J., LIU, K. & RELTON, J. (1995) Interleukin-1 receptor antagonist decreases the number of necrotic neurons in rats with middle cerebral artery occlusion. *Am J Pathol,* 147, 1477-1486.

GARGANO, J. W. & REEVES, M. J. (2007) Sex differences in stroke recovery and stroke-specific quality of life: results from a statewide stroke registry. *Stroke,* 38, 2541-8.

GELDERBLOM, M., LEYPOLDT, F., STEINBACH, K., BEHRENS, D., CHOE, C. U., SILER, D. A., ARUMUGAM, T. V., ORTHEY, E., GERLOFF, C., TOLOSA, E. & MAGNUS, T. (2009) Temporal and Spatial Dynamics of Cerebral Immune Cell Accumulation in Stroke. *Stroke,* 40, 1849-1857.

GENDRON, A., TEITELBAUM, J., COSSETTE, C., NUARA, S., DUMONT, M., GEADAH, D., DU SOUICH, P. & KOUASSI, E. (2002) Temporal effects of left versus right middle cerebral artery occlusion on spleen lymphocyte subsets and mitogenic response in Wistar rats. *Brain Res,* 955, 85-97.

GERARD, C. & ROLLINS, B. J. (2001) Chemokines and disease. *Nat Immunol,* 2, 108-15.

GIBOT, S., MASSIN, F., ALAUZET, C., MONTEMONT, C., LOZNIEWSKI, A., BOLLAERT, P. E. & LEVY, B. (2008) Effects of the TREM-1 pathway modulation during mesenteric ischemia-reperfusion in rats. *Crit Care Med,* 36, 504-10.

GINSBERG, M. D. (1997) The new language of cerebral ischemia. *AJNR Am J Neuroradiol,* 18, 1435-45.

GINSBERG, M. D. (2008) Neuroprotection for ischemic stroke: past, present and future. *Neuropharmacology,* 55, 363-89.

GINSBERG, M. D. (2009) Current status of neuroprotection for cerebral ischemia: synoptic overview. *Stroke,* 40, S111-4.

GIROUARD, H., WANG, G., GALLO, E. F., ANRATHER, J., ZHOU, P., PICKEL, V. M. & IADECOLA, C. (2009) NMDA Receptor Activation Increases Free Radical Production through Nitric Oxide and NOX2. *J. Neurosci.,* 29, 2545-2552.

GLADSTONE, D. J., BLACK, S. E. & HAKIM, A. M. (2002) Toward wisdom from failure: lessons from neuroprotective stroke trials and new therapeutic directions. *Stroke,* 33, 2123-36.

GLIMCHER, L. H. & MURPHY, K. M. (2000) Lineage commitment in the immune system: the T helper lymphocyte grows up. *Genes Dev,* 14, 1693-711.

GOLDIN, S. M., SUBBARAO, K., SHARMA, R., KNAPP, A. G., FISCHER, J. B., DALY, D., DURANT, G. J., REDDY, N. L., HU, L. Y., MAGAR, S., PERLMAN, M. E., CHEN, J., GRAHAM, S. H., HOLT, W. F., BERLOVE, D. & MARGOLIN, L. D. (1995) Neuroprotective use-dependent blockers of Na+ and Ca2+ channels controlling presynaptic release of glutamate. *Ann N Y Acad Sci,* 765, 210-29.

GONG, C., QIN, Z., BETZ, A. L., LIU, X. H. & YANG, G. Y. (1998) Cellular localization of tumor necrosis factor alpha following focal cerebral ischemia in mice. *Brain Res,* 801, 1-8.

GOTO, S., MATSUKADO, Y., MIYAMOTO, E. & YAMADA, M. (1987) Morphological characterization of the rat striatal neurons expressing calcineurin immunoreactivity. *Neuroscience,* 22, 189-201.

GRAF, R., SAITO, K., HÜBEL, T., FUJITA, T., ROSNER, G. & HEISS, W.-D. (1995) Spreading depression-like DC-negativations turn into terminal depolarization after prolonged focal ischemia in cats. *J Cereb Blood Flow Metab,* 15 (Suppl 1), S15.

GREEN, S. P., CAIRNS, B., RAE, J., ERRETT-BARONCINI, C., HONGO, J. A., ERICKSON, R. W. & CURNUTTE, J. T. (2001) Induction of gp91-phox, a component of the phagocyte NADPH oxidase, in microglial cells during central nervous system inflammation. *J Cereb Blood Flow Metab,* 21, 374-84.

GRIENDLING, K., MINIERI, C., OLLERENSHAW, J. & ALEXANDER, R. (1994a) Angiotensin II stimulates NADH and NADPH oxidase activity in cultured vascular smooth muscle cells. *Circ Res,* 74, 1141-1148.

GRIENDLING, K. K., MINIERI, C. A., OLLERENSHAW, J. D. & ALEXANDER, R. W. (1994b) Angiotensin II stimulates NADH and NADPH oxidase activity in cultured vascular smooth muscle cells. *Circ Res,* 74, 1141-8.

GRIENDLING, K. K., SORESCU, D. & USHIO-FUKAI, M. (2000) NAD(P)H Oxidase : Role in Cardiovascular Biology and Disease. *Circ Res,* 86, 494-501.

GUZIK, T. J., HOCH, N. E., BROWN, K. A., MCCANN, L. A., RAHMAN, A., DIKALOV, S., GORONZY, J., WEYAND, C. & HARRISON, D. G. (2007) Role of the T cell in the genesis of angiotensin II induced hypertension and vascular dysfunction. *J Exp Med,* 204, 2449-60.

HAAS, E., MEYER, M. R., SCHURR, U., BHATTACHARYA, I., MINOTTI, R., NGUYEN, H. H., HEIGL, A., LACHAT, M., GENONI, M. & BARTON, M. (2007) Differential Effects of 17{beta}-Estradiol on Function and Expression of Estrogen Receptor {alpha}, Estrogen Receptor {beta}, and GPR30 in Arteries and Veins of Patients With Atherosclerosis. *Hypertension,* 49, 1358-1363.

HACKE, W., KASTE, M., BLUHMKI, E., BROZMAN, M., DAVALOS, A., GUIDETTI, D., LARRUE, V., LEES, K. R., MEDEGHRI, Z., MACHNIG, T., SCHNEIDER, D., VON KUMMER, R., WAHLGREN, N. & TONI, D. FOR THE ECASS INVESTIGATORS. (2008). Thrombolysis with alteplase 3 to 4.5 hours after actue ischemic stroke. *N Engl J Med,* 359, 1317-29.

HACKE, W., BROTT, T., CAPLAN, L., MEIER, D., FIESCHI, C., VON KUMMER, R., DONNAN, G., HEISS, W. D., WAHLGREN, N. G., SPRANGER, M., BOYSEN, G. & MARLER, J. R. (1999) Thrombolysis in acute ischemic stroke: controlled trials and clinical experience. *Neurology,* 53, S3-14.

HACKE, W., SCHWAB, S., HORN, M., SPRANGER, M., DE GEORGIA, M. & VON KUMMER, R. (1996) 'Malignant' Middle Cerebral Artery Territory Infarction: Clinical Course and Prognostic Signs. *Arch Neurol,* 53, 309-315.

HAEUSLER, K. G., SCHMIDT, W. U., FOHRING, F., MEISEL, C., HELMS, T., JUNGEHULSING, G. J., NOLTE, C. H., SCHMOLKE, K., WEGNER, B., MEISEL, A., DIRNAGL, U., VILLRINGER, A. & VOLK, H. D. (2008) Cellular immunodepression preceding infectious complications after acute ischemic stroke in humans. *Cerebrovasc Dis,* 25, 50-8.

HANSEN, A. J. & ZEUTHEN, T. (1981) Extracellular ion concentrations during spreading depression and ischemia in the rat brain cortex. *Acta Physiol Scand,* 113, 437-45.

HARING, H. P., BERG, E. L., TSURUSHITA, N., TAGAYA, M. & DEL ZOPPO, G. J. (1996) E-selectin appears in nonischemic tissue during experimental focal cerebral ischemia. *Stroke,* 27, 1386-91; discussion 1391-2.

HARRIS, A. K., ERGUL, A., KOZAK, A., MACHADO, L. S., JOHNSON, M. H. & FAGAN, S. C. (2005) Effect of neutrophil depletion on gelatinase expression, edema formation and hemorrhagic transformation after focal ischemic stroke. *BMC Neurosci,* 6, 49.

HARRISON, D. G., GUZIK, T. J., GORONZY, J. & WEYAND, C. (2008) Is hypertension an immunologic disease? *Curr Cardiol Rep,* 10, 464-9.

HATCHELL, D. L., WILSON, C. A. & SALOUPIS, P. (1994) Neutrophils plug capillaries in acute experimental retinal ischemia. *Microvasc Res,* 47, 344-54.

HATTORI, K., LEE, H., HURN, P. D., CRAIN, B. J., TRAYSTMAN, R. J. & DEVRIES, A. C. (2000) Cognitive deficits after focal cerebral ischemia in mice. *Stroke,* 31, 1939-44.

HEISS, W. D., GRAF, R. & WIENHARD, K. (2001) Relevance of experimental ischemia in cats for stroke management: a comparative reevaluation. *Cerebrovasc Dis,* 11, 73-81.

HEUSCHMANN, P. U., KOLOMINSKY-RABAS, P. L., MISSELWITZ, B., HERMANEK, P., LEFFMANN, C., JANZEN, R. W., ROTHER, J., BUECKER-NOTT, H. J. & BERGER, K. (2004) Predictors of in-hospital mortality and attributable risks of death after ischemic stroke: the German Stroke Registers Study Group. *Arch Intern Med,* 164, 1761-8.

HILBURGER, E. W., CONTE, E. J., MCGEE, D. W. & TAMMARIELLO, S. P. (2005) Localization of NADPH oxidase subunits in neonatal sympathetic neurons. *Neuroscience Letters,* 377, 16-19.

HOGAN, P. G., CHEN, L., NARDONE, J. & RAO, A. (2003) Transcriptional regulation by calcium, calcineurin, and NFAT. *Genes Dev,* 17, 2205-32.

HOSSMANN, K. A. (2008) Cerebral ischemia: models, methods and outcomes. *Neuropharmacology,* 55, 257-70.

HUANG, J., UPADHYAY, U. M. & TAMARGO, R. J. (2006) Inflammation in stroke and focal cerebral ischemia. *Surg Neurol,* 66, 232-45.

HUANG, R., SHUAIB, A. & HERTZ, L. (1993) Glutamate uptake and glutamate content in primary cultures of mouse astrocytes during anoxia, substrate deprivation and simulated ischemia under normothermic and hypothermic conditions. *Brain Research,* 618, 346-351.

HUGHES, P. M., ALLEGRINI, P. R., RUDIN, M., PERRY, V. H., MIR, A. K. & WIESSNER, C. (2002) Monocyte chemoattractant protein-1 deficiency is protective in a murine stroke model. *J Cereb Blood Flow Metab,* 22, 308-17.

HURN, P. D., SUBRAMANIAN, S., PARKER, S. M., AFENTOULIS, M. E., KALER, L. J., VANDENBARK, A. A. & OFFNER, H. (2007) T- and B-cell-deficient mice with experimental stroke have reduced lesion size and inflammation. *J Cereb Blood Flow Metab,* 27, 1798-805.

IADECOLA, C. (2004) Neurovascular regulation in the normal brain and in Alzheimer's disease. *Nat Rev Neurosci,* 5, 347-60.

IADECOLA, C., FORSTER, C., NOGAWA, S., CLARK, H. B. & ROSS, M. E. (1999) Cyclooxygenase-2 immunoreactivity in the human brain following cerebral ischemia. *Acta Neuropathol,* 98, 9-14.

IADECOLA, C., NIWA, K., NOGAWA, S., ZHAO, X., NAGAYAMA, M., ARAKI, E., MORHAM, S. & ROSS, M. E. (2001a) Reduced susceptibility to ischemic brain injury and N-methyl-D-aspartate-mediated neurotoxicity in cyclooxygenase-2-deficient mice. *Proc Natl Acad Sci U S A,* 98, 1294-9.

IADECOLA, C., SUGIMOTO, K., NIWA, K., KAZAMA, K. & ROSS, M. E. (2001b) Increased susceptibility to ischemic brain injury in cyclooxygenase-1-deficient mice. *J Cereb Blood Flow Metab,* 21, 1436-41.

IADECOLA, C., ZHANG, F., CASEY, R., CLARK, H. B. & ROSS, M. E. (1996) Inducible nitric oxide synthase gene expression in vascular cells after transient focal cerebral ischemia. *Stroke,* 27, 1373-80.

IADECOLA, C., ZHANG, F., CASEY, R., NAGAYAMA, M. & ROSS, M. E. (1997) Delayed reduction of ischemic brain injury and neurological deficits in mice lacking the inducible nitric oxide synthase gene. *J Neurosci,* 17, 9157-64.

IADECOLA, C., ZHANG, F., XU, S., CASEY, R. & ROSS, M. E. (1995) Inducible nitric oxide synthase gene expression in brain following cerebral ischemia. *J Cereb Blood Flow Metab,* 15, 378-84.

IIJIMA, T., MIES, G. & HOSSMANN, K. A. (1992) Repeated negative DC deflections in rat cortex following middle cerebral artery occlusion are abolished by MK-801: effect on volume of ischemic injury. *J Cereb Blood Flow Metab,* 12, 727-33.

IVACKO, J., SZAFLARSKI, J., MALINAK, C., FLORY, C., WARREN, J. S. & SILVERSTEIN, F. S. (1997) Hypoxic-ischemic injury induces monocyte chemoattractant protein-1 expression in neonatal rat brain. *J Cereb Blood Flow Metab,* 17, 759-70.

JACKMAN, K. A., MILLER, A. A., DE SILVA, T. M., CRACK, P. J., DRUMMOND, G. R. & SOBEY, C. G. (2009a) Reduction of cerebral infarct volume by apocynin requires pretreatment and is absent in Nox2-deficient mice. *Br J Pharmacol,* 156, 680-8.

JACKMAN, K. A., MILLER, A. A., DRUMMOND, G. R. & SOBEY, C. G. (2009b) Importance of NOX1 for angiotensin II-induced cerebrovascular superoxide production and cortical infarct volume following ischemic stroke. *Brain Res,* 1286, 215-20.

JACKSON, S. H., DEVADAS, S., KWON, J., PINTO, L. A. & WILLIAMS, M. S. (2004) T cells express a phagocyte-type NADPH oxidase that is activated after T cell receptor stimulation. *Nat Immunol,* 5, 818-27.

JAIN, K. K. (2000) Neuroprotection in cerebrovascular disease. *Expert Opin Investig Drugs,* 9, 695-711.

JANDER, S., KRAEMER, M., SCHROETER, M., WITTE, O. W. & STOLL, G. (1995) Lymphocytic infiltration and expression of intercellular adhesion molecule-1 in photochemically induced ischemia of the rat cortex. *J Cereb Blood Flow Metab,* 15, 42-51.

JIANG, N., CHOPP, M. & CHAHWALA, S. (1998) Neutrophil inhibitory factor treatment of focal cerebral ischemia in the rat. *Brain Res,* 788, 25-34.

JOHNSTON, S. C., FUNG, L. H., GILLUM, L. A., SMITH, W. S., BRASS, L. M., LICHTMAN, J. H. & BROWN, A. N. (2001) Utilization of intravenous tissue-type plasminogen activator for ischemic stroke at academic medical centers: the influence of ethnicity. *Stroke,* 32, 1061-8.

JORGENSEN, H. S., SPERLING, B., NAKAYAMA, H., RAASCHOU, H. O. & OLSEN, T. S. (1994) Spontaneous reperfusion of cerebral infarcts in patients with acute stroke. Incidence, time course, and clinical outcome in the Copenhagen Stroke Study. *Arch Neurol,* 51, 865-73.

JUSTICIA, C., MARTIN, A., ROJAS, S., GIRONELLA, M., CERVERA, A., PANES, J., CHAMORRO, A. & PLANAS, A. M. (2006) Anti-VCAM-1 antibodies did not protect against ischemic damage either in rats or in mice. *J Cereb Blood Flow Metab,* 26, 421-32.

KAHLES, T., KOHNEN, A., HEUMUELLER, S., RAPPERT, A., BECHMANN, I., LIEBNER, S., WITTKO, I. M., NEUMANN-HAEFELIN, T., STEINMETZ, H., SCHROEDER, K. & BRANDES, R. P. (2010) NADPH oxidase Nox1 contributes to ischemic injury in experimental stroke in mice. *Neurobiol Dis,* 40, 185-92.

KAHLES, T., LUEDIKE, P., ENDRES, M., GALLA, H. J., STEINMETZ, H., BUSSE, R., NEUMANN-HAEFELIN, T. & BRANDES, R. P. (2007) NADPH oxidase plays a central role in blood-brain barrier damage in experimental stroke. *Stroke,* 38, 3000-6.

KAMINUMA, O., KITAMURA, F., MIYATAKE, S., YAMAOKA, K., MIYOSHI, H., INOKUMA, S., TATSUMI, H., NEMOTO, S., KITAMURA, N., MORI, A. & HIROI, T. (2009) T-box 21 transcription factor is responsible for distorted T(H)2 differentiation in human peripheral CD4+ T cells. *J Allergy Clin Immunol,* 123, 813-23 e3.

KAPINYA, K. J., PRASS, K. & DIRNAGL, U. (2002). Isoflurane induced prolonged protection against cerebral ischemia in mice: a redox sensitive mechanism? *Neuroreport,* 13, 1431-5.

KATZAN, I. L., HAMMER, M. D., HIXSON, E. D., FURLAN, A. J., ABOU-CHEBL, A. & NADZAM, D. M. (2004) Utilization of intravenous tissue plasminogen activator for acute ischemic stroke. *Arch Neurol,* 61, 346-50.

KEATING, D. J., DUBACH, D., ZANIN, M. P., YU, Y., MARTIN, K., ZHAO, Y.-F., CHEN, C., PORTA, S., ARBONES, M. L., MITTAZ, L. & PRITCHARD, M. A. (2008) DSCR1/RCAN1 regulates vesicle exocytosis and fusion pore kinetics: implications for Down syndrome and Alzheimer's disease. *Hum. Mol. Genet.,* 17, 1020-1030.

KHATRI, P., NEFF, J., BRODERICK, J. P., KHOURY, J. C., CARROZZELLA, J. & TOMSICK, T. (2005) Revascularization end points in stroke interventional trials: recanalization versus reperfusion in IMS-I. *Stroke,* 36, 2400-3.

KIELIAN, T., BARRY, B. & HICKEY, W. F. (2001) CXC Chemokine Receptor-2 Ligands Are Required for Neutrophil-Mediated Host Defense in Experimental Brain Abscesses1. *J Immunol,* 166, 4634-4643.

KIM, M. J., SHIN, K.-S., CHUNG, Y.-B., JUNG, K. W., CHA, C. I. & HOON SHIN, D. (2005) Immunohistochemical study of p47Phox and gp91Phox distributions in rat brain. *Brain Research,* 1040, 178-186.

KIM, Y. S., CHO, K. O., LEE, H. J., KIM, S. Y., SATO, Y. & CHO, Y. J. (2006) Down syndrome candidate region 1 increases the stability of the IkappaBalpha protein: implications for its anti-inflammatory effects. *J Biol Chem,* 281, 39051-61.

KINGSBURY, T. J. & CUNNINGHAM, K. W. (2000) A conserved family of calcineurin regulators. *Genes Dev,* 14, 1595-604.

KINOUCHI, H., EPSTEIN, C. J., MIZUI, T., CARLSON, E., CHEN, S. F. & CHAN, P. H. (1991) Attenuation of focal cerebral ischemic injury in transgenic mice overexpressing CuZn superoxide dismutase. *Proc Natl Acad Sci U S A,* 88, 11158-62.

KIRINO, T. (2000) Delayed neuronal death. *Neuropathology,* 20 Suppl, S95-7.

KLEINSCHNITZ, C., GRUND, H., WINGLER, K., ARMITAGE, M. E., JONES, E., MITTAL, M., BARIT, D., SCHWARZ, T., GEIS, C., KRAFT, P., BARTHEL, K., SCHUHMANN, M. K., HERRMANN, A. M., MEUTH, S. G., STOLL, G., MEURER, S., SCHREWE, A., BECKER, L., GAILUS-DURNER, V. R., FUCHS, H., KLOPSTOCK, T., DE ANGELIS, M. H., JANDELEIT-DAHM, K., SHAH, A. M., WEISSMANN, N. & SCHMIDT, H. H. H. W. (2010a) Post-Stroke Inhibition of Induced NADPH Oxidase Type 4 Prevents Oxidative Stress and Neurodegeneration. *PLoS Biol,* 8, e1000479.

KLEINSCHNITZ, C., SCHWAB, N., KRAFT, P., HAGEDORN, I., DREYKLUFT, A., SCHWARZ, T., AUSTINAT, M., NIESWANDT, B., WIENDL, H. & STOLL, G.

(2010b) Early detrimental T-cell effects in experimental cerebral ischemia are neither related to adaptive immunity nor thrombus formation. *Blood,* 115, 3835-42.

KOENNECKE, H. C., NOHR, R., LEISTNER, S. & MARX, P. (2001) Intravenous tPA for ischemic stroke team performance over time, safety, and efficacy in a single-center, 2-year experience. *Stroke,* 32, 1074-8.

KOISTINAHO, M. & KOISTINAHO, J. (2005) Interactions between Alzheimer's disease and cerebral ischemia--focus on inflammation. *Brain Res Brain Res Rev,* 48, 240-50.

KOIZUMI, J.-I., YOSHIDA, Y., NAKAZAWA, T. & OONEDA, G. (1986) A new experimental model of cerebral embolism in rats in which recirculation can be introduced in the ischemic area. *Japanese Journal of Stroke,* 8, 1-8.

KONDO, T., REAUME, A. G., HUANG, T.-T., CARLSON, E., MURAKAMI, K., CHEN, S. F., HOFFMAN, E. K., SCOTT, R. W., EPSTEIN, C. J. & CHAN, P. H. (1997) Reduction of CuZn-Superoxide Dismutase Activity Exacerbates Neuronal Cell Injury and Edema Formation after Transient Focal Cerebral Ischemia. *J. Neurosci.,* 17, 4180-4189.

KORN, T., BETTELLI, E., OUKKA, M. & KUCHROO, V. K. (2009) IL-17 and Th17 Cells. *Annu Rev Immunol,* 27, 485-517.

KOSTULAS, N., PELIDOU, S. H., KIVISAKK, P., KOSTULAS, V. & LINK, H. (1999) Increased IL-1beta, IL-8, and IL-17 mRNA expression in blood mononuclear cells observed in a prospective ischemic stroke study. *Stroke,* 30, 2174-9.

KUBOKI, S., SHIN, T., HUBER, N., EISMANN, T., GALLOWAY, E., SCHUSTER, R., BLANCHARD, J., EDWARDS, M. J. & LENTSCH, A. B. (2008) Hepatocyte signaling through CXC chemokine receptor-2 is detrimental to liver recovery after ischemia/reperfusion in mice. *Hepatology,* 48, 1213-23.

KUMAI, Y., OOBOSHI, H., TAKADA, J., KAMOUCHI, M., KITAZONO, T., EGASHIRA, K., IBAYASHI, S. & IIDA, M. (2004) Anti-monocyte chemoattractant protein-1 gene therapy protects against focal brain ischemia in hypertensive rats. *J Cereb Blood Flow Metab,* 24, 1359-68.

KUNZ, A., ANRATHER, J., ZHOU, P., ORIO, M. & IADECOLA, C. (2007) Cyclooxygenase-2 does not contribute to postischemic production of reactive oxygen species. *J Cereb Blood Flow Metab,* 27, 545-51.

KUSAKA, I., KUSAKA, G., ZHOU, C., ISHIKAWA, M., NANDA, A., GRANGER, D. N., ZHANG, J. H. & TANG, J. (2004) Role of AT1 receptors and NAD(P)H oxidase in diabetes-aggravated ischemic brain injury. *Am J Physiol Heart Circ Physiol,* 286, H2442-51.

LAHA, R. K., DUJOVNY, M., BARRIONUEVO, P. J., DECASTRO, S. C., HELLSTROM, H. R. & MAROON, J. C. (1978) Protective effects of methyl prednisolone and dimethyl sulfoxide in experimental middle cerebral artery embolectomy. *J Neurosurg,* 49, 508-16.

LAU, D. & BALDUS, S. (2006) Myeloperoxidase and its contributory role in inflammatory vascular disease. *Pharmacol Ther,* 111, 16-26.

LEE, J., CACALANO, G., CAMERATO, T., TOY, K., MOORE, M. W. & WOOD, W. I. (1995) Chemokine binding and activities mediated by the mouse IL-8 receptor. *J Immunol,* 155, 2158-64.

LEE, J. I. & BURCKART, G. J. (1998) Nuclear factor kappa B: important transcription factor and therapeutic target. *J Clin Pharmacol,* 38, 981-93.

LEMKE, R., GADIENT, R. A., SCHLIEBS, R., BIGL, V. & PATTERSON, P. H. (1996) Neuronal expression of leukemia inhibitory factor (LIF) in the rat brain. *Neurosci Lett,* 215, 205-8.

LI, F. M. D., SILVA, M. D. B. S., SOTAK, C. H. P. & FISHER, M. M. D. (2000) Temporal evolution of ischemic injury evaluated with diffusion-, perfusion-, and T2-weighted MRI. *Neurology,* 54, 689-696.

LI, J., BAUD, O., VARTANIAN, T., VOLPE, J. J. & ROSENBERG, P. A. (2005) Peroxynitrite generated by inducible nitric oxide synthase and NADPH oxidase mediates microglial toxicity to oligodendrocytes. *Proc Natl Acad Sci U S A,* 102, 9936-41.

LI, Y., CHOPP, M., JIANG, N., YAO, F. & ZALOGA, C. (1995) Temporal profile of in situ DNA fragmentation after transient middle cerebral artery occlusion in the rat. *J Cereb Blood Flow Metab,* 15, 389-97.

LIESZ, A., HAGMANN, S., ZSCHOCHE, C., ADAMEK, J., ZHOU, W., SUN, L., HUG, A., ZORN, M., DALPKE, A., NAWROTH, P. & VELTKAMP, R. (2009a) The spectrum of systemic immune alterations after murine focal ischemia: immunodepression versus immunomodulation. *Stroke,* 40, 2849-58.

LIESZ, A., SURI-PAYER, E., VELTKAMP, C., DOERR, H., SOMMER, C., RIVEST, S., GIESE, T. & VELTKAMP, R. (2009b) Regulatory T cells are key cerebroprotective immunomodulators in acute experimental stroke. *Nat Med,* 15, 192-9.

LILIENBAUM, A. & ISRAEL, A. (2003) From Calcium to NF-{kappa}B Signaling Pathways in Neurons. *Mol. Cell. Biol.,* 23, 2680-2698.

LIMATOLA, C., CIOTTI, M. T., MERCANTI, D., VACCA, F., RAGOZZINO, D., GIOVANNELLI, A., SANTONI, A., EUSEBI, F. & MILEDI, R. (2000) The chemokine growth-related gene product beta protects rat cerebellar granule cells from apoptotic cell death through alpha-amino-3-hydroxy-5-methyl-4-isoxazolepropionate receptors. *Proc Natl Acad Sci U S A,* 97, 6197-201.

LINDSBERG, P. J., CARPEN, O., PAETAU, A., KARJALAINEN-LINDSBERG, M. L. & KASTE, M. (1996) Endothelial ICAM-1 expression associated with inflammatory cell response in human ischemic stroke. *Circulation,* 94, 939-45.

LIPPERT, U., ZACHMANN, K., HENZ, B. M. & NEUMANN, C. (2004) Human T lymphocytes and mast cells differentially express and regulate extra- and intracellular CXCR1 and CXCR2. *Exp Dermatol,* 13, 520-5.

LIPTON, P. (1999) Ischemic cell death in brain neurons. *Physiol Rev,* 79, 1431-568.

LIU, T., MCDONNELL, P., YOUNG, P., WHITE, R., SIREN, A., HALLENBECK, J., BARONE, F. & FEURESTEIN, G. (1993) Interleukin-1 beta mRNA expression in ischemic rat cortex. *Stroke,* 24, 1746-1750.

LODDICK, S. A. & ROTHWELL, N. J. (1996) Neuroprotective effects of human recombinant interleukin-1 receptor antagonist in focal cerebral ischaemia in the rat. *J Cereb Blood Flow Metab,* 16, 932-40.

LOIHL, A. K., ASENSIO, V., CAMPBELL, I. L. & MURPHY, S. (1999) Expression of nitric oxide synthase (NOS)-2 following permanent focal ischemia and the role of nitric oxide in infarct generation in male, female and NOS-2 gene-deficient mice. *Brain Res,* 830, 155-64.

LUDWIG, A., EHLERT, J. E., FLAD, H.-D. & BRANDT, E. (2000) Identification of Distinct Surface-Expressed and Intracellular CXC-Chemokine Receptor 2 Glycoforms in Neutrophils: N-Glycosylation Is Essential for Maintenance of Receptor Surface Expression. *J Immunol,* 165, 1044-1052.

MACKAY, C. R. (2001) Chemokines: immunology's high impact factors. *Nat Immunol,* 2, 95-101.

MALLE, E., FURTMULLER, P. G., SATTLER, W. & OBINGER, C. (2007). Myeloperoxidase: a target for new drug development? *Br J Pharmacol,* 152, 838-54.

MANOLIO, T. A., KRONMAL, R. A., BURKE, G. L., O'LEARY, D. H. & PRICE, T. R. (1996) Short-term predictors of incident stroke in older adults. The Cardiovascular Health Study. *Stroke,* 27, 1479-86.

MARKUS, R., REUTENS, D. C., KAZUI, S., READ, S., WRIGHT, P., CHAMBERS, B. R., SACHINIDIS, J. I., TOCHON-DANGUY, H. J. & DONNAN, G. A. (2003) Topography and Temporal Evolution of Hypoxic Viable Tissue Identified by 18F-Fluoromisonidazole Positron Emission Tomography in Humans After Ischemic Stroke. *Stroke,* 34, 2646-2652.

MARTIN, R. L., LLOYD, H. G. & COWAN, A. I. (1994) The early events of oxygen and glucose deprivation: setting the scene for neuronal death? *Trends Neurosci,* 17, 251-7.

MARUI, N., OFFERMANN, M. K., SWERLICK, R., KUNSCH, C., ROSEN, C. A., AHMAD, M., ALEXANDER, R. W. & MEDFORD, R. M. (1993) Vascular cell adhesion molecule-1 (VCAM-1) gene transcription and expression are regulated through an antioxidant-sensitive mechanism in human vascular endothelial cells. *J Clin Invest,* 92, 1866-74.

MATSUO, Y., KIHARA, T., IKEDA, M., NINOMIYA, M., ONODERA, H. & KOGURE, K. (1995) Role of neutrophils in radical production during ischemia and reperfusion of the

rat brain: effect of neutrophil depletion on extracellular ascorbyl radical formation. *J Cereb Blood Flow Metab,* 15, 941-7.

MATSUO, Y., ONODERA, H., SHIGA, Y., NAKAMURA, M., NINOMIYA, M., KIHARA, T. & KOGURE, K. (1994) Correlation between myeloperoxidase-quantified neutrophil accumulation and ischemic brain injury in the rat. Effects of neutrophil depletion. *Stroke,* 25, 1469-75.

MATTSON, M. P., CULMSEE, C. & YU, Z. F. (2000) Apoptotic and antiapoptotic mechanisms in stroke. *Cell Tissue Res,* 301, 173-87.

MCCANN, S. K., DUSTING, G. J. & ROULSTON, C. L. (2008) Early increase of Nox4 NADPH oxidase and superoxide generation following endothelin-1-induced stroke in conscious rats. *Journal of Neuroscience Research,* 86, 2524-2534.

MCCOLL, B. W., ROTHWELL, N. J. & ALLAN, S. M. (2007) Systemic Inflammatory Stimulus Potentiates the Acute Phase and CXC Chemokine Responses to Experimental Stroke and Exacerbates Brain Damage via Interleukin-1- and Neutrophil-Dependent Mechanisms. *J. Neurosci.,* 27, 4403-4412.

MIES, G., IIJIMA, T. & HOSSMANN, K. A. (1993) Correlation between peri-infarct DC shifts and ischaemic neuronal damage in rat. *Neuroreport,* 4, 709-11.

MIETTINEN, S., FUSCO, F. R., YRJANHEIKKI, J., KEINANEN, R., HIRVONEN, T., ROIVAINEN, R., NARHI, M., HOKFELT, T. & KOISTINAHO, J. (1997) Spreading depression and focal brain ischemia induce cyclooxygenase-2 in cortical neurons through N-methyl-D-aspartic acid-receptors and phospholipase A2. *Proc Natl Acad Sci U S A,* 94, 6500-5.

MILLER, A. A., DRUMMOND, G. R., DE SILVA, T. M., MAST, A. E., HICKEY, H., WILLIAMS, J. P., BROUGHTON, B. R. & SOBEY, C. G. (2009) NADPH oxidase activity is higher in cerebral versus systemic arteries of four animal species: role of Nox2. *Am J Physiol Heart Circ Physiol,* 296, H220-5.

MILLER, A. A., DRUMMOND, G. R., SCHMIDT, H. H. & SOBEY, C. G. (2005) NADPH oxidase activity and function are profoundly greater in cerebral versus systemic arteries. *Circ Res,* 97, 1055-62.

MINAMI, M. & SATOH, M. (2003) Chemokines and their receptors in the brain: Pathophysiological roles in ischemic brain injury. *Life Sciences,* 74, 321-327.

MOLINA, C. A., BARRETO, A. D., TSIVGOULIS, G., SIERZENSKI, P., MALKOFF, M. D., RUBIERA, M., GONZALES, N., MIKULIK, R., PATE, G., OSTREM, J., SINGLETON, W., MANVELIAN, G., UNGER, E. C., GROTTA, J. C., SCHELLINGER, P. D. & ALEXANDROV, A. V. (2009) Transcranial ultrasound in clinical sonothrombolysis (TUCSON) trial. *Ann Neurol,* 66, 28-38.

MUGGE, A., HEISTAD, D., PADGETT, R., WAACK, B., DENSEN, P. & LOPEZ, J. (1991) Mechanisms of contraction induced by human leukocytes in normal and atherosclerotic arteries. *Circ Res,* 69, 871-880.

MURAKAMI, K., KONDO, T., KAWASE, M., LI, Y., SATO, S., CHEN, S. F. & CHAN, P. H. (1998) Mitochondrial Susceptibility to Oxidative Stress Exacerbates Cerebral Infarction That Follows Permanent Focal Cerebral Ischemia in Mutant Mice with Manganese Superoxide Dismutase Deficiency. *J. Neurosci.,* 18, 205-213.

MURPHY, K., TRAVERS, P. & WALPORT, M. (2008) Chapter 8: T Cell-Mediated Immunity. *Janeway's Immuno Biology.* 7th Edition ed., Garland Science, Taylor & Francis Group, LLC.

NATIONAL HEART, LUNG AND BLOOD INSTITUTE (NHLBI). (2006) *Incidence and Prevalence: 2006 Chart book on Cardiovascular and Lung Diseases.*

NATIONAL STROKE FOUNDATION (NSF). (2010) Facts, figures and statistics. Viewed July 25 2010, <http://www.strokefoundation.com.au/facts-figures-and-stats>

NAWASHIRO, H., MARTIN, D. & HALLENBECK, J. M. (1997) Inhibition of Tumor Necrosis Factor and Amelioration of Brain Infarction in Mice. *J Cereb Blood Flow Metab,* 17, 229-232.

NEDERGAARD, M. & HANSEN, A. J. (1993) Characterization of cortical depolarizations evoked in focal cerebral ischemia. *J Cereb Blood Flow Metab,* 13, 568-74.

NILUPUL PERERA, M., MA, H. K., ARAKAWA, S., HOWELLS, D. W., MARKUS, R., ROWE, C. C. & DONNAN, G. A. (2006) Inflammation following stroke. *J Clin Neurosci,* 13, 1-8.

NISHI, T., MAIER, C. M., HAYASHI, T., SAITO, A. & CHAN, P. H. (2005) Superoxide dismutase 1 overexpression reduces MCP-1 and MIP-1 alpha expression after transient focal cerebral ischemia. *J Cereb Blood Flow Metab,* 25, 1312-24.

NOGAWA, S., ZHANG, F., ROSS, M. E. & IADECOLA, C. (1997) Cyclo-oxygenase-2 gene expression in neurons contributes to ischemic brain damage. *J Neurosci,* 17, 2746-55.

NOH, K.-M. & KOH, J.-Y. (2000) Induction and Activation by Zinc of NADPH Oxidase in Cultured Cortical Neurons and Astrocytes. *J. Neurosci.,* 20, 111RC-.

O'NEILL, M. J. & CLEMENS, J. A. (2000) Rodent Models of Focal Cerebral Ischemia. *Curr Protoc Neurosci,* 12, 9.6.1-9.9.32.

OFFNER, H., SUBRAMANIAN, S., PARKER, S. M., AFENTOULIS, M. E., VANDENBARK, A. A. & HURN, P. D. (2006a) Experimental stroke induces massive, rapid activation of the peripheral immune system. *J Cereb Blood Flow Metab,* 26, 654-65.

OFFNER, H., SUBRAMANIAN, S., PARKER, S. M., WANG, C., AFENTOULIS, M. E., LEWIS, A., VANDENBARK, A. A. & HURN, P. D. (2006b) Splenic atrophy in

experimental stroke is accompanied by increased regulatory T cells and circulating macrophages. *J Immunol,* 176, 6523-31.

OSTWALD, S. K., WASSERMAN, J. & DAVIS, S. (2006) Medications, comorbidities, and medical complications in stroke survivors: the CAReS study. *Rehabil Nurs,* 31, 10-4.

PAHL, H. L. (1999) Activators and target genes of Rel/NF-kappaB transcription factors. *Oncogene,* 18, 6853-66.

PARK, E. M., CHO, S., FRYS, K. A., GLICKSTEIN, S. B., ZHOU, P., ANRATHER, J., ROSS, M. E. & IADECOLA, C. (2006) Inducible nitric oxide synthase contributes to gender differences in ischemic brain injury. *J Cereb Blood Flow Metab,* 26, 392-401.

PAXINOS, G. & FRANKLIN, K. B. J. (2001) *The Mouse Brain in Steriotaxic Coordinates*, Academic Press.

PETRAULT, O., OUK, T., GAUTIER, S., LAPRAIS, M., GELE, P., BASTIDE, M. & BORDET, R. (2005) Pharmacological neutropenia prevents endothelial dysfunction but not smooth muscle functions impairment induced by middle cerebral artery occlusion. *Br J Pharmacol,* 144, 1051-8.

PLANAS, A. M., SORIANO, M. A., RODRIGUEZ-FARRE, E. & FERRER, I. (1995) Induction of cyclooxygenase-2 mRNA and protein following transient focal ischemia in the rat brain. *Neurosci Lett,* 200, 187-90.

POPIVANOVA, B. K., KOIKE, K., TONCHEV, A. B., ISHIDA, Y., KONDO, T., OGAWA, S., MUKAIDA, N., INOUE, M. & YAMASHIMA, T. (2003) Accumulation of microglial cells expressing ELR motif-positive CXC chemokines and their receptor CXCR2 in monkey hippocampus after ischemia-reperfusion. *Brain Res,* 970, 195-204.

PORTA, S., MARTI, E., DE LA LUNA, S. & ARBONES, M. L. (2007) Differential expression of members of the RCAN family of calcineurin regulators suggests selective functions for these proteins in the brain. *Eur J Neurosci,* 26, 1213-26.

PRASS, K., MEISEL, C., HOFLICH, C., BRAUN, J., HALLE, E., WOLF, T., RUSCHER, K., VICTOROV, I. V., PRILLER, J., DIRNAGL, U., VOLK, H. D. & MEISEL, A. (2003) Stroke-induced immunodeficiency promotes spontaneous bacterial infections and is mediated by sympathetic activation reversal by poststroke T helper cell type 1-like immunostimulation. *J Exp Med,* 198, 725-36.

PRENCIPE, M., FERRETTI, C., CASINI, A. R., SANTINI, M., GIUBILEI, F. & CULASSO, F. (1997) Stroke, disability, and dementia: results of a population survey. *Stroke,* 28, 531-6.

PUBMED. Search string: (neuroprotection [ti] OR neuroprotective [ti]) AND (stroke OR cerebral ischemia OR cerebral ischaemia). 2010. http://www.ncbi.nlm.nih.gov/pubmed/

PUMA, C., DANIK, M., QUIRION, R., RAMON, F. & WILLIAMS, S. (2001) The chemokine interleukin-8 acutely reduces Ca(2+) currents in identified cholinergic septal neurons expressing CXCR1 and CXCR2 receptor mRNAs. *J Neurochem,* 78, 960-71.

PURUSHOTHAMAN, D. & SARIN, A. (2009) Cytokine-dependent regulation of NADPH oxidase activity and the consequences for activated T cell homeostasis. *J Exp Med,* 206, 1515-23.

QUALITY STANDARDS SUBCOMMITTEE OF THE AMERICAN ACADEMY OF NEUROLOGY (QSSAAN). (1996) Practice advisory: thrombolytic therapy for acute ischemic stroke--summary statement. *Neurology,* 47, 835-9.

QUAST, M. J., HUANG, N. C., HILLMAN, G. R. & KENT, T. A. (1993) The evolution of acute stroke recorded by multimodal magnetic resonance imaging. *Magnetic Resonance Imaging,* 11, 465-471.

RACHIDI, M. & LOPES, C. (2008) Mental retardation and associated neurological dysfunctions in Down syndrome: a consequence of dysregulation in critical chromosome 21 genes and associated molecular pathways. *Eur J Paediatr Neurol,* 12, 168-82.

RAO, A., LUO, C. & HOGAN, P. G. (1997) Transcription factors of the NFAT family: regulation and function. *Annu Rev Immunol,* 15, 707-47.

RAO, V. L., BOWEN, K. K. & DEMPSEY, R. J. (2001) Transient focal cerebral ischemia down-regulates glutamate transporters GLT-1 and EAAC1 expression in rat brain. *Neurochem Res,* 26, 497-502.

RELTON, J. K., MARTIN, D., THOMPSON, R. C. & RUSSELL, D. A. (1996) Peripheral administration of Interleukin-1 Receptor antagonist inhibits brain damage after focal cerebral ischemia in the rat. *Exp Neurol,* 138, 206-13.

ROGALEWSKI, A., SCHNEIDER, A., RINGELSTEIN, E. B. & SCHABITZ, W. R. (2006) Toward a multimodal neuroprotective treatment of stroke. *Stroke,* 37, 1129-36.

ROLLINS, B. J. (1997) Chemokines. *Blood,* 90, 909-28.

ROMANIC, A. M., WHITE, R. F., ARLETH, A. J., OHLSTEIN, E. H., BARONE, F. C. & DAWSON, V. L. (1998) Matrix Metalloproteinase Expression Increases After Cerebral Focal Ischemia in Rats : Inhibition of Matrix Metalloproteinase-9 Reduces Infarct Size • Editorial Comment: Inhibition of Matrix Metalloproteinase-9 Reduces Infarct Size. *Stroke,* 29, 1020-1030.

ROSSI, D. & ZLOTNIK, A. (2000) The biology of chemokines and their receptors. *Annu Rev Immunol,* 18, 217-42.

ROTHERMEL, B., VEGA, R. B., YANG, J., WU, H., BASSEL-DUBY, R. & WILLIAMS, R. S. (2000) A Protein Encoded within the Down Syndrome Critical Region Is Enriched in Striated Muscles and Inhibits Calcineurin Signaling. *J. Biol. Chem.,* 275, 8719-8725.

RUSSELL, J. H. & LEY, T. J. (2002) Lymphocyte-mediated cytotoxicity. *Annu Rev Immunol,* 20, 323-70.

RYEOM, S., GREENWALD, R. J., SHARPE, A. H. & MCKEON, F. (2003) The threshold pattern of calcineurin-dependent gene expression is altered by loss of the endogenous inhibitor calcipressin. *Nat Immunol,* 4, 874-81.

SAIRANEN, T., RISTIMAKI, A., KARJALAINEN-LINDSBERG, M. L., PAETAU, A., KASTE, M. & LINDSBERG, P. J. (1998) Cyclooxygenase-2 is induced globally in infarcted human brain. *Ann Neurol,* 43, 738-47.

SAKAGUCHI, S., ONO, M., SETOGUCHI, R., YAGI, H., HORI, S., FEHERVARI, Z., SHIMIZU, J., TAKAHASHI, T. & NOMURA, T. (2006) Foxp3+ CD25+ CD4+ natural regulatory T cells in dominant self-tolerance and autoimmune disease. *Immunol Rev,* 212, 8-27.

SAMPEI, K., MANDIR, A. S., ASANO, Y., WONG, P. C., TRAYSTMAN, R. J., DAWSON, V. L., DAWSON, T. M. & HURN, P. D. (2000) Stroke outcome in double-mutant antioxidant transgenic mice. *Stroke,* 31, 2685-91.

SANNA, B., BRANDT, E. B., KAISER, R. A., PFLUGER, P., WITT, S. A., KIMBALL, T. R., VAN ROOIJ, E., DE WINDT, L. J., ROTHENBERG, M. E., TSCHOP, M. H., BENOIT, S. C. & MOLKENTIN, J. D. (2006) Modulatory calcineurin-interacting proteins 1 and 2 function as calcineurin facilitators in vivo. *Proc Natl Acad Sci U S A,* 103, 7327-32.

SANTANA, M. A., PEDRAZA-ALVA, G., OLIVARES-ZAVALETA, N., MADRID-MARINA, V., HOREJSI, V., BURAKOFF, S. J. & ROSENSTEIN, Y. (2000) CD43-mediated Signals Induce DNA Binding Activity of AP-1, NF-AT, and NFkappa B Transcription Factors in Human T Lymphocytes. *J. Biol. Chem.,* 275, 31460-31468.

SANTANA, M. A. & ROSENSTEIN, Y. (2003) What it takes to become an effector T cell: the process, the cells involved, and the mechanisms. *J Cell Physiol,* 195, 392-401.

SANTIZO, R. A., ANDERSON, S., YE, S., KOENIG, H. M. & PELLIGRINO, D. A. (2000) Effects of estrogen on leukocyte adhesion after transient forebrain ischemia. *Stroke,* 31, 2231-5.

SAQQUR, M., UCHINO, K., DEMCHUK, A. M., MOLINA, C. A., GARAMI, Z., CALLEJA, S., AKHTAR, N., OROUK, F. O., SALAM, A., SHUAIB, A. & ALEXANDROV, A. V. (2007) Site of arterial occlusion identified by transcranial Doppler predicts the response to intravenous thrombolysis for stroke. *Stroke,* 38, 948-54.

SCHALLER, B. & GRAF, R. (2004) Cerebral ischemia and reperfusion: the pathophysiologic concept as a basis for clinical therapy. *J Cereb Blood Flow Metab,* 24, 351-71.

SCHILLING, M., BESSELMANN, M., LEONHARD, C., MUELLER, M., RINGELSTEIN, E. B. & KIEFER, R. (2003) Microglial activation precedes and predominates over macrophage infiltration in transient focal cerebral ischemia: a study in green fluorescent protein transgenic bone marrow chimeric mice. *Exp Neurol,* 183, 25-33.

SCHMERBACH, K., SCHEFE, J. H., KRIKOV, M., MULLER, S., VILLRINGER, A., KINTSCHER, U., UNGER, T. & THOENE-REINEKE, C. (2008) Comparison between single and combined treatment with candesartan and pioglitazone following transient focal ischemia in rat brain. *Brain Res,* 1208, 225-33.

SCHMID-ELSAESSER, R., ZAUSINGER, S., HUNGERHUBER, E., BAETHMANN, A., REULEN, H.-J. & GARCIA, J. H. (1998) A Critical Reevaluation of the Intraluminal Thread Model of Focal Cerebral Ischemia : Evidence of Inadvertent Premature Reperfusion and Subarachnoid Hemorrhage in Rats by Laser-Doppler Flowmetry • Editorial Comment: Evidence of Inadvertent Premature Reperfusion and Subarachnoid Hemorrhage in Rats by Laser-Doppler Flowmetry. *Stroke,* 29, 2162-2170.

SCHNEIDER, A., MARTIN-VILLALBA, A., WEIH, F., VOGEL, J., WIRTH, T. & SCHWANINGER, M. (1999) NF-kappaB is activated and promotes cell death in focal cerebral ischemia. *Nat Med,* 5, 554-9.

SCHWAB, J. M., NGUYEN, T. D., MEYERMANN, R. & SCHLUESENER, H. J. (2001) Human focal cerebral infarctions induce differential lesional interleukin-16 (IL-16) expression confined to infiltrating granulocytes, CD8+ T-lymphocytes and activated microglia/macrophages. *J Neuroimmunol,* 114, 232-41.

SEDER, R. A. & AHMED, R. (2003) Similarities and differences in CD4+ and CD8+ effector and memory T cell generation. *Nat Immunol,* 4, 835-42.

SELEMIDIS, S., SOBEY, C. G., WINGLER, K., SCHMIDT, H. H. & DRUMMOND, G. R. (2008) NADPH oxidases in the vasculature: molecular features, roles in disease and pharmacological inhibition. *Pharmacol Ther,* 120, 254-91.

SEMPLE, B. D., KOSSMANN, T. & MORGANTI-KOSSMANN, M. C. (2010) Role of chemokines in CNS health and pathology: a focus on the CCL2/CCR2 and CXCL8/CXCR2 networks. *J Cereb Blood Flow Metab,* 30, 459-73.

SENES, S. (2006) How we manage stroke in Australia. AUSTRALIAN INSTITUTE OF HEALTH AND WELFARE (Ed.) CARDIOVASCULAR DISEASE SERIES. Number 24

SERRANO, F., KOLLURI, N. S., WIENTJES, F. B., CARD, J. P. & KLANN, E. (2003) NADPH oxidase immunoreactivity in the mouse brain. *Brain Research,* 988, 193-198.

SESHADRI, S., BEISER, A., KELLY-HAYES, M., KASE, C. S., AU, R., KANNEL, W. B. & WOLF, P. A. (2006) The Lifetime Risk of Stroke: Estimates From the Framingham Study. *Stroke,* 37, 345-350.

SHARKEY, J. & BUTCHER, S. P. (1994) Immunophilins mediate the neuroprotective effects of FK506 in focal cerebral ischaemia. *Nature,* 371, 336-9.

SHARKEY, J., CRAWFORD, J. H., BUTCHER, S. P. & MARSTON, H. M. (1996) Tacrolimus (FK506) ameliorates skilled motor deficits produced by middle cerebral artery occlusion in rats. *Stroke,* 27, 2282-6.

SHICHITA, T., SUGIYAMA, Y., OOBOSHI, H., SUGIMORI, H., NAKAGAWA, R., TAKADA, I., IWAKI, T., OKADA, Y., IIDA, M., CUA, D. J., IWAKURA, Y. & YOSHIMURA, A. (2009) Pivotal role of cerebral interleukin-17-producing γδT cells in the delayed phase of ischemic brain injury. *Nature Medicine,* 15, 946-950.

SHIMIZU, S., SIMON, R. P. & GRAHAM, S. H. (1997) Dimethylsulfoxide (DMSO) treatment reduces infarction volume after permanent focal cerebral ischemia in rats. *Neurosci Lett,* 239, 125-7.

SHIODA, N., HAN, F., MORIGUCHI, S. & FUKUNAGA, K. (2007) Constitutively active calcineurin mediates delayed neuronal death through Fas-ligand expression via activation of NFAT and FKHR transcriptional activities in mouse brain ischemia. *J Neurochem,* 102, 1506-17.

SHIODA, N., MORIGUCHI, S., SHIRASAKI, Y. & FUKUNAGA, K. (2006) Generation of constitutively active calcineurin by calpain contributes to delayed neuronal death following mouse brain ischemia. *J Neurochem,* 98, 310-20.

SHUAIB, A., LEES, K. R., LYDEN, P., GROTTA, J., DAVALOS, A., DAVIS, S. M., DIENER, H. C., ASHWOOD, T., WASIEWSKI, W. W. & EMERIBE, U. (2007) NXY-059 for the treatment of acute ischemic stroke. *N Engl J Med,* 357, 562-71.

SLEVIN, M., KRUPINSKI, J., MITSIOS, N., PERIKLEOUS, C., CUADRADO, E., MONTANER, J., SANFELIU, C., LUQUE, A., KUMAR, S., KUMAR, P. & GAFFNEY, J. (2008) Leukaemia inhibitory factor is over-expressed by ischaemic brain tissue concomitant with reduced plasma expression following acute stroke. *Eur J Neurol,* 15, 29-37.

SMITH, W. S., SUNG, G., SAVER, J., BUDZIK, R., DUCKWILER, G., LIEBESKIND, D. S., LUTSEP, H. L., RYMER, M. M., HIGASHIDA, R. T., STARKMAN, S., GOBIN, Y. P., FREI, D., GROBELNY, T., HELLINGER, F., HUDDLE, D., KIDWELL, C., KOROSHETZ, W., MARKS, M., NESBIT, G. & SILVERMAN, I. E. (2008) Mechanical thrombectomy for acute ischemic stroke: final results of the Multi MERCI trial. *Stroke,* 39, 1205-12.

STEFFAN, N., BREN, G., FRANTZ, B., TOCCI, M., O'NEILL, E. & PAYA, C. (1995) Regulation of IkB alpha phosphorylation by PKC- and Ca(2+)-dependent signal transduction pathways. *J Immunol,* 155, 4685-4691.

STEVENS, S. L., BAO, J., HOLLIS, J., LESSOV, N. S., CLARK, W. M. & STENZEL-POORE, M. P. (2002) The use of flow cytometry to evaluate temporal changes in inflammatory cells following focal cerebral ischemia in mice. *Brain Res,* 932, 110-9.

STINS, M. F., GILLES, F. & KIM, K. S. (1997) Selective expression of adhesion molecules on human brain microvascular endothelial cells. *J Neuroimmunol,* 76, 81-90.

STOWE, A. M., ADAIR-KIRK, T. L., GONZALES, E. R., PEREZ, R. S., SHAH, A. R., PARK, T. S. & GIDDAY, J. M. (2009) Neutrophil elastase and neurovascular injury following focal stroke and reperfusion. *Neurobiol Dis,* 35, 82-90.

STRIETER, R. M., STANDIFORD, T. J., HUFFNAGLE, G. B., COLLETTI, L. M., LUKACS, N. W. & KUNKEL, S. L. (1996) "The good, the bad, and the ugly." The role of chemokines in models of human disease. *J Immunol,* 156, 3583-6.

STRONG, A. J., SMITH, S. E., WHITTINGTON, D. J., MELDRUM, B. S., PARSONS, A. A., KRUPINSKI, J., HUNTER, A. J., PATEL, S. & ROBERTSON, C. (2000) Factors influencing the frequency of fluorescence transients as markers of peri-infarct depolarizations in focal cerebral ischemia. *Stroke,* 31, 214-22.

SUDLOW, C. L. & WARLOW, C. P. (1997) Comparable studies of the incidence of stroke and its pathological types: results from an international collaboration. International Stroke Incidence Collaboration. *Stroke,* 28, 491-9.

SUGHRUE, M. E., CONNOLLY, E. S., JR, KRAMS, M., LEES, K. R., HACKE, W., GRIEVE, A. P., ORGOGOZO, J.-M. & FORD, G. A. (2004) Effectively Bridging the Preclinical/Clinical Gap: The Results of the ASTIN Trial * Response. *Stroke,* 35, e81-82.

TAKAGI, K., GINSBERG, M. D., GLOBUS, M. Y., DIETRICH, W. D., MARTINEZ, E., KRAYDIEH, S. & BUSTO, R. (1993) Changes in amino acid neurotransmitters and cerebral blood flow in the ischemic penumbral region following middle cerebral artery occlusion in the rat: correlation with histopathology. *J Cereb Blood Flow Metab,* 13, 575-85.

TAKAGI, K., ZHAO, W., BUSTO, R. & GINSBERG, M. D. (1995) Local hemodynamic changes during transient middle cerebral artery occlusion and recirculation in the rat: a [14C]iodoantipyrine autoradiographic study. *Brain Res,* 691, 160-8.

TANG, L. L., YE, K., YANG, X. F. & ZHENG, J. S. (2007) Apocynin attenuates cerebral infarction after transient focal ischaemia in rats. *J Int Med Res,* 35, 517-22.

TANG, X. N., CAIRNS, B., CAIRNS, N. & YENARI, M. A. (2008) Apocynin improves outcome in experimental stroke with a narrow dose range. *Neuroscience,* 154, 556-62.

TANI, M., FUENTES, M. E., PETERSON, J. W., TRAPP, B. D., DURHAM, S. K., LOY, J. K., BRAVO, R., RANSOHOFF, R. M. & LIRA, S. A. (1996) Neutrophil infiltration, glial reaction, and neurological disease in transgenic mice expressing the chemokine N51/KC in oligodendrocytes. *J Clin Invest,* 98, 529-39.

TARKOWSKI, E., ROSENGREN, L., BLOMSTRAND, C., WIKKELSO, C., JENSEN, C., EKHOLM, S. & TARKOWSKI, A. (1995) Early Intrathecal Production of Interleukin-6 Predicts the Size of Brain Lesion in Stroke. *Stroke,* 26, 1393-1398.

THEODOROU, G. L., MAROUSI, S., ELLUL, J., MOUGIOU, A., THEODORI, E., MOUZAKI, A. & KARAKANTZA, M. (2008) T helper 1 (Th1)/Th2 cytokine expression shift of peripheral blood CD4+ and CD8+ T cells in patients at the post-acute phase of stroke. *Clin Exp Immunol,* 152, 456-63.

TOUZANI, O., YOUNG, A. R., DERLON, J.-M., BEAUDOUIN, V., MARCHAL, G., RIOUX, P., MEZENGE, F., BARON, J.-C. & MACKENZIE, E. T. (1995) Sequential Studies of Severely Hypometabolic Tissue Volumes After Permanent Middle Cerebral

Artery Occlusion : A Positron Emission Tomographic Investigation in Anesthetized Baboons. *Stroke,* 26, 2112-2119.

TOWFIGHI, A., OVBIAGELE, B. & SAVER, J. L. (2010) Therapeutic Milestone: Stroke Declines From the Second to the Third Leading Organ- and Disease-Specific Cause of Death in the United States. *Stroke,* 41, 499-503.

TRACEY, K. J. & CERAMI, A. (1994) Tumor necrosis factor: a pleiotropic cytokine and therapeutic target. *Annu Rev Med,* 45, 491-503.

TRUSHIN, S. A., PENNINGTON, K. N., ALGECIRAS-SCHIMNICH, A. & PAYA, C. V. (1999) Protein kinase C and calcineurin synergize to activate IkappaB kinase and NF-kappaB in T lymphocytes. *J Biol Chem,* 274, 22923-31.

TSIVGOULIS, G., EGGERS, J., RIBO, M., PERREN, F., SAQQUR, M., RUBIERA, M., SERGENTANIS, T. N., VADIKOLIAS, K., LARRUE, V., MOLINA, C. A. & ALEXANDROV, A. V. (2010) Safety and efficacy of ultrasound-enhanced thrombolysis: a comprehensive review and meta-analysis of randomized and nonrandomized studies. *Stroke,* 41, 280-7.

TSUCHIYA, D., HONG, S., KAYAMA, T., PANTER, S. S. & WEINSTEIN, P. R. (2003) Effect of suture size and carotid clip application upon blood flow and infarct volume after permanent and temporary middle cerebral artery occlusion in mice. *Brain Res,* 970, 131-9.

UCHINO, H., ELMER, E., UCHINO, K., LI, P. A., HE, Q. P., SMITH, M. L. & SIESJO, B. K. (1998) Amelioration by cyclosporin A of brain damage in transient forebrain ischemia in the rat. *Brain Res,* 812, 216-26.

UGAZIO, A. G., MACCARIO, R., NOTARANGELO, L. D. & BURGIO, G. R. (1990) Immunology of Down syndrome: a review. *Am J Med Genet Suppl,* 7, 204-12.

UNO, H., MATSUYAMA, T., AKITA, H., NISHIMURA, H. & SUGITA, M. (1997) Induction of Tumor Necrosis Factor-[alpha] in the Mouse Hippocampus Following Transient Forebrain Ischemia. *J Cereb Blood Flow Metab,* 17, 491-499.

URRA, X., CERVERA, A., VILLAMOR, N., PLANAS, A. M. & CHAMORRO, A. (2009) Harms and benefits of lymphocyte subpopulations in patients with acute stroke. *Neuroscience,* 158, 1174-83.

VACHON, P., BEAUDRY, F., MARIER, J. F., STE-MARIE, L. & MONTGOMERY, J. (2002) Cyclosporin A in blood and brain tissue following intra-carotid injections in normal and stroke-induced rats. *Brain Res,* 943, 1-8.

VALLES, A., GRIJPINK-ONGERING, L., DE BREE, F. M., TUINSTRA, T. & RONKEN, E. (2006) Differential regulation of the CXCR2 chemokine network in rat brain trauma: implications for neuroimmune interactions and neuronal survival. *Neurobiol Dis,* 22, 312-22.

VAN DER WORP, H. B., DE HAAN, P., MORREMA, E. & KALKMAN, C. J. (2005) Methodological quality of animal studies on neuroprotection in focal cerebral ischaemia. *J Neurol,* 252, 1108-14.

VAN WIJNGAARDEN, J. D. H., DIRKS, M., HUIJSMAN, R., NIESSEN, L. W., FABBRICOTTI, I. N., DIPPEL, D. W. J. & THE PROMOTING ACUTE THROMBOLYSIS FOR ISCHAEMIC STROKE INVESTIGATORS (2009) Hospital Rates of Thrombolysis for Acute Ischemic Stroke: The Influence of Organizational Culture. *Stroke,* 40, 3390-3392.

VEGA, R. B., ROTHERMEL, B. A., WEINHEIMER, C. J., KOVACS, A., NASEEM, R. H., BASSEL-DUBY, R., WILLIAMS, R. S. & OLSON, E. N. (2003) Dual roles of modulatory calcineurin-interacting protein 1 in cardiac hypertrophy. *Proc Natl Acad Sci U S A,* 100, 669-74.

VERNINO, S., BROWN, R. D., JR., SEJVAR, J. J., SICKS, J. D., PETTY, G. W. & O'FALLON, W. M. (2003) Cause-specific mortality after first cerebral infarction: a population-based study. *Stroke,* 34, 1828-32.

VIKMAN, P., ANSAR, S., HENRIKSSON, M., STENMAN, E. & EDVINSSON, L. (2007) Cerebral ischemia induces transcription of inflammatory and extracellular-matrix-related genes in rat cerebral arteries. *Exp Brain Res,* 183, 499-510.

VILA, N., CASTILLO, J., DAVALOS, A. & CHAMORRO, A. (2000) Proinflammatory cytokines and early neurological worsening in ischemic stroke. *Stroke,* 31, 2325-9.

VILLA, P., TRIULZI, S., CAVALIERI, B., DI BITONDO, R., BERTINI, R., BARBERA, S., BIGINI, P., MENNINI, T., GELOSA, P., TREMOLI, E., SIRONI, L. & GHEZZI, P. (2007) The interleukin-8 (IL-8/CXCL8) receptor inhibitor reparixin improves neurological deficits and reduces long-term inflammation in permanent and transient cerebral ischemia in rats. *Mol Med,* 13, 125-33.

WALDER, C. E., GREEN, S. P., DARBONNE, W. C., MATHIAS, J., RAE, J., DINAUER, M. C., CURNUTTE, J. T. & THOMAS, G. R. (1997) Ischemic stroke injury is reduced in mice lacking a functional NADPH oxidase. *Stroke,* 28, 2252-8.

WANG, P. Y., KAO, C. H., MUI, M. Y. & WANG, S. J. (1993) Leukocyte infiltration in acute hemispheric ischemic stroke. *Stroke,* 24, 236-40.

WANG, Q., TANG, X. N. & YENARI, M. A. (2007) The inflammatory response in stroke. *J Neuroimmunol,* 184, 53-68.

WANG, X., ELLISON, J. A., SIREN, A. L., LYSKO, P. G., YUE, T. L., BARONE, F. C., SHATZMAN, A. & FEUERSTEIN, G. Z. (1998) Prolonged expression of interferon-inducible protein-10 in ischemic cortex after permanent occlusion of the middle cerebral artery in rat. *J Neurochem,* 71, 1194-204.

WANG, X., LI, X., YAISH-OHAD, S., SARAU, H. M., BARONE, F. C. & FEUERSTEIN, G. Z. (1999) Molecular cloning and expression of the rat monocyte chemotactic protein-3 gene: a possible role in stroke. *Brain Res Mol Brain Res,* 71, 304-12.

WANG, X., XU, L., WANG, H., ZHAN, Y., PURE, E. & FEUERSTEIN, G. Z. (2002) CD44 deficiency in mice protects brain from cerebral ischemia injury. *J Neurochem,* 83, 1172-9.

WANG, X., YUE, T.-L., BARONE, F., WHITE, R., GAGNON, R. & FEUERSTEIN, G. (1994) Concomitant cortical expression of TNF-α and IL-1β mRNAs follows early response gene expression in transient focal ischemia. *Molecular and Chemical Neuropathology,* 23, 103-114.

WATSON, K. & FAN, G. H. (2005) Macrophage inflammatory protein 2 inhibits beta-amyloid peptide (1-42)-mediated hippocampal neuronal apoptosis through activation of mitogen-activated protein kinase and phosphatidylinositol 3-kinase signaling pathways. *Mol Pharmacol,* 67, 757-65.

WEISBROT-LEFKOWITZ, M., REUHL, K., PERRY, B., CHAN, P. H., INOUYE, M. & MIROCHNITCHENKO, O. (1998) Overexpression of human glutathione peroxidase protects transgenic mice against focal cerebral ischemia/reperfusion damage. *Brain Res Mol Brain Res,* 53, 333-8.

WELLONS, J. C., 3RD, SHENG, H., LASKOWITZ, D. T., BURKHARD MACKENSEN, G., PEARLSTEIN, R. D. & WARNER, D. S. (2000) A comparison of strain-related susceptibility in two murine recovery models of global cerebral ischemia. *Brain Res,* 868, 14-21.

WEN, Y., YANG, S., LIU, R., PEREZ, E., YI, K. D., KOULEN, P. & SIMPKINS, J. W. (2004) Estrogen attenuates nuclear factor-kappa B activation induced by transient cerebral ischemia. *Brain Res,* 1008, 147-54.

WHITE, J. R., LEE, J. M., YOUNG, P. R., HERTZBERG, R. P., JUREWICZ, A. J., CHAIKIN, M. A., WIDDOWSON, K., FOLEY, J. J., MARTIN, L. D., GRISWOLD, D. E. & SARAU, H. M. (1998) Identification of a potent, selective non-peptide CXCR2 antagonist that inhibits interleukin-8-induced neutrophil migration. *J Biol Chem,* 273, 10095-8.

WISNIEWSKI, K. E., WISNIEWSKI, H. M. & WEN, G. Y. (1985) Occurrence of neuropathological changes and dementia of Alzheimer's disease in Down's syndrome. *Ann Neurol,* 17, 278-82.

WUYTS, A., HAELENS, A., PROOST, P., LENAERTS, J., CONINGS, R., OPDENAKKER, G. & VAN DAMME, J. (1996) Identification of mouse granulocyte chemotactic protein-2 from fibroblasts and epithelial cells. Functional comparison with natural KC and macrophage inflammatory protein-2. *J Immunol,* 157, 1736-1743.

WYLLER, T. B., SODRING, K. M., SVEEN, U., LJUNGGREN, A. E. & BAUTZ-HOLTER, E. (1997) Are there gender differences in functional outcome after stroke? *Clin Rehabil,* 11, 171-9.

XIA, C. F., SMITH, R. S., JR., SHEN, B., YANG, Z. R., BORLONGAN, C. V., CHAO, L. & CHAO, J. (2006) Postischemic brain injury is exacerbated in mice lacking the kinin B2 receptor. *Hypertension,* 47, 752-61.

YANG, G., CHAN, P. H., CHEN, J., CARLSON, E., CHEN, S. F., WEINSTEIN, P., EPSTEIN, C. J. & KAMII, H. (1994) Human copper-zinc superoxide dismutase transgenic mice are highly resistant to reperfusion injury after focal cerebral ischemia. *Stroke,* 25, 165-70.

YANG, J., ROTHERMEL, B., VEGA, R. B., FREY, N., MCKINSEY, T. A., OLSON, E. N., BASSEL-DUBY, R. & WILLIAMS, R. S. (2000) Independent signals control expression of the calcineurin inhibitory proteins MCIP1 and MCIP2 in striated muscles. *Circ Res,* 87, E61-8.

YEH, T.-H., HWANG, H.-M., CHEN, J.-J., WU, T., LI, A. H. & WANG, H.-L. (2005) Glutamate transporter function of rat hippocampal astrocytes is impaired following the global ischemia. *Neurobiology of Disease,* 18, 476-483.

YILMAZ, G., ARUMUGAM, T. V., STOKES, K. Y. & GRANGER, D. N. (2006) Role of T lymphocytes and interferon-gamma in ischemic stroke. *Circulation,* 113, 2105-12.

YOKOTA, C., KAJI, T., KUGE, Y., INOUE, H., TAMAKI, N. & MINEMATSU, K. (2004) Temporal and topographic profiles of cyclooxygenase-2 expression during 24 h of focal brain ishemia in rats. *Neurosci Lett,* 357, 219-22.

YOSHIMOTO, T. & SIESJO, B. K. (1999) Posttreatment with the immunosuppressant cyclosporin A in transient focal ischemia. *Brain Res,* 839, 283-91.

ZERNECKE, A., WEBER, K. S., ERWIG, L. P., KLUTH, D. C., SCHROPPEL, B., REES, A. J. & WEBER, C. (2001) Combinatorial model of chemokine involvement in glomerular monocyte recruitment: role of CXC chemokine receptor 2 in infiltration during nephrotoxic nephritis. *J Immunol,* 166, 5755-62.

ZHANG, F., ECKMAN, C., YOUNKIN, S., HSIAO, K. K. & IADECOLA, C. (1997) Increased Susceptibility to Ischemic Brain Damage in Transgenic Mice Overexpressing the Amyloid Precursor Protein. *J. Neurosci.,* 17, 7655-7661.

ZHANG, L., ZHANG, Z. G., ZHANG, R. L., LU, M., KRAMS, M. & CHOPP, M. (2003) Effects of a Selective CD11b/CD18 Antagonist and Recombinant Human Tissue Plasminogen Activator Treatment Alone and in Combination in a Rat Embolic Model of Stroke. *Stroke,* 34, 1790-1795.

ZHANG, R., CHOPP, M., ZHANG, Z., JIANG, N. & POWERS, C. (1998a) The expression of P- and E-selectins in three models of middle cerebral artery occlusion. *Brain Res,* 785, 207-14.

ZHANG, R. L., ZHANG, Z. G. & CHOPP, M. (1999) Increased therapeutic efficacy with rt-PA and anti-CD18 antibody treatment of stroke in the rat. *Neurology,* 52, 273-9.

ZHANG, W., POTROVITA, I., TARABIN, V., HERRMANN, O., BEER, V., WEIH, F., SCHNEIDER, A. & SCHWANINGER, M. (2005) Neuronal activation of NF-kappaB contributes to cell death in cerebral ischemia. *J Cereb Blood Flow Metab,* 25, 30-40.

ZHANG, Y. Q., SHI, J., RAJAKUMAR, G., DAY, A. L. & SIMPKINS, J. W. (1998b) Effects of gender and estradiol treatment on focal brain ischemia. *Brain Res,* 784, 321-4.

ZHANG, Z., CHOPP, M., GOUSSEV, A. & POWERS, C. (1998c) Cerebral vessels express interleukin 1beta after focal cerebral ischemia. *Brain Res,* 784, 210-7.

ZILBERSTEIN, G., LEVY, R., RACHINSKY, M., FISHER, A., GREEMBERG, L., SHAPIRA, Y., APPELBAUM, A. & ROYTBLAT, L. (2002) Ketamine attenuates neutrophil activation after cardiopulmonary bypass. *Anesth Analg,* 95, 531-6.

ZLOTNIK, A. & YOSHIE, O. (2000) Chemokines: a new classification system and their role in immunity. *Immunity,* 12, 121-7.

ZOUGGARI, Y., AIT-OUFELLA, H., WAECKEL, L., VILAR, J., LOINARD, C., COCHAIN, C., RECALDE, A., DURIEZ, M., LEVY, B. I., LUTGENS, E., MALLAT, Z. & SILVESTRE, J. S. (2009) Regulatory T cells modulate postischemic neovascularization. *Circulation,* 120, 1415-25.